STROMAL CONTRIBUTION TO PANCREATIC CANCER PATHOGENESIS

by

Esha Mathew

A dissertation submitted in partial fulfillment
of the requirements for the degree of
Doctor of Philosophy
(Cellular and Molecular Biology)
in the University of Michigan
2015

Doctoral Committee

Assistant Professor Marina Pasca di Magliano, Chair
Assistant Professor Benjamin L. Allen
Associate Professor Ronald J. Buckanovich
Professor Deborah L. Gumucio
Professor Linda C. Samuelson

© Esha Mathew

2015

To my parents, who encourage and inspire.

ACKNOWLEDGEMENTS

Graduate school is the most gratifying learning experience I have ever had. This is largely thanks to my many people I was privileged to know and work with during my time at Michigan.

My family - Mom, Appa, and Divij – have been a wonderful support system these past few years. Mom and Appa, thank you for always supporting my educational pursuits and not glazing over when I babble on about my experiments. And to my brother Divij – arguing with you, whether it's about to best way to quantify macrophages or the fastest way to measure the volume of a donut, is more fun than I will ever admit aloud. To my best friends – Ann Marie, Jackie, Katie, Lee, Randi, Rebecca, and Sarah – you are an incredible group of women, and I am so lucky to have you as friends. And to my dear friends in graduate school – especially Gabriel and Nathan – thanks for keeping me sane the past five years, always being ready with a cup of tea, and for reminding me that a life outside of the lab is important too.

I owe so much to my mentor, Marina Pasca di Magliano. I wish I could properly articulate how much I appreciate your abilities as a scientist and mentor, as well as a tremendous role model. Your support of my interests, both inside and outside of lab has allowed me to shape my own educational trajectory and pursue my interests wherever they take me.

Also, a big thank you to the wonderful Pasca Lab – Yaqing Zhang, Arthur Brannon III, Heather Schofield, and Paloma Garcia, as well as former lab members Meredith Collins, Marsha Thomas, and Kevin Kane; going to lab was something I looked forward to largely because of you all. Yaqing, you are the most patient and knowledgeable person I know – I'm going to sincerely miss brainstorming and troubleshooting experiments with you! Arthur and Heather – I'm lucky to have people I can talk to, not just about science, but also about social justice, wild turkeys, and how much better the Patriots are than any other team.

I would like to thank my thesis committee: Deb Gumucio, Linda Samuelson, Ron Buckanovich, and Ben Allen, for their guidance. In particular, I'd like to thank Ron and his lab for advice and reagents, as well as Ben and his lab, without which a large portion of this work would not have been possible. To the amazing staff at the Flow Cytometry Core and Microscopy and Image Analysis Laboratory (MIL) – a big thanks for your incredible reservoirs of patience when helping me troubleshoot experiments.

Michigan is filled with wonderful resources and people, too many to name here, who have influenced me in meaningful ways. The Michigan experience has had a lasting impact on me, and for that I will be forever grateful.

TABLE OF CONTENTS

LIST OF FIGURES

Figure

LIST OF TABLES

Table

LIST OF ABBREVIATIONS

βgal	β-galactosidase
BOC	Brother of Cdon
CA-MSC	Carcinoma-associated Mesenchymal Stem Cell
CAM Assay	Chick Chorioallantoic Membrane Assay
CC3	Cleaved caspase 3
CCK	Cholecystokinin
CDON	CAM-related/Downregulated by Oncogenes
CK19	Cytokeratin 19
DAPI	4',6-diamidino-2-phenylindole
DMSO	Dimethyl sulfoxide
ECM	Extracellular Matrix
G-CSF	Granulocyte colony-stimulating factor
GAPDH	Glyceraldehde 3-phosphate dehydrogenase
GAS1	Growth Arrest Specific 1
GM-CSF	Granulocyte/macrophage colony-stimulating factor
HH	Hedgehog
HHIP1	Hedgehog interacting protein 1
IHH	Indian hedgehog
iKras*	inducible Kras mouse

IL6	Interleukin-6
KC	Pft1a-Cre;LSLKras^{G12D} mouse
KPC	Pft1a-Cre;LSLKras^{G12D};p53$^{R127H/+}$ mouse
M-CSF	macrophage colony-stimulating factor
MSC	mesenchymal stem cell
P-MSC	normal pancreas mesenchymal stem cell
PanIN	Pancreatic Intraepithelial Neoplasia
Ptf1a	Pancreas transcription factor 1 subunit alpha
PTCH1	Patched1
RT-qPCR	Real time quantitative PCR
SHH	Sonic Hedgehog
SMA	Smooth muscle actin
SMO	Smoothened
TGFβ	Transforming growth factor β

ABSTRACT

The overarching goal of this work is to understand the contribution of the stroma to pancreatic tumorigenesis. Pancreatic cancer is among the deadliest of human malignancies and few specific treatments exist for this disease. Median survival following diagnosis is six months, a dismal prognosis that has not changed in fifty years. A hallmark of pancreatic cancer is an extensive desmoplastic stroma consisting of fibroblasts, immune cells, and extracellular matrix. The signaling pathways and cellular components involved in inducing this desmoplastic reaction are an area of active investigation, with the hope of elucidating pathways to target in the clinic. Overexpression of the Hedgehog (HH) ligand occurs in roughly 75% of human pancreatic cancers. Interestingly, HH ligands secreted by the tumor cells act on the tumor stroma to activate signaling in a paracrine manner. However, pathway components that activate hedgehog signaling in the target cells are not fully elucidated, and represent potential druggable targets.

In the first part of this dissertation, I determined the function of three HH co-receptors, Boc, Cdon, and Gas1, on pancreatic tumor growth. While inhibition of HH signaling proved effective in early preclinical tests, clinical trials in humans were terminated due to acceleration of disease. My work indicated that the dosage of HH signaling is an important consideration in pancreatic cancer; while a complete blockade

of the pathway abrogated tumor growth, partial inhibition, such as that observed in the clinic, led to larger, more vascular tumors, which may account for the disappointing clinical trials. Next, I studied the role of the HH pathway on pancreatitis and recovery. Pancreatitis is a risk factor for pancreatic cancer, and currently no treatment beyond palliative care exists for a disease characterized by progressive fibrosis and loss of tissue function. While descriptive reports have identified HH signaling in pancreatitis, studies as to its functional importance are lacking. Here, I identify a role for Gli1, a transcription factor activated by HH signaling, in pancreatitis and repair. Lastly, I characterized the role of the mesenchymal stem cell (MSC) in pancreatic cancer. Fibroblasts in the tumor microenvironment are treated as a homogenous group of cells, despite evidence that multiple subtypes exist. One such subtype is the MSC, a multipotent cell that has profound effects on tumorigenesis in several solid tumors. In pancreatic cancer, I identified a role for MSCs to direct the behavior of another stromal cell type, the macrophage, with the ultimate effect of promoting tumor growth.

Taken together, this dissertation work will provide insight into the complex and dynamic microenvironment of pancreatic cancer.

CHAPTER ONE

Introduction[1]

Pancreatic Cancer

Current Outlook

Pancreatic cancer is a highly malignant disease with a median survival of 6 months. Fewer than 5% of patients survive 5 years post-diagnosis, and only 15% of patients qualify for a surgical resection of the tumor, which is currently the most effective clinical option (1). Even among patients who qualify for resection and adjuvant chemotherapy, the median survival rate is only two years (2). Unfortunately, the currently used drug regimen is only marginally more efficacious than palliative care. While pancreatic cancer is currently the fourth leading cause of cancer deaths in the United States, it is expected to surpass breast, prostate and colorectal cancers to become the second leading cause of cancer deaths by 2030 (3,4). Thus, a better understanding of pancreatic tumor biology is imperative for developing much-needed treatments.

Overview

[1]Portions of this chapter have been submitted as an invited review to *Cellular and Molecular Life Sciences*: Mathew, E, Allen BA, and Pasca di Magliano, M. Tentative title: Hedgehog Signaling in Pancreatic Cancer

Pancreatic cancer, or pancreatic adenocarcinoma, arises from the exocrine pancreas and is the focus of this dissertation. The vast majority of pancreatic malignancies arise from the exocrine compartment. In contrast, cancers arising from the endocrine pancreas, known as pancreatic neuroendocrine tumors (PNETs), are rarer, but have a much better prognosis (5). Pancreatitis is a known risk factor for pancreatic cancer, and is the leading cause for gastrointestinal-related hospitalization in the United States (6,7). There are two forms of pancreatitis - acute and chronic. Both are characterized by improper production and activation of digestive enzymes in the pancreas, leading to acinar cell loss and fibroinflammatory infiltration. Unlike acute pancreas, which resolves over time, chronic pancreatitis requires continued medical intervention due to irreversible fibrosis and progressive loss of both endocrine and exocrine pancreas. However, only 5% of those suffering from chronic pancreatitis progress to pancreatic cancer (8).

Pancreatic cancer is thought to progress through precursor lesions that have been characterized both histologically and based on their gene mutation profile. The most common precursor lesion is the Pancreatic Intraepithelial Neoplasia (PanIN), although other neoplasms, such as Intraductal mucinous papillary neoplasm (IMPNs) and mucinous cystic neoplasms (MCNs) are also known to progress to cancer, although rarely (for review, see (9) or (10)). PanINs are categorized into stages 1 through 3, based on increasing cellular atypia. Almost all cases of pancreatic cancer are linked to an activating mutation in the GTPase KRAS, most commonly G12D and G12V (11-13), which are observed starting in low-grade PanIN lesions. Higher grades of PanIN lesions are also associated with loss of tumor suppressors including P53, INK4a/ARF and

SMAD4 (14-16). Along with PanIN progression, pancreatic cancer is characterized by a prominent desmoplasia – the accumulation of activated fibroblasts, extracellular matrix, and immune cells that persist throughout tumorigenesis. Up to 90% of a bulk tumor can consist of this reactive stroma, which is considered the highest of all solid epithelial malignancies (1).

Treatment Options

Pancreatic cancer is largely refractory to chemotherapy. The cancer cells themselves are resistant to apoptosis-inducing agents (17), and the reactive stroma creates a poorly perfused environment that nurtures tumor growth and suppresses the immune system (for review, see (18)). Along with a high degree of reactive stroma, pancreatic cancer is characterized by hypovascularity; tumors have significantly fewer functional blood vessels than normal pancreas (19). Gemcitabine has long been the standard of care for pancreatic cancer (recently replaced by Folfirinox). However, most patients have little clinical response to this agent. An emerging mode of treatment is the combination of agents that target both the tumor itself as well as signals from the microenvironment (for review, see (1)). While such approaches have shown efficacy in mouse models of pancreatic cancer, they remain unproven in the clinical setting.

Mouse Models of Pancreatic Cancer

Mouse models of pancreatic cancer have provided further insight into the cellular and molecular mechanisms that drive progression, maintenance, and metastasis of pancreatic cancer. The models that are considered most faithful to the human disease are based on the expression of an oncogenic form of Kras, usually a $Kras^{G12D}$ allele,

using a pancreas epithelium-specific promoter (for review, see (20)). The most commonly used model, called the KC mouse, combines a pancreas-specific Cre, such as Pft1a-Cre or Pdx1-Cre, with a conditional mutant $Kras^{G12D}$ allele inserted into its endogenous locus (21). Notwithstanding the expression of oncogenic Kras starting during embryonic stages, KC mice are born with a normal pancreas. However, over time, PanIN lesions do develop (21). Tumor formation in KC mice is rare. The deletion of P53 or presence of a mutant form of P53 (R172H) creates the KPC mouse and accelerates both PanIN and tumor formation (22). The KPC mouse also replicates the resistance to gemcitabine commonly observed in human patients (19). Other pancreatic cancer models combine KC mice with deletion of other tumor suppressors such as CDKN2a or PTEN (23,24).

Alternatively, PanIN progression can be accelerated in KC mice by inducing pancreatitis. Administration of the cholecystokinin (CCK) agonist caerulein induces the excessive secretion and premature activation of digestive enzymes that in turn causes acinar cell death, which leads to acinar de-differentiation to duct-like cells in a process known as acinar-ductal metaplasia (ADM) (25). Caerulein-induced pancreatitis is characterized by edema and infiltration of immune cells. Wildtype mice undergo tissue repair within a week of caerulein administration. However, KC mice do not undergo repair; instead, the pancreatitis synergizes with oncogenic Kras to drive the development of low-grade PanIN lesions and the accumulation of desmoplastic stroma.

The models described above all feature continuous activation of oncogenic Kras upon Cre expression, which occurs during pancreatic development (21,22). A different model of pancreatic cancer is the iKras* mouse. Expression of $Kras^{G12D}$ in this model is

inducible *and* reversible (26). Like KC mice, iKras* mice develop PanINs sporadically and with long latency, but this process can be accelerated by inducing CCK-mediated pancreatitis. Interestingly, if oncogenic Kras is inactivated at early stages of PanIN-development, the pancreas undergoes full recovery. The acinar cells re-differentiate, and the fibroinflammatory stroma completely resolves away (26). Thus, the iKras* mouse represents a system to study the pathogenesis of pancreatic cancer during initiation and progression, but also tissue dynamics following Kras inactivation. Both the iKras* and KPC mice replicate the salient features of human disease including aberrant secretion of HH ligand and accumulation of desmoplastic stroma (22,27).

Hedgehog Signaling in the Pancreas

Hedgehog Pathway Overview

The Hedgehog (HH) pathway is highly conserved and plays an important role in a wide range of physiological processes. During development, HH signaling acts as a classic morphogen to define specific cell fates in a concentration- and time-dependent manner (for review, see (28)). The Hedgehog (*Hh*) gene was originally identified in a mutagenesis screen in *Drosophila;* larvae containing homozygous mutations in *Hh* display segmentation defects resulting in a continuous lawn of denticles (29). Unlike *Drosophila*, which possesses a single *Hh* gene, mammals have three: Sonic Hedgehog (Shh), Indian Hedgehog (Ihh), and Desert Hedgehog (Dhh). During mammalian development, expression of these three *Hh* genes depends on tissue and temporal context. *Shh*, the best-studied and most widely expressed of the three, is expressed in a broad range of tissues throughout embryonic development. *Ihh* expression is more

restricted than *Shh*, and has been best-studied in the context of endochondral bone formation (30). *Dhh* expression is largely restricted to the testes where it is essential for spermatogenesis (31), although it also controls peripheral nerve sheath formation (32).

HH pathway activity depends on genes involved in the formation of primary cilia. All three ligands initiate canonical HH signaling by binding to the 12-pass transmembrane protein Patched 1 (PTCH1), located in the ciliary membrane. In the absence of HH ligand, PTCH1 inhibits the function of another 7-pass transmembrane protein Smoothened (SMO). Binding of HH ligand to PTCH1 triggers its endocytosis, thus abrogating SMO inhibition. SMO can then localize to the cilia (33), where it mediates HH signal transduction through activation of the GLI family of transcription factors. As another level of pathway regulation, the protein Supressor of Fused (SUFU) can sequester GLI proteins in the cytoplasm, thereby controlling their transcriptional activity (34,35,36) (**for pathway schematic, see Figure 1.1)**.

In mammals, there are three GLI proteins (GLI1, GLI2, and GLI3) with different functional properties. While GLI1 functions exclusively as a transcriptional activator, GLI2 and GLI3 can act as either transcriptional activators or repressors. Genetic studies indicate that GLI2 functions primarily as a transcriptional activator, while GLI3 acts mainly as a transcriptional repressor (37,38). Although GLI target genes are not fully elucidated, a number of HH pathway genes, including *Gli1, Ptch1, Ptch2 and Hhip* are direct transcriptional targets of the pathway (28), thus providing an additional mechanism of feedback regulation of the pathway activity.

More recently, screens in *Shh* mutant mice identified additional co-receptors that also bind HH ligands. These receptors, GPI-anchored Growth arrest-specific 1 (GAS1), along with single pass transmembrane CAMrelated/down-regulated by oncogenes (CDON), and Brother of Cdo (BOC), were all shown to all cooperate with PTCH1 to promote HH signaling during development (39-42). Notably, removal of all three co-receptors resulted in the complete disruption of HH-mediated neural tube patterning, despite the presence of PTCH1, indicating the importance of these co-receptors in developmental processes (43). Thus, these co-receptors comprise a wider network of proteins required for HH pathway activation; their role in mediating HH signaling in adult tissues and disease, however, is still poorly understood.

Hedgehog Signaling in Pancreatic Development

Repression of HH signaling is required for proper pancreas development, as determined by experiments in chicks and mice. Early ectopic expression of SHH driven by the *Pdx1* promoter resulted in a small, poorly developed pancreas. Within the tissue, differentiated epithelial cells were present, but failed to organize properly, and mucinous lesions resembling the intestinal epithelium were present in the tissue rudiment. The surrounding mesenchyme was converted into smooth muscle cells resembling intestinal mesenchyme (44-46). SHH expression at later developmental stages, after the onset of pancreas specification and morphogenesis, resulted in a decrease in both the exocrine and endocrine pancreatic epithelium, and an expansion of the mesenchyme (47). Expression of HH ligand in the fully developed pancreas, driven by the acinar cell specific *Cela1* promoter, resulted in an expansion in mesenchymal cells; no defect was noted in the epithelial compartment aside from displacement of acinar cells due to the

expansion of pancreatic mesenchyme (48). While over-activation of HH pathway activity led to abnormal pancreatic development, pathway inhibition experiments resulted in an expansion of pancreatic tissue. In chick embryos, SMO inhibition led to ectopic pancreas formation (49), and mice lacking *Shh* had a significant increase in pancreatic mass and endocrine cells relative to body size (50).

Removal of *Hhip*, a HH pathway inhibitor, also resulted in impaired pancreatic morphogenesis and reduced tissue mass. Interestingly, acinar cell differentiation was not impeded; rather, the endocrine cells were reduced in number (51). Taken together, these studies support the role of HH as a negative regulator of pancreatic development, and they point at a critical dosage-dependent role of this signaling pathway, as even a minor perturbation in the pathway leads to impaired pancreatic development.

Hedgehog Signaling in Pancreatitis

Several studies have reported increased SHH expression in the epithelium of human patients with chronic pancreatitis, thus providing a descriptive link between ligand expression in chronic inflammation and neoplasia (52,53). However, the functional consequences of HH ligand expression during inflammation remain to be elucidated in mouse models.

In the normal adult pancreas, all three HH ligands are undetectable, but pathway effectors, such as GAS1 and GLI1 are expressed in a subset of the stromal cells (46,54,55) **(Figure 1.2)**, and HHIP expression is observed in islets (51). Lack of active HH signaling is not unexpected, as this is typically restricted to adult epithelium tissues with high turnover, such as the gut and skin (for review, see (56)). Although active

Hedgehog pathway activity is quiescent in the pancreas during development and homeostasis, accumulating evidence indicates that it is essential for pancreatic recovery following tissue damage (51,54,57).

Hedgehog Signaling in Pancreatic Cancer

The first description of aberrant HH secretion in pancreatic cancer was provided by two studies (46,58). Although initially autocrine signaling was proposed, later studies indicated that HH ligands did not stimulate the tumor cells that secreted them. HH response was instead detected in stromal cells within the tumors. Administration of the SMO inhibitor cyclopamine to subcutaneously injected tumors reduced tumor growth compared to vehicle-treated cohorts (59). This effect was linked to HH-response of the infiltrating fibroblasts, as *Smo* deletion in fibroblasts significantly reduced their ability to promote tumor growth compared to their HH-responsive counterparts (59). Thus, canonical signaling in pancreatic tumors occurred in a paracrine manner, and the HH-responsiveness of fibroblasts was associated with their ability to promote tumor growth. Evidence linking HH signaling to desmoplasia was demonstrated using a transformed epithelial cell line (T-HPNE) experimentally induced to overexpress SHH (T-HPNE.SHH). Orthotopic injection of T-HPNE.SHH cells resulted in a significant increase of SMA+ myofibroblasts and ECM components compared to tumors from T-HPNE cells (60). Taken together, these data supported a model wherein tumor-derived HH promoted the expansion of activated fibroblasts and desmoplasia that in turn promoted tumor growth (**Figure 1.3**).

The notion that HH signaling acts in a paracrine manner in pancreatic cancer was furthered by two studies demonstrating that autocrine HH activation is dispensable in the pancreatic epithelium. The first implemented a conditional deletion of *Smo* in the pancreatic epithelium, thus disabling canonical activation of the pathway in these cells. Deletion of *Smo* did not affect $KRAS^{G12D}$ mediated tumorigenesis (61). In a complementary experiment, a constitutively active form of SMO (SMOM2), first identified in basal cell carcinoma, was conditionally expressed in the pancreatic epithelium. Even the addition of $Kras^{G12D}$ did not accelerate tumorigenesis compared to epithelium harboring only $Kras^{G12D}$ (62). Thus, autocrine HH signaling in epithelial cells does not appear to play a role in pancreatic carcinogenesis.

An intriguing finding was that cell-autonomous activation of Hedgehog signaling in the epithelium was compatible with normal pancreas development in contrast with ligand overexpression studies. This was shown using mice with either constitutively active SMO or a dominant active form of Gli2 in the epithelium (27,62). In the context of dominant active Gli2, the primary cilia was found to regulate activation of HH signaling; with intact cilia, mice with a dominant active form of Gli2 still could not efficiently activate the pathway. However, upon the ablation of primary cilia, HH activation of the pathway was observed in the epithelium leading to loss of both endocrine and exocrine tissue and expansion of pancreatic progenitor cells (63). Whether the cilia plays a regulatory role in pancreatic cancer has yet to be explored, although counterintuitively, the presence of primary cilia in pancreatic cancer was correlated with poorer overall survival in human patients (64).

Epithelial Gli1 in Pancreatic Cancer.

Along with HH signaling to the surrounding stroma, non-canonical *Gli1* expression and activation in tumor cells has been described in human pancreatic cancer (46,58). Similarly, KPC mice have detectable *Gli1* expression both in PanINs and in cancer cells, although to a much lower level than the surrounding stroma. Likewise, expression of *GLI1* in human pancreatic cancer samples was significantly higher in the stroma compared to the epithelium (61,62). Unlike what was observed in stromal cells, Gli1 expression in the epithelium was not decreased when SMO was inactivated, indicating non-canonical regulation of its expression (61). Ectopic expression of a dominant active form of GLI2 or GLI1 in the pancreatic epithelium did not induce PanIN formation, although GLI2 induced the formation of undifferentiated, sarcomatoid tumors (27). However, when combined with $KRAS^{G12D}$, both dominant active GLI2 and GLI1 accelerated PanIN formation (27,65). Conversely, in a mouse model of pancreatic cancer bearing a dominant repressor form of GLI3-which represses GLI1 and GLI2 mediated gene transcription in epithelial cells- $KRAS^{G12D}$-driven PanIN formation was reduced, whereas survival was prolonged (65). While the effects of GLI1 activation in the epithelium are not completely understood, some indication as to the mechanism of activation derives from *in vitro* studies that linked TGFβ signaling and NFκB signaling to GLI1 (52,61,66).

Therapeutic Implications of Hedgehog Signaling in Cancer

Clinical Modes of HH Pathway Inhibition

The involvement of HH signaling in multiple malignancies, including basal cell carcinomas and medulloblastomas, as well as several gastrointestinal cancers,

underscores the clinical importance of Hedgehog pathway antagonists. The most widely used HH antagonists in the clinic target SMO, thus preventing all downstream signaling. Cyclopamine, a natural compound present in the corn lily, was the first identified SMO antagonist (67,68), and can inhibit HH signaling in mouse cells at an IC_{50} = 300 nM (68). Cyclopamine is not suitable for clinical use due to its poor pharmacokinetics, including structural complexity, instability in acid and poor aqueous solubility (69), although it still retains widespread use in preclinical experiments. However, alternate compounds have been commercially synthesized that improve the bioavailability and pharmacokinetic properties of cyclopamine, including GDC-0449 and IPI-926 (70,71).

Genentech: GDC-0449, also referred to as Vismodegib or Erivedge, was the first SMO inhibitor to pass phase II clinical trials, and is currently approved for treatment of locally advanced or metastatic basal cell carcinomas (BCC). In preclinical data, GDC-0449 inhibited GLI1 expression in 10T1/2 embryonic fibroblasts at an IC50 = 13nM (71). A pilot study of GDC-0449 in a single patient with metastatic medulloblastoma resulted in a dramatic, although transient, reduction in tumor burden; rapid relapse was due to the selection of a SMO variant (D473H) resistant to inhibition (72,73). Currently, the National Cancer Institute has sponsored Phase I clinical trials to test the efficacy of GDC-0449 in children with medulloblastoma (NCT00822458). In pancreatic cancer, while early studies combining chemotherapy (gemcitabine) and GDC-0449 did not demonstrate clinical utility (74), additional trials in pancreatic cancer, along with other solid tumors, are in progress (NCT01088815, NCT01064622).

Infinity Pharmaceuticals: IPI-926, also known as Saridegib, is a semisynthetic analog of cyclopamine. It is still an investigational drug and is not currently approved for use by the FDA (70), although it has demonstrated potency in preclinical experiments using mouse models of medulloblastoma (75). *In vitro*, IPI-926 could inhibit Gli1 expression in 10T1/2 embryonic fibroblasts at an IC_{50} of 9 nM, and interestingly, was also effective against the D473H *SMO* mutant (IC_{50} = 244 nM) that conferred resistance to GDC-0449 (75). In a Phase I trial, IPI-926 was effective against BCC that had not been previously treated with GDC-0449; patients previously treated with GDC-0449 showed little response to IPI-926, indicating some therapeutic overlap between the two agents, although the shared mechanism behind this resistance is unclear (76).

In addition to the inhibitors described above, alternative HH-antagonists have been synthesized by other companies including Novartis (LDE225/Erismodegib/Odozmo) (77), Bristol-Myers Squibb (BMS-833923/XL139)(78) and Pfizer (PF-04449913/Glasdegib) (79) and are also in clinical trials. Given the potential of HH inhibitors to treat HH-dysregulated cancers and the recurring issue of drug-resistance, the continued development of multiple HH inhibitors is clinically important.

HH Pathway Inhibition in Pancreatic Cancer

As a preclinical study of HH signaling inhibition in pancreatic cancer, tumor-bearing KPC mice were treated with gemcitabine and the HH inhibitor IPI-926. Either gemcitabine or IPI-926 had little effect when used as single agent. However, in combination, they conferred a survival benefit (19). This effect was attributed to

improved perfusion of the tumors, due to an increase in vascularization, which was the result of a reduction of the stromal fibroblast population and of the accumulation of extracellular matrix. These and other results indicating the benefits of targeting the stroma through HH inhibition led to clinical trials in human pancreatic cancer patients (NCT01130142). However, in late 2013, these trials were terminated as patients treated with both HH inhibition and chemotherapy had faster disease progression than those on chemotherapy alone (80). Clinical trials of another HH inhibitor GDC-0449 (Genentech) combined with gemcitabine in pancreatic cancer did not improve outcome compared to gemcitabine alone (74).

In the wake of the disappointing clinical trials, several studies emerged that added complexity to the role of HH signaling in pancreatic cancer. First, the duration of HH inhibition was found to affect cancer progression. While short-term inhibition of HH signaling in KPC mice with IPI-926 resulted in increased intratumoral vasculature and better drug perfusion (19), long-term treatment of KPC mice, starting at the PanIN stage, resulted in poorer survival (81). GDC-0449 administration also accelerated PanIN progression and tumor burden in KPC mice (82). Similarly, genetic deletion of *Shh* from the epithelium of KPC mice resulted in accelerated tumor progression and lethality (81,82). Intriguingly, while a similar experimental scheme was implemented in the two studies, the results are only partially overlapping. While both studies found reduced survival in mice lacking epithelial SHH, the nature of the tumors that formed was different. In one case (81), instead of a classic presentation of pancreatic cancer, with duct-like structures surrounded by abundant stroma, deletion of SHH resulted in tumors reminiscent of sarcomatoid tumors in a subset of human patients. In the second study

(82), the tumors had abundant stroma, although a mild reduction in this compartment was observed. Interestingly, the sarcomatoid tumors in KPC;*Shh*$^{f/f}$ were highly vascularized, which sensitized them to antivascular agents, which are typically ineffective in pancreatic cancer (83).

Taken together, interpreting the results from these different studies is difficult, but some speculations can be made. *Shh* deletion in the pancreas epithelium resulted in a compensatory upregulation of *Ihh* (81). Thus, it is possible that the end result of Shh depletion is a reduction, rather than complete ablation, of HH signaling in the pancreas. Many studies link reduced HH signaling to increased vascularization (19,55,81). While increased tumor vasculature might allow better drug perfusion, pancreatic cancer cells have a high propensity to develop resistance to gemcitabine. Thus, the end result of increasing the tumor vasculature might be to promote tumor growth.

The Microenvironment of Pancreatic Cancer

Despite the clinical inefficacy thus far of targeting the Hh pathway in pancreatic cancer, the microenvironment contains multiple cell types and signaling pathways that collectively influence tumorigenesis. The manner in which these stromal components act upon each other and upon tumors cells is an area of active investigation.

Macrophages

Macrophages are a prominent population in the stroma of both human and mouse pancreatic cancers (84,85). In mice, macrophages are the dominant population of leukocytes present in the stroma. These cells start accumulating in the pancreas during the PanIN stage, and persist throughout tumorigenesis (85).

Macrophages are highly plastic cells than can further polarize into a classically activated subtype or an alternatively activated subtype; each is associated with a particular cytokine and chemokine profile. Classically activated macrophages, also termed M1 macrophages, are typically associated with anti-tumor behavior, and express markers including iNOS and CD11c (86,87). Alternatively activated macrophages, also referred to as M2 macrophages, are thought to promote tumor growth, and express CD206 and Arg1, among others (88,89). In human pancreatic cancer, alternatively activated macrophages are prevalent in the tumor stroma (90). Moreover, their increased infiltration in human pancreatic cancer was associated with a poorer prognosis (90), and was also shown to promote epithelial-to-mesenchymal transition (EMT) of pancreatic cancer cells *in vitro* (88). In mice, blockade of macrophage growth factor CSF1 (M-CSF) slowed tumor growth by enhancing the infiltration of cytotoxic T cells, which are normally excluded from the microenvironment, and thus cannot employ their anti-tumor function (91). Interestingly, CSF1 blockade specifically depleted the CD206+ population of cells, supporting the accumulating evidence that alternatively activated macrophages generally act to promote tumor growth.

Mesenchymal Stem Cells

The fibroblast population itself is heterogeneous and comprised of ill-defined subtypes (92). Unlike immune cells, which have better defined subtypes and tools with which to identify and study them, fibroblasts do not. Few surface markers exist to separate fibroblast populations, and thus they are often treated experimentally as a homogenous group of cells. Recently however, a fibroblast-like cell has been identified in the stroma of several solid, epithelial tumors – the Mesenchymal Stem Cell (MSC).

While macrophages have been described in the pancreatic cancer stroma, the presence and activity of MSCs has not, although they have been noted in the normal pancreas (93). MSCs are multipotent cells capable of differentiating into osteoblasts, chondrocytes, and adipocytes. Aside from their hallmark multipotency, MSCs can be identified by a panel of cell surface markers, namely $CD44^{+}/CD49a^{+}/CD73^{+}/CD90^{+}$, and negative for markers of hematopoietic and endothelial lineages (94).

Originally discovered in the bone marrow (95), these cells are now thought to reside in virtually all adult organs, including the pancreas (96). Functional studies have described MSCs as 'medicinal signaling cells' due to their ability to both stimulate epithelial cell growth after injury and modulate the immune system (97-99). MSCs were also found to play an active role in tumor growth in a context-dependent manner. In breast carcinoma, MSCs significantly increased cancer cell metastasis via CCL5 expression upon co-injection with cancer cells into mice (100). A study in ovarian carcinoma found that stromal MSCs supported tumor growth by secretion of BMP pathway proteins (101). More recently, a study on stromal MSCs in lymphomas found that MSC tumor promotion was abrogated upon depletion of macrophages, although the requirement of a particular subset of macrophages was not determined (102). Regardless of the specific mechanism, these studies clearly show that MSCs affect tumorigenesis and are thus an important component of the tumor microenvironment. Moreover, notwithstanding the extensive desmoplastic reaction in pancreatic cancer, interaction between stromal cell populations remains largely unexplored.

Dissertation Overview

In this dissertation, I explore multiple aspects of the role of the microenvironment in pancreatic cancer pathogenesis. In Chapter Two, HH co-receptors BOC, CDON, and GAS1, whose function in pancreatic cancer is unknown, are evaluated for their role in promoting tumor growth. While combined Hedgehog inhibition and chemotherapy has shown promise in preclinical models of pancreatic cancer (19), human clinical trials have been disappointing (74,80). Moreover, even when HH pathway inhibition through SMO antagonism is effective in cancer, the development of drug-resistance is an issue (72,73); thus multiple modes to inhibit the HH pathway aside from SMO inhibition are clinically valuable. In Chapter Two, which has been published (55), I find that GAS1, BOC, and CDON are expressed in fibroblasts in the reactive stroma of pancreatic cancer, the predominant cell population responding to tumor-derived HH. Further, through use of mouse models with genetic deletions of these co-receptors, I identify a previously unappreciated dosage-dependent role for HH signaling in pancreatic tumor growth.

In Chapter Three, which has also been published (54), I focus on the role of HH signaling in pancreatitis and recovery. Tissue recovery is a complex process that involves crosstalk between the damaged epithelium and surrounding cells, such as fibroblasts and immune cells (for review, see (103) or (104)). In pancreatitis, further understanding the molecular mechanisms behind tissue damage and repair are important given that pancreatitis is a risk factor for cancer and no specific treatment exists for it. While SHH expression has been described in human pancreatitis (52,53), its functional consequences remain to be explored experimentally. In Chapter Three, I

focus on understanding the role of Hedgehog signaling in pancreatic repair, using two modes of injury: caerulein-induced pancreatitis, and $Kras^{G12D}$ inactivation. Mice lacking a copy of *Gli1* or mice treated with a HH inhibitor are unable to properly remodel the injury-induced fibroinflammatory stroma; this impaired repair process is specifically linked to impaired secretion of immunomodulating cytokines from pancreatic fibroblasts, indicating a role for HH signaling in fibroblast-immune cell crosstalk during pancreas recovery.

Further insight into the heterogeneity of the microenvironment is explored in Chapter Four. Unlike immune cells, fibroblasts do not have panels of cell-surface markers and experimental tools with which to identify and study subsets within this population of cells. Thus, although fibroblast heterogeneity within the cancer microenvironment has been acknowledged (92,105), fibroblasts are still typically treated as a homogenous population of cells. In Chapter Four, I identify a subset of fibroblast-like cells in the pancreas – the MSC - and describe their ability to promote tumor growth. Tumor-derived MSCs depend on macrophages to promote tumor growth, and can direct the polarization of alternatively activated macrophages, thereby impacting tumor growth. Finally, in Chapter Five, further questions and directions identified by this dissertation work will be discussed.

Figures

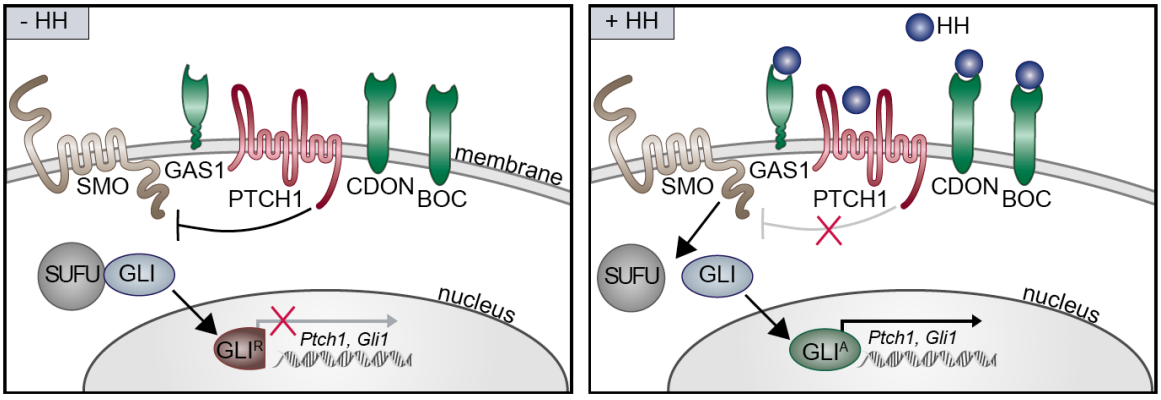

Figure 1.1: HH signaling

In the absence of HH ligand, PTCH1 inhibits SMO. Upon binding of HH ligand to PTCH1, its inhibitory function ceases and SMO then can initiate HH signaling, culminating in the activation of the GLI family of transcription factors. In addition to PTCH1, co-receptors BOC, CDON, and GAS1 can also bind HH ligand and activate HH signaling.

(*cartoon credit: Dr. Ben Allen)*

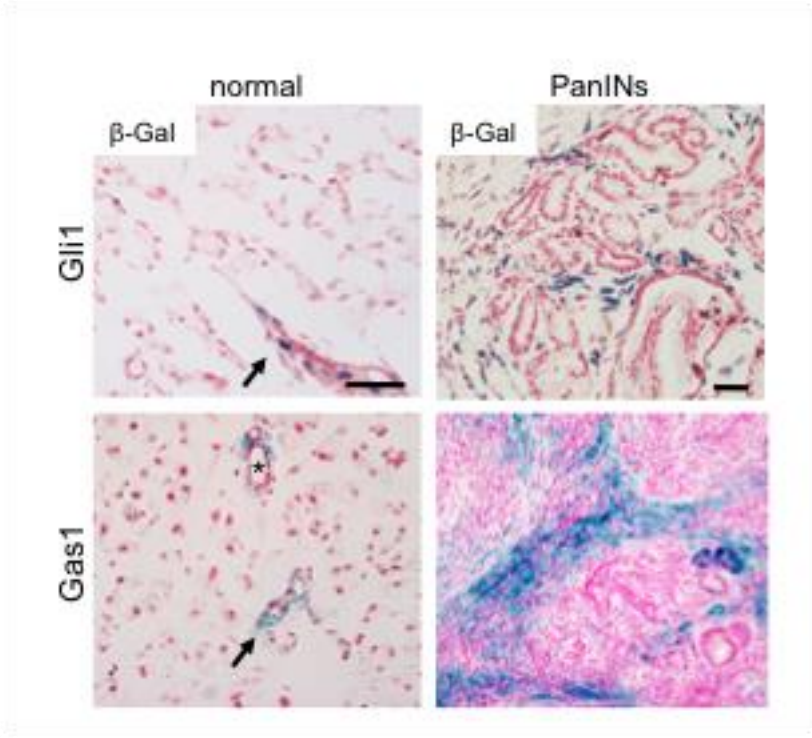

Figure 1.2: HH pathway components Gli1 and Gas1 are expressed in the pancreas. In the pancreas of untreated $Gli1^{Lacz/+}$ or $Gas1^{\tau LacZ/+}$ mice, GLI1 and GAS1 are expressed in a perivascular and periductal manner (left). Asterisks (*) marks ducts and black arrows mark blood vessels. Scale bar 20μm. Analysis of neoplastic pancreas from $KC;Gli1^{LacZ/+}$ or $KC;Gas1^{\tau LacZ/+}$ shows that during tumorigenesis, GLI1 and GAS1 are expressed throughout the accumulating reactive stroma (right). Scale bar 50μm

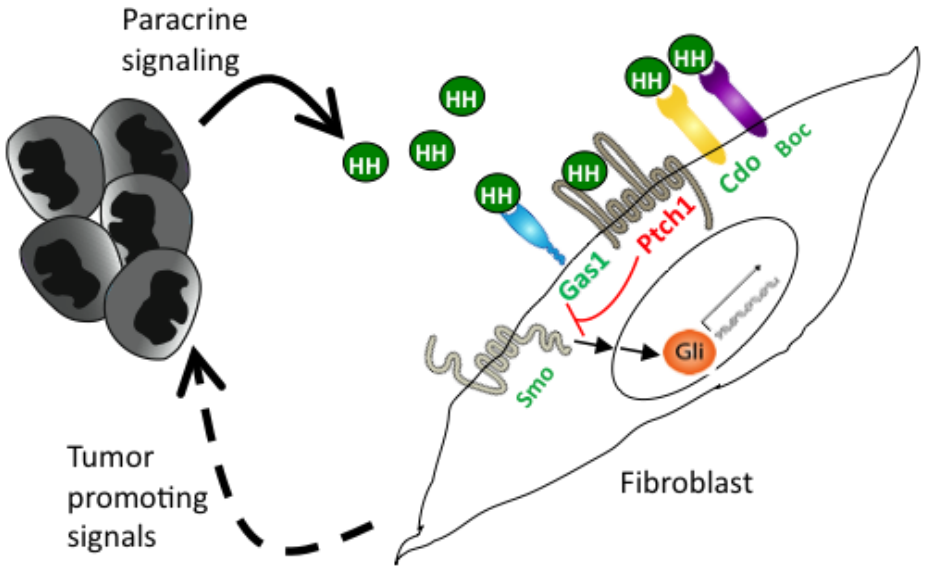

Figure 1.3: Paracrine HH signaling in pancreatic cancer.

In pancreatic cancer, HH ligand from tumor cells activate the pathway in surrounding fibroblasts, which in turn signal back to the tumor; the nature of this response is poorly understood.

References

1. Neesse, A., Michl, P., Frese, K. K., Feig, C., Cook, N., Jacobetz, M. A., Lolkema, M. P., Buchholz, M., Olive, K. P., Gress, T. M., and Tuveson, D. A. (2011) Stromal biology and therapy in pancreatic cancer. *Gut* **60**, 861-868
2. Mayo, S. C., Nathan, H., Cameron, J. L., Olino, K., Edil, B. H., Herman, J. M., Hirose, K., Schulick, R. D., Choti, M. A., Wolfgang, C. L., and Pawlik, T. M. (2012) Conditional survival in patients with pancreatic ductal adenocarcinoma resected with curative intent. *Cancer* **118**, 2674-2681
3. Herszenyi, L., and Tulassay, Z. (2010) Epidemiology of gastrointestinal and liver tumors. *Eur Rev Med Pharmacol Sci* **14**, 249-258
4. Rahib, L., Smith, B. D., Aizenberg, R., Rosenzweig, A. B., Fleshman, J. M., and Matrisian, L. M. (2014) Projecting cancer incidence and deaths to 2030: the unexpected burden of thyroid, liver, and pancreas cancers in the United States. *Cancer Res* **74**, 2913-2921
5. Halfdanarson, T. R., Rabe, K. G., Rubin, J., and Petersen, G. M. (2008) Pancreatic neuroendocrine tumors (PNETs): incidence, prognosis and recent trend toward improved survival. *Ann Oncol* **19**, 1727-1733
6. Malka, D., Hammel, P., Maire, F., Rufat, P., Madeira, I., Pessione, F., Levy, P., and Ruszniewski, P. (2002) Risk of pancreatic adenocarcinoma in chronic pancreatitis. *Gut* **51**, 849-852
7. Peery, A. F., Dellon, E. S., Lund, J., Crockett, S. D., McGowan, C. E., Bulsiewicz, W. J., Gangarosa, L. M., Thiny, M. T., Stizenberg, K., Morgan, D. R., Ringel, Y., Kim, H. P., Dibonaventura, M. D., Carroll, C. F., Allen, J. K., Cook, S. F., Sandler, R. S., Kappelman, M. D., and Shaheen, N. J. (2012) Burden of gastrointestinal disease in the United States: 2012 update. *Gastroenterology* **143**, 1179-1187 e1171-1173
8. Raimondi, S., Lowenfels, A. B., Morselli-Labate, A. M., Maisonneuve, P., and Pezzilli, R. (2010) Pancreatic cancer in chronic pancreatitis; aetiology, incidence, and early detection. *Best Pract Res Clin Gastroenterol* **24**, 349-358
9. Hezel, A. F., Kimmelman, A. C., Stanger, B. Z., Bardeesy, N., and Depinho, R. A. (2006) Genetics and biology of pancreatic ductal adenocarcinoma. *Genes Dev* **20**, 1218-1249
10. Morris, J. P. t., Wang, S. C., and Hebrok, M. (2010) KRAS, Hedgehog, Wnt and the twisted developmental biology of pancreatic ductal adenocarcinoma. *Nat Rev Cancer* **10**, 683-695
11. Biankin, A. V., Waddell, N., Kassahn, K. S., Gingras, M. C., Muthuswamy, L. B., Johns, A. L., Miller, D. K., Wilson, P. J., Patch, A. M., Wu, J., Chang, D. K., Cowley, M. J., Gardiner, B. B., Song, S., Harliwong, I., Idrisoglu, S., Nourse, C., Nourbakhsh, E., Manning, S., Wani, S., Gongora, M., Pajic, M., Scarlett, C. J., Gill J., Pinho, A. V., Rooman, I., Anderson, M., Holmes, O., Leonard, C., Taylor, D., Wood, S., Xu, Q., Nones, K., Fink, J. L., Christ, A., Bruxner, T., Cloonan, N., Kolle, G., Newell, F., Pinese, M., Mead, R. S., Humphris, J. L., Kaplan, W., Jones, M. D., Colvin, E. K., Nagrial, A. M., Humphrey, E. S., Chou, A., Chin, V. T., Chantrill, L. A., Mawson, A., Samra, J. S., Kench, J. G., Lovell, J. A., Daly, R. J., Merrett, N. D., Toon, C., Epari, K., Nguyen, N. Q., Barbour, A., Zeps, N.,

Kakkar, N., Zhao, F., Wu, Y. Q., Wang, M., Muzny, D. M., Fisher, W. E., Brunicardi, F. C., Hodges, S. E., Reid, J. G., Drummond, J., Chang, K., Han, Y., Lewis, L. R., Dinh, H., Buhay, C. J., Beck, T., Timms, L., Sam, M., Begley, K., Brown, A., Pai, D., Panchal, A., Buchner, N., De Borja, R., Denroche, R. E., Yung, C. K., Serra, S., Onetto, N., Mukhopadhyay, D., Tsao, M. S., Shaw, P. A., Petersen, G. M., Gallinger, S., Hruban, R. H., Maitra, A., Iacobuzio-Donahue, C. A., Schulick, R. D., Wolfgang, C. L., Morgan, R. A., Lawlor, R. T., Capelli, P., Corbo, V., Scardoni, M., Tortora, G., Tempero, M. A., Mann, K. M., Jenkins, N. A., Perez-Mancera, P. A., Adams, D. J., Largaespada, D. A., Wessels, L. F., Rust, A. G., Stein, L. D., Tuveson, D. A., Copeland, N. G., Musgrove, E. A., Scarpa, A., Eshleman, J. R., Hudson, T. J., Sutherland, R. L., Wheeler, D. A., Pearson, J. V., McPherson, J. D., Gibbs, R. A., and Grimmond, S. M. (2012) Pancreatic cancer genomes reveal aberrations in axon guidance pathway genes. *Nature* **491**, 399-405

12. Jones, S., Zhang, X., Parsons, D. W., Lin, J. C., Leary, R. J., Angenendt, P., Mankoo, P., Carter, H., Kamiyama, H., Jimeno, A., Hong, S. M., Fu, B., Lin, M. T., Calhoun, E. S., Kamiyama, M., Walter, K., Nikolskaya, T., Nikolsky, Y., Hartigan, J., Smith, D. R., Hidalgo, M., Leach, S. D., Klein, A. P., Jaffee, E. M., Goggins, M., Maitra, A., Iacobuzio-Donahue, C., Eshleman, J. R., Kern, S. E., Hruban, R. H., Karchin, R., Papadopoulos, N., Parmigiani, G., Vogelstein, B., Velculescu, V. E., and Kinzler, K. W. (2008) Core signaling pathways in human pancreatic cancers revealed by global genomic analyses. *Science* **321**, 1801-1806
13. Waddell, N., Pajic, M., Patch, A. M., Chang, D. K., Kassahn, K. S., Bailey, P., Johns, A. L., Miller, D., Nones, K., Quek, K., Quinn, M. C., Robertson, A. J., Fadlullah, M. Z., Bruxner, T. J., Christ, A. N., Harliwong, I., Idrisoglu, S., Manning, S., Nourse, C., Nourbakhsh, E., Wani, S., Wilson, P. J., Markham, E., Cloonan, N., Anderson, M. J., Fink, J. L., Holmes, O., Kazakoff, S. H., Leonard, C., Newell, F., Poudel, B., Song, S., Taylor, D., Wood, S., Xu, Q., Wu, J., Pinese, M., Cowley, M. J., Lee, H. C., Jones, M. D., Nagrial, A. M., Humphris, J., Chantrill, L. A., Chin, V., Steinmann, A. M., Mawson, A., Humphrey, E. S., Colvin, E. K., Chou, A., Scarlett, C. J., Pinho, A. V., Giry-Laterriere, M., Rooman, I., Samra, J. S., Kench, J. G., Pettitt, J. A., Merrett, N. D., Toon, C., Epari, K., Nguyen, N. Q., Barbour, A., Zeps, N., Jamieson, N. B., Graham, J. S., Niclou, S. P., Bjerkvig, R., Grutzmann, R., Aust, D., Hruban, R. H., Maitra, A., Iacobuzio-Donahue, C. A., Wolfgang, C. L., Morgan, R. A., Lawlor, R. T., Corbo, V., Bassi, C., Falconi, M., Zamboni, G., Tortora, G., Tempero, M. A., Gill, A. J., Eshleman, J. R., Pilarsky, C., Scarpa, A., Musgrove, E. A., Pearson, J. V., Biankin, A. V., and Grimmond, S. M. (2015) Whole genomes redefine the mutational landscape of pancreatic cancer. *Nature* **518**, 495-501
14. Scarpa, A., Capelli, P., Mukai, K., Zamboni, G., Oda, T., Iacono, C., and Hirohashi, S. (1993) Pancreatic adenocarcinomas frequently show p53 gene mutations. *Am J Pathol* **142**, 1534-1543
15. Wilentz, R. E., Geradts, J., Maynard, R., Offerhaus, G. J., Kang, M., Goggins, M., Yeo, C. J., Kern, S. E., and Hruban, R. H. (1998) Inactivation of the p16 (INK4A)

tumor-suppressor gene in pancreatic duct lesions: loss of intranuclear expression. *Cancer Res* **58**, 4740-4744

16. Wilentz, R. E., Iacobuzio-Donahue, C. A., Argani, P., McCarthy, D. M., Parsons, J. L., Yeo, C. J., Kern, S. E., and Hruban, R. H. (2000) Loss of expression of Dpc4 in pancreatic intraepithelial neoplasia: evidence that DPC4 inactivation occurs late in neoplastic progression. *Cancer Res* **60**, 2002-2006
17. Burris, H. A., 3rd, Moore, M. J., Andersen, J., Green, M. R., Rothenberg, M. L., Modiano, M. R., Cripps, M. C., Portenoy, R. K., Storniolo, A. M., Tarassoff, P., Nelson, R., Dorr, F. A., Stephens, C. D., and Von Hoff, D. D. (1997) Improvements in survival and clinical benefit with gemcitabine as first-line therapy for patients with advanced pancreas cancer: a randomized trial. *J Clin Oncol* **15**, 2403-2413
18. Feig, C., Gopinathan, A., Neesse, A., Chan, D. S., Cook, N., and Tuveson, D. A. (2012) The pancreas cancer microenvironment. *Clin Cancer Res* **18**, 4266-4276
19. Olive, K. P., Jacobetz, M. A., Davidson, C. J., Gopinathan, A., McIntyre, D., Honess, D., Madhu, B., Goldgraben, M. A., Caldwell, M. E., Allard, D., Frese, K. K., Denicola, G., Feig, C., Combs, C., Winter, S. P., Ireland-Zecchini, H., Reichelt, S., Howat, W. J., Chang, A., Dhara, M., Wang, L., Ruckert, F., Grutzmann, R., Pilarsky, C., Izeradjene, K., Hingorani, S. R., Huang, P., Davies, S. E., Plunkett, W., Egorin, M., Hruban, R. H., Whitebread, N., McGovern, K., Adams, J., Iacobuzio-Donahue, C., Griffiths, J., and Tuveson, D. A. (2009) Inhibition of Hedgehog signaling enhances delivery of chemotherapy in a mouse model of pancreatic cancer. *Science* **324**, 1457-1461
20. Westphalen, C. B., and Olive, K. P. (2012) Genetically engineered mouse models of pancreatic cancer. *Cancer J* **18**, 502-510
21. Hingorani, S. R., Petricoin, E. F., Maitra, A., Rajapakse, V., King, C., Jacobetz, M. A., Ross, S., Conrads, T. P., Veenstra, T. D., Hitt, B. A., Kawaguchi, Y., Johann, D., Liotta, L. A., Crawford, H. C., Putt, M. E., Jacks, T., Wright, C. V., Hruban, R. H., Lowy, A. M., and Tuveson, D. A. (2003) Preinvasive and invasive ductal pancreatic cancer and its early detection in the mouse. *Cancer Cell* **4**, 437-450
22. Hingorani, S. R., Wang, L., Multani, A. S., Combs, C., Deramaudt, T. B., Hruban, R. H., Rustgi, A. K., Chang, S., and Tuveson, D. A. (2005) Trp53R172H and KrasG12D cooperate to promote chromosomal instability and widely metastatic pancreatic ductal adenocarcinoma in mice. *Cancer Cell* **7**, 469-483
23. Aguirre, A. J., Bardeesy, N., Sinha, M., Lopez, L., Tuveson, D. A., Horner, J., Redston, M. S., and DePinho, R. A. (2003) Activated Kras and Ink4a/Arf deficiency cooperate to produce metastatic pancreatic ductal adenocarcinoma. *Genes Dev* **17**, 3112-3126
24. Ying, H., Elpek, K. G., Vinjamoori, A., Zimmerman, S. M., Chu, G. C., Yan, H., Fletcher-Sananikone, E., Zhang, H., Liu, Y., Wang, W., Ren, X., Zheng, H., Kimmelman, A. C., Paik, J. H., Lim, C., Perry, S. R., Jiang, S., Malinn, B., Protopopov, A., Colla, S., Xiao, Y., Hezel, A. F., Bardeesy, N., Turley, S. J., Wang, Y. A., Chin, L., Thayer, S. P., and DePinho, R. A. (2011) PTEN is a major tumor suppressor in pancreatic ductal adenocarcinoma and regulates an NF-kappaB-cytokine network. *Cancer Discov* **1**, 158-169

25. Morris, J. P. t., Cano, D. A., Sekine, S., Wang, S. C., and Hebrok, M. (2010) Beta-catenin blocks Kras-dependent reprogramming of acini into pancreatic cancer precursor lesions in mice. *J Clin Invest* **120**, 508-520
26. Collins, M. A., Bednar, F., Zhang, Y., Brisset, J. C., Galban, S., Galban, C. J., Rakshit, S., Flannagan, K. S., Adsay, N. V., and Pasca di Magliano, M. (2012) Oncogenic Kras is required for both the initiation and maintenance of pancreatic cancer in mice. *J Clin Invest* **122**, 639-653
27. Pasca di Magliano, M., Sekine, S., Ermilov, A., Ferris, J., Dlugosz, A. A., and Hebrok, M. (2006) Hedgehog/Ras interactions regulate early stages of pancreatic cancer. *Genes Dev* **20**, 3161-3173
28. Dessaud, E., McMahon, A. P., and Briscoe, J. (2008) Pattern formation in the vertebrate neural tube: a sonic hedgehog morphogen-regulated transcriptional network. *Development* **135**, 2489-2503
29. Nusslein-Volhard, C., and Wieschaus, E. (1980) Mutations affecting segment number and polarity in Drosophila. *Nature* **287**, 795-801
30. Vortkamp, A., Lee, K., Lanske, B., Segre, G. V., Kronenberg, H. M., and Tabin, C. J. (1996) Regulation of rate of cartilage differentiation by Indian hedgehog and PTH-related protein. *Science* **273**, 613-622
31. Bitgood, M. J., Shen, L., and McMahon, A. P. (1996) Sertoli cell signaling by Desert hedgehog regulates the male germline. *Curr Biol* **6**, 298-304
32. Parmantier, E., Lynn, B., Lawson, D., Turmaine, M., Namini, S. S., Chakrabarti, L., McMahon, A. P., Jessen, K. R., and Mirsky, R. (1999) Schwann cell-derived Desert hedgehog controls the development of peripheral nerve sheaths. *Neuron* **23**, 713-724
33. Corbit, K. C., Aanstad, P., Singla, V., Norman, A. R., Stainier, D. Y., and Reiter, J. F. (2005) Vertebrate Smoothened functions at the primary cilium. *Nature* **437**, 1018-1021
34. Kogerman, P., Grimm, T., Kogerman, L., Krause, D., Unden, A. B., Sandstedt, B., Toftgard, R., and Zaphiropoulos, P. G. (1999) Mammalian suppressor-of-fused modulates nuclear-cytoplasmic shuttling of Gli-1. *Nat Cell Biol* **1**, 312-319
35. Humke, E. W., Dorn, K. V., Milenkovic, L., Scott, M. P., and Rohatgi, R. (2010) The output of Hedgehog signaling is controlled by the dynamic association between Suppressor of Fused and the Gli proteins. *Genes Dev* **24**, 670-682
36. Jia, J., Kolterud, A., Zeng, H., Hoover, A., Teglund, S., Toftgard, R., and Liu, A. (2009) Suppressor of Fused inhibits mammalian Hedgehog signaling in the absence of cilia. *Dev Biol* **330**, 452-460
37. Pan, Y., Bai, C. B., Joyner, A. L., and Wang, B. (2006) Sonic hedgehog signaling regulates Gli2 transcriptional activity by suppressing its processing and degradation. *Mol Cell Biol* **26**, 3365-3377
38. Wang, B., Fallon, J. F., and Beachy, P. A. (2000) Hedgehog-regulated processing of Gli3 produces an anterior/posterior repressor gradient in the developing vertebrate limb. *Cell* **100**, 423-434
39. Allen, B. L., Tenzen, T., and McMahon, A. P. (2007) The Hedgehog-binding proteins Gas1 and Cdo cooperate to positively regulate Shh signaling during mouse development. *Genes Dev* **21**, 1244-1257

40. Martinelli, D. C., and Fan, C. M. (2007) Gas1 extends the range of Hedgehog action by facilitating its signaling. *Genes Dev* **21**, 1231-1243
41. Tenzen, T., Allen, B. L., Cole, F., Kang, J. S., Krauss, R. S., and McMahon, A. P. (2006) The cell surface membrane proteins Cdo and Boc are components and targets of the Hedgehog signaling pathway and feedback network in mice. *Dev Cell* **10**, 647-656
42. Zhang, W., Kang, J. S., Cole, F., Yi, M. J., and Krauss, R. S. (2006) Cdo functions at multiple points in the Sonic Hedgehog pathway, and Cdo-deficient mice accurately model human holoprosencephaly. *Dev Cell* **10**, 657-665
43. Allen, B. L., Song, J. Y., Izzi, L., Althaus, I. W., Kang, J. S., Charron, F., Krauss, R. S., and McMahon, A. P. (2011) Overlapping roles and collective requirement for the coreceptors GAS1, CDO, and BOC in SHH pathway function. *Dev Cell* **20**, 775-787
44. Apelqvist, A., Ahlgren, U., and Edlund, H. (1997) Sonic hedgehog directs specialised mesoderm differentiation in the intestine and pancreas. *Curr Biol* **7**, 801-804
45. Hebrok, M., Kim, S. K., and Melton, D. A. (1998) Notochord repression of endodermal Sonic hedgehog permits pancreas development. *Genes Dev* **12**, 1705-1713
46. Thayer, S. P., di Magliano, M. P., Heiser, P. W., Nielsen, C. M., Roberts, D. J., Lauwers, G. Y., Qi, Y. P., Gysin, S., Fernandez-del Castillo, C., Yajnik, V., Antoniu, B., McMahon, M., Warshaw, A. L., and Hebrok, M. (2003) Hedgehog is an early and late mediator of pancreatic cancer tumorigenesis. *Nature* **425**, 851-856
47. Kawahira, H., Scheel, D. W., Smith, S. B., German, M. S., and Hebrok, M. (2005) Hedgehog signaling regulates expansion of pancreatic epithelial cells. *Dev Biol* **280**, 111-121
48. Fendrich, V., Oh, E., Bang, S., Karikari, C., Ottenhof, N., Bisht, S., Lauth, M., Brossart, P., Katsanis, N., Maitra, A., and Feldmann, G. (2011) Ectopic overexpression of Sonic Hedgehog (Shh) induces stromal expansion and metaplasia in the adult murine pancreas. *Neoplasia* **13**, 923-930
49. Kim, S. K., and Melton, D. A. (1998) Pancreas development is promoted by cyclopamine, a hedgehog signaling inhibitor. *Proc Natl Acad Sci U S A* **95**, 13036-13041
50. Hebrok, M., Kim, S. K., St Jacques, B., McMahon, A. P., and Melton, D. A. (2000) Regulation of pancreas development by hedgehog signaling. *Development* **127**, 4905-4913
51. Kawahira, H., Ma, N. H., Tzanakakis, E. S., McMahon, A. P., Chuang, P. T., and Hebrok, M. (2003) Combined activities of hedgehog signaling inhibitors regulate pancreas development. *Development* **130**, 4871-4879
52. Nakashima, H., Nakamura, M., Yamaguchi, H., Yamanaka, N., Akiyoshi, T., Koga, K., Yamaguchi, K., Tsuneyoshi, M., Tanaka, M., and Katano, M. (2006) Nuclear factor-kappaB contributes to hedgehog signaling pathway activation through sonic hedgehog induction in pancreatic cancer. *Cancer Res* **66**, 7041-7049

53. Strobel, O., Rosow, D. E., Rakhlin, E. Y., Lauwers, G. Y., Trainor, A. G., Alsina, J., Fernandez-Del Castillo, C., Warshaw, A. L., and Thayer, S. P. (2010) Pancreatic duct glands are distinct ductal compartments that react to chronic injury and mediate Shh-induced metaplasia. *Gastroenterology* **138**, 1166-1177
54. Mathew, E., Collins, M. A., Fernandez-Barrena, M. G., Holtz, A. M., Yan, W., Hogan, J. O., Tata, Z., Allen, B. L., Fernandez-Zapico, M. E., and di Magliano, M. P. (2014) The transcription factor GLI1 modulates the inflammatory response during pancreatic tissue remodeling. *J Biol Chem* **289**, 27727-27743
55. Mathew, E., Zhang, Y., Holtz, A. M., Kane, K. T., Song, J. Y., Allen, B. L., and Pasca di Magliano, M. (2014) Dosage-dependent regulation of pancreatic cancer growth and angiogenesis by hedgehog signaling. *Cell Rep* **9**, 484-494
56. Petrova, R., and Joyner, A. L. (2014) Roles for Hedgehog signaling in adult organ homeostasis and repair. *Development* **141**, 3445-3457
57. Fendrich, V., Esni, F., Garay, M. V., Feldmann, G., Habbe, N., Jensen, J. N., Dor, Y., Stoffers, D., Jensen, J., Leach, S. D., and Maitra, A. (2008) Hedgehog signaling is required for effective regeneration of exocrine pancreas. *Gastroenterology* **135**, 621-631
58. Berman, D. M., Karhadkar, S. S., Maitra, A., Montes De Oca, R., Gerstenblith, M. R., Briggs, K., Parker, A. R., Shimada, Y., Eshleman, J. R., Watkins, D. N., and Beachy, P. A. (2003) Widespread requirement for Hedgehog ligand stimulation in growth of digestive tract tumours. *Nature* **425**, 846-851
59. Yauch, R. L., Gould, S. E., Scales, S. J., Tang, T., Tian, H., Ahn, C. P., Marshall, D., Fu, L., Januario, T., Kallop, D., Nannini-Pepe, M., Kotkow, K., Marsters, J. C., Rubin, L. L., and de Sauvage, F. J. (2008) A paracrine requirement for hedgehog signalling in cancer. *Nature* **455**, 406-410
60. Bailey, J. M., Swanson, B. J., Hamada, T., Eggers, J. P., Singh, P. K., Caffery, T., Ouellette, M. M., and Hollingsworth, M. A. (2008) Sonic hedgehog promotes desmoplasia in pancreatic cancer. *Clin Cancer Res* **14**, 5995-6004
61. Nolan-Stevaux, O., Lau, J., Truitt, M. L., Chu, G. C., Hebrok, M., Fernandez-Zapico, M. E., and Hanahan, D. (2009) GLI1 is regulated through Smoothened-independent mechanisms in neoplastic pancreatic ducts and mediates PDAC cell survival and transformation. *Genes Dev* **23**, 24-36
62. Tian, H., Callahan, C. A., DuPree, K. J., Darbonne, W. C., Ahn, C. P., Scales, S. J., and de Sauvage, F. J. (2009) Hedgehog signaling is restricted to the stromal compartment during pancreatic carcinogenesis. *Proc Natl Acad Sci U S A* **106**, 4254-4259
63. Cervantes, S., Lau, J., Cano, D. A., Borromeo-Austin, C., and Hebrok, M. (2010) Primary cilia regulate Gli/Hedgehog activation in pancreas. *Proc Natl Acad Sci U S A* **107**, 10109-10114
64. Emoto, K., Masugi, Y., Yamazaki, K., Effendi, K., Tsujikawa, H., Tanabe, M., Kitagawa, Y., and Sakamoto, M. (2014) Presence of primary cilia in cancer cells correlates with prognosis of pancreatic ductal adenocarcinoma. *Hum Pathol* **45**, 817-825
65. Rajurkar, M., De Jesus-Monge, W. E., Driscoll, D. R., Appleman, V. A., Huang, H., Cotton, J. L., Klimstra, D. S., Zhu, L. J., Simin, K., Xu, L., McMahon, A. P., Lewis, B. C., and Mao, J. (2012) The activity of Gli transcription factors is

essential for Kras-induced pancreatic tumorigenesis. *Proc Natl Acad Sci U S A* **109**, E1038-1047

66. Dennler, S., Andre, J., Alexaki, I., Li, A., Magnaldo, T., ten Dijke, P., Wang, X. J., Verrecchia, F., and Mauviel, A. (2007) Induction of sonic hedgehog mediators by transforming growth factor-beta: Smad3-dependent activation of Gli2 and Gli1 expression in vitro and in vivo. *Cancer Res* **67**, 6981-6986
67. Cooper, M. K., Porter, J. A., Young, K. E., and Beachy, P. A. (1998) Teratogen-mediated inhibition of target tissue response to Shh signaling. *Science* **280**, 1603-1607
68. Chen, J. K., Taipale, J., Cooper, M. K., and Beachy, P. A. (2002) Inhibition of Hedgehog signaling by direct binding of cyclopamine to Smoothened. *Genes Dev* **16**, 2743-2748
69. Lipinski, R. J., Hutson, P. R., Hannam, P. W., Nydza, R. J., Washington, I. M., Moore, R. W., Girdaukas, G. G., Peterson, R. E., and Bushman, W. (2008) Dose- and route-dependent teratogenicity, toxicity, and pharmacokinetic profiles of the hedgehog signaling antagonist cyclopamine in the mouse. *Toxicol Sci* **104**, 189-197
70. Tremblay, M. R., Lescarbeau, A., Grogan, M. J., Tan, E., Lin, G., Austad, B. C., Yu, L. C., Behnke, M. L., Nair, S. J., Hagel, M., White, K., Conley, J., Manna, J. D., Alvarez-Diez, T. M., Hoyt, J., Woodward, C. N., Sydor, J. R., Pink, M., MacDougall, J., Campbell, M. J., Cushing, J., Ferguson, J., Curtis, M. S., McGovern, K., Read, M. A., Palombella, V. J., Adams, J., and Castro, A. C. (2009) Discovery of a potent and orally active hedgehog pathway antagonist (IPI-926). *J Med Chem* **52**, 4400-4418
71. Robarge, K. D., Brunton, S. A., Castanedo, G. M., Cui, Y., Dina, M. S., Goldsmith, R., Gould, S. E., Guichert, O., Gunzner, J. L., Halladay, J., Jia, W., Khojasteh, C., Koehler, M. F., Kotkow, K., La, H., Lalonde, R. L., Lau, K., Lee, L., Marshall, D., Marsters, J. C., Jr., Murray, L. J., Qian, C., Rubin, L. L., Salphati, L., Stanley, M. S., Stibbard, J. H., Sutherlin, D. P., Ubhayaker, S., Wang, S., Wong, S., and Xie, M. (2009) GDC-0449-a potent inhibitor of the hedgehog pathway. *Bioorg Med Chem Lett* **19**, 5576-5581
72. Rudin, C. M., Hann, C. L., Laterra, J., Yauch, R. L., Callahan, C. A., Fu, L., Holcomb, T., Stinson, J., Gould, S. E., Coleman, B., LoRusso, P. M., Von Hoff, D. D., de Sauvage, F. J., and Low, J. A. (2009) Treatment of medulloblastoma with hedgehog pathway inhibitor GDC-0449. *N Engl J Med* **361**, 1173-1178
73. Yauch, R. L., Dijkgraaf, G. J., Alicke, B., Januario, T., Ahn, C. P., Holcomb, T., Pujara, K., Stinson, J., Callahan, C. A., Tang, T., Bazan, J. F., Kan, Z., Seshagiri, S., Hann, C. L., Gould, S. E., Low, J. A., Rudin, C. M., and de Sauvage, F. J. (2009) Smoothened mutation confers resistance to a Hedgehog pathway inhibitor in medulloblastoma. *Science* **326**, 572-574
74. Kim, E. J., Sahai, V., Abel, E. V., Griffith, K. A., Greenson, J. K., Takebe, N., Khan, G. N., Blau, J. L., Craig, R., Balis, U. G., Zalupski, M. M., and Simeone, D. M. (2014) Pilot clinical trial of hedgehog pathway inhibitor GDC-0449 (vismodegib) in combination with gemcitabine in patients with metastatic pancreatic adenocarcinoma. *Clin Cancer Res* **20**, 5937-5945

75. Lee, M. J., Hatton, B. A., Villavicencio, E. H., Khanna, P. C., Friedman, S. D., Ditzler, S., Pullar, B., Robison, K., White, K. F., Tunkey, C., LeBlanc, M., Randolph-Habecker, J., Knoblaugh, S. E., Hansen, S., Richards, A., Wainwright, B. J., McGovern, K., and Olson, J. M. (2012) Hedgehog pathway inhibitor saridegib (IPI-926) increases lifespan in a mouse medulloblastoma model. *Proc Natl Acad Sci U S A* **109**, 7859-7864
76. Jimeno, A., Weiss, G. J., Miller, W. H., Jr., Gettinger, S., Eigl, B. J., Chang, A. L., Dunbar, J., Devens, S., Faia, K., Skliris, G., Kutok, J., Lewis, K. D., Tibes, R., Sharfman, W. H., Ross, R. W., and Rudin, C. M. (2013) Phase I study of the Hedgehog pathway inhibitor IPI-926 in adult patients with solid tumors. *Clin Cancer Res* **19**, 2766-2774
77. Pan, S., Wu, X., Jiang, J., Gao, W., Wan, Y., Cheng, D., Han, D., Liu, J., Englund, N. P., Wang, Y., Peukert, S., Miller-Moslin, K., Yuan, J., Guo, R., Matsumoto, M., Vattay, A., Jiang, Y., Tsao, J., Sun, F., Pferdekamper, A. C., Dodd, S., Tuntland, T., Maniara, W., Kelleher, J. F., 3rd, Yao, Y. M., Warmuth, M., Williams, J., and Dorsch, M. (2010) Discovery of NVP-LDE225, a Potent and Selective Smoothened Antagonist. *ACS Med Chem Lett* **1**, 130-134
78. Steven B. Gendreau, D. H., Ching- Ping Ho, Anne Lewin, Tara Lin, Akil Merchant, R. Bruce Rowley, Qiuju Wang, William Matsui, and Joseph Fargnoli2. (2009) Preclinical characterization of BMS- 833923 (XL139), a hedgehog (HH) pathway inhibitor in early clinical development. *Molecular Cancer Therepeutics* **8**
79. Munchhof, M. J., Li, Q., Shavnya, A., Borzillo, G. V., Boyden, T. L., Jones, C. S., LaGreca, S. D., Martinez-Alsina, L., Patel, N., Pelletier, K., Reiter, L. A., Robbins, M. D., and Tkalcevic, G. T. (2012) Discovery of PF-04449913, a Potent and Orally Bioavailable Inhibitor of Smoothened. *ACS Med Chem Lett* **3**, 106-111
80. Amakye, D., Jagani, Z., and Dorsch, M. (2013) Unraveling the therapeutic potential of the Hedgehog pathway in cancer. *Nat Med* **19**, 1410-1422
81. Rhim, A. D., Oberstein, P. E., Thomas, D. H., Mirek, E. T., Palermo, C. F., Sastra, S. A., Dekleva, E. N., Saunders, T., Becerra, C. P., Tattersall, I. W., Westphalen, C. B., Kitajewski, J., Fernandez-Barrena, M. G., Fernandez-Zapico, M. E., Iacobuzio-Donahue, C., Olive, K. P., and Stanger, B. Z. (2014) Stromal elements act to restrain, rather than support, pancreatic ductal adenocarcinoma. *Cancer Cell* **25**, 735-747
82. Lee, J. J., Perera, R. M., Wang, H., Wu, D. C., Liu, X. S., Han, S., Fitamant, J., Jones, P. D., Ghanta, K. S., Kawano, S., Nagle, J. M., Deshpande, V., Boucher, Y., Kato, T., Chen, J. K., Willmann, J. K., Bardeesy, N., and Beachy, P. A. (2014) Stromal response to Hedgehog signaling restrains pancreatic cancer progression. *Proc Natl Acad Sci U S A* **111**, E3091-3100
83. Kindler, H. L., Niedzwiecki, D., Hollis, D., Sutherland, S., Schrag, D., Hurwitz, H., Innocenti, F., Mulcahy, M. F., O'Reilly, E., Wozniak, T. F., Picus, J., Bhargava, P., Mayer, R. J., Schilsky, R. L., and Goldberg, R. M. (2010) Gemcitabine plus bevacizumab compared with gemcitabine plus placebo in patients with advanced pancreatic cancer: phase III trial of the Cancer and Leukemia Group B (CALGB 80303). *J Clin Oncol* **28**, 3617-3622
84. Komura, T., Sakai, Y., Harada, K., Kawaguchi, K., Takabatake, H., Kitagawa, H., Wada, T., Honda, M., Ohta, T., Nakanuma, Y., and Kaneko, S. (2015)

Inflammatory features of pancreatic cancer highlighted by monocytes/macrophages and CD4+ T cells with clinical impact. *Cancer Sci* **106**, 672-686
85. Clark, C. E., Hingorani, S. R., Mick, R., Combs, C., Tuveson, D. A., and Vonderheide, R. H. (2007) Dynamics of the immune reaction to pancreatic cancer from inception to invasion. *Cancer Res* **67**, 9518-9527
86. Ma, J., Liu, L., Che, G., Yu, N., Dai, F., and You, Z. (2010) The M1 form of tumor-associated macrophages in non-small cell lung cancer is positively associated with survival time. *BMC Cancer* **10**, 112
87. Engstrom, A., Erlandsson, A., Delbro, D., and Wijkander, J. (2014) Conditioned media from macrophages of M1, but not M2 phenotype, inhibit the proliferation of the colon cancer cell lines HT-29 and CACO-2. *Int J Oncol* **44**, 385-392
88. Liu, C. Y., Xu, J. Y., Shi, X. Y., Huang, W., Ruan, T. Y., Xie, P., and Ding, J. L. (2013) M2-polarized tumor-associated macrophages promoted epithelial-mesenchymal transition in pancreatic cancer cells, partially through TLR4/IL-10 signaling pathway. *Lab Invest* **93**, 844-854
89. Mantovani, A., Sozzani, S., Locati, M., Allavena, P., and Sica, A. (2002) Macrophage polarization: tumor-associated macrophages as a paradigm for polarized M2 mononuclear phagocytes. *Trends Immunol* **23**, 549-555
90. Kurahara, H., Shinchi, H., Mataki, Y., Maemura, K., Noma, H., Kubo, F., Sakoda, M., Ueno, S., Natsugoe, S., and Takao, S. (2011) Significance of M2-polarized tumor-associated macrophage in pancreatic cancer. *J Surg Res* **167**, e211-219
91. Zhu, Y., Knolhoff, B. L., Meyer, M. A., Nywening, T. M., West, B. L., Luo, J., Wang-Gillam, A., Goedegebuure, S. P., Linehan, D. C., and DeNardo, D. G. (2014) CSF1/CSF1R blockade reprograms tumor-infiltrating macrophages and improves response to T-cell checkpoint immunotherapy in pancreatic cancer models. *Cancer Res* **74**, 5057-5069
92. Sugimoto, H., Mundel, T. M., Kieran, M. W., and Kalluri, R. (2006) Identification of fibroblast heterogeneity in the tumor microenvironment. *Cancer Biol Ther* **5**, 1640-1646
93. Crisan, M., Chen, C. W., Corselli, M., Andriolo, G., Lazzari, L., and Peault, B. (2009) Perivascular multipotent progenitor cells in human organs. *Ann N Y Acad Sci* **1176**, 118-123
94. Dominici, M., Le Blanc, K., Mueller, I., Slaper-Cortenbach, I., Marini, F., Krause, D., Deans, R., Keating, A., Prockop, D., and Horwitz, E. (2006) Minimal criteria for defining multipotent mesenchymal stromal cells. The International Society for Cellular Therapy position statement. *Cytotherapy* **8**, 315-317
95. Friedenstein, A. J., Deriglasova, U. F., Kulagina, N. N., Panasuk, A. F., Rudakowa, S. F., Luria, E. A., and Ruadkow, I. A. (1974) Precursors for fibroblasts in different populations of hematopoietic cells as detected by the in vitro colony assay method. *Exp Hematol* **2**, 83-92
96. Crisan, M., Yap, S., Casteilla, L., Chen, C. W., Corselli, M., Park, T. S., Andriolo, G., Sun, B., Zheng, B., Zhang, L., Norotte, C., Teng, P. N., Traas, J., Schugar, R., Deasy, B. M., Badylak, S., Buhring, H. J., Giacobino, J. P., Lazzari, L., Huard, J., and Peault, B. (2008) A perivascular origin for mesenchymal stem cells in multiple human organs. *Cell Stem Cell* **3**, 301-313

97. Caplan, A. I., and Correa, D. (2011) The MSC: an injury drugstore. *Cell Stem Cell* **9**, 11-15
98. Le Blanc, K., and Mougiakakos, D. (2012) Multipotent mesenchymal stromal cells and the innate immune system. *Nat Rev Immunol* **12**, 383-396
99. Semont, A., Francois, S., Mouiseddine, M., Francois, A., Sache, A., Frick, J., Thierry, D., and Chapel, A. (2006) Mesenchymal stem cells increase self-renewal of small intestinal epithelium and accelerate structural recovery after radiation injury. *Adv Exp Med Biol* **585**, 19-30
100. Karnoub, A. E., Dash, A. B., Vo, A. P., Sullivan, A., Brooks, M. W., Bell, G. W., Richardson, A. L., Polyak, K., Tubo, R., and Weinberg, R. A. (2007) Mesenchymal stem cells within tumour stroma promote breast cancer metastasis. *Nature* **449**, 557-563
101. McLean, K., Gong, Y., Choi, Y., Deng, N., Yang, K., Bai, S., Cabrera, L., Keller, E., McCauley, L., Cho, K. R., and Buckanovich, R. J. (2011) Human ovarian carcinoma-associated mesenchymal stem cells regulate cancer stem cells and tumorigenesis via altered BMP production. *J Clin Invest* **121**, 3206-3219
102. Ren, G., Zhao, X., Wang, Y., Zhang, X., Chen, X., Xu, C., Yuan, Z. R., Roberts, A. I., Zhang, L., Zheng, B., Wen, T., Han, Y., Rabson, A. B., Tischfield, J. A., Shao, C., and Shi, Y. (2012) CCR2-dependent recruitment of macrophages by tumor-educated mesenchymal stromal cells promotes tumor development and is mimicked by TNFalpha. *Cell Stem Cell* **11**, 812-824
103. Eming, S. A., Martin, P., and Tomic-Canic, M. (2014) Wound repair and regeneration: mechanisms, signaling, and translation. *Sci Transl Med* **6**, 265sr266
104. Klingberg, F., Hinz, B., and White, E. S. (2013) The myofibroblast matrix: implications for tissue repair and fibrosis. *J Pathol* **229**, 298-309
105. Erez, N., Truitt, M., Olson, P., Arron, S. T., and Hanahan, D. (2010) Cancer-Associated Fibroblasts Are Activated in Incipient Neoplasia to Orchestrate Tumor-Promoting Inflammation in an NF-kappaB-Dependent Manner. *Cancer Cell* **17**, 135-147

CHAPTER TWO

Dosage-Dependent Regulation of Pancreatic Cancer Growth and Angiogenesis by Hedgehog Signaling[1]

Abstract

Pancreatic cancer, a hypovascular and highly desmoplastic cancer, is characterized by tumor expression of Hedgehog (HH) ligands that signal to fibroblasts in the surrounding stroma, which in turn promote tumor survival and growth. However, the mechanisms and consequences of stromal HH pathway activation are not well understood. Here we show that the HH co-receptors GAS1, BOC, and CDON are expressed in cancer-associated fibroblasts. Deletion of two co-receptors (*Gas1* and *Boc*) in fibroblasts reduces HH-responsiveness. Strikingly, these fibroblasts promote greater tumor growth in vivo that correlates with increased tumor-associated vascularity. In contrast, deletion of all three co-receptors (*Gas1, Boc* and *Cdon*) results in the near complete abrogation of HH signaling and a corresponding failure to promote tumorigenesis and angiogenesis. Collectively, these data identify a novel role for HH-

[1] Originally published as: Mathew, E., Zhang, Y., Holtz, A. M., Kane, K. T., Song, J. Y., Allen, B. L., and Pasca di Magliano, M. (2014) Dosage-dependent regulation of pancreatic cancer growth and angiogenesis by hedgehog signaling. *Cell Rep* **9**, 484-494 (doi:10.1016/j.celrep.2014.09.010)

dosage in pancreatic cancer promotion and may explain the clinical failure of HH pathway blockade as a therapeutic approach in pancreatic cancer.

Introduction

Pancreatic cancer, one of the deadliest human malignancies, is almost invariably associated with oncogenic mutations of Kras and the inappropriate activation of embryonic signaling pathways (1,2). Pancreatic cancer is preceded by precursor lesions, the most common of which are Pancreatic Intraepithelial Neoplasias (PanINs) (3). Notably, tissue-specific expression of mutant Kras in mice recapitulates the step-wise progression of the human disease and constitutes a reasonable mouse model of pancreatic cancer (4).

Aberrant activation of Hedgehog (HH) signaling is observed in pancreatic cancer in both humans (5,6) and mice (7). In pancreatic cancer, the HH pathway is proposed to act in a paracrine manner, where epithelial tumor cells secrete HH ligands that signal to cells of the tumor stroma (8). HH signaling is activated by ligand binding to the twelve-pass transmembrane protein Patched (PTCH1), which relieves an inhibitory effect on a second, GPCR-like protein, Smoothened (SMO) (9). De-repression of SMO results in a cascade of events that ultimately leads to the activation of GLI transcription factors and modulated target gene expression. HH pathway genes such as *PTCH1* and *GLI1* are direct transcriptional targets, thus establishing a feedback loop that regulates the level of pathway activity (10,11).

In tumors classically associated with cell-autonomous activation of HH signaling, such as basal cell carcinoma and medulloblastoma, HH inhibition has emerged as a therapeutic strategy (12,13). Small molecule inhibitors that target SMO have been successfully developed to inhibit signaling and induce tumor regression (13). HH inhibitors have also been applied to tumor types that rely on paracrine HH signaling (8). While SMO inhibition in the clinic has met with initial success, the emergence of drug-resistant *SMO* mutations in tumors (14) underscores the need for alternative approaches to restrict HH pathway function.

GAS1, BOC and CDON are cell surface-associated proteins that bind HH ligands and function as pathway activators (15-18). During neural tube development, GAS1, BOC and CDON are required for HH signal transduction (19). However, despite their collective requirement during HH-dependent embryogenesis, the role of these proteins has not been explored in adult tissues and organs, and their potential contribution to disease, including cancer, is currently unknown.

Here, we investigated GAS1, BOC and CDON expression and function in pancreatic cancer to determine whether they constitute potential novel therapeutic targets. We found that all three co-receptors were expressed in the adult pancreas and upregulated in pancreatic cancer stroma. We also observed that, similar to their role in embryogenesis, these co-receptors were required to mediate HH signal transduction in pancreatic fibroblasts. Counter to prevailing paradigms, while deletion of two co-receptors (*Gas1* and *Boc*) in pancreatic fibroblasts led to reduced HH-responsiveness, this resulted in increased tumor growth. In contrast, deletion of all three co-receptors

(*Gas1, Boc* and *Cdon*) abrogated HH signaling and blocked tumor promotion. Notably, the tumor promoting effects of reduced HH signaling were due to increased angiogenesis mediated by the tumor stroma. These findings uncover a novel dosage-dependent role of HH signaling in the regulation of tumor angiogenesis in pancreatic cancer.

Materials and Methods

Mice

Mice were housed in specific pathogen-free facilities of the University of Michigan Comprehensive Cancer Center. This study was approved by the University of Michigan University Committee on Use and Care of Animals (UCUCA) guidelines. Ptf1a-Cre mice (20) were intercrossed with LSL-Kras^{G12D} (4) to generate Ptf1a-Cre;LSL-Kras^{G12D} (KC) animals. KC mutant mice were further crossed with mice bearing reporter alleles Gas1$^{LacZ/+}$ (16) or Boc$^{AP/+}$ (21) to generate KC;Gas1$^{LacZ/+}$ or KC;Boc$^{AP/+}$. Acute pancreatitis was induced by two 8-hourly series of intraperitoneal injections with caerulein (Sigma) at a concentration of 75ug/kg over a 48-hour period, as previously described (22).

Cell Culture

Primary mouse pancreatic fibroblast lines were derived from E18.5 wildtype or Gas1$^{-/-}$;Boc$^{-/-}$ pancreata. Embryonic pancreas were minced via vigorous pipetting then immediately plated. MEFs were isolated and established using the methods of Todaro and Green (23). Samples were cultured in IMDM supplemented with 10% FBS and 1%

penicillin/streptomycin (Gibco). For HH signaling assays, plated cells were serum-starved (IMDM supplemented with 0.5% serum) for 36h prior to addition of conditioned media, and samples collected at indicated timepoints.

Immunohistochemistry/Immunofluorescence

Histology and immunohistochemistry/immunofluorescence stainings were performed as previously described (24). Primary antibodies used were β-Gal (1:200, Abcam), CD45 (1:200, BDPharm), CD31 (1:100, BDPharm), Ki67 (1:100, Vector Laboratories), αSMA (1:1000, Sigma), E-cadherin (1:100, Cell Signaling), Vimentin (1:100, Cell Signaling), and Cleaved Caspase-3 (Cell Signaling). Images from immunohistochemical stains were obtained with an Olympus BX-51 microscope, Olympus DP71 digital camera, and CellSens standard v1.6 software. For immunofluorescence, Alexa Fluor (Invitrogen) secondary antibodies were used. DAPI (Invitrogen) was used to counterstain cell nuclei. Images from immunofluorescence stains were obtained using an Olympus IX-71 confocal microscope and FluoView FV500/IX software.

RT-qPCR

Tissue for RNA extraction was prepared through overnight incubation in RNAlater-ICE (Ambion) at -20^{o}C, then isolated using RNeasy Protect (Qiagen) according the manufacturer's instructions. Reverse transcription reactions were conducted using a High-Capacity cDNA Reverse Transcription Kit (Applied Biosystems). Samples for RT-qPCR were prepared with 1x SYBR Green PCR Master Mix (Applied Biosystems) and primers: *Gli1*, 5´-tggactctcttgacctggacaac-3´ (forward) and 5´-ggccctgggcctcatc-

3´(reverse); *Ptch1*, 5´- ttgtggaagccacagaaaacc -3´ (forward) and 5´-tgtctggagtccggatgga -3´(reverse); *Gapdh* was used as the housekeeping gene expression control. All primers were optimized for amplification under reaction conditions as follows: 95°C 10 minutes, followed by 40 cycles of 95°C 15 seconds and 60°C 1 minute. All samples underwent melt curve analysis following the amplification protocol.

Subcutaneous Tumor Models

5 x 10^5 tumor cells were injected alone or in combination with an equal number of fibroblasts into the flanks of CB17/SCID mice (Charles River, stock/strain #236) at a 1:1 ratio of complete medium and Matrigel (BD Biosciences #356234). Tumor size was measured weekly by caliper.

Chick Chorioallantoic Membrane (CAM) Assay

The CAM assay was performed as described previously (25). Briefly, 3 x 10^5 tumor cells were seeded alone or with an equal number of fibroblasts atop the CAM of E11.5 fertilized eggs. After three days of incubation at 37°C, the tumor cells and surrounding CAM were dissected, fixed in 4% paraformaldehyde and imaged with a Nikon SMZ1500 Scope and NIS-Elements D Imaging software.

Statistical Analysis

The data is expressed as the mean ± SEM. One-way ANOVA with a Tukey post-test and Student's t-tests were used to compare data. A p value <0.05 was considered

statistically significant. Significance values indicated by asterisks are as follows: *p<0.05, **p < 0.01, ***p < 0.0005, ****p < 0.0001

Results

GAS1, BOC, and CDON are Expressed in Fibroblasts and Stellate Cells in the Normal Adult and Neoplastic Pancreas.

Given the requirement of the HH co-receptors GAS1, BOC and CDON in embryonic development (19), we sought to identify a role for these HH pathway components in adult tissue. To determine if GAS1, BOC and CDON were expressed in the normal pancreas, during pancreatitis, and/or in the neoplastic pancreas, we harvested pancreata from adult wildtype or Ptf1aCre;LSL-Kras^{G12D} (KC) mice (4). KC pancreata were harvested three weeks following the induction of acute pancreatitis using the CCK agonist caerulein; this treatment synergizes with oncogenic Kras to drive tissue-wide PanIN formation and the accumulation of a fibroinflammatory stroma (22,26). Wildtype pancreata were harvested from either untreated adult animals or from animals one day after caerulein treatment, at the peak of pancreatitis. Expression of all three co-receptors, as measured by RT-qPCR analysis, was barely detectable in control tissue (untreated adult pancreata), but was significantly increased in KC pancreata. In addition, we observed a significant increase in *Boc* expression and a modest increase in *Gas1* and *Cdon* expression in the pancreatitis samples (**Figure 2.1A**).

To determine the cellular compartment in which these co-receptors are expressed, we crossed mice bearing reporter alleles of *Gas1* (*Gas1*$^{LacZ/+}$; (16)) or *Boc*

(*Boc*$^{PLAP/+}$; (21)) into the KC model of pancreatic cancer (**Figure 2.1B**). Pancreata were harvested from adult animals three weeks after inducing acute pancreatitis. Analysis of control pancreata revealed a perivascular and periductal expression pattern for *Gas1* and *Boc*, as well as in scattered cells throughout the parenchyma (**Figure 2.1B**). Strikingly, in KC tissues, *Gas1* and *Boc* expression expanded throughout the stroma surrounding PanIN lesions (**Figure 2.1B**).

To confirm that the RT-qPCR and reporter allele expression data correlated with increased co-receptor protein levels, we performed antibody detection of GAS1, BOC and CDON in pancreatic tissue (**Figure 2.2**). Consistent with our gene expression data, we detected limited stromal expression of GAS1, BOC and CDON in the normal pancreas (**Figure 2.2A**), and increased co-receptor expression in the stroma surrounding PanIN lesions and tumor cells in KC and KPC mice (**Figures 2.2B and 2.2C**). These data suggest that GAS1, BOC and CDON are expressed in a population of stromal cells in the adult pancreas that expands during PanIN formation.

To identify the specific cell type within the stroma expressing these co-receptors, we performed antibody staining of tissue from PanIN-bearing KC;*Gas1*$^{LacZ/+}$ pancreata (**Figures 2.3 and 2.4**). *Gas1*^{LacZ} expression was excluded from epithelial (E-cadherin+) and hematopoeitic (CD45+) cells (**Figure 2.3A, white arrows**). Similarly, β-galactosidase (β-gal) was not detected in endothelial cells lining the blood vessels (**Figure 2.3B**). In contrast, we detected widespread co-expression of β-gal with smooth muscle actin (SMA), a marker of activated fibroblasts (**Figure 2.3C**, **yellow arrows**), throughout the stroma, except immediately surrounding blood vessels (Fig. 2.1E). *Gas1*

expression in fibroblasts was confirmed by co-staining with antibodies directed against β-gal and Vimentin (**Figure 2.3D**, **yellow arrows**), another fibroblast marker (27). We also performed antibody staining of tissue from PanIN-bearing KC;*Boc*$^{PLAP/+}$ pancreata (**Figure 2.5**). Antibody detection of alkaline phosphatase (AP) co-localized with SMA (**Figure 2.5A**), suggesting that *Gas1* and *Boc* were co-expressed in a population of fibroblasts in the pancreas. In contrast, no co-localization was observed of AP with either E-cadherin (**Figure 2.5B**) or CK19 (**Figure 2.5C**), both epithelial markers. Thus, *Boc* expression was confined to the mesenchymal compartment. Finally, we performed RT-qPCR analysis of primary mouse pancreatic tumor cells, fibroblasts, and flow-sorted macrophages from the Pft1a-Cre;LSL-Kras^{G12D};p53$^{R172H/+}$(KPC) (7) and iKras (24) pancreatic cancer models. We detected expression of Sonic HH ligand (*Shh*) only in the tumor cells (**Figure 2.6A**), whereas only fibroblasts expressed *Gas1* (**Figure 2.6B**). Macrophages, another prominent stromal cell population did not express *Shh* or *Gas1* (**Figures 2.6A and 2.6B**).

Two alternative models could explain the increase in Gas1, Cdon and Boc expression in the neoplastic pancreas– increased expression on a per cell basis, or increased expression due to increased numbers of fibroblasts expressing these co-receptors. To distinguish between these two possibilities, we normalized the expression of the co-receptors to the mesenchymal marker *Vimentin*. Using this approach, we observed no change in *Gas1*, *Cdon* and *Boc* expression in the neoplastic pancreas compared to control (**Figure 2.6C**). Thus, the increase in co-receptor expression is caused by an increase in the number of co-receptor expressing cells within the tissue.

To determine whether our findings were relevant to human samples, we performed RT-qPCR on resected human pancreatic cancer samples and adjacent uninvolved pancreas. Upregulation of all three co-receptors was detected in the tumor samples (**Figure 2.7A**). To determine which compartment expressed the co-receptors, we obtained RNA from primary human tumor cells and primary human cancer associated fibroblasts (CAFs). We found elevated co-receptor expression in the CAF population, but not in the tumor cells (**Figure 2.7B**). As expected, *VIMENTIN* and *E-CADHERIN* were restricted to the CAF and tumor compartments respectively, thus confirming the identity of the samples (**Figure 2.7C**). These data suggest that upregulation of HH co-receptors is a phenomenon observed in human pancreatic cancer and recapitulated in mouse models of this disease.

Together, these data demonstrate that Gas1, Boc, and, Cdon are expressed in fibroblasts in both normal and PanIN-bearing pancreata and that their expression increases during pancreatic tumorigenesis as activated fibroblasts accumulate in the pancreas. Notably, this expression pattern resembles that observed for Ptch1 in KC mice (28), thus placing these co-receptors in the same cell population previously reported to respond to HH signaling in pancreatic cancer.

GAS1 and BOC Mediate HH-responsiveness in Pancreatic Fibroblasts

GAS1, BOC and CDON promote HH signaling in the developing neural tube in a ligand-dependent manner (19). To determine whether these co-receptors are required to transduce HH signals in fibroblasts, we generated wildtype and *Gas1*$^{-/-}$*;Boc*$^{-/-}$ mouse

embryonic fibroblasts (MEFs) and treated them with control or SHH conditioned medium. The cells were harvested 48 hours after treatment and analyzed for HH target gene expression (*Gli1* and *Ptch1*). We found significantly attenuated, although measurable levels of *Gli1* and *Ptch1* expression in SHH-CM treated *Gas1*$^{-/-}$*;Boc* $^{-/-}$ MEFs compared to wildtype MEFs (**Figure 2.8A**).

Activation of HH signaling in fibroblasts has been reported to promote tumor growth in co-transplantation experiments (8). Thus, we predicted that *Gas1*$^{-/-}$*;Boc*$^{-/-}$ MEFs would display reduced tumor-promoting ability compared to wildtype MEFs. To test this hypothesis, we co-injected the human pancreatic cancer cell lines Hs766T and MiaPaCa with either wildtype or *Gas1*$^{-/-}$*;Boc*$^{-/-}$ MEFs in immune compromised mice (**for schematic, see Figure 2.8B**). Surprisingly, tumor cells co-injected with *Gas1*$^{-/-}$*;Boc*$^{-/-}$ MEFs grew significantly larger than tumor cells injected alone or co-injected with wildtype MEFs (**Figures 2.8C and 2.8D**). Analysis of these tumors revealed comparable epithelial histology for all experimental cohorts, including the accumulation of a collagen-rich stroma (**Figure 2.9A**). However, blood vessel density was dramatically increased in tumors co-injected with *Gas1*$^{-/-}$*;Boc*$^{-/-}$ MEFs compared to tumor cells alone or co-injected with wildtype MEFs (**Figures 2.9A and 2.9B**).

To study this phenomenon in a more physiologically relevant system, we replaced MEFs with primary pancreatic fibroblasts isolated from either wildtype or *Gas1*$^{-/-}$*;Boc*$^{-/-}$ E18.5 mouse embryos (**Figure 2.10A**). Despite the perinatal lethality of *Gas1*$^{-/-}$*;Boc*$^{-/-}$ embryos (19), histological analysis of E18.5 pancreata revealed no gross abnormalities (data not shown). To assess HH-responsiveness, we treated wildtype

and *Gas1*$^{-/-}$;*Boc*$^{-/-}$ pancreatic fibroblasts with control or SHH-conditioned media and extracted RNA 24 hours later. Similar to the MEF lines, SHH treatment induced robust expression of both *Gli1* and *Ptch1* in wildtype pancreatic fibroblasts, whereas this response was significantly attenuated in *Gas1*$^{-/-}$;*Boc*$^{-/-}$ pancreatic fibroblasts (**Figure 2.10A**). Thus, HH co-receptors are required for normal HH signaling in both MEFs and pancreatic fibroblasts.

We then repeated subcutaneous co-injection experiments of tumor cells and fibroblasts, this time using pancreatic fibroblasts instead of MEFs and primary human pancreatic tumor cells (1319; (29,30)) instead of human pancreatic tumor cell lines. 1319 cells were injected alone or in combination with either genotype of pancreatic fibroblasts into mice. Notably, 1319 cells express *SHH* in culture at levels comparable to Hs766T cells (**Figure 2.10B**). Injection of 1319 cells alone formed subcutaneous tumors that were larger upon co-injection with wildtype fibroblasts, as expected (**Figure 2.11A**) (8). However, co-injection with *Gas1*$^{-/-}$;*Boc*$^{-/-}$ pancreatic fibroblasts resulted in even larger tumors (**Figure 2.11A**). Tumor histology from each cohort was similar as assessed by H&E and Gomori staining, with a marked ductal morphology and abundant stroma, thus resembling the most common histology of human pancreatic cancer (**Figure 2.11B**) (31). However, CD31 immunostaining revealed a dramatic increase in vasculature within tumors co-injected with *Gas1*$^{-/-}$;*Boc*$^{-/-}$ pancreatic fibroblasts (**Figures 2.11C and 2.11D**). The *Gas1*$^{-/-}$;*Boc*$^{-/-}$ fibroblasts were detected in close association with blood vessels, as determined by β-gal immunostaining (**Figure 2.11D**). Thus, stromal deletion of *Gas1* and *Boc*, tested in both MEFs and pancreatic fibroblasts, results in

attenuated HH-responsiveness that paradoxically increases tumor growth. Given the heterogeneity of stromal fibroblasts (27), these *Gas1* and *Boc* expressing fibroblasts may represent a subset of cells in which HH ligands inhibit an angiogenic response.

Dosage-dependent Stromal HH Signaling Differentially Promotes Pancreatic Tumor Growth.

Our data contrast with previous studies in which SMO blockade in the stroma inhibits pancreatic tumor growth (8,32). Notably, despite the significantly reduced response to HH signaling in *Gas1*$^{-/-}$*;Boc*$^{-/-}$ fibroblasts, these cells are not completely refractory to HH pathway stimulation (**Figure 2.8A and 2.10A**). One possibility is that the level of HH pathway activation differentially affects pancreatic tumor growth.

To understand the relationship between HH signaling dosage and tumor promotion, we tested *Gas1*$^{-/-}$*Boc*$^{-/-}$*;Cdon*$^{-/-}$ MEFs. Of note, we could not use pancreatic fibroblasts as triple null embryos die at E9.5 (19) at the onset of pancreas development. *Gas1*$^{-/-}$*Boc*$^{-/-}$*;Cdon*$^{-/-}$ MEFs had nearly undetectable activation of HH target genes when exposed to SHH conditioned medium (**Figure 2.12A**). We co-transplanted human pancreatic 1319 tumor cells alone, or with three different cohorts of MEFs: wildtype, *Gas1*$^{-/-}$*;Boc*$^{-/-}$ and *Gas1*$^{-/-}$*Boc*$^{-/-}$*;Cdon*$^{-/-}$ (**see schematic in Figure 2.12B**). Again, wildtype MEFs promoted tumor growth compared to tumor cells alone, and *Gas1*$^{-/-}$*;Boc*$^{-/-}$ MEFs promoted tumor growth further (**Figures 2.12C and 2.12D**). In contrast, tumors co-injected with *Gas1*$^{-/-}$*;Boc*$^{-/-}$*;Cdon*$^{-/-}$ MEFs were comparable both in growth rate and size at dissection to tumor cells alone (**Figure 2.12C and 2.12D**). These data are

consistent with the reduced tumor-promoting ability of *Smo*$^{-/-}$ MEFs that are completely refractory to HH stimulation (8).

Although tumor size varied between the different experimental groups, the histology was similar, with ductal structures surrounded by collagen rich stroma (**Figure 2.13A**). Cell death was similar in all experimental cohorts (**Figure 2.13B**), however we detected increased intratumoral proliferation in co-injections with tumor cells and *Gas1*$^{-/-}$*;Boc*$^{-/-}$ MEFs; this effect was abrogated in co-injections with *Gas1*$^{-/-}$*;Boc*$^{-/-}$*;Cdon*$^{-/-}$ MEFs (**Figure 2.13C**).

To verify that the co-injected MEFs persisted within the tumor at the time of analysis, we took advantage of lineage tracing provided by the expression of the β-gal reporter from the *Gas1* locus in these cells. By β-gal staining and quantitation we detected that both double and triple knock-out cells were present within the tumors (**Figure 2.14A**). Notably, the level of *SHH* ligand, produced by the tumor cells (detected with human-specific primers and normalized to human *CYCLOPHILIN*) did not change among the different groups (**Figure 2.14B**).

Genetic inactivation of Shh in multiple mouse models of pancreatic cancer resulted in variable reduction of stroma accumulation in different settings (33,34). To further investigate potential changes to the stroma in our model, we quantified the relative ratio of mesenchymal cells within the tumors (identified by immunostaining for Vimentin), and observed no measurable change (**Figures 2.15A and 2.15B**). Furthermore, RT-qPCR analysis for *Collagen I* revealed no difference among the

different cohorts (**Figure 2.15C**), indicating no changes in fibrosis. The differences between the two experimental groups might derive from the different timing of HH pathway alteration. Interestingly, analysis of pre- and post-treatment biopsies of liver metastases in a recent clinical trial of the HH inhibitor GDC-0449 revealed only a mild reduction of fibrosis in half the patients, and no changes in fibrosis in the other half, consistent with our findings (Dr. Diane Simeone, University of Michigan, personal communication).

While the accumulation of fibroblasts within the stroma did not change, the number of blood vessels was significantly increased in tumors co-injected with *Gas1*$^{-/-}$*;Boc*$^{-/-}$ MEFs but not in tumors co-injected with *Gas1*$^{-/-}$*;Boc*$^{-/-}$*;Cdon*$^{-/-}$ MEFs compared with control, as quantified by CD31 immunostaining (**Figures 2.16A and 2.16B**). A similar increase in vasculature was previously observed following genetic ablation of *Shh* or following drug-mediated inhibition of SMO, although the mechanism remained to be investigated (32-34). Thus, reduced HH response promotes tumor vascularity and growth, whereas complete HH pathway blockade fails to promote tumor vascularity and growth.

Reduced HH Signaling Promotes Angiogenesis.

To determine the mechanism by which reduced HH signaling promotes tumor growth and vascularity, we measured the expression of several angiogenic factors by RT-qPCR (**Figures 2.17A and 2.17B**). Along with VEGFa, the angiopoietins (ANGPT1 and ANGPT2) encompass a family of factors that act on the vascular endothelium (35).

In both *Gas1*$^{-/-}$*;Boc*$^{-/-}$ MEFs and pancreatic fibroblasts, *Angpt2* was upregulated compared to control pancreatic fibroblasts and MEFs respectively; in contrast, *Angpt2* expression in *Gas1*$^{-/-}$*;Boc*$^{-/-}$*;Cdon*$^{-/-}$ MEFs was comparable to wildtype MEFS (**Figures 2.17A and 2.17B**). The expression of other angiogenic factors varied between MEFs and pancreatic fibroblasts, although in all cases, reduced HH signaling resulted in increased expression of angiogenic factors, while the abrogation of HH signaling inhibited angiogenic gene expression (**Figures 2.17A and 2.17B**). For example, *Angpt1* expression was significantly upregulated in *Gas1*$^{-/-}$*;Boc*$^{-/-}$ pancreatic fibroblasts (**Figure 2.17A**), while *Vegfa* , previously described as a HH target in stromal perivascular cells (36) was upregulated in *Gas1*$^{-/-}$*;Boc*$^{-/-}$ MEFs (**Figure 2.17B**). The specific gene programs activated were not identical, possibly indicating distinct properties of fibroblasts of different origins.

To determine whether the change in expression of the angiogenic factors depended on ligand-mediated HH signaling, we treated wildtype or *Gas1*$^{-/-}$*;Boc*$^{-/-}$ pancreatic fibroblasts with control-conditioned medium or SHH-conditioned medium. SHH treatment induced expression of *Vegfa* and *Angpt1*, while repressing expression of *Angpt2* (**Figure 2.18A**) consistent with previous publications (Lee et al., 2007; Zhang et al., 2011). The induction of *Vegfa* and overall expression levels were similar in *Gas1*$^{-/-}$*;Boc*$^{-/-}$ pancreatic fibroblasts. In contrast, both *Angpt1* and *Angpt2* had higher basal expression levels in *Gas1*$^{-/-}$*;Boc*$^{-/-}$ pancreatic fibroblasts, but the extent of relative induction or repression in response to SHH was reduced compared to wildtype

fibroblasts, indicating that both ligand-dependent and ligand-independent mechanisms regulated the expression of these angiogenic factors (**Figures 2.18A and 2.18B**).

To further dissect the angiogenic properties of fibroblasts lacking *Gas1* and *Boc*, we used the chick chorioallantoic membrane (CAM) assay. *Gas1*$^{-/-}$*;Boc*$^{-/-}$ pancreatic fibroblasts and MEFs implanted alone atop the CAM induced the formation of more blood vessels than wildtype MEFs. Notably, this pro-angiogenic effect was not detected in *Gas1*$^{-/-}$*;Boc*$^{-/-}$*;Cdon*$^{-/-}$ MEFs (**Figure 2.18C**).

We next co-implanted human pancreatic 1319 tumor cells with wildtype or *Gas1*$^{-/-}$*;Boc*$^{-/-}$ pancreatic fibroblasts. Wildtype fibroblasts promoted tumor growth in CAM assays, in agreement with our observations in the mouse (**Figures 2.19A and 2.19B**). Again, *Gas1*$^{-/-}$*;Boc*$^{-/-}$ pancreatic fibroblasts promoted the growth of even larger, more vascularized tumors (**Figures 2.19A and 2.19B**). Similar results were obtained using a primary mouse pancreatic cancer cell line (30) derived from the KPC (7) pancreatic cancer model (**Figure 2.19C)**.

We then tested *Gas1*$^{-/-}$*;Boc*$^{-/-}$*;Cdon*$^{-/-}$ MEFs in this assay and observed reduced tumor growth and vascularization (**Figures 2.19D and 2.19E**), indicating that tumor promotion and angiogenesis are specifically linked to the degree of HH-responsiveness. Similar to the subcutaneous tumor injections, *Gas1*$^{-/-}$*;Boc*$^{-/-}$*;Cdon*$^{-/-}$ fibroblasts did not impact tumor growth compared to tumor cells alone (**Figures 2.19D and 2.19E**).

Discussion

The Hedgehog co-receptors GAS1, BOC and CDON are required to mediate HH signaling during embryonic development (19), but their potential role in adult tissues and in disease remained largely unexplored. Here, we show that these co-receptors are expressed in pancreatic cancer (**Figures 2.1 and 2.7**) and modulate the levels of HH-responsiveness in pancreatic fibroblasts (**Figures 2.18A, 2.10A and 2.12A**). Despite initial expectations that fibroblasts with reduced HH-responsiveness would be impaired in their ability to support tumor growth, surprisingly, we found that these cells promoted tumor growth to a significantly greater extent than wildtype fibroblasts (**Figures 2.8 and 2.11**). Although HH pathway inhibition showed promise in mouse models of pancreatic cancer (32), clinical trials in humans were unsuccessful (37). Treatment with HH inhibitors in human patients are likely to result in a strong reduction, but not complete inactivation, of HH signaling, since the drugs are continuously metabolized and excreted in between doses. Here we show that HH dosage is a key consideration in cancer treatment, where reduced levels of HH signaling evoke a potent angiogenic response (**Figure 2.20**). Thus, an angiogenic response might constitute a clinical readout of successful, but partial, HH blockade in vivo. While dosage-specific HH response has not been considered in cancer, developmental biology provides ample evidence of HH target genes activated at specific thresholds of signaling (for review, see (38)). Further, although angiogenic blockade has not been used in pancreatic cancer due to its hypovascularity, our results raise the possibility that HH pathway blockade in pancreatic cancer may render tumors susceptible to anti-angiogenic therapy. A recent study

indicates a possible benefit of this combination therapy on a mesenchymal subtype of pancreatic cancer in genetically engineered mice (34). Whether the failure of the recent HH inhibition trials in pancreatic cancer are due to an increase in angiogenesis should be investigated.

Another aspect of interest is the finding that MEFs and pancreatic fibroblasts have differences in HH-mediated gene regulation. The differences among fibroblasts populations in different organs are poorly understood, and might play an important role in cancer treatment, as fibroblasts at the metastatic sites might respond differently to treatment compared to fibroblasts at the primary site. HH signaling has been associated with pancreatic cancer metastasis (39), indicating the need for further studies aimed at characterizing HH response in fibroblasts derived from the pancreas and from common metastatic sites (such as liver and lung).

Acknowledgements

We thank Drs. Diane Simeone, Meghna Waghray, Lidong Wang, and Ethan Abel (University of Michigan) for providing the 1319 human primary tumor cells, providing human sample RNA, and sharing unpublished data. We thank Dr. Chandan Kumar (University of Michigan) for sharing his expertise on publicly available gene-expression datasets. We also thank Dr. Andrew Rhim and Dr. Angelina Londono-Joshi (University of Michigan) for sharing unpublished data. We thank Dr. Deb Gumucio for critical reading of the manuscript. This project was supported by the University of Michigan Biological Sciences Scholar Program, the University of Michigan Comprehensive

Cancer Center, NCI-1R01CA151588-01 to Marina Pasca di Magliano (MPdM) and 1R21CA167122-01 to Ben Allen and Marina Pasca di Magliano. Esha Mathew was supported by a University of Michigan Program in Cellular and Molecular Biology training grant (NIH T32 GM007315) and a University of Michigan Gastrointestinal Training Grant (NIH T32 DK094775). Alexander Holtz was supported by a University of Michigan Program in Cellular and Molecular Biology training grant (NIH T32 GM007315) and an NIH predoctoral fellowship (F31 NS081806). Ben Allen was supported by an American Heart Association Scientist Development Grant (11SDG6380000).

Figures

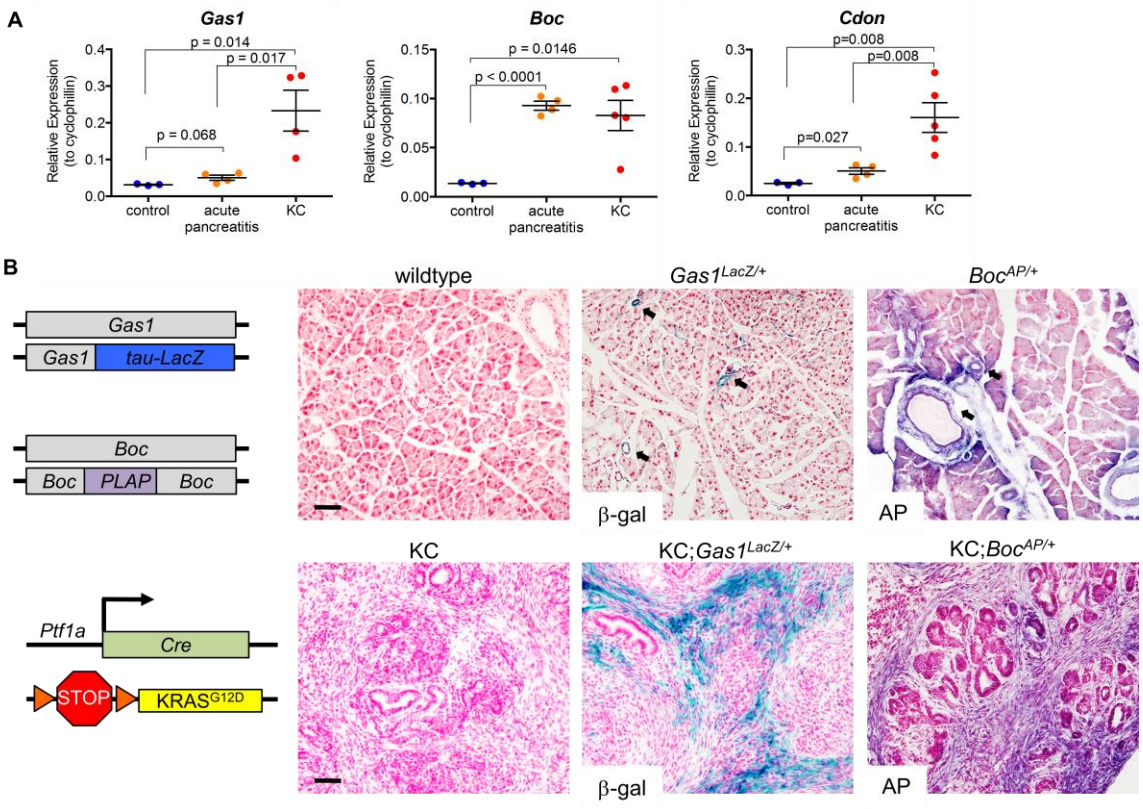

Figure 2.1: Gas1, Boc, and Cdon are expressed in the normal and neoplastic pancreas

(A) RT-qPCR analysis for *Gas1, Boc, and Cdon* in control (n=3), acute pancreatitis (n=4), and KC pancreata 3 wk following caerulein-induced pancreatitis (n=5). (B) Schematic of Gas1 and Boc reporter strains and KC model (left panels). Beta-galactosidase (β-gal) and Alkaline Phosphatase (AP) staining for Gas1 and Boc reporter expression in normal and neoplastic pancreata (right panels). Scale bars, 50μm.

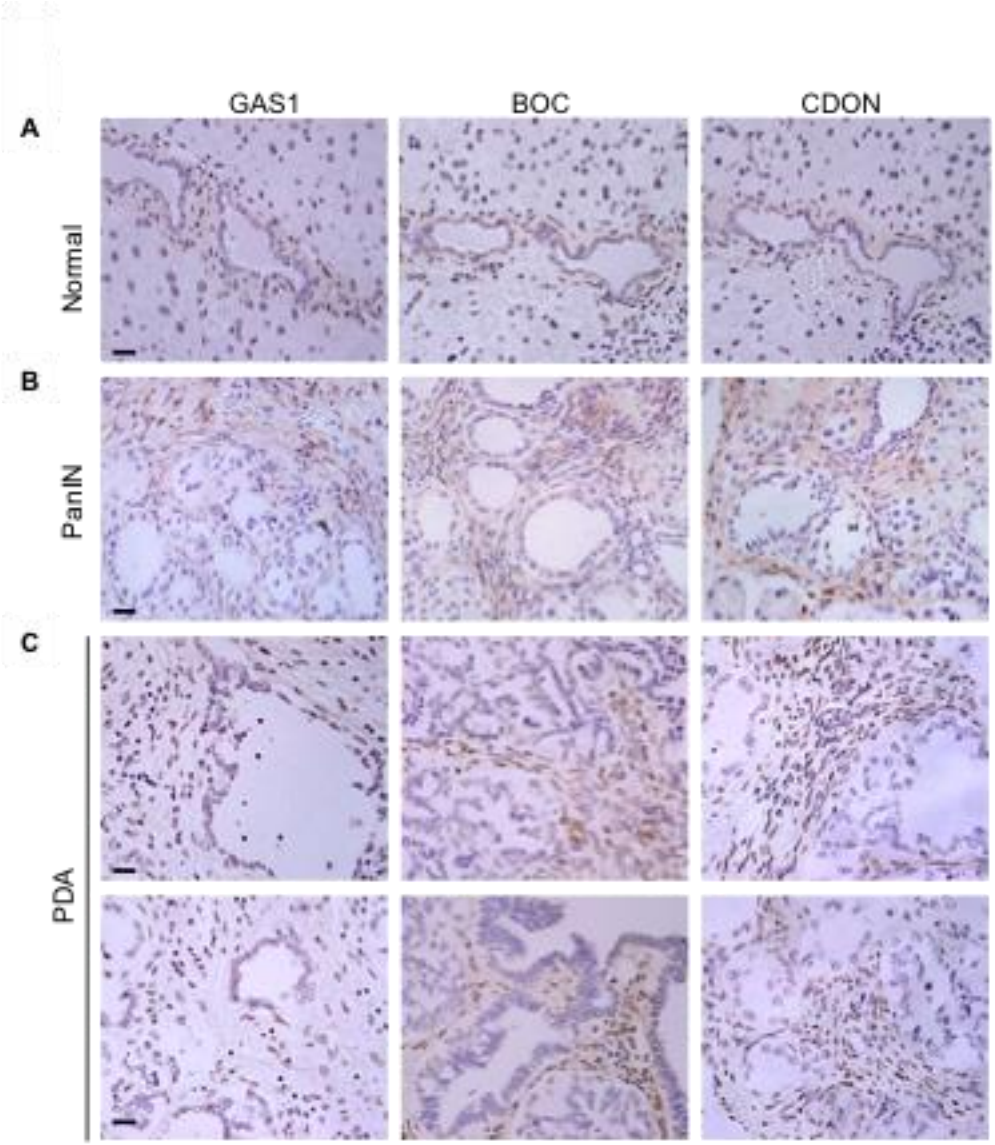

Figure 2.2: GAS1, BOC, and CDON are expressed in the normal and neoplastic pancreas

Antibody detection of GAS1, BOC, and CDON in (A) normal pancreas from wildtype mice, (B) PanIN-bearing pancreas from KC mice 3 weeks following caerulein-induced pancreatitis, or (C) tumor bearing mouse pancreata from KPC mice. Scale bars, 20μm.

(Data/Image Credit: Dr. Yaqing Zhang)

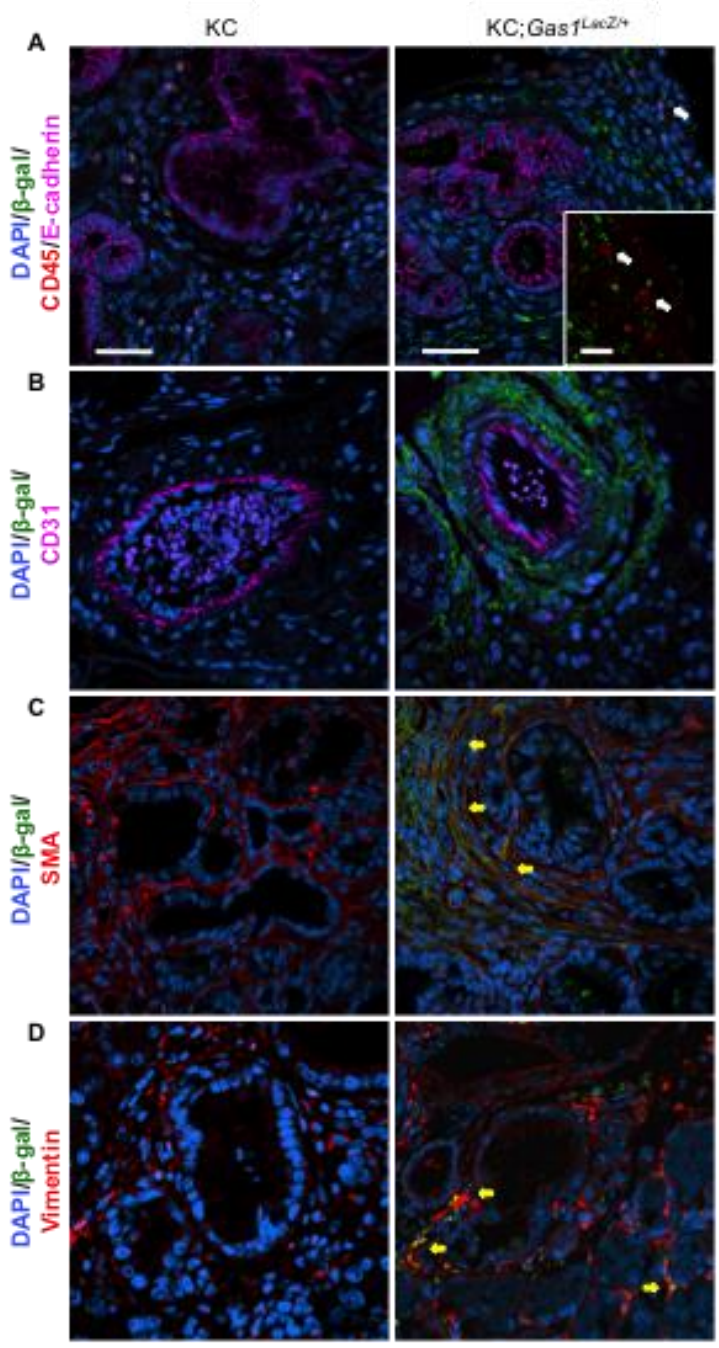

Figure 2.3: Gas1 is co-expressed with SMA and Vimentin in the neoplastic pancreas

Antibody detection of *Gas1*$^{LacZ/+}$ β-gal (green) and (A) CD45/E-cadherin (red/magenta), (B) CD31 (magenta), (C) SMA (red), and (D) Vimentin (red) in KC and KC;*Gas1*$^{LacZ/+}$ PanIN lesions. DAPI (blue) marks nuclei. White arrows indicate separate β-gal and CD45 expression; yellow arrows indicate co-expression of β-gal with SMA and Vimentin. Scale bar, 20μm.

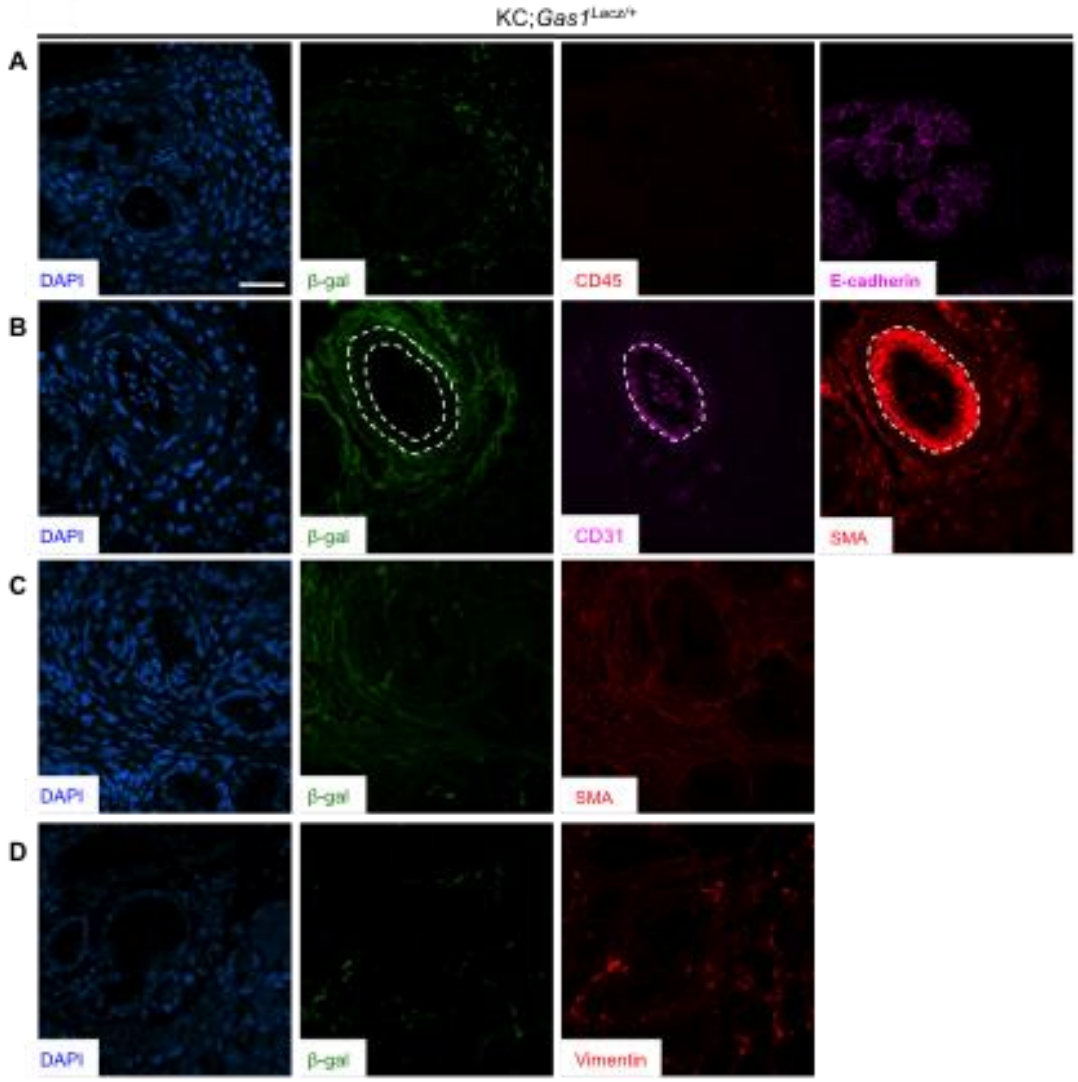

Figure 2.4: Gas1 is expressed by fibroblasts in the neoplastic pancreas

Individual channel images of (A) DAPI (blue), β-gal (green), CD45 (red), and E-cadherin (magenta); (B) DAPI (blue), β-gal (green), CD31 (magenta), and SMA (red); (C) DAPI (blue), β-gal (green), and SMA (red); and (D) DAPI (blue), β-gal (green), and Vimentin (red) in KC;*Gas1*$^{LacZ/+}$ PanIN lesions. Scale bar, 20μm

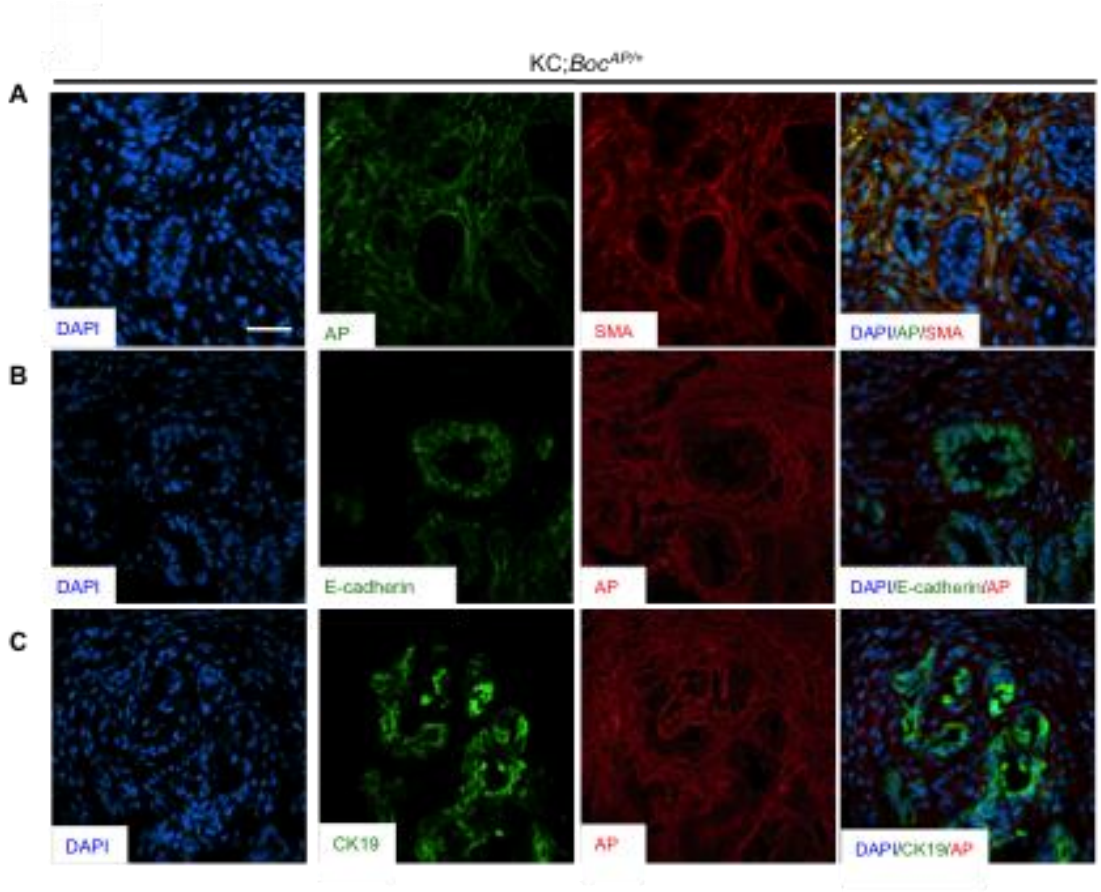

Figure 2.5: Boc is expressed by fibroblasts in the neoplastic pancreas

Individual channel images of (A) DAPI (blue), AP (green) and SMA (red). (B) DAPI (blue), E-cadherin (green) and AP (red); and (C) DAPI (blue), CK19 (green) and AP (red) in KC;*Boc*$^{PLAP/+}$ PanIN lesions. Scale bar, 20μm.

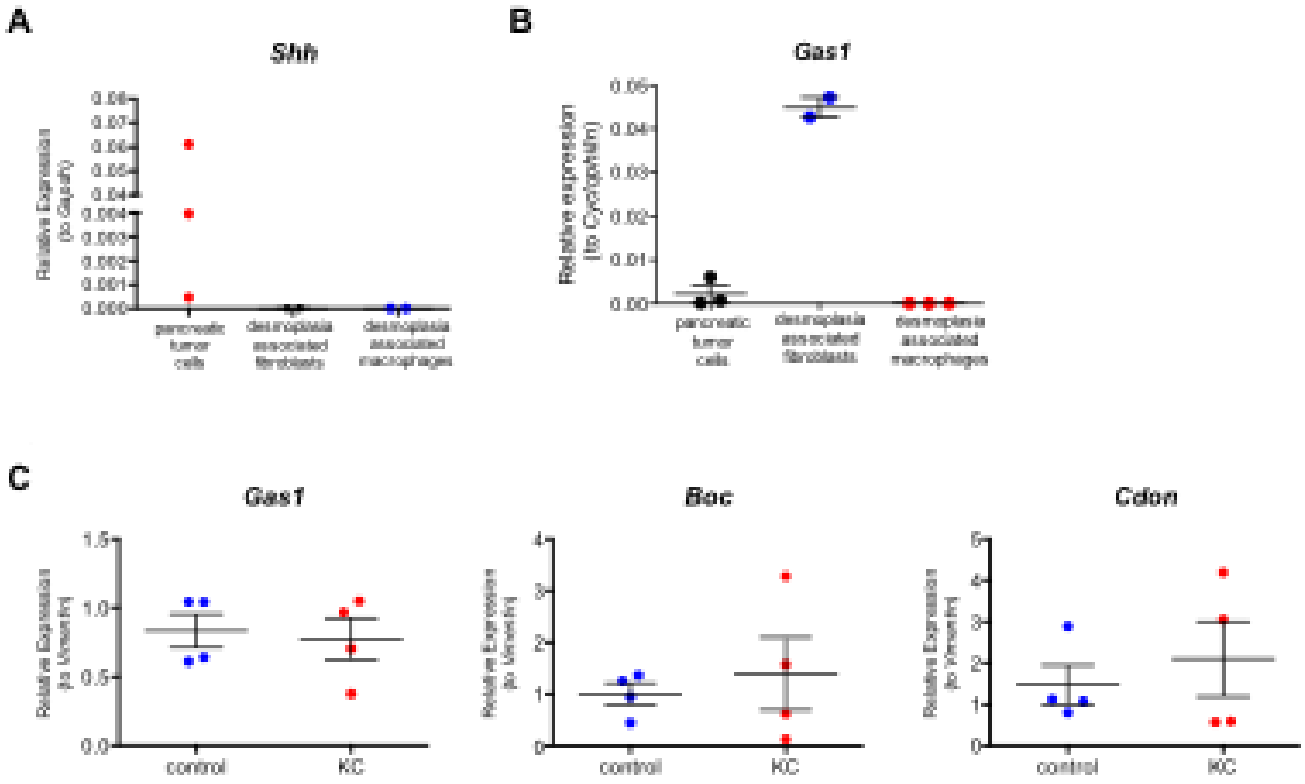

Figure 2.6: Shh expression is restricted to the pancreatic tumor cells, whereas HH co-receptor expression is restricted to fibroblasts

(A) *Shh* expression in mouse pancreatic tumor cells, fibroblasts and flow cytometry-isolated $CD11b^{+};F4/80^{+}$ macrophages. (B) *Gas1* expression in mouse pancreatic tumor cells, fibroblasts, and flow cytometry-isolated $CD11b^{+};F4/80^{+}$ macrophages. (C) RT-qPCR analysis of *Gas1*, *Boc*, and *Cdon* normalized to *Vimentin* expression in control and KC pancreas.

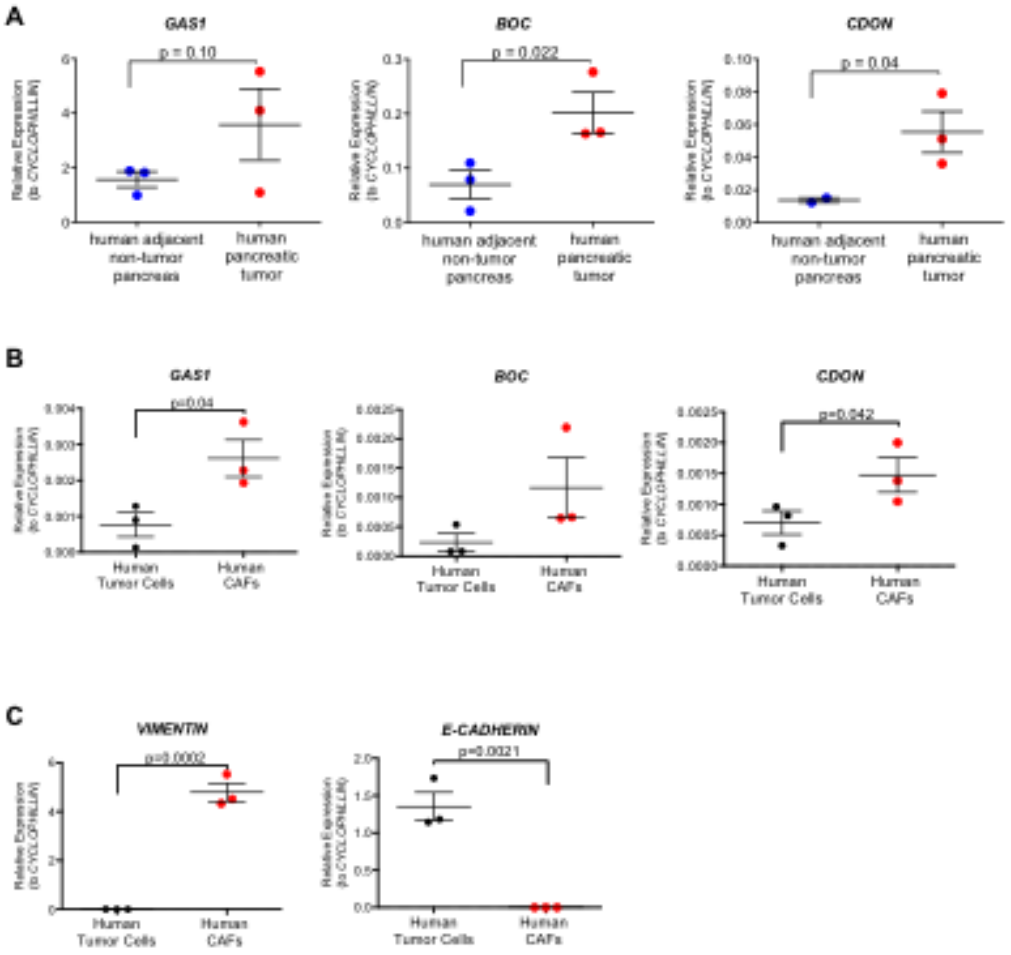

Figure 2.7: Gas1, Boc, and Cdon are expressed in human pancreatic cancer associated fibroblasts.

A) *GAS1*, *BOC* and *CDON* expression in human pancreatic tumor tissue, and adjacent, non-tumor pancreas. (B) RT-qPCR analysis of *GAS1*, *BOC* and *CDON* expression in primary human tumor cells and cancer associated fibroblasts (CAFs). (C) VIMENTIN and E-CADHERIN expression in primary human tumor cells and human CAFs.

cDNA from human tumor samples and human tumor cells and CAFs generously provided by Dr. Diane Simeone

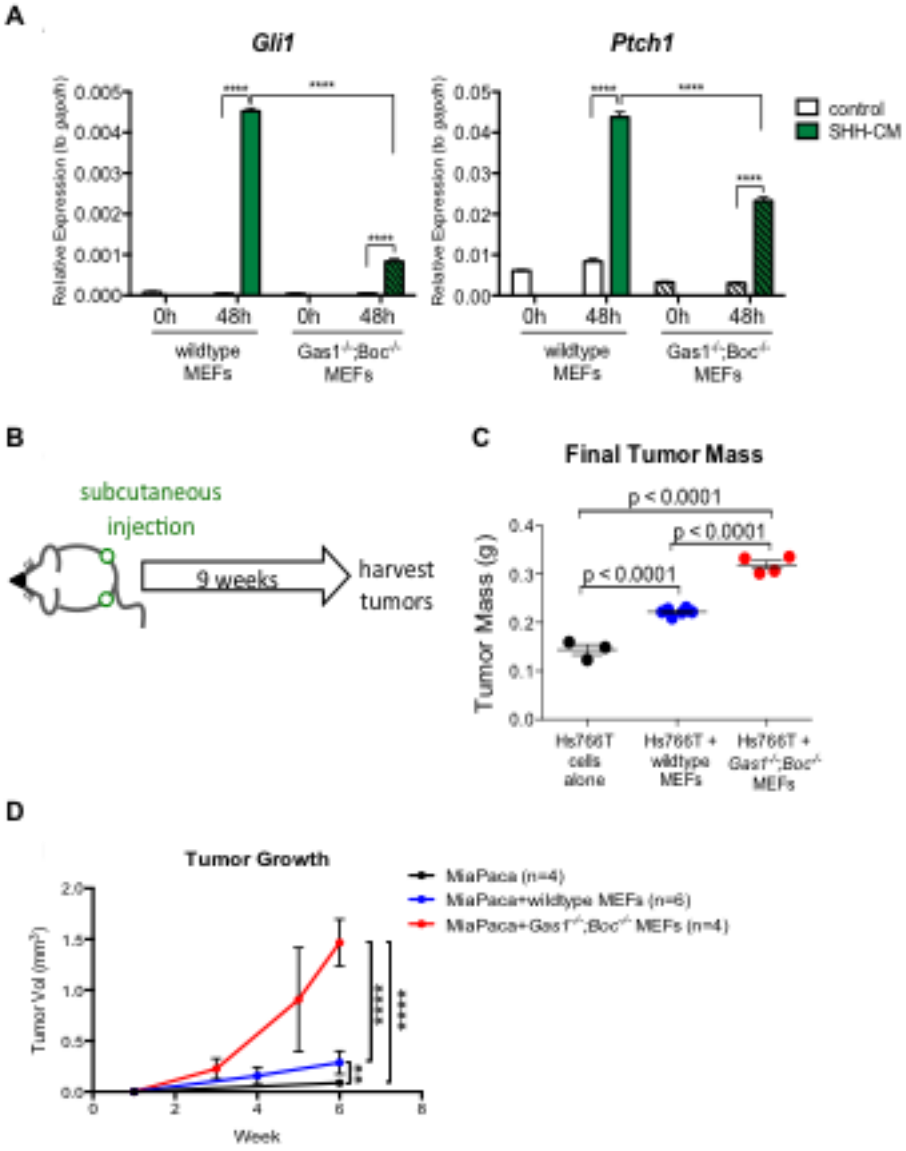

Figure 2.8: Stromal deletion of Gas1 and Boc impairs HH-responsiveness, but promotes tumor growth.

(A) RT-qPCR analysis of *Gli1* and *Ptch1* on SHH-stimulated MEFs. (B) Schematic of subcutaneous tumor injection experiment. (C) Quantitation of final tumor size in co-injection experiments of MEFs with Hs766T human tumor cell line. (D) Tumor growth curve for co-injection experiments of MEFs with MiaPaca human tumor cell line.

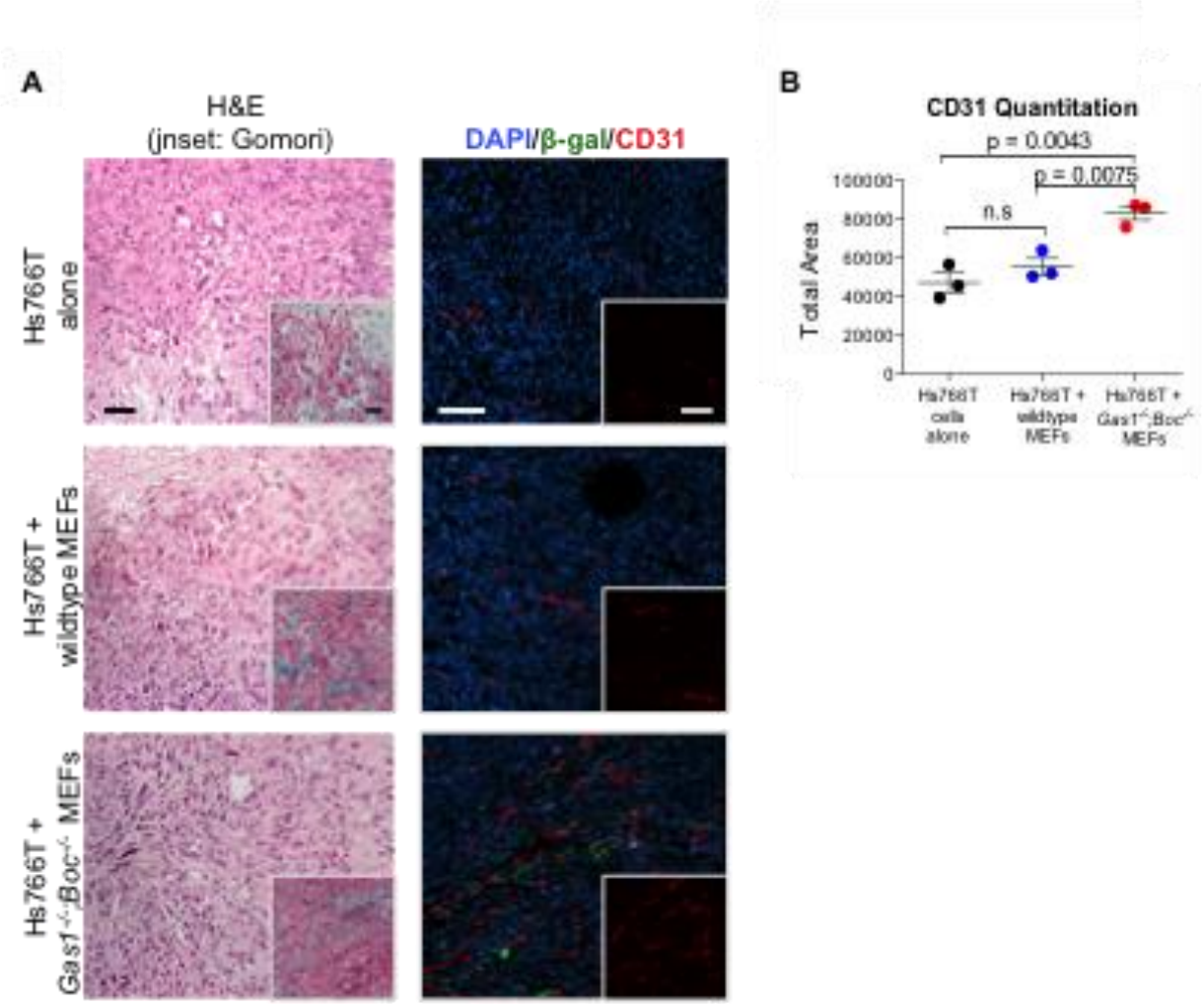

Figure 2.9: Stromal deletion of Gas1 and Boc impairs promotes the growth of large, vascularized tumors

(A) Histopathological analysis of tumors following co-injection of Hs766T cells with MEFs. Scale bar, 50μm, inset scale bar 50μm. H&E staining (left panels) and Gomori trichrome (inset, left panels). Antibody detection of β-gal (green) and CD31 (red); right panels). DAPI (blue) marks nuclei. Scale bar 50μm, inset scale bar 50μm. (B) Quantitation of CD31 staining.

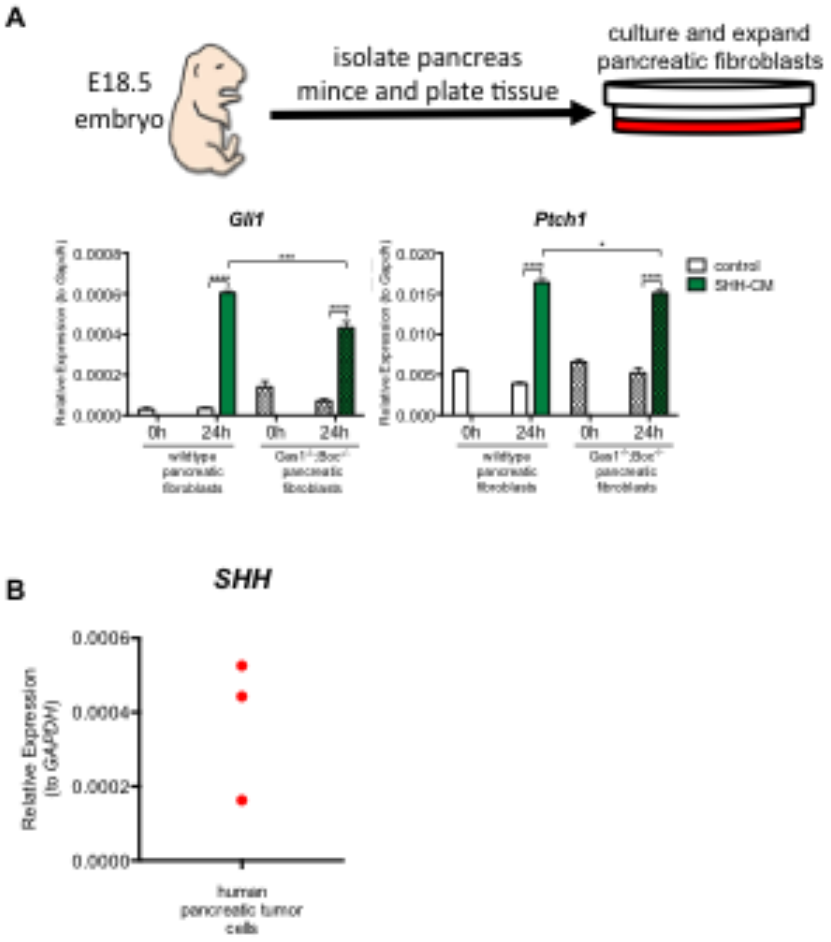

Figure 2.10: *Gas1*$^{-/-}$*;Boc*$^{-/-}$ pancreatic fibroblasts have impaired HH-responsiveness, similarly to MEFs.

(A) Schematic of pancreatic fibroblast isolation. RT-qPCR analysis of *Gli1* and *Ptch1* on SHH-stimulated pancreatic fibroblasts. (B) Expression of *SHH* in human pancreatic tumor cells; moving from highest expression to lowest: Hs766T human pancreatic tumor cell line, 1319 human pancreatic tumor primary cells, UM2 human pancreatic tumor primary cells.

1319 and UM2 primary human pancreatic cells generously provided by Dr. Diane Simeone

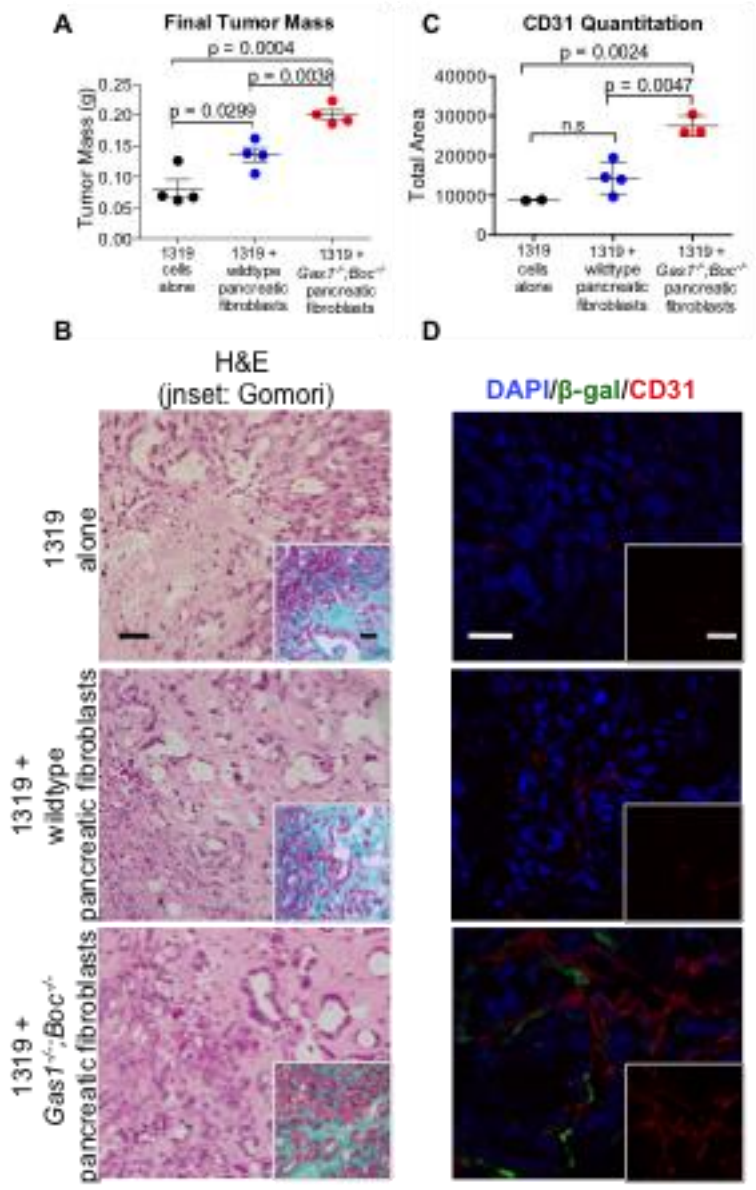

Figure 2.11: *Gas1*$^{-/-}$*;Boc*$^{-/-}$ pancreatic fibroblasts promote the growth of large, vascularized tumors.

(A) Quantitation of final tumor size in co-injection experiments with 1319 primary tumor cells human tumor cells with pancreatic fibroblasts. (B) Histopathological analysis of tumors following co-injections. H&E staining and Gomori trichrome (inset). Scale bar, 20μm, inset scale bar, 20μm. (C) Quantitation of CD31 staining. (D) Antibody detection of β-gal (green) and CD31 (red). DAPI (blue) marks nuclei. Scale bar, 20μm, inset scale bar 20μm.

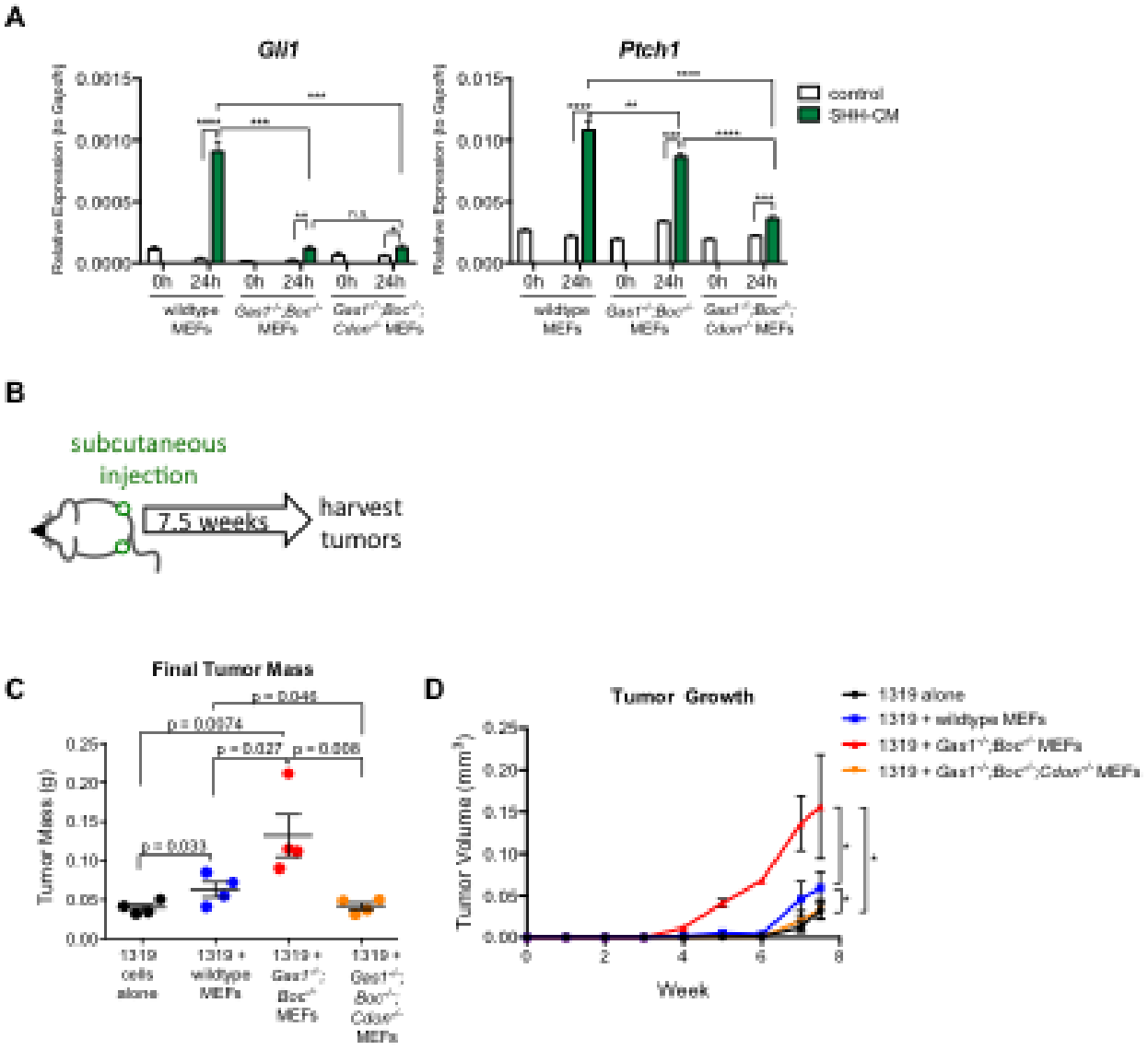

Figure 2.12: Dosage-dependant HH signaling differentially promotes pancreatic tumor growth.

(A) RT-qPCR analysis for *Gli1* and *Ptch1* on SHH-stimulated MEFs. (B) Schematic of subcutaneous tumor injection experiment. (C) Quantitation of final tumor size. (D) Growth curve for subcutaneous tumors.

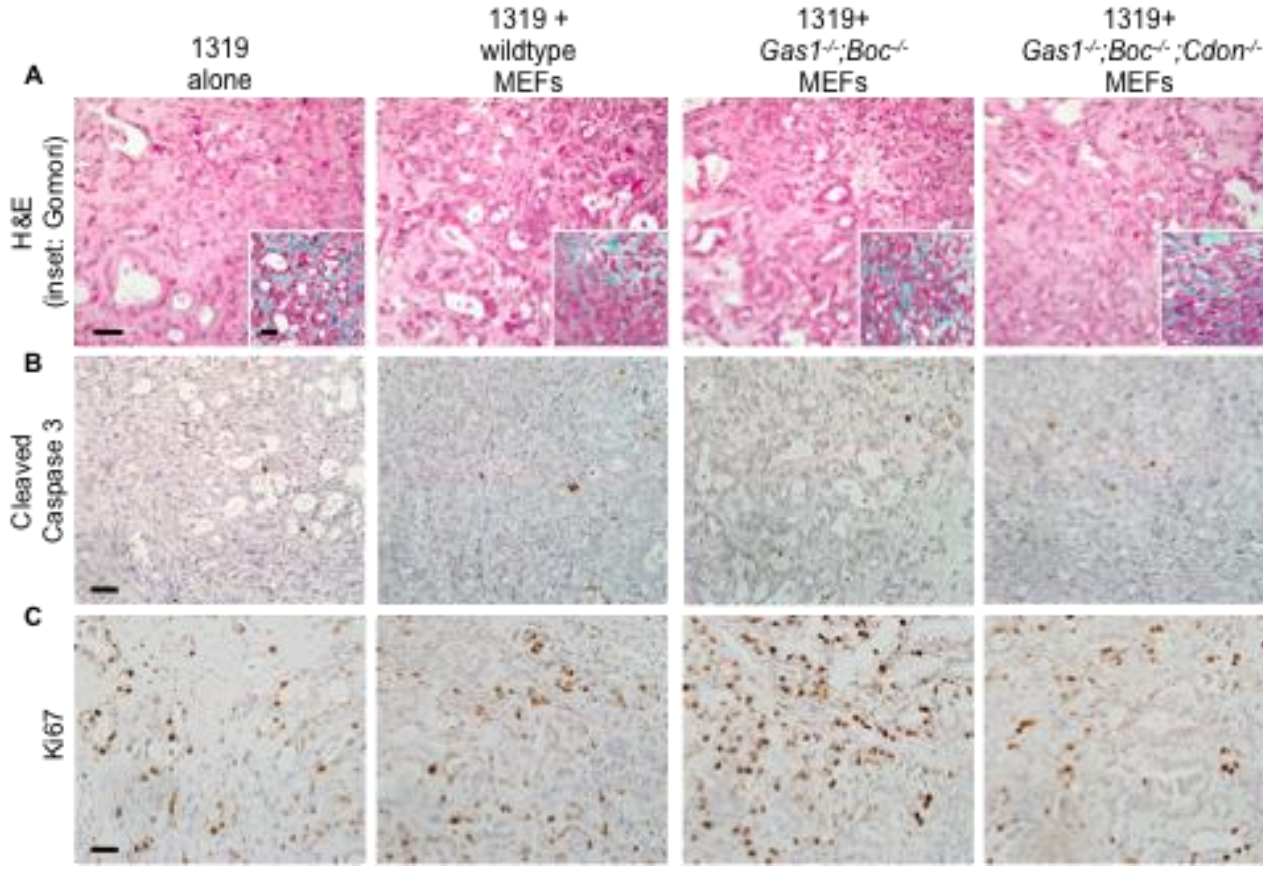

Figure 2.13: Dosage-dependant HH signaling differentially promotes pancreatic tumor proliferation.

(A) Histopathological analysis of tumors following co-injection of 1319 cells with MEFs. H&E staining and Gomori trichrome (inset). Scale bar, 20μm, inset scale bar 20μm. Antibody detection of (B) Cleaved Caspase 3 and (C) Ki67. Scale bar, 20μm.

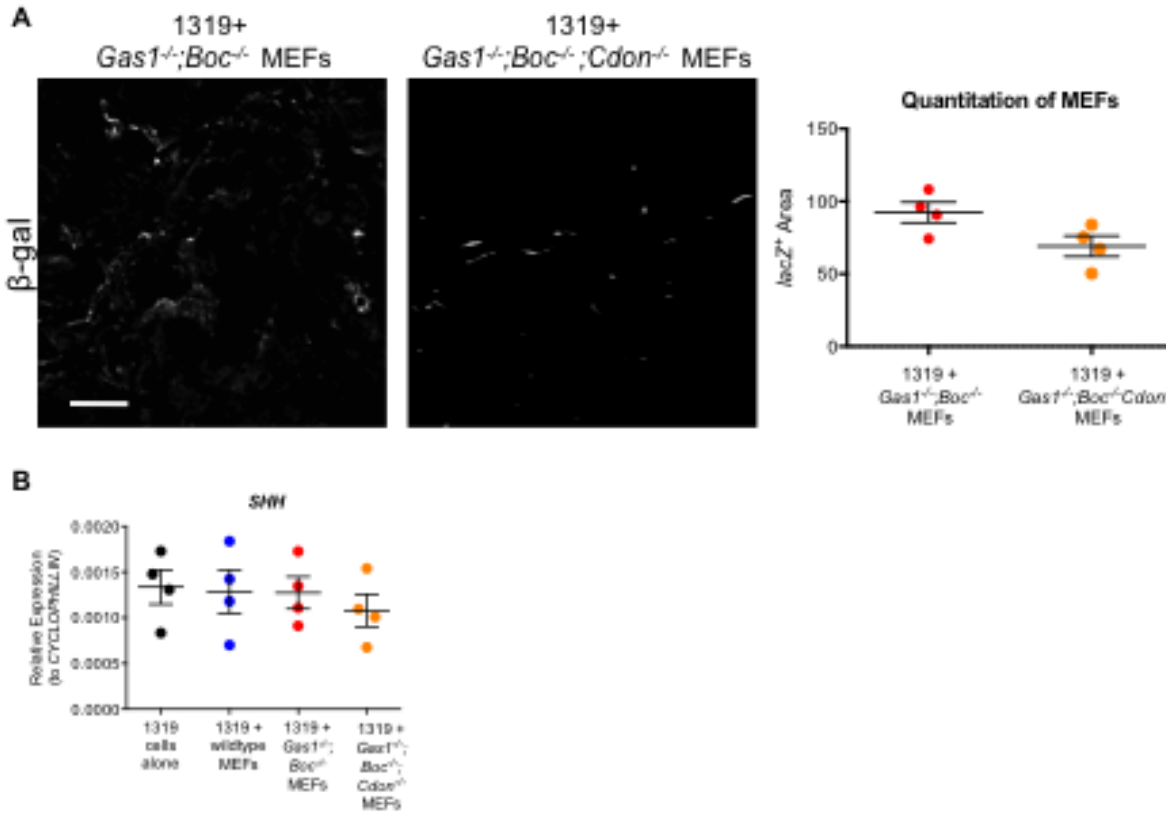

Figure 2.14: Co-injected fibroblasts and HH ligand expression persist in subcutaneous tumors.

(A) β-gal reporter expression in subcutaneous tumor cohorts. Scale bar, 20μm. Quantitation of β-gal staining. (B) RT-qPCR analysis of *SHH* in subcutaneous experiment cohorts with MEF lines

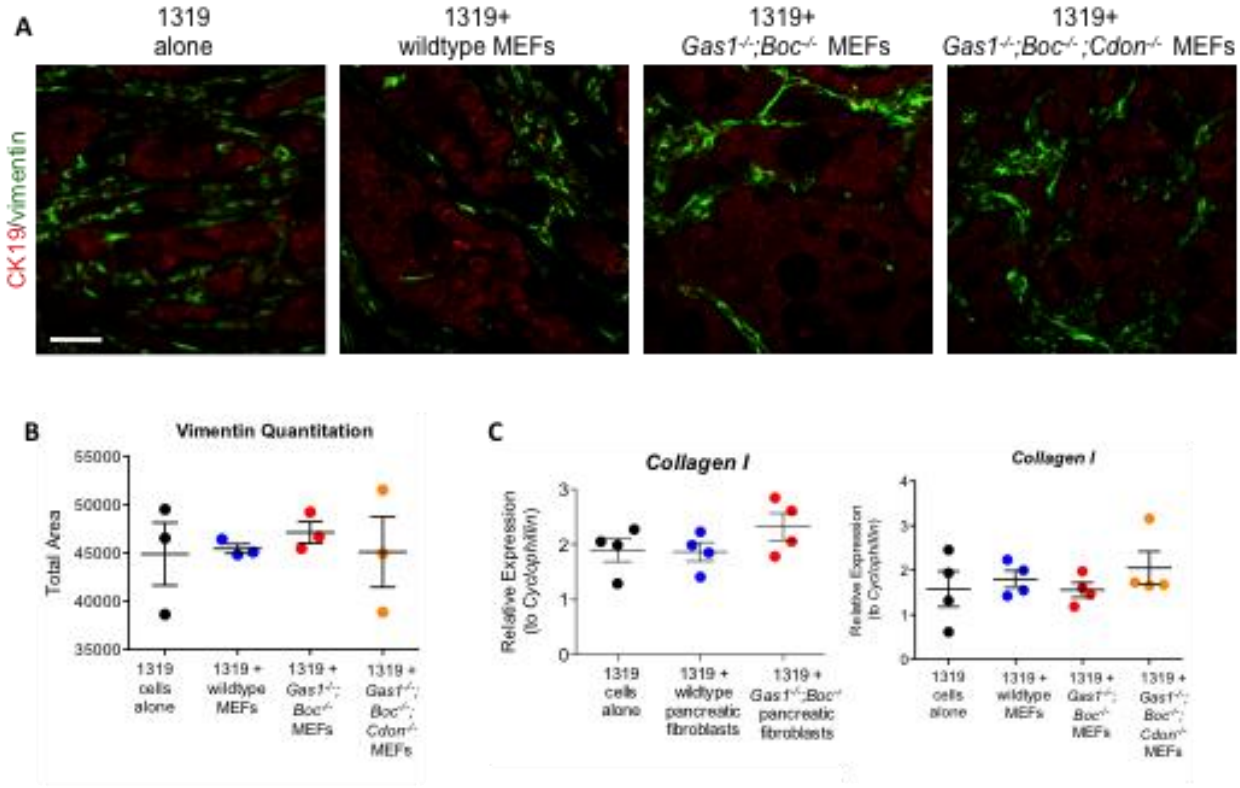

Figure 2.15: Dosage-dependent HH signaling does not affect ECM deposition.

(A) Antibody detection of Vimentin (green) and Ck19 (red) Scale bar, 20μm. (B) Quantitation of Vimentin staining. (C) RT-qPCR analysis of *Collagen I* expression in subcutaneous experiments with pancreatic fibroblasts (left graph) and MEFs (right graph).

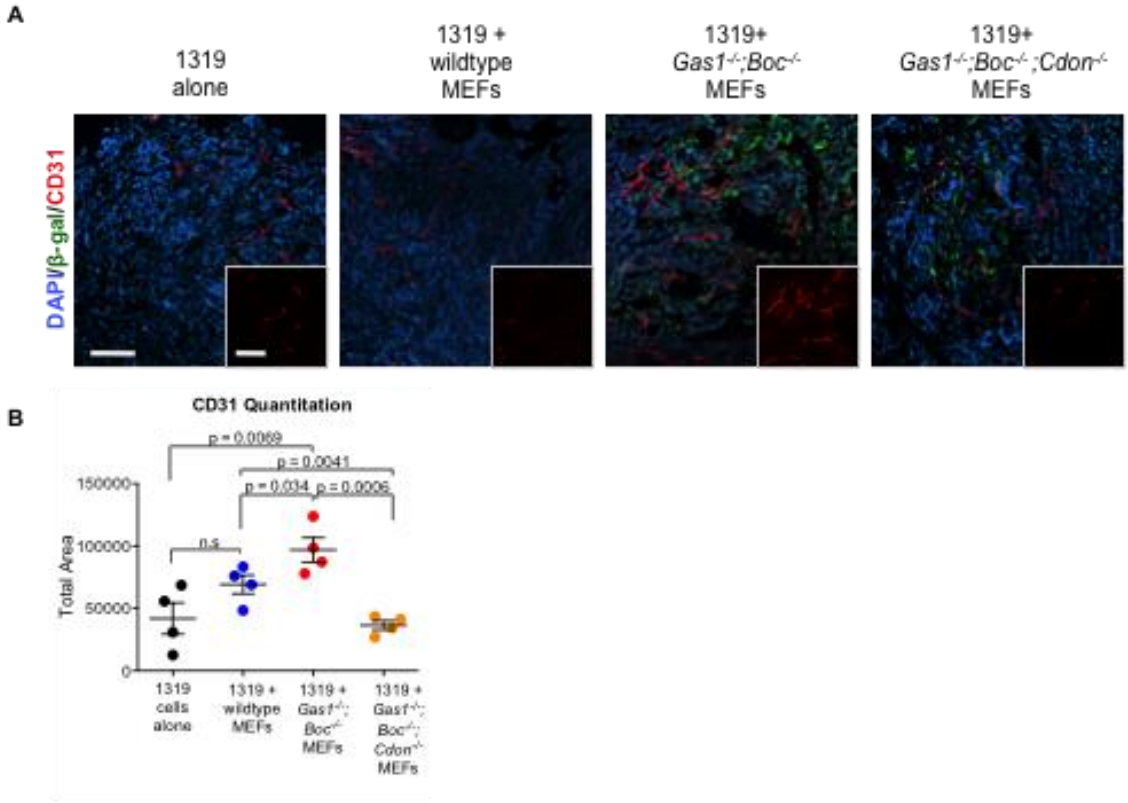

Figure 2.16: Dosage-dependant HH signaling differentially promotes pancreatic tumor vascularity.

(A) Antibody detection of β-gal (green) and CD31 (red) in tumor tissue following co-injection of 1319 cells with MEFs. DAPI (blue) marks nuclei. Scale bar 50μm, inset scale bar 50μm. (B) Quantitation of CD31 staining.

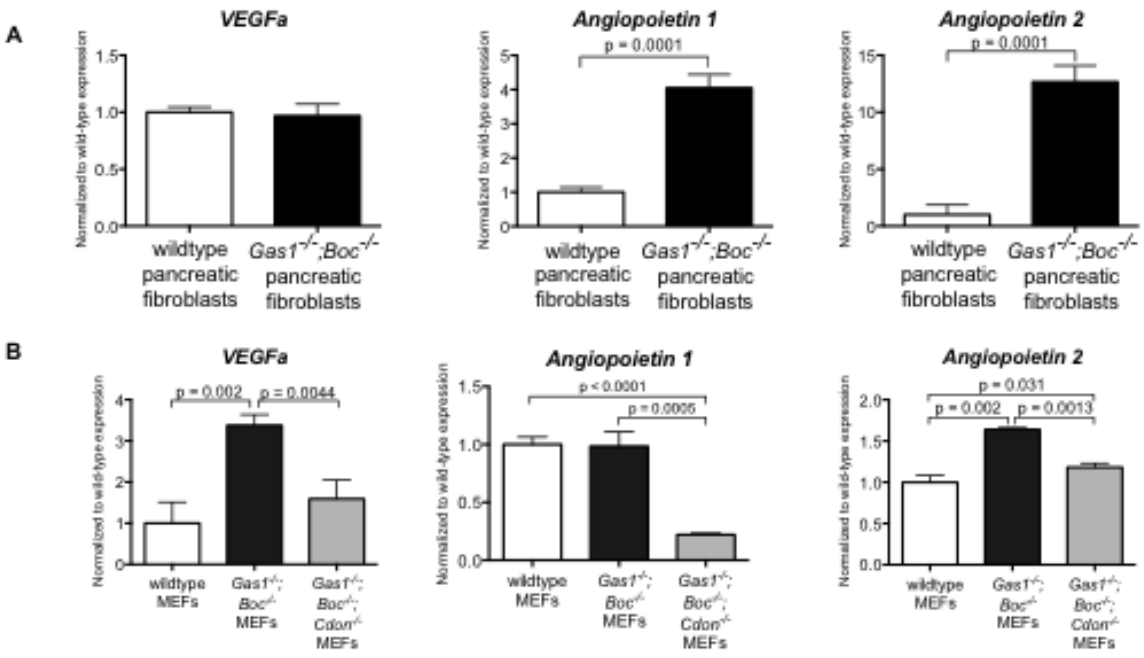

Figure 2.17: Differential expression of angiogenic factors in fibroblasts.

RT-qPCR analysis of *Vegfa*, *Anpgt1*, and *Anpgt2* in (A) pancreatic fibroblasts and (B) in MEFs.

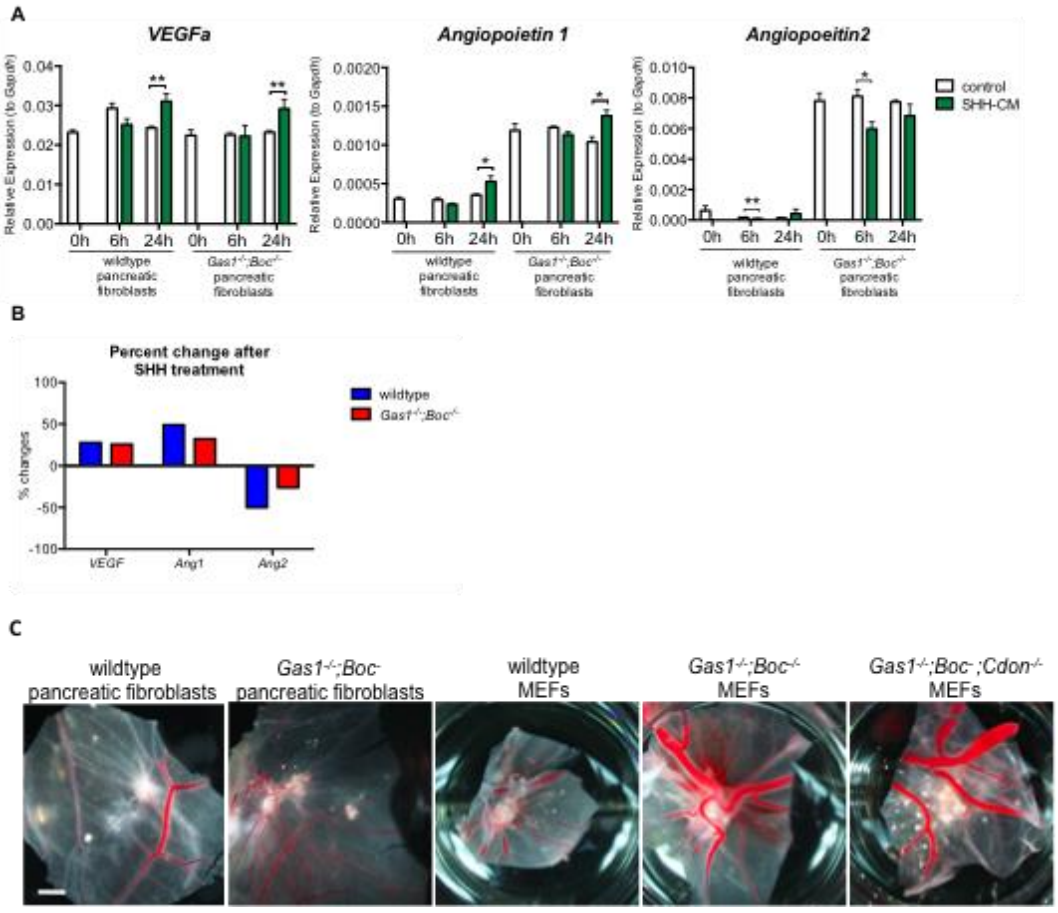

Figure 2.18: Angiogenesis regulation by fibroblasts in response to modulation of Hedgehog signaling.

(A) RT-qPCR analysis of *Vegfa*, Angiopoietin *1* and *Angiopoietin 2* in pancreatic fibroblasts. (B) Percent change in angiogenic gene expression in pancreatic fibroblasts in response to SHH treatment. (C) Chicken chorioallantoic membrane (CAM) assays with pancreatic fibroblasts and MEFs. Scale bar, 2mm.

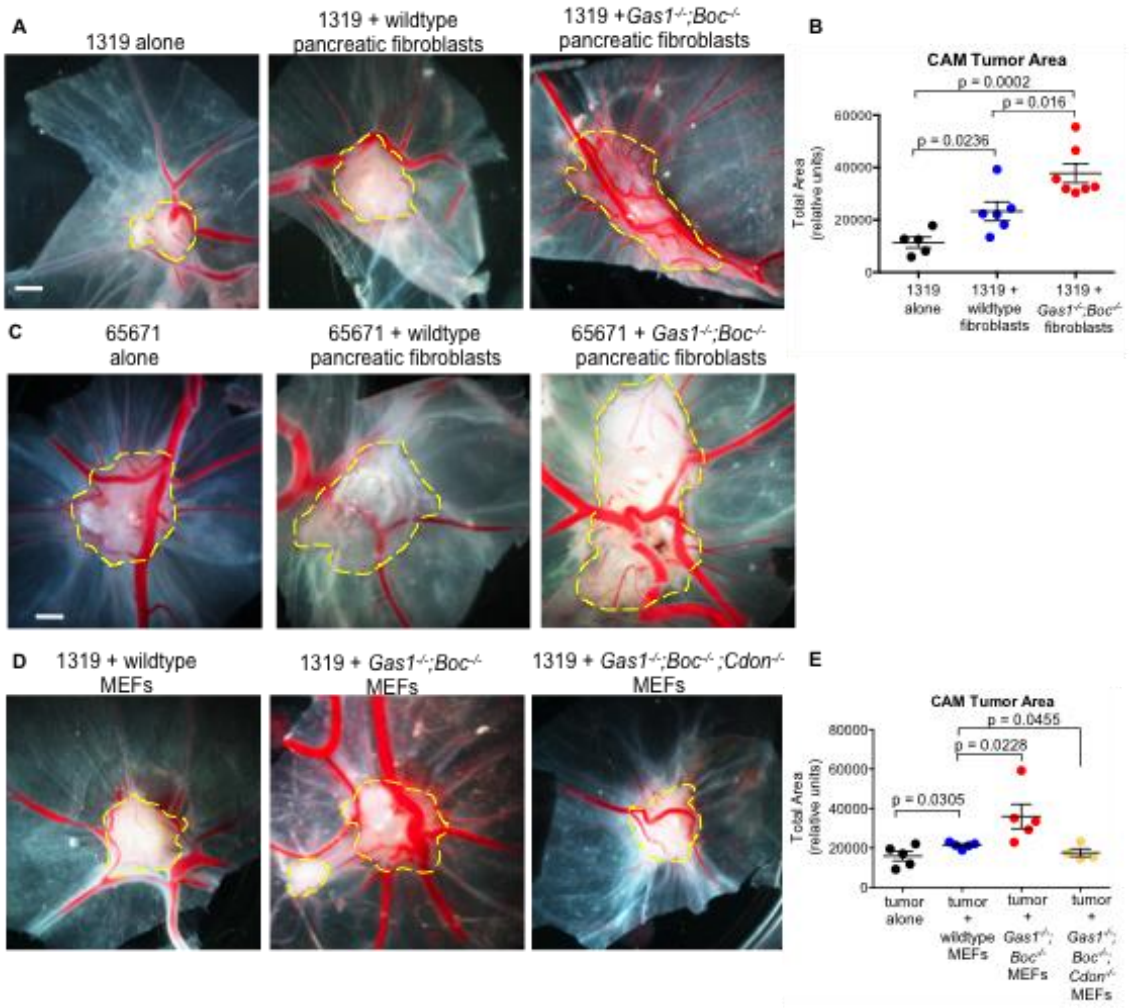

Figure 2.19: Dosage-dependant HH signaling differentially promotes pancreatic tumor growth and vascularity in CAM assays.

(A) Chicken CAM assay with 1319 cells and pancreatic fibroblasts. (B) Quantitation of CAM tumor area. (C) CAM assays with KPC mouse derived tumor cells (65671) and pancreatic fibroblasts. Scale, bar 2mm. (D) Chicken CAM assay with 1319 cells and MEFs. (E) Quantitation of CAM tumor area. Scale bar, 2mm.

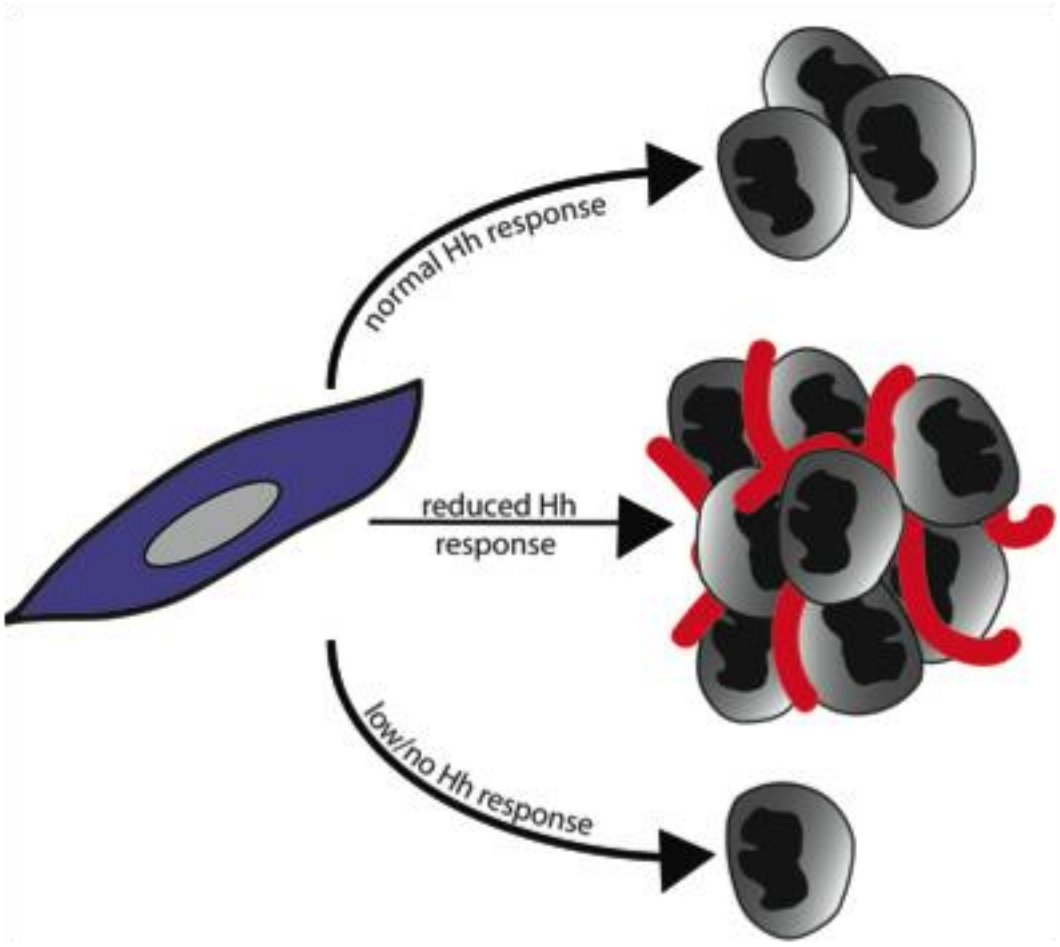

Figure 2.20: Working model of dosage-dependent regulation of tumor growth and angiogenesis by Hedgehog signaling.

Fibroblasts with all three co-receptors, and thus a normal HH response, respond to tumor-derived HH ligand by promoting tumor growth. In contrast, fibroblasts missing all three co-receptors, and thus a severely reduced ability to respond to HH, do not promote tumor growth. However, fibroblasts missing two co-receptors, with a moderately reduced ability to respond to HH, promote the growth of large, vascular tumors compared to normal fibroblasts. Taken together, this points towards a dosage-dependant effect of HH signaling on tumor growth and angiogenesis.

References

1. Jones, S., Zhang, X., Parsons, D. W., Lin, J. C., Leary, R. J., Angenendt, P., Mankoo, P., Carter, H., Kamiyama, H., Jimeno, A., Hong, S. M., Fu, B., Lin, M. T., Calhoun, E. S., Kamiyama, M., Walter, K., Nikolskaya, T., Nikolsky, Y., Hartigan, J., Smith, D. R., Hidalgo, M., Leach, S. D., Klein, A. P., Jaffee, E. M., Goggins, M., Maitra, A., Iacobuzio-Donahue, C., Eshleman, J. R., Kern, S. E., Hruban, R. H., Karchin, R., Papadopoulos, N., Parmigiani, G., Vogelstein, B., Velculescu, V. E., and Kinzler, K. W. (2008) Core signaling pathways in human pancreatic cancers revealed by global genomic analyses. *Science* **321**, 1801-1806
2. Hruban, R. H., Adsay, N. V., Albores-Saavedra, J., Compton, C., Garrett, E. S., Goodman, S. N., Kern, S. E., Klimstra, D. S., Kloppel, G., Longnecker, D. S., Luttges, J., and Offerhaus, G. J. (2001) Pancreatic intraepithelial neoplasia: a new nomenclature and classification system for pancreatic duct lesions. *Am J Surg Pathol* **25**, 579-586
3. Klimstra, D. S., and Longnecker, D. S. (1994) K-ras mutations in pancreatic ductal proliferative lesions. *Am J Pathol* **145**, 1547-1550
4. Hingorani, S. R., Petricoin, E. F., Maitra, A., Rajapakse, V., King, C., Jacobetz, M. A., Ross, S., Conrads, T. P., Veenstra, T. D., Hitt, B. A., Kawaguchi, Y., Johann, D., Liotta, L. A., Crawford, H. C., Putt, M. E., Jacks, T., Wright, C. V., Hruban, R. H., Lowy, A. M., and Tuveson, D. A. (2003) Preinvasive and invasive ductal pancreatic cancer and its early detection in the mouse. *Cancer Cell* **4**, 437-450
5. Berman, D. M., Karhadkar, S. S., Maitra, A., Montes De Oca, R., Gerstenblith, M. R., Briggs, K., Parker, A. R., Shimada, Y., Eshleman, J. R., Watkins, D. N., and Beachy, P. A. (2003) Widespread requirement for Hedgehog ligand stimulation in growth of digestive tract tumours. *Nature* **425**, 846-851
6. Thayer, S. P., di Magliano, M. P., Heiser, P. W., Nielsen, C. M., Roberts, D. J., Lauwers, G. Y., Qi, Y. P., Gysin, S., Fernandez-del Castillo, C., Yajnik, V., Antoniu, B., McMahon, M., Warshaw, A. L., and Hebrok, M. (2003) Hedgehog is an early and late mediator of pancreatic cancer tumorigenesis. *Nature* **425**, 851-856
7. Hingorani, S. R., Wang, L., Multani, A. S., Combs, C., Deramaudt, T. B., Hruban, R. H., Rustgi, A. K., Chang, S., and Tuveson, D. A. (2005) Trp53R172H and KrasG12D cooperate to promote chromosomal instability and widely metastatic pancreatic ductal adenocarcinoma in mice. *Cancer Cell* **7**, 469-483
8. Yauch, R. L., Gould, S. E., Scales, S. J., Tang, T., Tian, H., Ahn, C. P., Marshall, D., Fu, L., Januario, T., Kallop, D., Nannini-Pepe, M., Kotkow, K., Marsters, J. C., Rubin, L. L., and de Sauvage, F. J. (2008) A paracrine requirement for hedgehog signalling in cancer. *Nature* **455**, 406-410
9. Carpenter, D., Stone, D. M., Brush, J., Ryan, A., Armanini, M., Frantz, G., Rosenthal, A., and de Sauvage, F. J. (1998) Characterization of two patched

receptors for the vertebrate hedgehog protein family. *Proc Natl Acad Sci U S A* **95**, 13630-13634
10. Agren, M., Kogerman, P., Kleman, M. I., Wessling, M., and Toftgard, R. (2004) Expression of the PTCH1 tumor suppressor gene is regulated by alternative promoters and a single functional Gli-binding site. *Gene* **330**, 101-114
11. Dai, P., Akimaru, H., Tanaka, Y., Maekawa, T., Nakafuku, M., and Ishii, S. (1999) Sonic Hedgehog-induced activation of the Gli1 promoter is mediated by GLI3. *J Biol Chem* **274**, 8143-8152
12. Molckovsky, A., and Siu, L. L. (2008) First-in-class, first-in-human phase I results of targeted agents: highlights of the 2008 American society of clinical oncology meeting. *J Hematol Oncol* **1**, 20
13. Rudin, C. M., Hann, C. L., Laterra, J., Yauch, R. L., Callahan, C. A., Fu, L., Holcomb, T., Stinson, J., Gould, S. E., Coleman, B., LoRusso, P. M., Von Hoff, D. D., de Sauvage, F. J., and Low, J. A. (2009) Treatment of medulloblastoma with hedgehog pathway inhibitor GDC-0449. *N Engl J Med* **361**, 1173-1178
14. Yauch, R. L., Dijkgraaf, G. J., Alicke, B., Januario, T., Ahn, C. P., Holcomb, T., Pujara, K., Stinson, J., Callahan, C. A., Tang, T., Bazan, J. F., Kan, Z., Seshagiri, S., Hann, C. L., Gould, S. E., Low, J. A., Rudin, C. M., and de Sauvage, F. J. (2009) Smoothened mutation confers resistance to a Hedgehog pathway inhibitor in medulloblastoma. *Science* **326**, 572-574
15. Allen, B. L., Tenzen, T., and McMahon, A. P. (2007) The Hedgehog-binding proteins Gas1 and Cdo cooperate to positively regulate Shh signaling during mouse development. *Genes Dev* **21**, 1244-1257
16. Martinelli, D. C., and Fan, C. M. (2007) Gas1 extends the range of Hedgehog action by facilitating its signaling. *Genes Dev* **21**, 1231-1243
17. Tenzen, T., Allen, B. L., Cole, F., Kang, J. S., Krauss, R. S., and McMahon, A. P. (2006) The cell surface membrane proteins Cdo and Boc are components and targets of the Hedgehog signaling pathway and feedback network in mice. *Dev Cell* **10**, 647-656
18. Zhang, W., Kang, J. S., Cole, F., Yi, M. J., and Krauss, R. S. (2006) Cdo functions at multiple points in the Sonic Hedgehog pathway, and Cdo-deficient mice accurately model human holoprosencephaly. *Dev Cell* **10**, 657-665
19. Allen, B. L., Song, J. Y., Izzi, L., Althaus, I. W., Kang, J. S., Charron, F., Krauss, R. S., and McMahon, A. P. (2011) Overlapping roles and collective requirement for the coreceptors GAS1, CDO, and BOC in SHH pathway function. *Dev Cell* **20**, 775-787
20. Kawaguchi, Y., Cooper, B., Gannon, M., Ray, M., MacDonald, R. J., and Wright, C. V. (2002) The role of the transcriptional regulator Ptf1a in converting intestinal to pancreatic progenitors. *Nat Genet* **32**, 128-134
21. Zhang, W., Hong, M., Bae, G. U., Kang, J. S., and Krauss, R. S. (2011) Boc modifies the holoprosencephaly spectrum of Cdo mutant mice. *Dis Model Mech* **4**, 368-380
22. Morris, J. P. t., Cano, D. A., Sekine, S., Wang, S. C., and Hebrok, M. (2010) Beta-catenin blocks Kras-dependent reprogramming of acini into pancreatic cancer precursor lesions in mice. *J Clin Invest* **120**, 508-520

23. Todaro, G. J., and Green, H. (1963) Quantitative studies of the growth of mouse embryo cells in culture and their development into established lines. *J Cell Biol* **17**, 299-313
24. Collins, M. A., Bednar, F., Zhang, Y., Brisset, J. C., Galban, S., Galban, C. J., Rakshit, S., Flannagan, K. S., Adsay, N. V., and Pasca di Magliano, M. (2012) Oncogenic Kras is required for both the initiation and maintenance of pancreatic cancer in mice. *J Clin Invest* **122**, 639-653
25. Kunzi-Rapp, K., Genze, F., Kufer, R., Reich, E., Hautmann, R. E., and Gschwend, J. E. (2001) Chorioallantoic membrane assay: vascularized 3-dimensional cell culture system for human prostate cancer cells as an animal substitute model. *J Urol* **166**, 1502-1507
26. Guerra, C., Schuhmacher, A. J., Canamero, M., Grippo, P. J., Verdaguer, L., Perez-Gallego, L., Dubus, P., Sandgren, E. P., and Barbacid, M. (2007) Chronic pancreatitis is essential for induction of pancreatic ductal adenocarcinoma by K-Ras oncogenes in adult mice. *Cancer Cell* **11**, 291-302
27. Sugimoto, H., Mundel, T. M., Kieran, M. W., and Kalluri, R. (2006) Identification of fibroblast heterogeneity in the tumor microenvironment. *Cancer Biol Ther* **5**, 1640-1646
28. Tian, H., Callahan, C. A., DuPree, K. J., Darbonne, W. C., Ahn, C. P., Scales, S. J., and de Sauvage, F. J. (2009) Hedgehog signaling is restricted to the stromal compartment during pancreatic carcinogenesis. *Proc Natl Acad Sci U S A* **106**, 4254-4259
29. Li, C., Heidt, D. G., Dalerba, P., Burant, C. F., Zhang, L., Adsay, V., Wicha, M., Clarke, M. F., and Simeone, D. M. (2007) Identification of pancreatic cancer stem cells. *Cancer Res* **67**, 1030-1037
30. Zhang, Y., Morris, J. P. t., Yan, W., Schofield, H. K., Gurney, A., Simeone, D. M., Millar, S. E., Hoey, T., Hebrok, M., and Pasca di Magliano, M. (2013) Canonical wnt signaling is required for pancreatic carcinogenesis. *Cancer Res* **73**, 4909-4922
31. Collisson, E. A., Sadanandam, A., Olson, P., Gibb, W. J., Truitt, M., Gu, S., Cooc, J., Weinkle, J., Kim, G. E., Jakkula, L., Feiler, H. S., Ko, A. H., Olshen, A. B., Danenberg, K. L., Tempero, M. A., Spellman, P. T., Hanahan, D., and Gray, J. W. (2011) Subtypes of pancreatic ductal adenocarcinoma and their differing responses to therapy. *Nat Med* **17**, 500-503
32. Olive, K. P., Jacobetz, M. A., Davidson, C. J., Gopinathan, A., McIntyre, D., Honess, D., Madhu, B., Goldgraben, M. A., Caldwell, M. E., Allard, D., Frese, K. K., Denicola, G., Feig, C., Combs, C., Winter, S. P., Ireland-Zecchini, H., Reichelt, S., Howat, W. J., Chang, A., Dhara, M., Wang, L., Ruckert, F., Grutzmann, R., Pilarsky, C., Izeradjene, K., Hingorani, S. R., Huang, P., Davies, S. E., Plunkett, W., Egorin, M., Hruban, R. H., Whitebread, N., McGovern, K., Adams, J., Iacobuzio-Donahue, C., Griffiths, J., and Tuveson, D. A. (2009) Inhibition of Hedgehog signaling enhances delivery of chemotherapy in a mouse model of pancreatic cancer. *Science* **324**, 1457-1461
33. Lee, J. J., Perera, R. M., Wang, H., Wu, D. C., Liu, X. S., Han, S., Fitamant, J., Jones, P. D., Ghanta, K. S., Kawano, S., Nagle, J. M., Deshpande, V., Boucher,

Y., Kato, T., Chen, J. K., Willmann, J. K., Bardeesy, N., and Beachy, P. A. (2014) Stromal response to Hedgehog signaling restrains pancreatic cancer progression. *Proc Natl Acad Sci U S A* **111**, E3091-3100

34. Rhim, A. D., Oberstein, P. E., Thomas, D. H., Mirek, E. T., Palermo, C. F., Sastra, S. A., Dekleva, E. N., Saunders, T., Becerra, C. P., Tattersall, I. W., Westphalen, C. B., Kitajewski, J., Fernandez-Barrena, M. G., Fernandez-Zapico, M. E., Iacobuzio-Donahue, C., Olive, K. P., and Stanger, B. Z. (2014) Stromal elements act to restrain, rather than support, pancreatic ductal adenocarcinoma. *Cancer Cell* **25**, 735-747
35. Augustin, H. G., Koh, G. Y., Thurston, G., and Alitalo, K. (2009) Control of vascular morphogenesis and homeostasis through the angiopoietin-Tie system. *Nat Rev Mol Cell Biol* **10**, 165-177
36. Chen, W., Tang, T., Eastham-Anderson, J., Dunlap, D., Alicke, B., Nannini, M., Gould, S., Yauch, R., Modrusan, Z., DuPree, K. J., Darbonne, W. C., Plowman, G., de Sauvage, F. J., and Callahan, C. A. (2011) Canonical hedgehog signaling augments tumor angiogenesis by induction of VEGF-A in stromal perivascular cells. *Proc Natl Acad Sci U S A* **108**, 9589-9594
37. Amakye, D., Jagani, Z., and Dorsch, M. (2013) Unraveling the therapeutic potential of the Hedgehog pathway in cancer. *Nat Med* **19**, 1410-1422
38. Jessell, T. M. (2000) Neuronal specification in the spinal cord: inductive signals and transcriptional codes. *Nat Rev Genet* **1**, 20-29
39. Feldmann, G., Dhara, S., Fendrich, V., Bedja, D., Beaty, R., Mullendore, M., Karikari, C., Alvarez, H., Iacobuzio-Donahue, C., Jimeno, A., Gabrielson, K. L., Matsui, W., and Maitra, A. (2007) Blockade of hedgehog signaling inhibits pancreatic cancer invasion and metastases: a new paradigm for combination therapy in solid cancers. *Cancer Res* **67**, 2187-2196

CHAPTER THREE

The Transcription Factor Gli1 Modulates the Inflammatory Response During Pancreatic Tissue Remodeling.[1]

Abstract

Pancreatic cancer, one of the deadliest human malignancies, is almost uniformly associated with a mutant, constitutively active form of the oncogene Kras. Studies in genetically engineered mouse models have defined a requirement for oncogenic KRAS in both the formation of PanINs -the most common precursor lesions to pancreatic cancer- and in the maintenance and progression of these lesions. Previous work using an inducible model allowing tissue-specific and reversible expression of oncogenic Kras in the pancreas indicates that inactivation of this GTPase at the PanIN stage promotes pancreatic tissue repair. Here, we extend these findings to identify GLI1, a transcriptional effector of the Hedgehog pathway, as a central player in pancreatic tissue repair upon Kras inactivation. Deletion of a single allele of Gli1 results in improper stromal remodeling and perdurance of the inflammatory infiltrate characteristic of

[1] Originally published as: Mathew, E., Collins, M., Fernandez-Barrena, M.G., Holtz, A.M., Yan, W., Hogan, J.O., Tata, Z., Allen, B.L., Fernandez-Zapico, M.E., and Pasca di Magliano, M. (2014) The Transcription Factor Gli1 Modulates the Inflammatory Response During Pancreatic Tissue Remodeling. *Journal of Biol. Chem.* **289**(40): 27727-27743. (doi:10.1074/jbc.M114.556563)

pancreatic tumorigenesis. Strikingly, this partial loss of Gli1 affects activated fibroblasts in the pancreas, and the recruitment of immune cells that are vital for tissue recovery. Analysis of the mechanism using expression and chromatin immunoprecipitation assays identified a subset of cytokines including IL-6, mIL-8, Mcp-1 and M-csf (Csf1) as direct GLI1 target genes potentially mediating this phenomenon. Finally, we demonstrate that canonical Hedgehog signaling, a known regulator of Gli1 activity, is required for pancreas recovery. Collectively, these data delineate a new pathway controlling tissue repair and highlight the importance of GLI1 in regulation of the pancreatic microenvironment during this cellular process.

Introduction

Pancreatic cancer is among the deadliest of human malignancies. The median survival is less than 6 months, and this prognosis has not changed in almost 50 years (1). Pancreatic cancer is preceded by precursor lesions, the most frequent being pancreatic intraepithelial neoplasias (PanINs) (2). Both PanINs and pancreatic cancer are almost uniformly associated with the presence of a mutant form of KRAS, most commonly $KRAS^{G12D}$ (2-5). In mice, pancreatic cancer can be modeled by expressing oncogenic Kras in the pancreas epithelium (6,7). The induction of pancreatitis, a known risk factor for the development of pancreatic cancer (8), in mice expressing oncogenic Kras leads to rapid PanIN formation (9-11). In wildtype mice, the acute inflammatory response during pancreatitis is followed by rapid tissue repair over the course of several days (12). In contrast, mice bearing mutant Kras undergo rapid fibrosis and PanIN development upon induction of pancreatitis (11,13). Although the biology of these

phenomenona is clearly established, the molecular mechanism modulating tissue repair remains elusive.

In the current study, we identified a novel mechanism underlying pancreas repair after pancreatitis and Kras-driven, inflammation-induced pancreatic carcinogenesis. We demonstrate that the transcription factor GLI1 is required for pancreatic tissue remodeling after damage. Our studies revealed that a reduction in the dosage of Gli1, through genetic inactivation of one Gli1 allele, caused impaired tissue repair following induction of pancreatitis, altering the remodeling of the stroma. Furthermore, we identified a subset of known immune system regulators as GLI1 direct targets including IL-6, mIL-8, Mcp-1 and M-csf (Csf1). Finally, we detected a reduction in the infiltration of macrophages, thus possibly explaining the impaired tissue remodeling. Our results define a novel mechanism controlling pancreatic tissue repair and identified a dosage-dependent role of the transcription factor GLI1 in the regulation of inflammatory responses in the pancreas.

Materials and Methods

Mice

Mice were housed in specific pathogen-free facilities of the University of Michigan Comprehensive Cancer Center. This study was approved by the University of Michigan University Committee on Use and Care of Animals (UCUCA) guidelines. p48Cre (Ptf1aCre) mice (14) were intercrossed with TetO-Kras^{G12D} (15) and Rosa26$^{rtTa/rtTa}$ (16) to generate p48Cre; TetO-Kras^{G12D}; Rosa26$^{rtTa/rtTa}$ (iKras*) triple mutants (17). Gli1$^{lacZ/lacZ}$

mice (18) (Jackson Laboratories stock #008211) were bred with iKras* animals to generate iKras*Gli1$^{lacZ/+}$ mice. LSL-Kras^{G12D} mice were bred with p48Cre and Gli1$^{lacZ/lacZ}$ mice to create KC double transgenics (7) and KC;Gli1$^{lacZ/+}$ triple transgenics. Doxycycline (DOX) (Sigma) was administered in the drinking water at a concentration of 0.2g/L in a solution of 5% sucrose and replaced every 3-4 days. Acute pancreatitis was induced by 2 series of 8 hourly intraperitoneal injections with caerulein (Sigma) at a concentration of 75µg/kg over a 48-hour period, as previously described (11).

Immunohistochemistry and Immunofluorescence

These assays were performed as previously described (17). Primary antibodies used were β-Gal/lacZ (1:200, Abcam), CD45 (1:200, BDPharm), CK19 (1:100, Iowa Developmental Hybridoma Bank), F4/80 (1:100, BMA Biomedicals), phospho-ERK1/2 (1:100, Cell Signaling), Ki67 (1:100, Vector Laboratories), SMA (1:1000, Sigma), and Vimentin (1:100, Cell Signaling). Images were taken with an Olympus BX-51 microscope, Olympus DP71 digital camera, and CellSens standard v1.6 software. For immunofluorescence, Alexa Fluor (Invitrogen) secondary antibodies were used. Cell nuclei were counterstained with DAPI (Invitrogen). The images were acquired using an Olympus IX-71 confocal microscope and FluoView FV500/IX software or a Leica Inverted SP5X confocal microscope with Leica Applications Suite Advanced Fluorescence (LAS AF) software.

Histopathology

Briefly, de-identified slides were examined by an expert pathologist (W.Y.). For each slide, 5 low magnification pictures were taken from the center, top right, top left, bottom right and bottom left locations in order to cover most of the area of each section. A minimum of 50 total acinar or ductal clusters was counted from at least 3 independent animals for each group, as previously described (19). Each cluster counted was classified as Acinar, Acinar-Ductal Metaplasia (ADM), PanIN1A, 1B, 2 or 3 based on the classification consensus (20). The data was expressed as percentage of total counted clusters. Error bars represent SEM.

Quantification of Trichrome Staining

Images of iKras* and iKras*Gli1$^{lacZ/+}$ Gomori Trichrome-stained sections were taken with a Leica MZFLIII dissection microscope and Olympus DP72 camera. Trichrome positive areas were determined with Image Pro Plus v4 software (MediaCybernetics). The data was expressed as a percent of trichrome positive area and averaged per timepoint. Error bars represent SEM.

Reverse Transcription Quantitative PCR (qRT-PCR)

Tissue for RNA extraction was prepared through overnight incubation in RNAlater-ICE (Ambion) at -20^{o}C, then isolated using RNeasy Protect (Qiagen) according to the manufacturer's instructions. Reverse transcription reactions were conducted using a High-Capacity cDNA Reverse Transcription Kit (Applied Biosystems). Samples for qRT-PCR were prepared with 1x SYBR Green PCR Master Mix (Applied Biosystems) and various primers listed in **Table 3.1**. All primers were optimized for amplification under

reaction conditions as follows: 95°C 10 minutes, followed by 40 cycles of 95°C 15 seconds and 60°C 1 minute. Melt curve analysis was performed for all samples after completion of the amplification protocol. *Cyclophilin* was used as the housekeeping gene expression control.

Cell Culture

Mouse-derived tumor cell lines were cultured for 3 days after which conditioned media was collected, centrifuged and filtered. For cell stimulation, conditioned media was mixed with low-serum media (0.5%) at a 1:1 ratio. Mouse pancreatic fibroblast lines were derived from WT and Gli1$^{lacZ/+}$ pancreata. Briefly, freshly isolated pancreas were minced with sterile scissors then digested in 1mg/mL collagenase. Digested samples were then filtered through a 100µm strainer and cultured in IMDM supplemented with 10% FBS and 1% penicillin/streptomycin (Gibco). Cells were serum-starved (IMDM supplemented with 0.5% serum) for 36 hours prior to addition of conditioned media, and samples collected 0 hours, 6 hours, and 24 hours following stimulation. Mouse NIH/3T3 cells (ATCC, VA) were plated at 200,000 cells/well in 6-well plates in DMEM + 10% FBS + penicillin/streptomycin. After 24 hours cells were switched to low serum media (DMEM + 0.5% FBS) and treated with 100µl of conditioned media from control vector -(pcDNA3) or Sonic Hedgehog N-Terminus (NShh-pcDNA3) transfected COS7 cells. RNA was extracted after 24 hours of treatment and subjected to qRT-PCR as described above. The mouse embryonic fibroblast line was a gift from Dr. Shilatifard (Stowers Institute for Medical Research, Kansas City, MO) (21) and it was cultured in DMEM (Invitrogen) supplemented with 10% FBS (SAFC BioScience).

Flow Cytometry

Single cell suspensions from the pancreas and spleen were prepared as follows: freshly isolated organs were minced with sterile scalpels prior to incubation in 1mg/mL collagenase (Sigma-Aldrich) in HBSS for 15min at 37°C. Cell suspensions were then passed through a 40µM strainer. Single cell suspensions were prepared in HBSS/2% FBS. Antibodies used were CD45-Pacific Orange (1:50, Invitrogen), Gr1-FITC (1:50, BD Pharm), F4/80-PE-CY5 (1:50, eBioscience), CD11b-APC-CY7 (1:50, BD Pharm), CD3-PE (1:50, BD Pharm), CD8-APC-CY7 (1:50, BD Pharm), CD4-Pacific Blue (1:50, BD Pharm), CD25-APC (1:50, BD Pharm), Foxp3-FITC (1:50, eBioscience). Flow cytometry analysis was performed on a CyanTM ADP Analyzer (Beckman Coulter) and data analyzed using Summit 4.3 Software.

Chromatin Immunoprecipitation Assay (ChIP)

ChiP was conducted following the Magna ChIP kit protocol (Upstate). Briefly, 4×10^6 cells, cultured in DMEM (Invitrogen) supplemented with 10% FBS (SAFC BioScience), were cross-linked with 1% formaldehyde directly into the media for 10 min at room temperature. The cells were then washed and scraped with phosphate-buffered saline and collected by centrifugation at 800 × g for 5 min at 4°C, resuspended in cell lysis buffer and incubated on ice for 15 min. The pellet was then resuspended in nuclear lysis buffer and sheared to fragment DNA to ~700 bp. Samples were then immunoprecipitated using a GLI1 antibody (Novus Biologicals), normal rabbit IgG (Upstate) overnight at 4 °C on a rotating wheel. Following immunoprecipitation, samples

were washed and eluted using the chromatin immunoprecipitation kit in accordance with the manufacturer's instructions. Cross-links were removed at 62°C for 2 h, followed by 10 min at 95°C, and immunoprecipitated DNA was purified (Upstate) and subsequently amplified by real-time PCR. PCR was performed using primer sets for areas containing potential Gli1 binding sites in the M-cp1, M-csf, IL-6 and IL-8 promoter sequence: M-cp1, 5´-caaatctcaggtccagggaag-3´ (forward) and 5´-gccaggcatagtcagttgt-3´(reverse); M-csf, 5´-gcaggatatctgacttgtgacc-3´(forward) and 5´-caacccattcctcccagttaag-3´(reverse); IL-6, 5´-gcagtgggatcagcactaacagat-3´ (forward) and 5´-cctggacaacagacagtaatgttg-3´(reverse); IL-8, 5´-caacagaactggtgcatctataag-3´ (forward) and 5´-gccaactgctctaggacat-3´(reverse); Gli1-negative region in Chromosome 11 5'-tcccaggagtggctagaa-3' (forward) and 5'-gctctgaggcagccttt-3' (reverse). Quantitative SYBR PCR was performed in triplicate for each sample or control using the C1000 Thermal Cycler (Bio-Rad).

Statistical Analysis

The data are expressed as the mean± standard deviation. One-way ANOVA with a Tukey post-test was used to compare data between groups. A P value <0.05 was considered statistically significant.

Results

Gli1 is Required for Pancreas Recovery Following Pancreatitis or Inactivation of Oncogenic Kras

To investigate the role of GLI1 in tissue repair following acute pancreatitis as well as during early stages of pancreatic carcinogenesis, we used a mouse model where one Gli1 allele was replaced with a lacZ cassette, generating a Gli1 hemizygous animal (18). We initially induced pancreatitis in wildtype (WT) and Gli1$^{lacZ/+}$ mice with the cholecystokinin agonist caerulein (22). Both WT and Gli1 $^{lacZ/+}$ mice exhibited the characteristic acinar damage and influx of immune cells and activated fibroblasts 2 days after pancreatitis induction (**Figures 3.1A and 3.1B**). However, while normal tissue architecture and function was restored in WT pancreata after one week (**Figure 3.1A**), 6 out of 10 Gli1 $^{lacZ/+}$ mice failed to resolve the fibroinflammatory response (**Figure 3.1B**, **black arrows**). Interestingly, the failure to resolve pancreatitis did not increase in Gli1$^{lacZ/lacZ}$ mice (**Figure 3.2**).

To determine whether Gli1 was similarly required to mediate pancreas repair following oncogenic Kras^{G12D} inactivation, we crossed Gli1$^{lacZ/lacZ}$ mice with the iKras* mouse model of pancreatic cancer -that allows for tissue-specific and reversible control of oncogenic Kras^{G12D}- to generate iKras*$^{Gli1lacZ/+}$ animals. In iKras* mice, activation and inactivation of the oncogene is obtained by the addition or removal of doxycycline (DOX) from the drinking water (**Figure 3.3A**). The iKras* mouse develops PanINs and a pronounced desmoplastic stroma upon oncogenic Kras activation followed by the induction of acute pancreatitis (17). Conversely, inactivation of oncogenic Kras expression in low-grade PanINs leads to complete tissue recovery. We administered DOX to 4 to 6 week old iKras* and iKras*Gli1$^{lacZ/+}$ mice to express Kras^{G12D} and then induced pancreatitis. We harvested pancreata 3 weeks later (n=3-5) (**Figure 3.3B**).

Both iKras* and iKras*Gli1$^{lacZ/+}$ mice exhibited a substantial acinar cell loss and PanIN formation with accumulation of desmoplastic stroma (**Figures 3.4A, 3.4B, and 3.5**). Thus, inactivation of one allele of Gli1 did not affect pancreatitis-driven PanIN formation in this model.

We then inactivated Kras^{G12D} expression, by removing DOX from the water, and harvested tissue after 3 days, 2 weeks, and 5 weeks (n=3-5). Notably, upon Kras^{G12D} inactivation, recovery of the acinar cell compartment was apparent after only 3 days in iKras* mice, whereas iKras*Gli1$^{lacZ/+}$ mice displayed delayed recovery of the acinar compartment (**Figures 3.4A, 3.4B, and 3.5**). Two weeks following Kras^{G12D} inactivation, recovery of the acinar compartment as well as comprehensive remodeling of the stroma was complete in iKras* mice. In contrast, iKras*Gli1$^{lacZ/+}$ mice retained low-grade PanIN lesions and displayed a prominent amount of stroma even at the 5 week time point (**Figure 3.4B and 3.5**). Using β-Gal staining to follow Gli1 expression, we found that Gli1 levels increased throughout the stroma after 3 weeks of oncogenic Kras activation, and persisted even after Kras inactivation (**Figure 3.4B**). These data suggest a critical role for Gli1 dosage during tissues recovery following both caerulein-induced pancreatitis and after inactivation of oncogenic Kras.

Loss of Gli1 Impairs Stromal Remodeling During Tissue Repair

To determine which cell types in the pancreas express Gli1, we performed co-immunofluorescence for β-Gal along with various epithelial, fibroblast, and immune cell markers in iKras*Gli1$^{lacZ/+}$ mice. First, we observed a distinct separation of β-Gal+ cells

and CK19, a marker for pancreatic ducts and PanINs, indicating that ducts and neoplastic epithelial cells did not express Gli1 (**Figure 3.6A**). In contrast, we identified widespread co-expression of β-Gal with SMA, a marker of activated fibroblasts, as well as co-localization with Vimentin, another fibroblast marker (**Figure 3.6B, and data not shown**). We additionally observed co-expression of Gli1 with a subset of the macrophages within the tissue, identified by the marker F4/80 (**Figure 3.6C**).

In order to determine whether the expression pattern of Gli1 was conserved in a different model of $Kras^{G12D}$-driven pancreatic carcinogenesis, we crossed $Gli1^{lacZ/+}$ reported mice with the KC mouse model of pancreatic cancer (Pft1a-Cre;LSL-$Kras^{G12D}$) (7). We collected pancreata from KC;$Gli1^{lacZ/+}$ mice 3 weeks following the induction of pancreatitis, when widespread PanINs are expected. Similar to our findings in the iKras*$Gli1^{lacZ/+}$ mice, β-Gal expression in KC;$Gli1^{lacZ/+}$ mice was detected in activated fibroblasts and in a subset of immune cells (expressing CD45) but not in epithelial cells (**Figures 3.7A-D**). Thus, stromal expression of Gli1 is common to caerulein-induced pancreatitis and 2 independent models of pancreatic cancer.

Next, we wanted to assess the stroma that failed to remodel in iKras*$Gli1^{lacZ/+}$ mice. Thus, we performed a Gomori Trichrome stain to visualize and quantify collagen deposition. Three weeks after $Kras^{G12D}$ activation, both iKras* and iKras*$Gli1^{lacZ/+}$ mice pancreata had an abundance of collagen deposition, which is a hallmark of the desmoplastic response in the neoplastic pancreas (23). The collagen deposition persisted at the 3 day timepoint, but fully resolved by 2 weeks following $Kras^{G12D}$ inactivation in iKras* mice. In contrast, in iKras*$Gli1^{lacZ/+}$ mice, abundant collagen

deposition was still observed throughout the stroma at 2 weeks, indicating a delay or impairment of the remodeling process (**Figures 3.8A and 3.8B**).

Both in iKras* and iKras*Gli1$^{lacZ/+}$ pancreatic tissues active proliferation (measured by Ki67 immunostaining) was observed in both the epithelial and stromal compartments 3 weeks following Kras^{G12D} activation (**Figure 3.9A**). Subsequent inactivation of oncogenic Kras shifted the majority of cell proliferation to the epithelial compartment in both genotypes (**Figure 3.9A**). Additionally, in the presence of oncogenic Kras, phospho-ERK1/2 (pERK1/2) - a downstream effector of Kras - was elevated in the epithelial compartment (**Figure 3.9B**). Upon Kras^{G12D} inactivation, pERK1/2 levels decreased in the epithelium and there was a transient increase in the stroma of iKras* pancreata, as previously described (17). Interestingly, in iKras*Gli1$^{lacZ/+}$ mice, elevated pERK1/2 levels in the stroma persisted even at 5 weeks following Kras^{G12D} inactivation (**Figure 3.9B**).

Finally, we assessed SMA expression to mark the reactive stromal compartment. Three weeks following induction of Kras^{G12D} expression, robust SMA expression was detected in the stroma of both sets of mice (**Figure 3.10A, black arrows**). This expression rapidly decreased in iKras* animals upon Kras^{G12D} inactivation. However, in iKras*Gli1$^{lacZ/+}$ mice, SMA expression persisted longer than in iKras* mice. By 2 weeks, however, most of the fibroblasts persisting in the pancreas did not express SMA (**Figure 3.10A**, **white arrows**), thus indicating that reduced Gli1 dosage impaired remodeling but did not cause sustained fibroblast activation.

Gli1 Regulates a Distinct Profile of Immune System Regulators

Knowing the function of Gli1 as an effector of the Hedgehog (HH) pathway, we assessed the expression of HH pathway components in both iKras* and iKras*Gli1$^{lacZ/+}$ mice. In the normal adult mouse pancreas, HH pathway components are not expressed at detectable levels. However, expression of HH pathway components increases in PanINs (24). In iKras*Gli1 $^{lacZ/+}$ mice, the expression of HH pathway components was reduced compared to iKras* mice, indicating that one allele of Gli1 was not sufficient to maintain the level of pathway activation found in PanINs. (**Figures 3.11A-F**). Upon Kras^{G12D} inactivation, expression of these HH pathway genes decreased over time. Intriguingly, we observed a spike of *Gli1* expression in iKras* mice after 2 weeks of Kras^{G12D} inactivation (**Figure 3.11A**), consistent with a role for this gene in pancreatic recovery and remodeling.

To investigate potential mechanisms by which Gli1 regulates pancreatic recovery, we assessed the expression of cytokines involved in tissue remodeling. First, we performed qRT-PCR analysis to assess differences in cytokine production between iKras* and iKras*Gli1$^{lacZ/+}$ pancreatic tissue (**scheme in Figure 3.12A**). We detected a significant decrease in IL-6 expression in iKras*Gli1$^{lacZ/+}$ pancreas (**Figure 3.12B**). Likewise, we detected a significant reduction in both Mcp-1 and the murine homolog of IL8 (mIL-8) in iKras*Gli1$^{lacZ/+}$ pancreata (**Figures 3.12C and 3.12D**). These cytokines all regulate leukocyte accumulation and function (25); however, only IL-6 was previously described as a GLI1 target (26). Additionally, transcription of M-csf, a critical factor for macrophage differentiation and function (27), was reduced in iKras*Gli1$^{lacZ/+}$ pancreas

(**Figure 3.12E**). These data suggest that GLI1 may regulate pancreas recovery through the expression of secreted factors involved in immune system function.

To test whether Gli1 loss affected cytokine production specifically in fibroblasts, we extracted pancreatic fibroblasts from untreated WT and Gli1$^{lacZ/+}$ mice (**scheme in Figure 3.13A**), followed by serum-starvation and treatment with either cancer cell conditioned media (CCM) from primary iKras* tumor cells (28) or control (Ctrl) media for 0, 6, and 24 hours; we then collected cells for RNA extraction (**scheme in Figure 3.13A**). In parallel, fibroblasts were treated with conditioned medium from control or SHH-expressing COS7 cells. As expected, Gli1 and Ptch1 expression increased in WT fibroblasts treated with SHH-expressing COS7 cell conditioned medium, as measured by qRT-PCR. Of note, Gli1 had a higher basal expression level but reduced Shh-dependent activation in Gli1$^{lacZ/+}$ fibroblasts. Moreover, the extent of Ptch1 activation was reduced in Gli1$^{lacZ/+}$ fibroblasts. (**Figure 3.13B**). Over the course of experimental repeats, we found that Gli1 expression in WT fibroblasts was inconsistently increased after 6 hours, but always significantly increased by 24 hours. Further, transcription of IL-6 was significantly increased 6 hours after exposure to CCM, in both WT and Gli1$^{lacZ/+}$ cells. At 24 hours however, WT fibroblasts sustained significantly greater levels of *IL-6* transcription than Gli1$^{lacZ/+}$ cells (**Figure 3.13C**). Expression of both *Mcp-1* and *mIL-8* were also significantly reduced in Gli1$^{lacZ/+}$ fibroblasts at both 6 hours and 24 hours post-treatment (**Figures 3.13D and 3.13E**). Moreover, transcription of *M-csf* was also significantly reduced at 6 hours in Gli1lacZ/+ fibroblasts compared to their WT counterparts; however, by 24 hours levels of *M-csf* transcription were the same (**Figure**

3.13F). Of note, as both WT and Gli1$^{lacZ/+}$ fibroblasts express a basal level of GLI proteins, activation of target genes could occur even before new Gli1 is transcribed. These results identify multiple potential GLI1-dependent cytokine targets in pancreatic fibroblasts.

To test whether these putative GLI1 targets were common to other fibroblast populations, we treated serum-starved NIH/3T3 cells with control-conditioned media (COS7-CM) or NSHH-conditioned medium (COS7-SHH) for 24 hours followed by assessment of cytokine expression by qRT-PCR (**scheme in Figure 3.14A**). We also included untreated cells to exclude any effects of the control-conditioned media. *Gli1* and *Ptch1* were up-regulated in response to NSHH treatment, confirming increased HH pathway activity in these cells (**Figure 3.14B**). While we did not observe significant changes in the expression of *Mcp-1* or *M-csf*, both *IL-6* and *mIL-8* were up-regulated in response to NSHH treatment (**Figure 3.14B**). Therefore, IL-6 and mIL-8 may be general HH targets in fibroblasts, while Mcp-1 and M-csf might be pancreas-specific.

Finally, we determined whether these cytokines were direct GLI1 target genes. Bioinformatic analysis identified putative GLI1 binding sites in the promoters of these cytokines (**Figure 3.15A**). To assess GLI1 binding to these sites we performed ChIP assays in mouse embryonic fibroblasts (MEFs). Endogenous GLI1 bound to the promoter of IL-6, mIL-8, Mcp-1 and M-csf (**Figures 3.15B-E**). We also observed GLI1 binding on the Cyclin D1 promoter (**Figure 3.15F**), used as a positive control (29,30). To control for the specificity of GLI1 binding, we performed PCR in a region lacking canonical GLI1-binding sites. Importantly, GLI1 binding was not detected in this region

(**Figure 3.15G**). Taken together, these data indicate that several cytokines important in immune cell recruitment and function are direct GLI1 transcriptional targets whose expression is reduced upon loss of a single Gli1 allele.

Immune Cell Infiltration is Regulated in a Gli1-dependent Manner

To define if the altered cytokine expression profiles detected in Gli1$^{lacZ/+}$ animals affected immune cell recruitment in vivo, we performed flow cytometry analysis on iKras* and iKras*Gli1$^{lacZ/+}$ mice 3 weeks after pancreatitis. We quantified both the myeloid and T lymphocyte subsets recruited to the neoplastic pancreas. Since B lymphocytes are not reported to function in the wound healing process, we did not quantify their numbers in this analysis (31).

We detected no difference in the overall population of CD45+ hematopoietic cells between iKras* and iKras*Gli1$^{lacZ/+}$ mice (**Figure 3.16A**). Previous work characterizing the immune infiltrate of pancreatic cancer revealed a prominent leukocyte population, predominantly F4/80+/CD11b+ macrophages, that developed during PanIN formation and persisted through tumor development (32). Comparison of iKras* and iKras*Gli1$^{lacZ/+}$ pancreata 3 weeks after Kras^{G12D} activation revealed lower F4/80 staining in the stroma of mice with reduced Gli1 dosage (**Figure 3.16B**). Flow cytometry analysis corroborated the decrease in CD11b+;F4/80+ macrophages (**Figure 3.16C**). Additional characterization of the myeloid populations revealed that immature myeloid cells (iMCs; Cd11b+;Gr-1+), a heterogeneous population of immature monocytes and granulocytes, was decreased in iKras*Gli1$^{lacZ/+}$ samples compared to iKras* tissues

(**Figure 3.16D**). Both polymophonuclear-derived iMCs (PMN-iMCs) and mononuclear-derived iMCs (Mo-iMCs) were reduced in iKras*Gli1$^{lacZ/+}$ pancreata (**Figures 3.16E and 3.16F**).

Analysis of T cell subsets revealed significantly elevated CD3+ lymphocyte populations in the iKras*Gli1$^{lacZ/+}$ pancreas (**Figure 3.17A**). More specifically, both CD3+/CD4+ Helper T helper cells (**Figure 3.17B**) and CD3+/CD8+ Cytotoxic T cells (**Figure 3.17C**) were significantly increased in iKras*Gli1 $^{lacZ/+}$ pancreas. However, levels of CD3+/CD4+/CD25+/FoxP3+ Regulatory T cells were equivalent between iKras* and iKras*Gli1 $^{lacZ/+}$ pancreas (**Figure 3.17D**). Thus, the changes in the myeloid cell subset correlated with the changes observed in the T cell populations. Moreover, upon matching qRT-PCR *Gli1* expression with flow analyzed immature myeloid cell populations for individual iKras*Gli1 $^{lacZ/+}$ mice, we found a positive correlation between Gli1 levels and myeloid cell infiltration (**Figure 3.17E**). Taken together, these data indicate a novel role for Gli1 in regulating the immune cell response in the neoplastic pancreas.

Reduced Gli1 Expression Decreases M2 Macrophage Recruitment to the Pancreas

During tissue recovery, macrophages play an important role in multiple aspects of the wound healing process (for review, see (33)). In particular, alternatively activated macrophages (M2) can digest cell debris and extracellular matrix (ECM) components to promote tissue remodeling (34,35). Given the importance of M2 macrophages in tissue recovery, we tested whether a reduction in Gli1 affected their recruitment. We

performed flow cytometry on pancreas after 3 weeks of $Kras^{G12D}$ activation, as well as 3 days following subsequent $Kras^{G12D}$ inactivation to detect numbers of M2 (CD11b+;CD64+;F4/80+;CD11c-;CD206+) and M1 (CD11b+;CD64+;F4/80+;CD206-;CD11c+) macrophages. In both iKras* and iKras*Gli1 $^{lacZ/+}$ mice, M2 macrophage numbers were comparably low at 3 weeks of $Kras^{G12D}$ activation. Interestingly, M2 macrophage numbers increased significantly upon $Kras^{G12D}$ inactivation in iKras* mice. However, we detected a significant decrease in M2 macrophages in iKras*Gli1 $^{lacZ/+}$ mice at this timepoint (**Figure 3.17F**). This population reduction was specific to M2 macrophages, as M1 macrophage populations were comparable between iKras* and iKras*Gli1 $^{lacZ/+}$ mice at both timepoints tested (**Figure 3.17G**). Thus, the specific macrophage population that is critical for tissue repair is decreased in iKras*$Gli1^{lacZ/+}$ mice.

Canonical Hedgehog Signaling is Required for Pancreas Recovery

To determine whether the loss of Gli1 affected pancreas tissue repair through the HH pathway (36), we used 2 complementary in vivo approaches. First, we investigated the ability of mice lacking expression of SHH ligand in the pancreatic epithelium (Pft1a-Cre;$Shh^{f/f}$) to recover from pancreatitis. Similar to $Gli1^{LacZ/+}$ mice, Pft1a-Cre;$Shh^{f/f}$ mice displayed defects in stromal remodeling 1 week after pancreatitis (**Figure 3.18**). Second, we used a pharmacological method to inhibit canonical HH signaling. PanIN-bearing iKras* mice were treated with either the Smo-antagonist LDE225 or with vehicle by oral gavage every 24 hours for 2 weeks following $Kras^{G12D}$ inactivation (**Figure 3.19A**). As expected, vehicle-treated iKras* mice showed complete recovery of the

epithelium and remodeling of the stroma. In contrast, the vast majority of LDE225-treated tissues did not recover (**Figures 3.19B and 3.19C**). Similar to iKras*Gli1$^{lacZ/+}$ mice, LDE225-treated iKras* pancreata showed improper stromal remodeling, with abundant residual collagen deposition (**Figure 3.19C, bottom row**). LDE225-treated mice also displayed SMA and pERK1/2 positivity throughout the stroma, indicating a reactive stroma that failed to resolve (**Figure 3.19C**). Thus, canonical HH signaling is necessary for PanIN regression and stromal remodeling in the pancreas.

To determine whether the cytokines we identified as GLI1 targets were regulated by canonical HH signaling, we treated WT pancreatic fibroblasts with CCM alone or with CCM and the selective Smoothened inhibitors SANT-1 or SANT-2 (**scheme in Figure 3.20A**) (37). After 6 hours of treatment, cells were collected for qRT-PCR analysis. CCM treatment induced expression of *IL-6*, *Mcp-1*, *mIL-8*, and *M-csf*, as seen previously. However, concomitant HH inhibition significantly reduced the level of induction, indicating that ligand-dependent HH signaling mediates activation of these targets (**Figure 3.20B**). Collectively, our in vivo and in vitro data reveals a requirement for canonical HH signaling for cytokine expression in fibroblasts and for pancreas tissue repair.

Discussion

The HH signaling pathway is essential for proper embryonic development and adult tissue homeostasis (38). HH signaling culminates in the modulation of the GLI1 family of transcription factors that in turn regulate the gene expression mediating HH-

dependant cellular responses (for review see (39)). Mammals possess 3 GLI transcription factors, GLI1, GLI2 and GLI3. While both Gli2 and Gli3 mutant mice die embryonically or perinatally due to a range of HH-dependent developmental defects, Gli1 mutant mice are viable and fertile, and reach adulthood with no apparent impairment (40). However, recent studies indicate that these mice have defects in regulating inflammation and tissue repair following injury (41). Specifically, mice hemizygous for Gli1 are more susceptible to intestinal inflammation and chemical-induced injury (42). Gli1+/- mice are also less susceptible to inflammation-induced metaplasia upon H. pylori infection (43). In humans, a variant of Gli1 with reduced transcriptional function confers higher susceptibility to irritable bowel disease mediated by an altered myeloid response (42). Thus, both in previous studies and in our work, Gli1 dosage appears to mediate critical aspects of myeloid cell function in the gastrointestinal system. These findings in could be explained with a threshold model, wherein the overall ratio of GLI activator and repressor are crucial for transcriptional output. Future studies will be required to examine the requirement for other GLI factors in pancreatic cancer. We have previously shown that GLI activity in pancreatic fibroblasts leads to expression of IL-6, an inflammatory cytokine that activates Stat3 in the pancreatic cancer cells (26). However, the regulation of Gli1 expression and its role in pancreatitis and tissue repair, and during the onset of pancreatic cancer has not been comprehensively addressed.

Here, we investigated the role of Gli1 during tissue repair in the pancreas. Unlike the stomach and intestine, which have a basal level of active HH signaling, components

of the HH pathway are undetectable in the normal pancreas both during development and in the adult tissue (24,44). However, HH signaling is activated during pancreatitis (45), as well as in pancreatic cancer (46,47). The specific role of Gli1 during those processes, however, was not previously explored. We investigated the effect of reducing Gli1 dosage in 2 pathologic contexts: induction of acute pancreatitis and pancreatitis-induced pancreatic carcinogenesis. Inactivation of a single copy of Gli1 disrupted tissue repair following both pancreatitis and oncogenic Kras inactivation.

We determined that Gli1 was primarily expressed in pancreatic fibroblasts. The primary function of fibroblasts is to secrete extracellular matrix proteins and thus provide structural integrity to connective tissues (48). However, these cells not only contribute to tissue homeostasis but also respond to epithelial damage. In addition to promoting epithelial recovery, fibroblasts secrete a range of immunomodulatory proteins, such as IL-6, MCP-1, and IL-8, which regulate immune cell function during both tissue damage and recovery (49,50). This function is critical, as improper immune cell recruitment has adverse effects on various aspects of tissue healing. Though fibroblast-mediated regulation of immune response is important for wound recovery, few studies have focused on the ability of these stromal cells to coordinate immune cell recruitment and function during neoplasia (51). In this study we found that Gli1$^{lacZ/+}$ fibroblasts had a significantly altered transcriptional profile compared to their WT counterparts in response to cancer cell conditioned media. Notably, loss of Gli1 resulted in lower transcriptional levels of multiple potent factors that regulate immune cell migration and function, such as M-csf, Mcp-1, and mIL-8. Consequently, we found that in vivo, the

profile of immune cells in the PanIN bearing pancreas is significantly altered; loss of Gli1 results in fewer myeloid cells and greater numbers of T cells.

The precise regulation of the immune response is critical for tissue recovery. In particular, the monocyte-macrophage population plays a vital role; these cells participate in wound debridement, the removal of extracellular matrix and dead or damaged cells (31). In the liver, macrophage depletion during recovery from inflammatory injury resulted in impaired stromal remodelling. However, depletion of macrophages during injury induction led to an overall reduction in scar matrix (52). Likewise, our data suggests that the improper recruitment of myeloid cells, particularly M2 macrophages, leads to improper pancreatic repair in iKras*Gli1$^{lacZ/+}$ mice.

In summary, our studies show that Gli1 is a key modulator of pancreatic inflammation, through transcriptional regulation of cytokine production in pancreatic fibroblasts. A working model summarizing our findings is provided in **Figure 3.21**.

Acknowledgments

This work was supported, in whole or in part, by National Institutes of Health Grants 1R01CA151588-01 (to Marina Pasca di Magliano) and 1R21CA167122-01 (to Ben Allen and Marina Pasca di Magliano). This work was also supported by the University of Michigan Biological Scholar. Both Esha Mathew (EM) and Meredith Collins (MC) contributed equally to this work. EM was supported by a National Institutes of Health Training Grant T32 GM007315 and T32 DK094775. MC was supported by

National Institutes of Health Training Grant 5-T32-HD007515. We thank Elizabeth Skendovich and Marsha Thomas for technical support

Figures

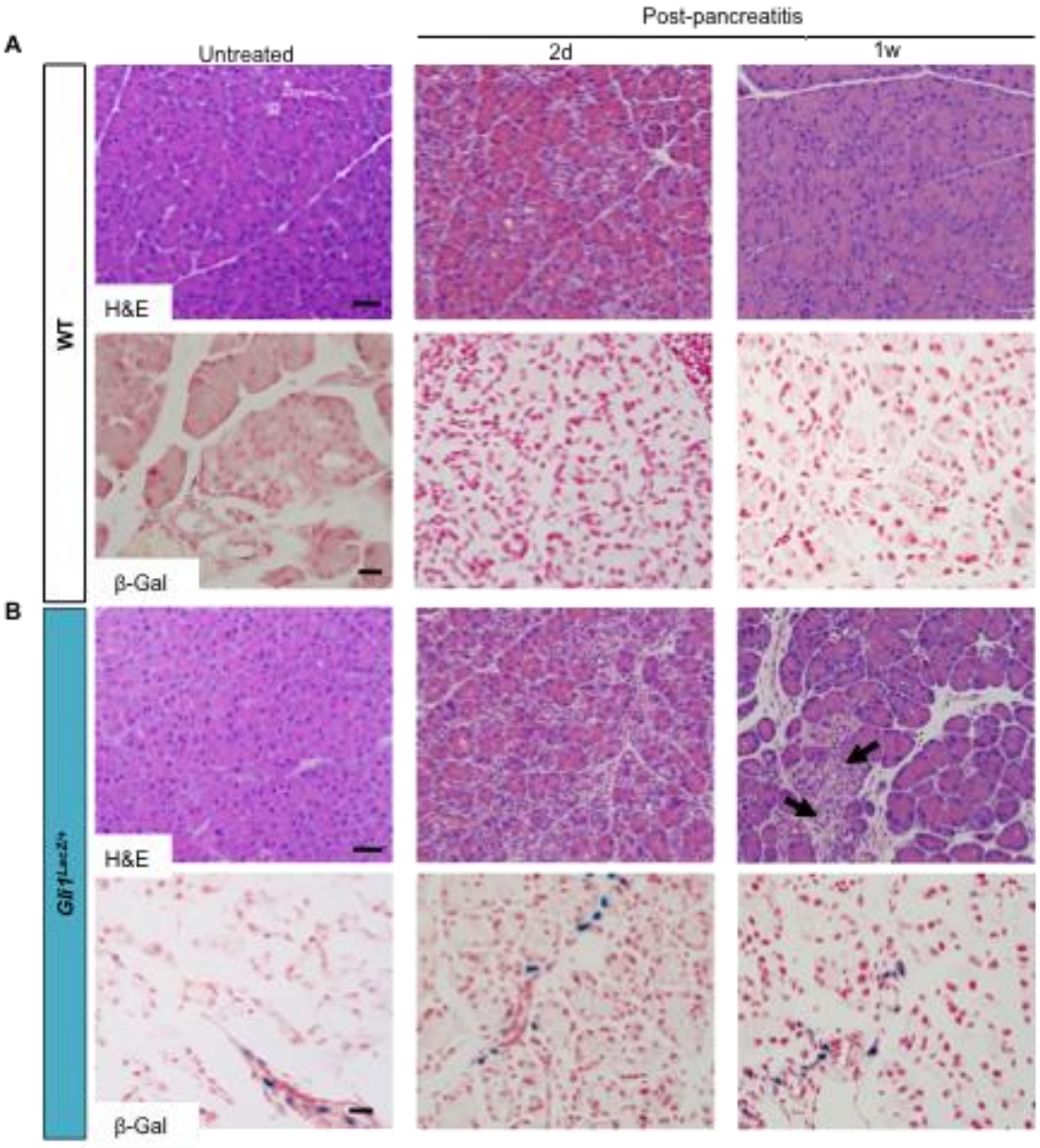

Figure 3.1: Reduced expression of Gli1 delays tissue repair following pancreatitis

(A) H&E (scale bars 50µm) and ß-Gal staining (scale bars 20µm) for (A) WT and (B) Gli1$^{lacZ/+}$ mice either untreated or 2d and 1w following pancreatitis. Gli1$^{lacZ/+}$ pancreata exhibit a delay in tissue recovery compared to WT, with some fibrotic areas remaining (black arrows) 1w post-pancreatitis.

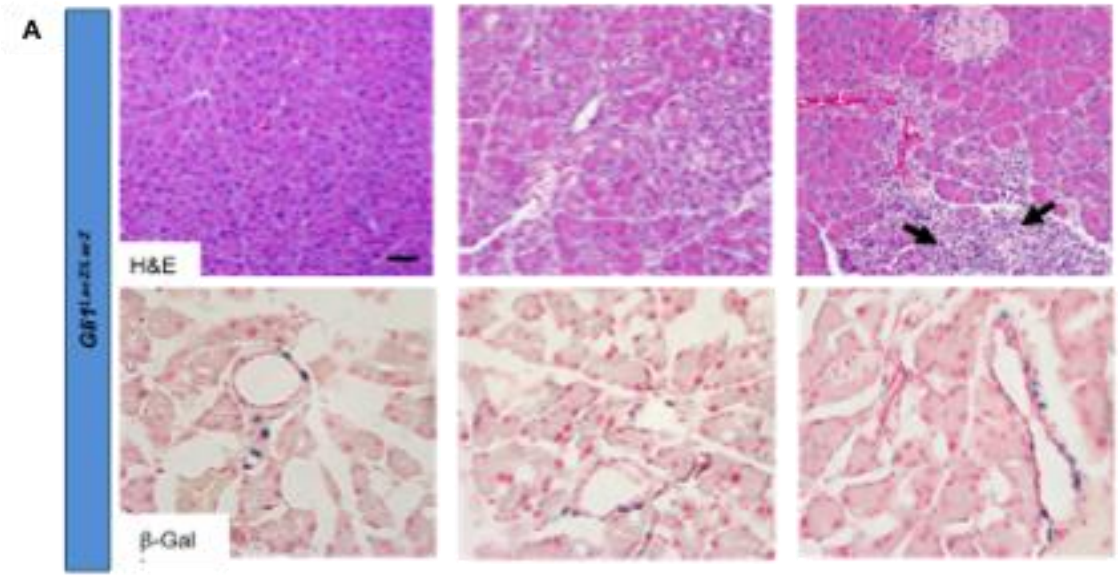

Figure 3.2: Deletion of Gli1 delays tissue repair following pancreatitis

(A) H&E (scale bars 50µm) and ß-Gal staining (scale bars 20µm) for $Gli1^{lacZ/lacZ}$ mice either untreated or 2d and 1w following pancreatitis. $Gli1^{lacZ/lacZ}$ pancreata, like $Gli1^{lacZ/+}$ pancreata, exhibit a delay in tissue recovery compared to WT, with some fibrotic areas remaining (black arrows) 1w post-pancreatitis.

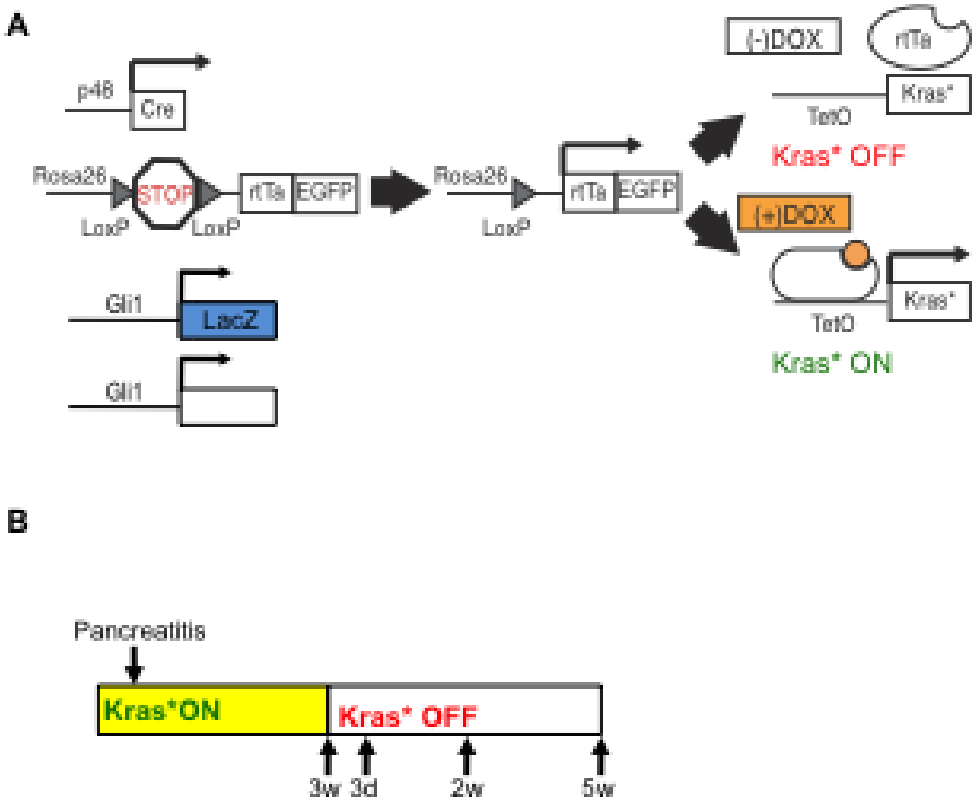

Figure 3.3: Reduced expression of Gli1 impairs tissue recovery following oncogenic Kras inactivation.

(A) Genetic makeup of iKras*Gli1$^{lacZ/+}$ mice. (B) Experimental Design. Kras*=Kras^{G12D}.

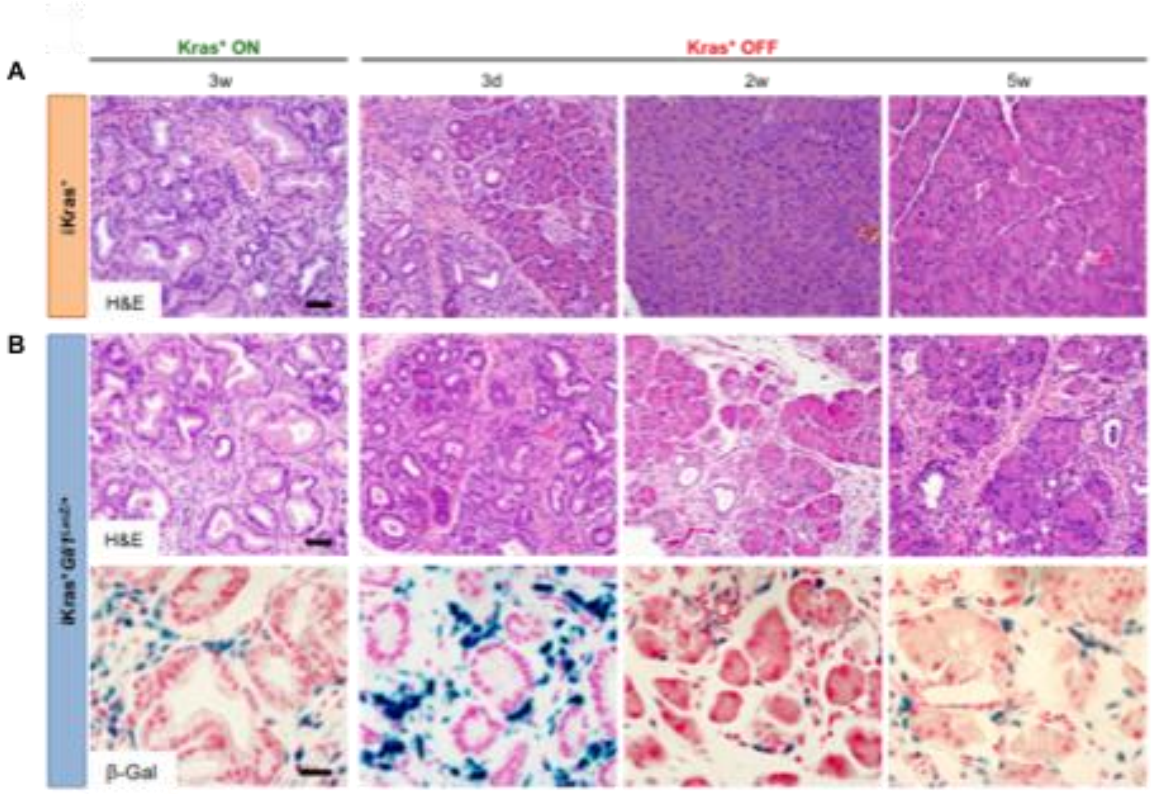

Figure 3.4: Reduced expression of Gli1 impairs tissue recovery following oncogenic Kras inactivation.

(A) H&E (scale bars 50µm) for iKras* and (B) H&E (scale bars 50µm) and ß-Gal staining (scale bars 20µm) iKras*Gli1$^{lacZ/+}$ pancreata with Kras* active (Kras* ON) for 3w, and following Kras* inactivation (Kras* OFF) 3d, 2w, and 5w.

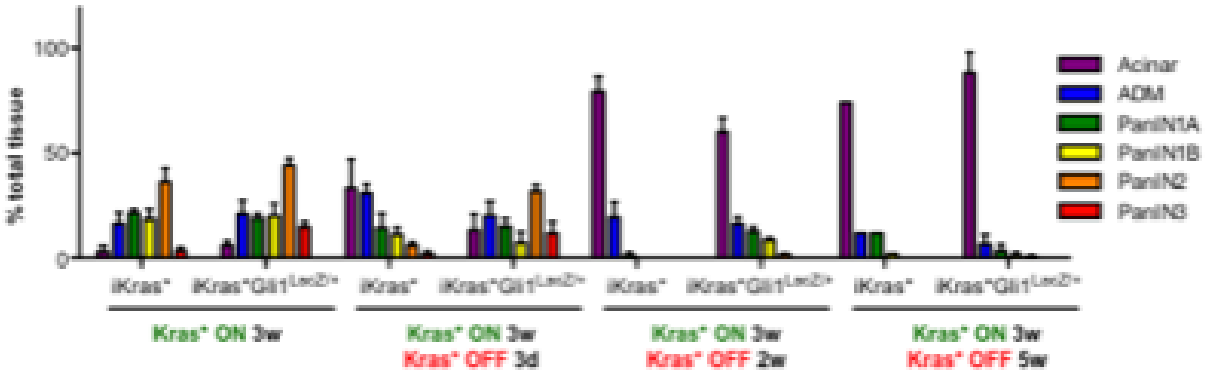

Figure 3.5: Histopathological analysis of impaired tissue recovery following oncogenic Kras inactivation.

Histopathological analysis of iKras* and iKras*Gli1$^{lacZ/+}$ tissues at the indicated time points, data represent mean ± SEM.

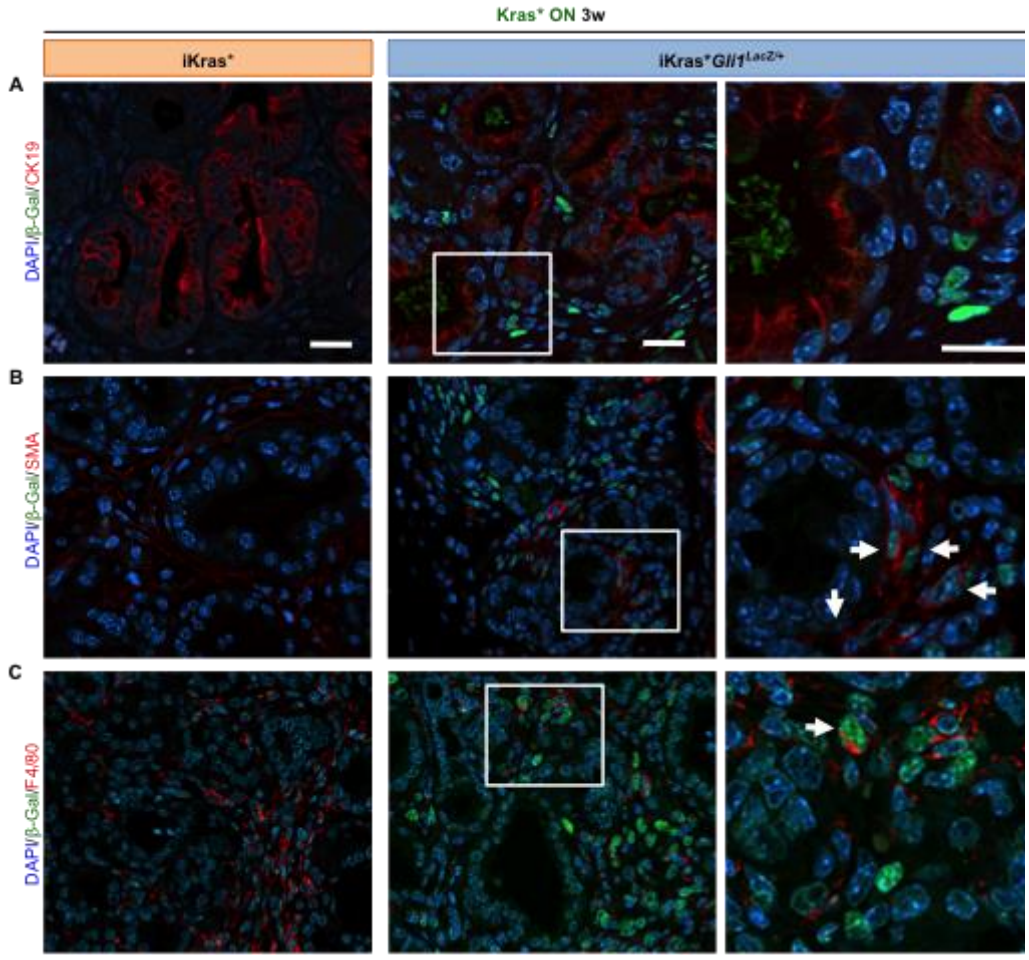

Figure 3.6: Identification of Gli1 expressing cells in the stroma

Co-immunofluorescence for ß-Gal (green) and (A) CK19, (B) SMA, and (C) F4/80 (red) in iKras* and iKras*Gli1^{lacZ}/+ PanIN lesions. Nuclei denoted by DAPI (blue). Scale bars 20µm.

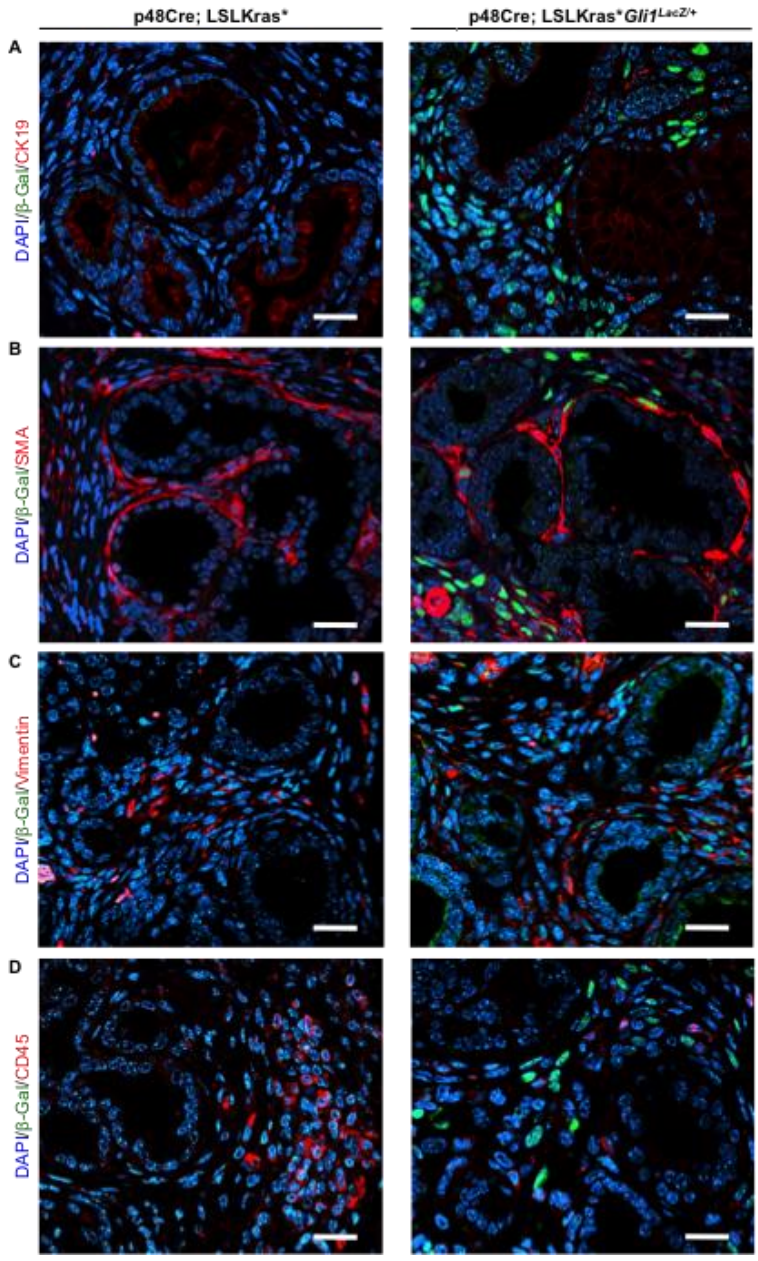

Figure 3.7: Identification of LacZ positive cells in KC mice

Coimmunofluorescence for ß-Gal (green) and (A) CK19, (B) SMA, (C) Vimentin, and (D) CD45 in KC and KC; Gli1$^{LacZ/+}$ mice 3 weeks post-pancreatitis. Nuclei denoted by DAPI (blue). Scale bars 20µm.

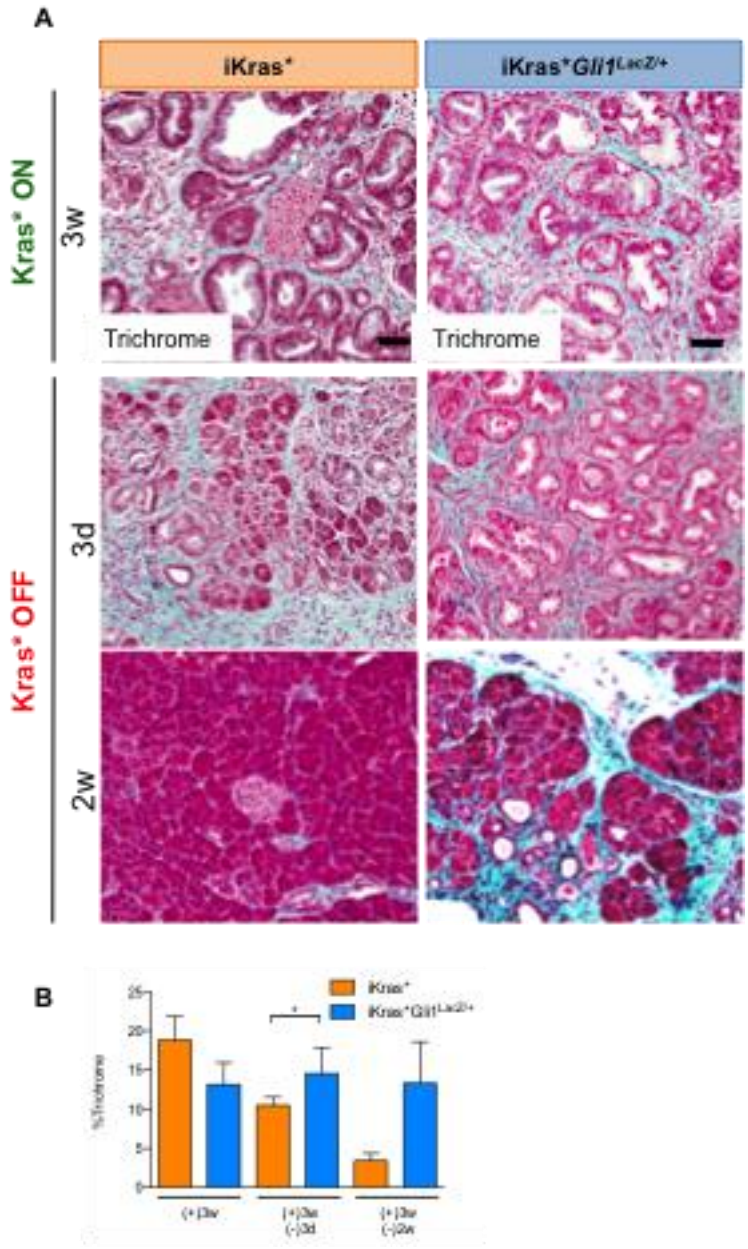

Figure 3.8: Gli1 is required for stroma remodeling.

(A) Gomori Trichrome staining of iKras* and iKras*Gli1$^{lacZ/+}$ pancreata. Scale bar 50um. (B) Quantification of Trichrome positive area (expressed as percentage of total area). Data represent mean ± SEM.

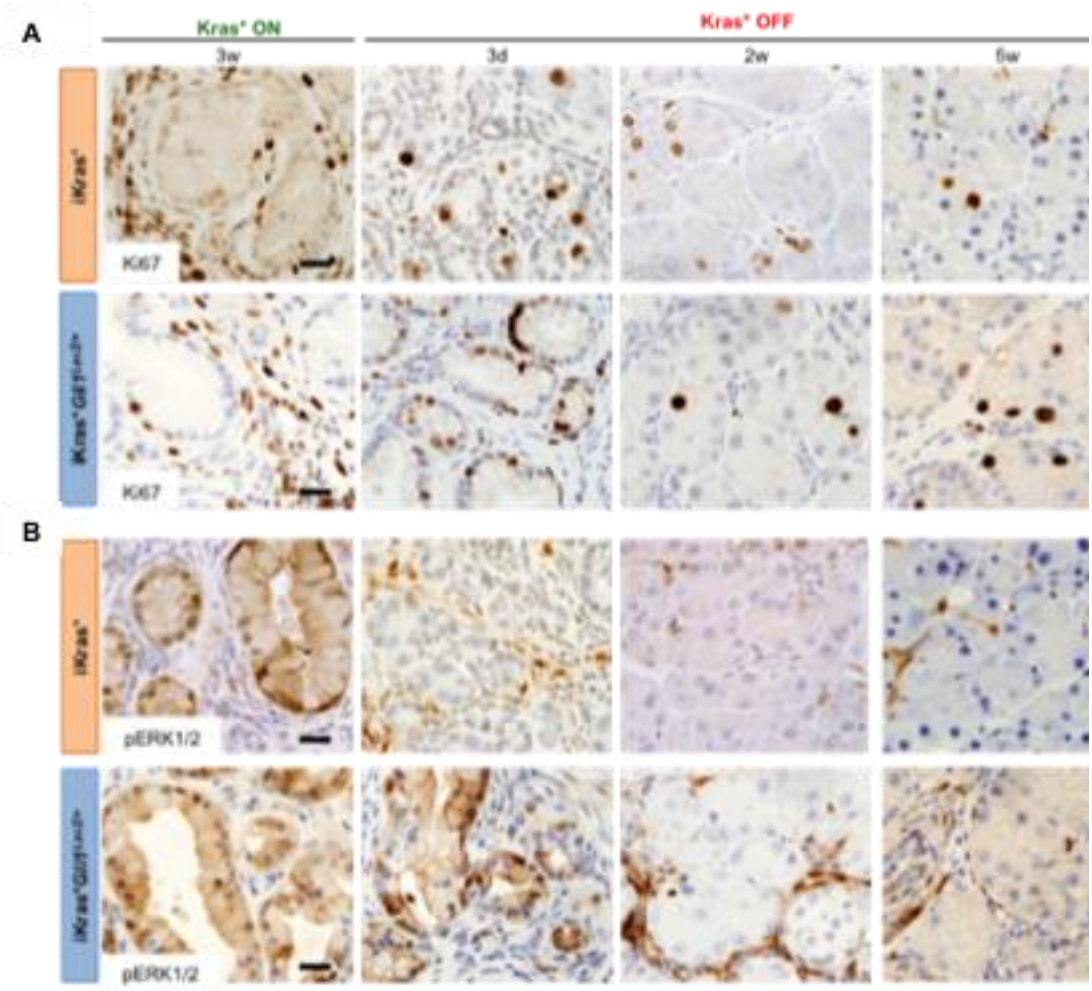

Figure 3.9: Gli1 is required for stroma remodeling.

Immunohistochemistry for (A) Ki67 and (B) pERK1/2 in iKras* and iKras*Gli1$^{lacZ/+}$ pancreata. Scale bars 20µm.

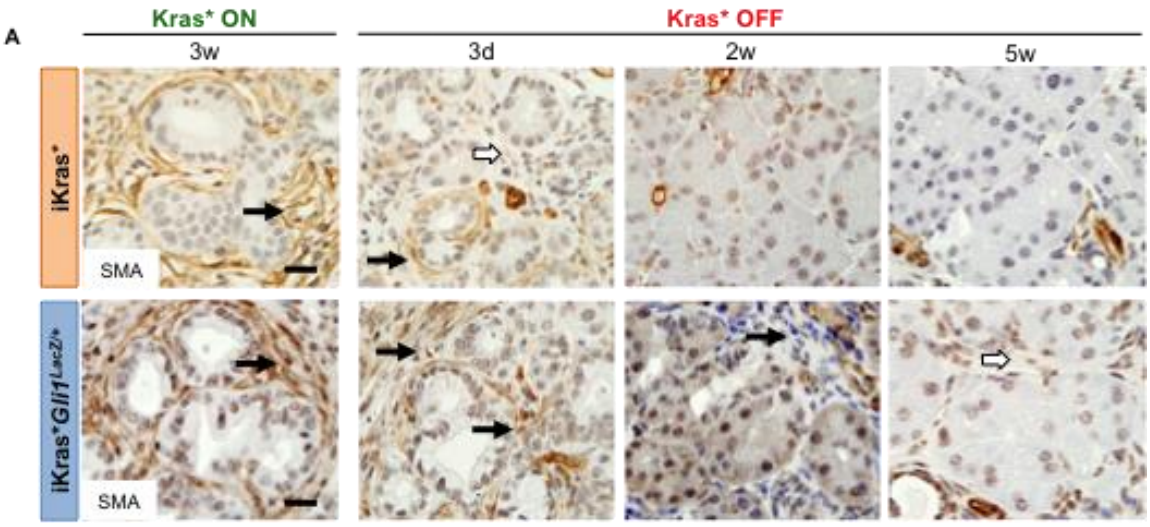

Figure 3.10: Characterization of iKras* and iKras*Gli1$^{lacZ/+}$ tissues upon Kras* inactivation.

(A) Immunohistochemistry for SMA in iKras* and iKras*Gli1$^{lacZ/+}$ pancreata. Black arrows indicate fibroblasts positive for SMA expression, white arrows indicate fibroblasts negative for SMA expression. Scale bars 20μm.

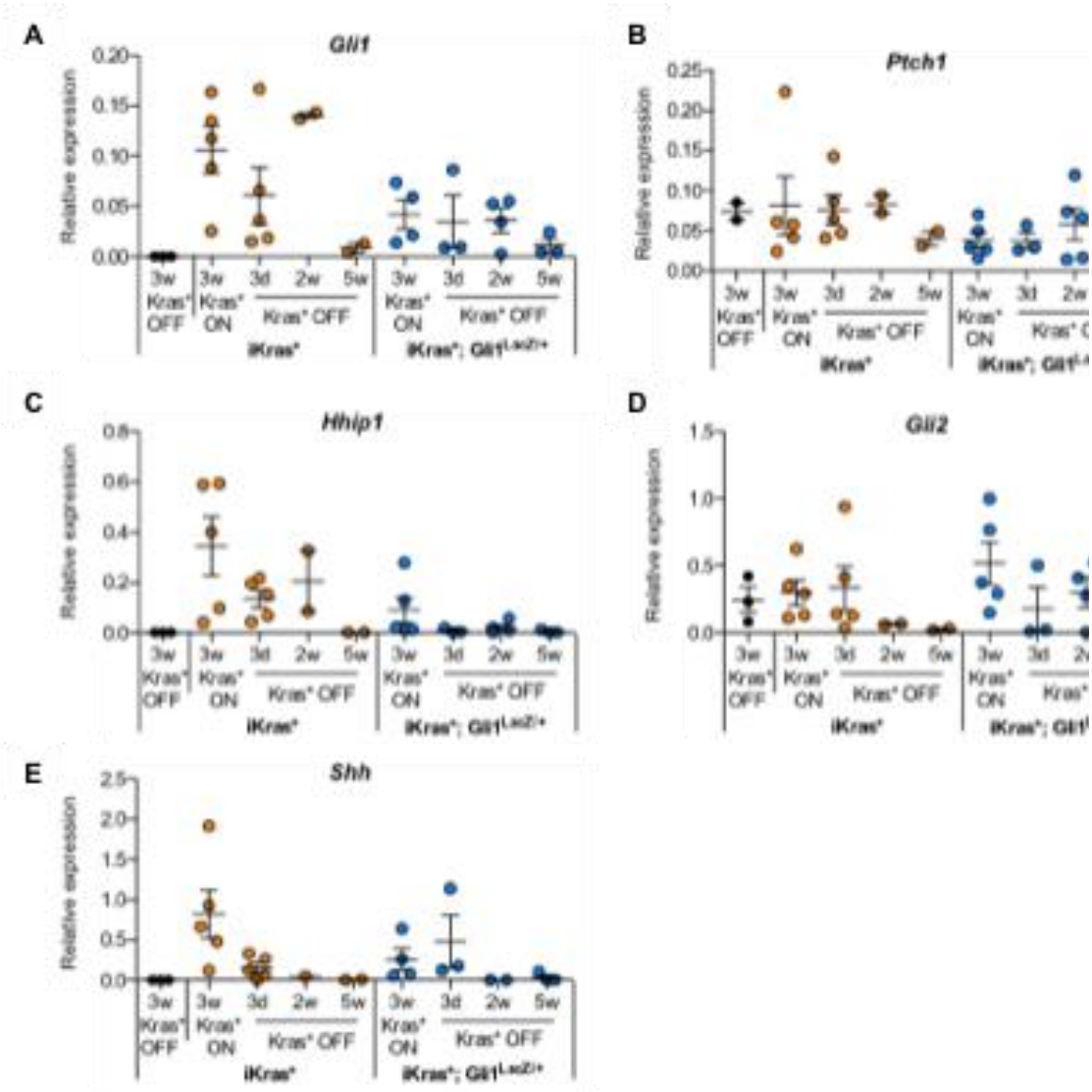

Figure 3.11: Characterization of HH signaling in iKras* and iKras*Gli1$^{lacZ/+}$ tissues upon Kras* inactivation.

qRT-PCR for HH signaling pathway components (A) *Gli1*, (B) *Ptch1*, (C) *Hhip1*, (D) *Gli2*, and (E) *Shh*.

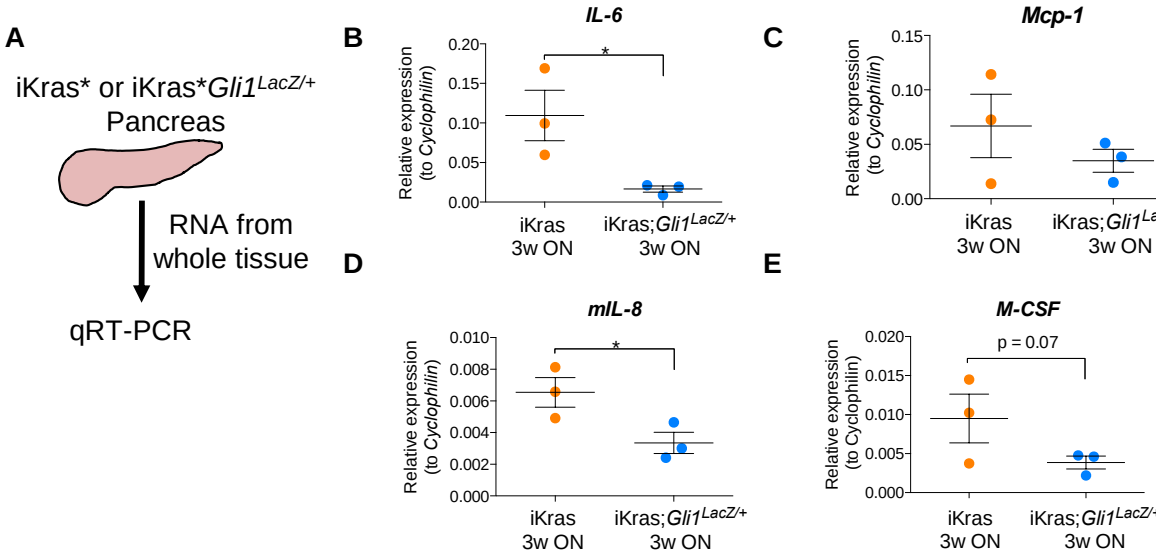

Figure 3.12: Reduced expression of Gli1 alters HH response and the cytokine transcriptional profile of pancreatic tissue.

(A) Experimental design. qRT-PCR analysis for (B) *IL-6* (C) *Mcp-1* (D) *mIL-8* and (E) *M-csf* in iKras* and iKras*Gli1$^{lacZ/+}$ pancreata.

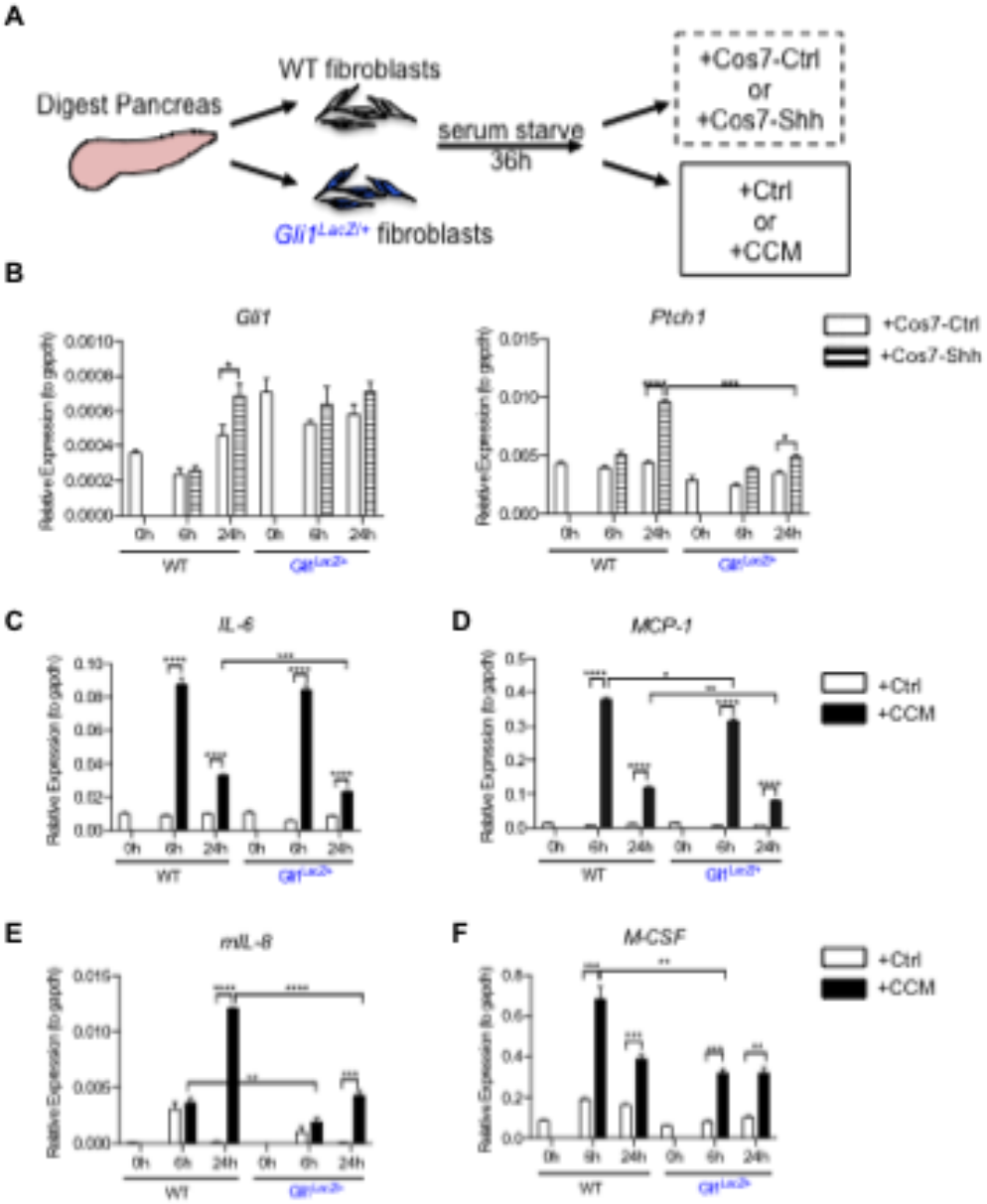

Figure 3.13: Reduced expression of Gli1 alters Hh response and the cytokine transcriptional profile of pancreatic fibroblasts.

(A) Experimental design. qRT-PCR analysis for (B) Hh target genes Gli1 and Ptch1 in both WT and $Gli1^{lacZ/+}$ fibroblasts following treatment with Cos7-ctrl or Cos7-Shh conditioned media. qRT-PCR analysis for cytokines (C) *IL-6*, (D) *Mcp-1*, (E) *mIL-8*, and (F) *M-csf* in both WT and $Gli1^{LacZ/+}$ fibroblasts following treatment with control (Ctrl) or cancer-cell conditioned media (CCM).

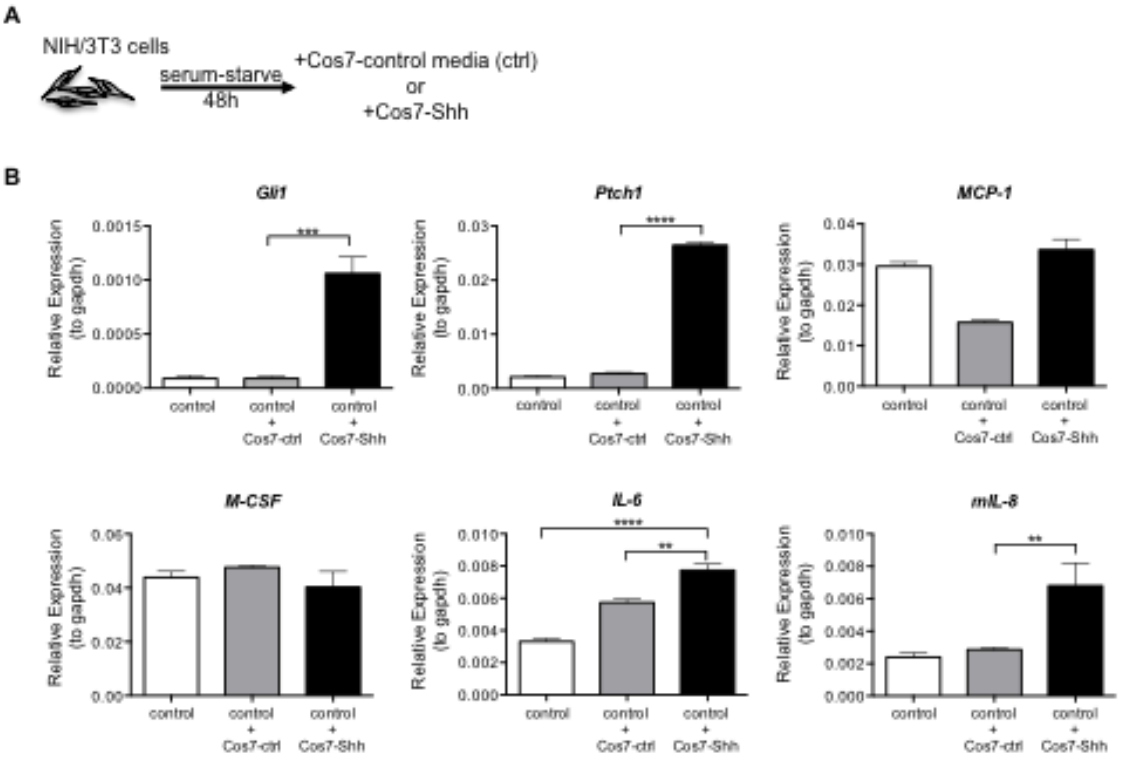

Figure 3.14: Identification of Gli1 target genes.

(A) Experimental design. (B) qRT-PCR analysis for HH target genes *Gli1* and *Ptch1*, and the cytokines *Mcp-1, M-Csf, IL-6*, and *mIL-8* in NIH3T3 cells following treatment with Cos7-ctrl or Cos7-Shh conditioned media.

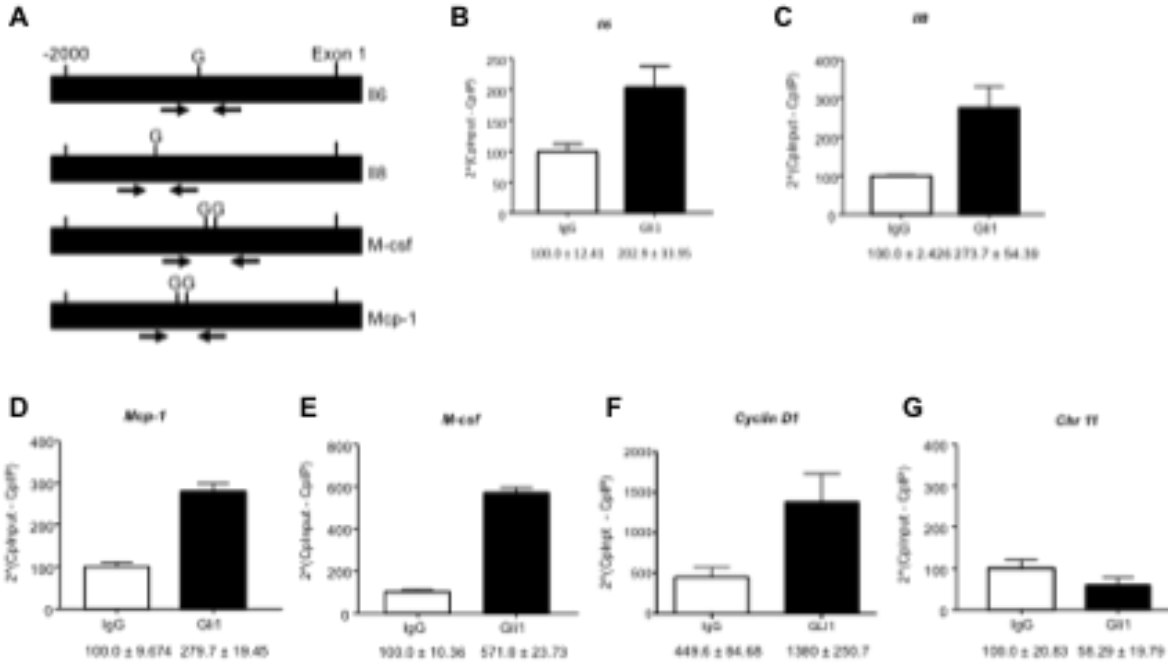

Figure 3.15: Identification of Gli1 binding sites.

(A) Putative GLI1 binding sites on cytokines' 5' region. (B-E) Chromatin immunoprecipitation assay on putative GLI1 binding regions, (F) on positive control Cyclin D1, and (G) on a region lacking GLI1 binding sites as a negative control.

(Data/Figure credit: Dr. Maite Fernandez-Barrena in the lab of Dr. Martin Fernandez-Zapico.)

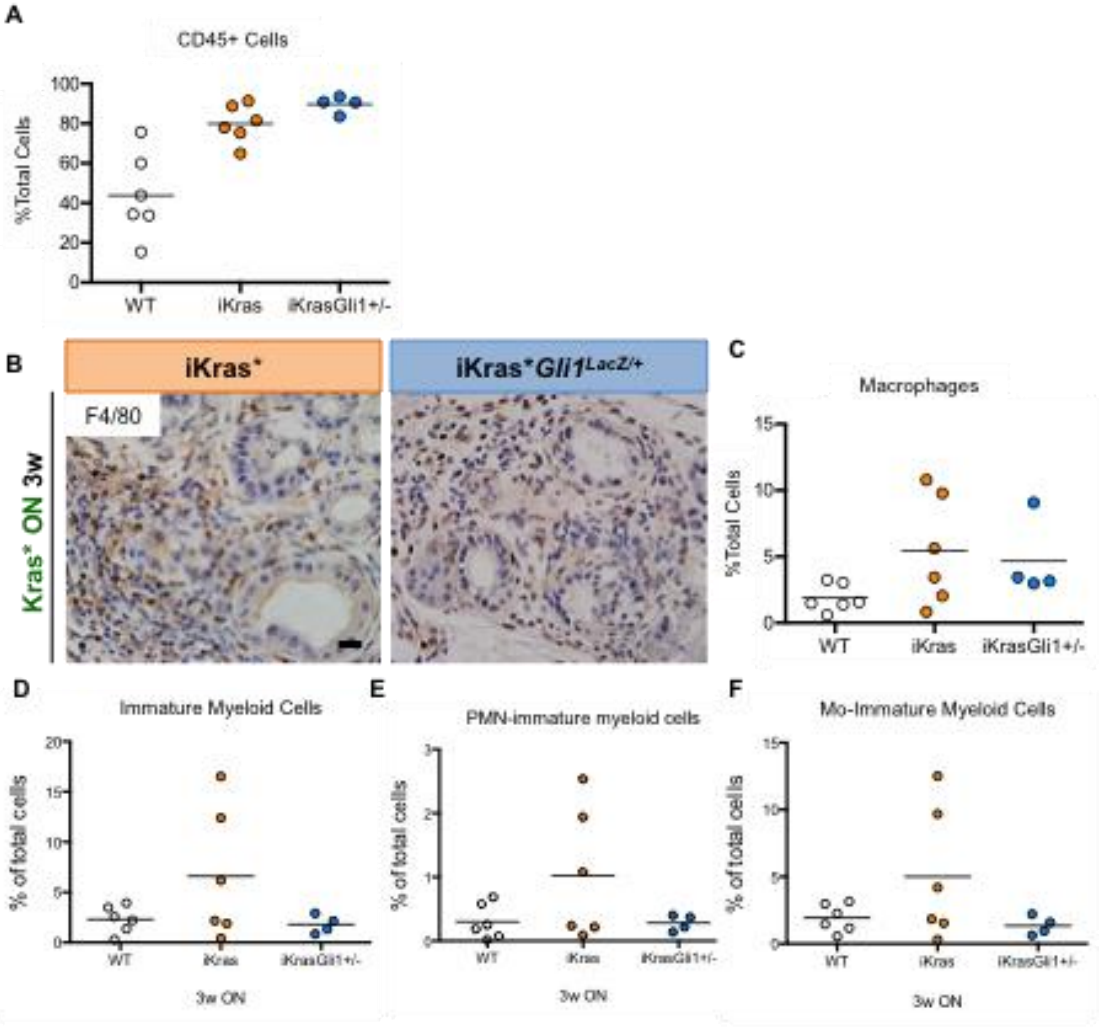

Figure 3.16: Tissues with reduced Gli1 expression have altered immune infiltration

(A) Flow cytometry analysis for CD45+ cells. (B) Immunohistochemistry for F4/80 macrophages in iKras* and iKras*Gli1$^{lacZ/+}$ pancreata. Flow cytometry analysis for (C) macrophages (D) immature myeloid cells (E) polymorphonuclear-derived immature myeloid cells, and (F) mononuclear-derived immature myeloid cells

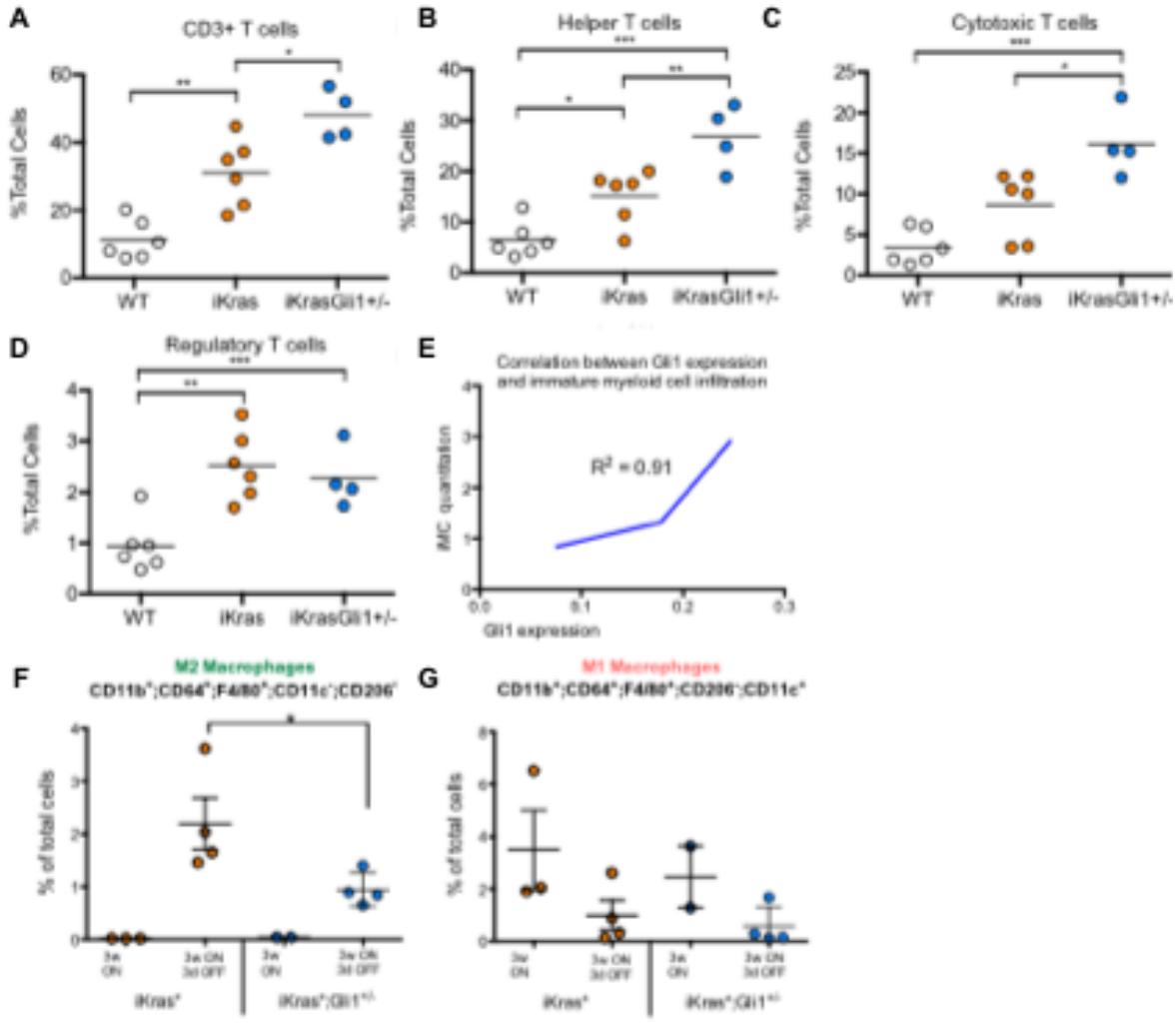

Figure 3.17: Tissues with reduced Gli1 expression have altered immune infiltration

Flow cytometry analysis for (A) CD3+ T cells (B) Helper T cells (C) Cytotoxic T cells, and (D) Regulatory T cells. (E) Correlation between *Gli1* expression and immature myeloid cell infiltration in iKras*Gli1$^{lacZ/+}$ pancreata. Flow cytometry analysis for (F) M2 macrophages and (G) M1 macrophages.

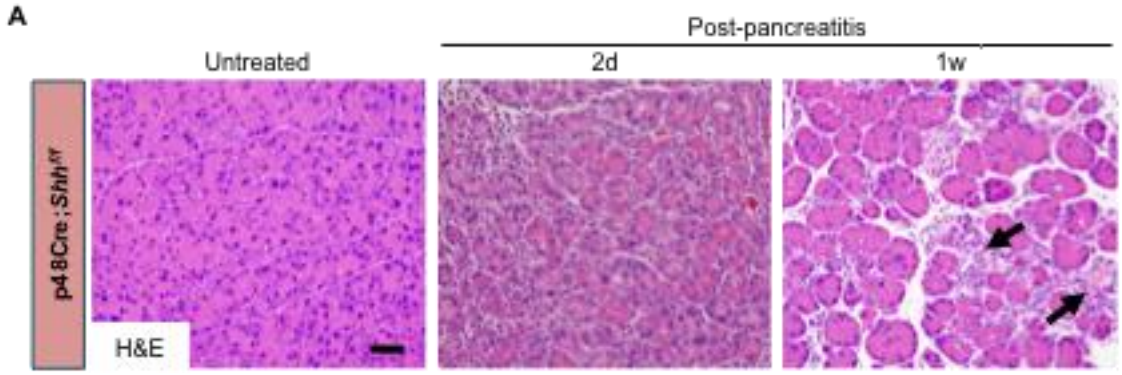

Figure 3.18: Canonical Hh signaling is essential for pancreatic tissue repair following injury

(A) H&E for p48Cre;*Shh*$^{f/f}$ pancreata either untreated or 2d and 1w following pancreatitis. Fibrotic areas are highlighted with black arrows.

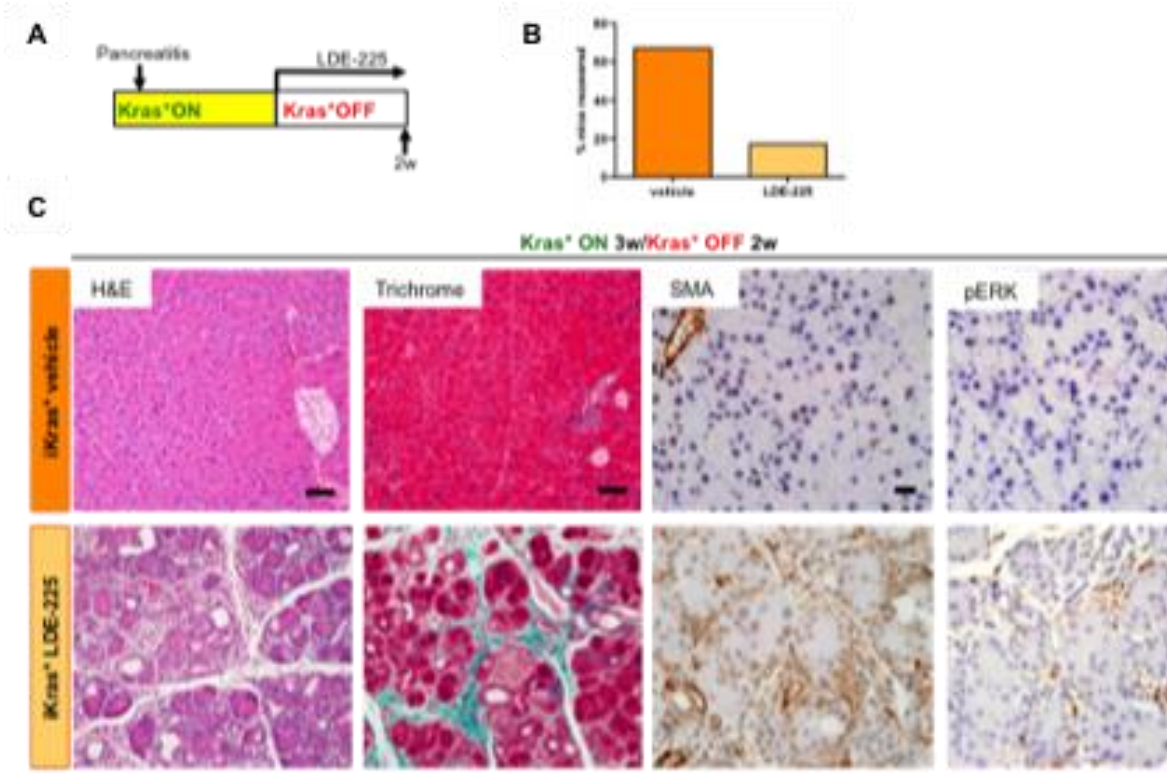

Figure 3.19: Inhibition of HH signaling impairs pancreatic tissue repair following injury

(A) Experimental Design (B) Quantitation of tissue repair (C) H&E (scale bars 50μm), Gomori Trichrome (scale bars 50μm), SMA immunostaining (scale bars 50μm), and pERK1/2 immunostaining (scale bars 50μm) for iKras* pancreata with Kras* active (Kras* ON) for 3w and subsequently inactivated (Kras* OFF) 2w. Mice were treated with vehicle or Smo antagonist LDE-225 during the 2 weeks following Kras* inactivation.

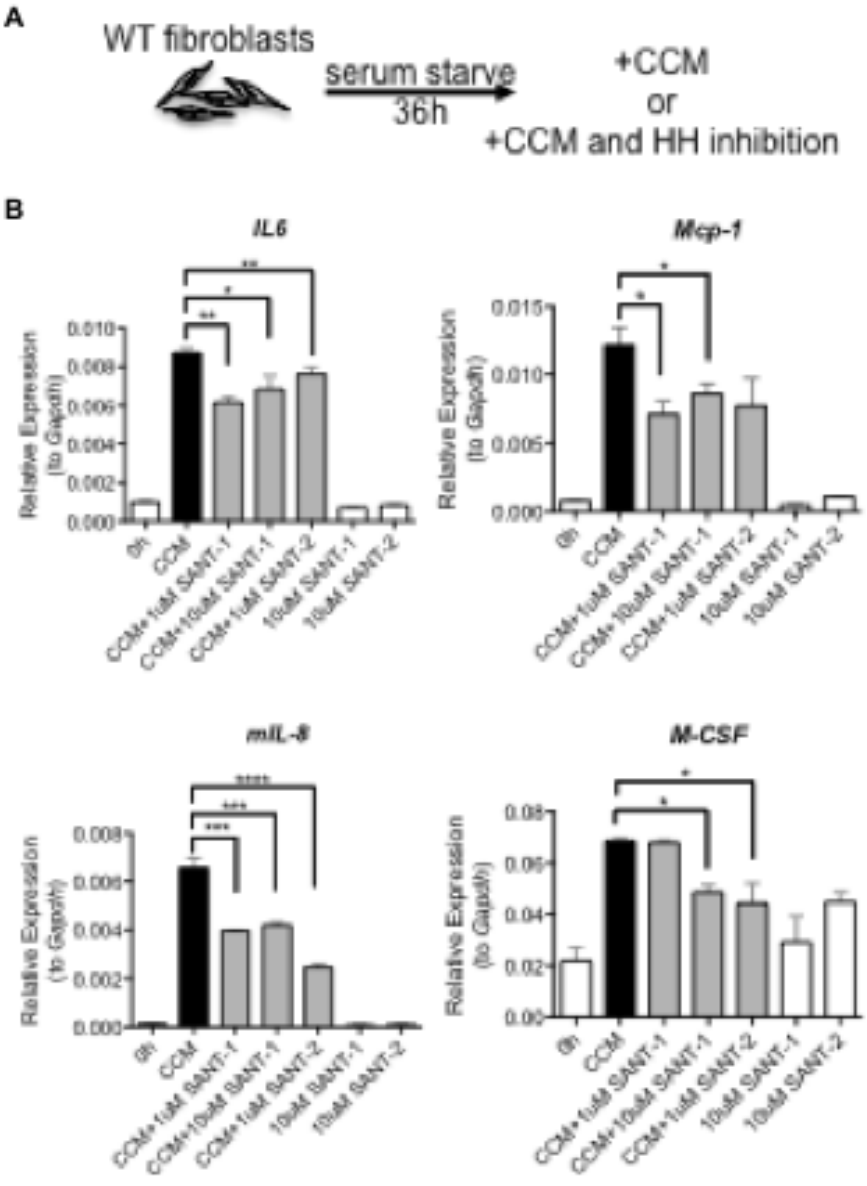

Figure 3.20: Canonical HH signaling is essential for cytokine secretion from pancreatic fibroblasts

(A) Experimental Design. (B) qRT-PCR analysis for cytokines IL-6, Mcp-1, mIL-8, and M-csf in WT pancreatic fibroblasts treated with cancer conditioned media (CCM) with and without concomitant HH inhibition.

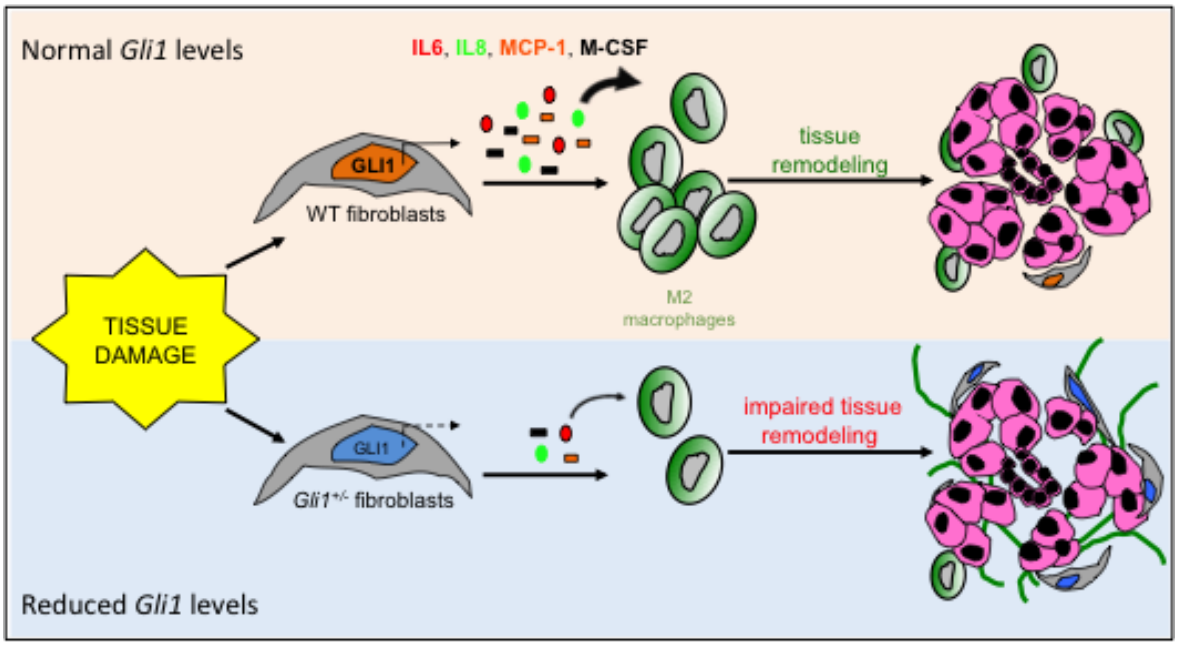

Figure 3.21: Working model of *Gli1* regulation of pancreas remodeling following injury

Following injury, pancreatic fibroblasts upregulate the expression of cytokines regulating myeloid cell recruitment and function. *Gli1* dosage is critical for this response. Reduced *Gli1* dosage leads to reduced cytokine expression and impaired recruitment of myeloid cells. Specifically, the recruitment of M2 macrophages -the myeloid population critical for injury repair and tissue remodeling- is reduced. Ultimately, reduction in *Gli1* dosage results improper pancreatic recovery.

Tables

Table 3.1: Primer sequences		
Gene	**Forward (5'-3')**	**Reverse (5'-3')**
TREKras	caaggacaaggtgtacagttatgtgact	gcctgcgacgcggcatctgc
Gli1	gcagtgggtaacatgagtgtct	aggcactagagttgaggaatttgt
Ptch1	ttgtggaagccacagaaaacc	tgtctggagtccggatgga
Hhip1	gctctcgtttaagctgctactg	caaacttcgcatctccttcaaag
Gli2	gtgcacagcagccccacactctc	ggtaatagtctgaagggttggtgcctgg
Shh	caaagctcacatccactgttctg	gaaacagccgccggattt
IL-6	ttccatccagttgccttcttgg	ttctcatttccacgatttcccag
Mcp-1	ttaaaaacctggatcggaaccaa	gcattagcttcagatttacgggt
IL-8	ctgcacccaaaccgaagtcat	ttgtcagaagccagcgttcac
M-csf	gacttcatgccagattgcc	ggtggctttagggtacagg
Cyclin D1	taggaaggagcctatcgtgtctca	caacagctcaagatggtggccatt

References

1. Rooman, I., and Real, F. X. (2012) Pancreatic ductal adenocarcinoma and acinar cells: a matter of differentiation and development? Gut 61, 449-458
2. Hruban, R. H., Adsay, N. V., Albores-Saavedra, J., Compton, C., Garrett, E. S., Goodman, S. N., Kern, S. E., Klimstra, D. S., Kloppel, G., Longnecker, D. S., Luttges, J., and Offerhaus, G. J. (2001) Pancreatic intraepithelial neoplasia: a new nomenclature and classification system for pancreatic duct lesions. Am J Surg Pathol 25, 579-586
3. Biankin, A. V., Waddell, N., Kassahn, K. S., Gingras, M. C., Muthuswamy, L. B., Johns, A. L., Miller, D. K., Wilson, P. J., Patch, A. M., Wu, J., Chang, D. K., Cowley, M. J., Gardiner, B. B., Song, S., Harliwong, I., Idrisoglu, S., Nourse, C., Nourbakhsh, E., Manning, S., Wani, S., Gongora, M., Pajic, M., Scarlett, C. J., Gill, A. J., Pinho, A. V., Rooman, I., Anderson, M., Holmes, O., Leonard, C., Taylor, D., Wood, S., Xu, Q., Nones, K., Fink, J. L., Christ, A., Bruxner, T., Cloonan, N., Kolle, G., Newell, F., Pinese, M., Mead, R. S., Humphris, J. L., Kaplan, W., Jones, M. D., Colvin, E. K., Nagrial, A. M., Humphrey, E. S., Chou, A., Chin, V. T., Chantrill, L. A., Mawson, A., Samra, J. S., Kench, J. G., Lovell, J. A., Daly, R. J., Merrett, N. D., Toon, C., Epari, K., Nguyen, N. Q., Barbour, A., Zeps, N., Kakkar, N., Zhao, F., Wu, Y. Q., Wang, M., Muzny, D. M., Fisher, W. E., Brunicardi, F. C., Hodges, S. E., Reid, J. G., Drummond, J., Chang, K., Han, Y., Lewis, L. R., Dinh, H., Buhay, C. J., Beck, T., Timms, L., Sam, M., Begley, K., Brown, A., Pai, D., Panchal, A., Buchner, N., De Borja, R., Denroche, R. E., Yung, C. K., Serra, S., Onetto, N., Mukhopadhyay, D., Tsao, M. S., Shaw, P. A., Petersen, G. M., Gallinger, S., Hruban, R. H., Maitra, A., Iacobuzio-Donahue, C. A., Schulick, R. D., Wolfgang, C. L., Morgan, R. A., Lawlor, R. T., Capelli, P., Corbo, V., Scardoni, M., Tortora, G., Tempero, M. A., Mann, K. M., Jenkins, N. A., Perez-Mancera, P. A., Adams, D. J., Largaespada, D. A., Wessels, L. F., Rust, A. G., Stein, L. D., Tuveson, D. A., Copeland, N. G., Musgrove, E. A., Scarpa, A., Eshleman, J. R., Hudson, T. J., Sutherland, R. L., Wheeler, D. A., Pearson, J. V., McPherson, J. D., Gibbs, R. A., and Grimmond, S. M. (2012) Pancreatic cancer genomes reveal aberrations in axon guidance pathway genes. Nature 491, 399-405
4. Jones, S., Zhang, X., Parsons, D. W., Lin, J. C., Leary, R. J., Angenendt, P., Mankoo, P., Carter, H., Kamiyama, H., Jimeno, A., Hong, S. M., Fu, B., Lin, M. T., Calhoun, E. S., Kamiyama, M., Walter, K., Nikolskaya, T., Nikolsky, Y., Hartigan, J., Smith, D. R., Hidalgo, M., Leach, S. D., Klein, A. P., Jaffee, E. M., Goggins, M., Maitra, A., Iacobuzio-Donahue, C., Eshleman, J. R., Kern, S. E., Hruban, R. H., Karchin, R., Papadopoulos, N., Parmigiani, G., Vogelstein, B., Velculescu, V. E., and Kinzler, K. W. (2008) Core signaling pathways in human pancreatic cancers revealed by global genomic analyses. Science 321, 1801-1806
5. Kanda, M., Matthaei, H., Wu, J., Hong, S. M., Yu, J., Borges, M., Hruban, R. H., Maitra, A., Kinzler, K., Vogelstein, B., and Goggins, M. (2012) Presence of

somatic mutations in most early-stage pancreatic intraepithelial neoplasia. Gastroenterology 142, 730-733 e739
6. Aguirre, A. J., Bardeesy, N., Sinha, M., Lopez, L., Tuveson, D. A., Horner, J., Redston, M. S., and DePinho, R. A. (2003) Activated Kras and Ink4a/Arf deficiency cooperate to produce metastatic pancreatic ductal adenocarcinoma. Genes Dev 17, 3112-3126
7. Hingorani, S. R., Petricoin, E. F., Maitra, A., Rajapakse, V., King, C., Jacobetz, M. A., Ross, S., Conrads, T. P., Veenstra, T. D., Hitt, B. A., Kawaguchi, Y., Johann, D., Liotta, L. A., Crawford, H. C., Putt, M. E., Jacks, T., Wright, C. V., Hruban, R. H., Lowy, A. M., and Tuveson, D. A. (2003) Preinvasive and invasive ductal pancreatic cancer and its early detection in the mouse. Cancer Cell 4, 437-450
8. Lowenfels, A. B., Maisonneuve, P., Cavallini, G., Ammann, R. W., Lankisch, P. G., Andersen, J. R., Dimagno, E. P., Andren-Sandberg, A., and Domellof, L. (1993) Pancreatitis and the risk of pancreatic cancer. International Pancreatitis Study Group. N Engl J Med 328, 1433-1437
9. Carriere, C., Young, A. L., Gunn, J. R., Longnecker, D. S., and Korc, M. (2011) Acute pancreatitis accelerates initiation and progression to pancreatic cancer in mice expressing oncogenic Kras in the nestin cell lineage. PLoS One 6, e27725
10. Guerra, C., Collado, M., Navas, C., Schuhmacher, A. J., Hernandez-Porras, I., Canamero, M., Rodriguez-Justo, M., Serrano, M., and Barbacid, M. (2011) Pancreatitis-induced inflammation contributes to pancreatic cancer by inhibiting oncogene-induced senescence. Cancer Cell 19, 728-739
11. Morris, J. P. t., Cano, D. A., Sekine, S., Wang, S. C., and Hebrok, M. (2010) Beta-catenin blocks Kras-dependent reprogramming of acini into pancreatic cancer precursor lesions in mice. J Clin Invest 120, 508-520
12. Jensen, J. N., Cameron, E., Garay, M. V., Starkey, T. W., Gianani, R., and Jensen, J. (2005) Recapitulation of elements of embryonic development in adult mouse pancreatic regeneration. Gastroenterology 128, 728-741
13. Guerra, C., Schuhmacher, A. J., Canamero, M., Grippo, P. J., Verdaguer, L., Perez-Gallego, L., Dubus, P., Sandgren, E. P., and Barbacid, M. (2007) Chronic pancreatitis is essential for induction of pancreatic ductal adenocarcinoma by K-Ras oncogenes in adult mice. Cancer Cell 11, 291-302
14. Kawaguchi, Y., Cooper, B., Gannon, M., Ray, M., MacDonald, R. J., and Wright, C. V. (2002) The role of the transcriptional regulator Ptf1a in converting intestinal to pancreatic progenitors. Nat Genet 32, 128-134
15. Fisher, G. H., Wellen, S. L., Klimstra, D., Lenczowski, J. M., Tichelaar, J. W., Lizak, M. J., Whitsett, J. A., Koretsky, A., and Varmus, H. E. (2001) Induction and apoptotic regression of lung adenocarcinomas by regulation of a K-Ras transgene in the presence and absence of tumor suppressor genes. Genes Dev 15, 3249-3262
16. Belteki, G., Haigh, J., Kabacs, N., Haigh, K., Sison, K., Costantini, F., Whitsett, J., Quaggin, S. E., and Nagy, A. (2005) Conditional and inducible transgene expression in mice through the combinatorial use of Cre-mediated recombination and tetracycline induction. Nucleic Acids Res 33, e51

17. Collins, M. A., Bednar, F., Zhang, Y., Brisset, J. C., Galban, S., Galban, C. J., Rakshit, S., Flannagan, K. S., Adsay, N. V., and Pasca di Magliano, M. (2012) Oncogenic Kras is required for both the initiation and maintenance of pancreatic cancer in mice. J Clin Invest 122, 639-653
18. Bai, C. B., Auerbach, W., Lee, J. S., Stephen, D., and Joyner, A. L. (2002) Gli2, but not Gli1, is required for initial Shh signaling and ectopic activation of the Shh pathway. Development 129, 4753-4761
19. Kojima, K., Vickers, S. M., Adsay, N. V., Jhala, N. C., Kim, H. G., Schoeb, T. R., Grizzle, W. E., and Klug, C. A. (2007) Inactivation of Smad4 accelerates Kras(G12D)-mediated pancreatic neoplasia. Cancer Res 67, 8121-8130
20. Hruban, R. H., Adsay, N. V., Albores-Saavedra, J., Anver, M. R., Biankin, A. V., Boivin, G. P., Furth, E. E., Furukawa, T., Klein, A., Klimstra, D. S., Kloppel, G., Lauwers, G. Y., Longnecker, D. S., Luttges, J., Maitra, A., Offerhaus, G. J., Perez-Gallego, L., Redston, M., and Tuveson, D. A. (2006) Pathology of genetically engineered mouse models of pancreatic exocrine cancer: consensus report and recommendations. Cancer Res 66, 95-106
21. Wang, P., Lin, C., Smith, E. R., Guo, H., Sanderson, B. W., Wu, M., Gogol, M., Alexander, T., Seidel, C., Wiedemann, L. M., Ge, K., Krumlauf, R., and Shilatifard, A. (2009) Global analysis of H3K4 methylation defines MLL family member targets and points to a role for MLL1-mediated H3K4 methylation in the regulation of transcriptional initiation by RNA polymerase II. Mol Cell Biol 29, 6074-6085
22. Saluja, A., Saito, I., Saluja, M., Houlihan, M. J., Powers, R. E., Meldolesi, J., and Steer, M. (1985) In vivo rat pancreatic acinar cell function during supramaximal stimulation with caerulein. Am J Physiol 249, G702-710
23. Hezel, A. F., Kimmelman, A. C., Stanger, B. Z., Bardeesy, N., and Depinho, R. A. (2006) Genetics and biology of pancreatic ductal adenocarcinoma. Genes Dev 20, 1218-1249
24. Pasca di Magliano, M., Sekine, S., Ermilov, A., Ferris, J., Dlugosz, A. A., and Hebrok, M. (2006) Hedgehog/Ras interactions regulate early stages of pancreatic cancer. Genes Dev 20, 3161-3173
25. Andoh, A., Takaya, H., Saotome, T., Shimada, M., Hata, K., Araki, Y., Nakamura, F., Shintani, Y., Fujiyama, Y., and Bamba, T. (2000) Cytokine regulation of chemokine (IL-8, MCP-1, and RANTES) gene expression in human pancreatic periacinar myofibroblasts. Gastroenterology 119, 211-219
26. Mills, L. D., Zhang, Y., Marler, R. J., Herreros-Villanueva, M., Zhang, L., Almada, L. L., Couch, F., Wetmore, C., Pasca di Magliano, M., and Fernandez-Zapico, M. E. (2013) Loss of the transcription factor GLI1 identifies a signaling network in the tumor microenvironment mediating KRAS oncogene-induced transformation. J Biol Chem 288, 11786-11794
27. Davies, L. C., Rosas, M., Jenkins, S. J., Liao, C. T., Scurr, M. J., Brombacher, F., Fraser, D. J., Allen, J. E., Jones, S. A., and Taylor, P. R. (2013) Distinct bone marrow-derived and tissue-resident macrophage lineages proliferate at key stages during inflammation. Nat Commun 4, 1886

28. Collins, M. A., Brisset, J. C., Zhang, Y., Bednar, F., Pierre, J., Heist, K. A., Galban, C. J., Galban, S., and di Magliano, M. P. (2012) Metastatic pancreatic cancer is dependent on oncogenic Kras in mice. PLoS One 7, e49707
29. Nakamura, I., Fernandez-Barrena, M. G., Ortiz-Ruiz, M. C., Almada, L. L., Hu, C., Elsawa, S. F., Mills, L. D., Romecin, P. A., Gulaid, K. H., Moser, C. D., Han, J. J., Vrabel, A., Hanse, E. A., Akogyeram, N. A., Albrecht, J. H., Monga, S. P., Sanderson, S. O., Prieto, J., Roberts, L. R., and Fernandez-Zapico, M. E. (2013) Activation of the transcription factor GLI1 by WNT signaling underlies the role of SULFATASE 2 as a regulator of tissue regeneration. J Biol Chem 288, 21389-21398
30. Eto, I. (2000) Molecular cloning and sequence analysis of the promoter region of mouse cyclin D1 gene: implication in phorbol ester-induced tumour promotion. Cell Prolif 33, 167-187
31. Martin, P., and Leibovich, S. J. (2005) Inflammatory cells during wound repair: the good, the bad and the ugly. Trends Cell Biol 15, 599-607
32. Clark, C. E., Hingorani, S. R., Mick, R., Combs, C., Tuveson, D. A., and Vonderheide, R. H. (2007) Dynamics of the immune reaction to pancreatic cancer from inception to invasion. Cancer Res 67, 9518-9527
33. Murray, P. J., and Wynn, T. A. (2011) Protective and pathogenic functions of macrophage subsets. Nat Rev Immunol 11, 723-737
34. O'Brien, J., Lyons, T., Monks, J., Lucia, M. S., Wilson, R. S., Hines, L., Man, Y. G., Borges, V., and Schedin, P. (2010) Alternatively activated macrophages and collagen remodeling characterize the postpartum involuting mammary gland across species. Am J Pathol 176, 1241-1255
35. Atabai, K., Jame, S., Azhar, N., Kuo, A., Lam, M., McKleroy, W., Dehart, G., Rahman, S., Xia, D. D., Melton, A. C., Wolters, P., Emson, C. L., Turner, S. M., Werb, Z., and Sheppard, D. (2009) Mfge8 diminishes the severity of tissue fibrosis in mice by binding and targeting collagen for uptake by macrophages. J Clin Invest 119, 3713-3722
36. Nolan-Stevaux, O., Lau, J., Truitt, M. L., Chu, G. C., Hebrok, M., Fernandez-Zapico, M. E., and Hanahan, D. (2009) GLI1 is regulated through Smoothened-independent mechanisms in neoplastic pancreatic ducts and mediates PDAC cell survival and transformation. Genes Dev 23, 24-36
37. Chen, J. K., Taipale, J., Young, K. E., Maiti, T., and Beachy, P. A. (2002) Small molecule modulation of Smoothened activity. Proc Natl Acad Sci U S A 99, 14071-14076
38. McMahon, A. P., Ingham, P. W., and Tabin, C. J. (2003) Developmental roles and clinical significance of hedgehog signaling. Curr Top Dev Biol 53, 1-114
39. Hui, C. C., and Angers, S. (2011) Gli proteins in development and disease. Annu Rev Cell Dev Biol 27, 513-537
40. Park, H. L., Bai, C., Platt, K. A., Matise, M. P., Beeghly, A., Hui, C. C., Nakashima, M., and Joyner, A. L. (2000) Mouse Gli1 mutants are viable but have defects in SHH signaling in combination with a Gli2 mutation. Development 127, 1593-1605

41. Shin, K., Lee, J., Guo, N., Kim, J., Lim, A., Qu, L., Mysorekar, I. U., and Beachy, P. A. (2011) Hedgehog/Wnt feedback supports regenerative proliferation of epithelial stem cells in bladder. Nature 472, 110-114
42. Lees, C. W., Zacharias, W. J., Tremelling, M., Noble, C. L., Nimmo, E. R., Tenesa, A., Cornelius, J., Torkvist, L., Kao, J., Farrington, S., Drummond, H. E., Ho, G. T., Arnott, I. D., Appelman, H. D., Diehl, L., Campbell, H., Dunlop, M. G., Parkes, M., Howie, S. E., Gumucio, D. L., and Satsangi, J. (2008) Analysis of germline GLI1 variation implicates hedgehog signalling in the regulation of intestinal inflammatory pathways. PLoS Med 5, e239
43. El-Zaatari, M., Kao, J. Y., Tessier, A., Bai, L., Hayes, M. M., Fontaine, C., Eaton, K. A., and Merchant, J. L. (2013) Gli1 deletion prevents Helicobacter-induced gastric metaplasia and expansion of myeloid cell subsets. PLoS One 8, e58935
44. Hebrok, M., Kim, S. K., and Melton, D. A. (1998) Notochord repression of endodermal Sonic hedgehog permits pancreas development. Genes Dev 12, 1705-1713
45. Fendrich, V., Esni, F., Garay, M. V., Feldmann, G., Habbe, N., Jensen, J. N., Dor, Y., Stoffers, D., Jensen, J., Leach, S. D., and Maitra, A. (2008) Hedgehog signaling is required for effective regeneration of exocrine pancreas. Gastroenterology 135, 621-631
46. Thayer, S. P., di Magliano, M. P., Heiser, P. W., Nielsen, C. M., Roberts, D. J., Lauwers, G. Y., Qi, Y. P., Gysin, S., Fernandez-del Castillo, C., Yajnik, V., Antoniu, B., McMahon, M., Warshaw, A. L., and Hebrok, M. (2003) Hedgehog is an early and late mediator of pancreatic cancer tumorigenesis. Nature 425, 851-856
47. Treier, M., Gleiberman, A. S., O'Connell, S. M., Szeto, D. P., McMahon, J. A., McMahon, A. P., and Rosenfeld, M. G. (1998) Multistep signaling requirements for pituitary organogenesis in vivo. Genes Dev 12, 1691-1704
48. Bowers, S. L., Borg, T. K., and Baudino, T. A. (2010) The dynamics of fibroblast-myocyte-capillary interactions in the heart. Ann N Y Acad Sci 1188, 143-152
49. Buckley, C. D., Pilling, D., Lord, J. M., Akbar, A. N., Scheel-Toellner, D., and Salmon, M. (2001) Fibroblasts regulate the switch from acute resolving to chronic persistent inflammation. Trends Immunol 22, 199-204
50. Ingerslev, H. C., Ossum, C. G., Lindenstrom, T., and Nielsen, M. E. (2010) Fibroblasts express immune relevant genes and are important sentinel cells during tissue damage in rainbow trout (Oncorhynchus mykiss). PLoS One 5, e9304
51. Silzle, T., Randolph, G. J., Kreutz, M., and Kunz-Schughart, L. A. (2004) The fibroblast: sentinel cell and local immune modulator in tumor tissue. Int J Cancer 108, 173-180
52. Duffield, J. S., Forbes, S. J., Constandinou, C. M., Clay, S., Partolina, M., Vuthoori, S., Wu, S., Lang, R., and Iredale, J. P. (2005) Selective depletion of macrophages reveals distinct, opposing roles during liver injury and repair. J Clin Invest 115, 56-65

CHAPTER FOUR

Mesenchymal Stem Cells promote pancreatic tumor growth by promoting M2 macrophage polarization[1]

Abstract

Pancreatic cancer is characterized by an extensive desmoplastic stroma, the functional relevance of which is poorly understood. Activated fibroblasts are a prevalent component of the stroma and traditionally, these cells have been considered as a homogenous population derived from pancreatic stellate cells. In this study, we highlight a previously unappreciated heterogeneity of the fibroblast population within the stroma. In particular, a subset of stromal fibroblasts have characteristics of Mesenchymal Stem Cells (MSCs). MSCs are present in the normal pancreas (P-MSCs), as well as in the carcinomatous pancreas (CA-MSCs). Here, we determine that CA-MSCs have increased tumor-promoting function compared with P-MSCs. This ability to promote tumor growth is associated with CA-MSCs' unique ability to promote alternative macrophage polarization. Thus, our study identifies a previously uncharacterized cell

[1] Manuscript currently in review at *Cancer Discovery.* Mathew, E., Brannon, A.L., Del Vecchio, A., Penny, M.K., Kane, K.T., Vinta, A., Buckanovich, R.J., and Pasca di Magliano, M. Tentative Title: Mesenchymal Stem Cells promote pancreatic tumor growth by promoting M2 macrophage polarization.

population within the stroma and sheds light on tumor-promoting interactions between different components of the stroma.

Introduction

Pancreatic cancer is among the deadliest of human malignancies. A prominent feature of pancreatic cancer is an extensive reactive stroma, which can comprise up to 90% of the overall tumor volume, the highest fraction of all solid, epithelial tumors (for review, see (1)). The accumulation of a desmoplastic stroma occurs from the onset of pancreatic carcinogenesis, and is evident in the precursor lesions of pancreatic cancer known as pancreatic intraepithelial neoplasia or PanINs (2). The cellular components of the stroma include fibroblasts, myofibroblasts, endothelial cells and infiltrating immune cells (3,4). Fibroblasts are an abundant and poorly characterized component of the stroma, thought to derive from pancreatic stellate cells. Fibroblasts within the stroma have been thought of as pro-tumor agents (5), but recent studies have challenged this concept indicating that stromal fibroblasts might act of restrain tumor growth (6,7). This controversy might in part reflect our limited understanding of cellular components of the stroma and their individual contribution to tumorigenesis.

The healthy pancreas includes different fibroblast populations. A population of mesenchymal stem cells (P-MSCs) was identified in the normal human and mouse pancreas (8-10); however, whether MSCs are present in pancreatic carcinoma and what their function might be during carcinogenesis remained unclear. MSCs were identified as a tumor-promoting stromal component in several epithelial cancers (11-13).

Interestingly, the manner in which MSCs promote tumorigenesis is distinct in each tumor context. In breast cancer, bone marrow derived MSCs promote the metastasis of tumor cells through a CCL5-mediated effect (12). In ovarian cancer, MSCs isolated from the tumor stroma secrete BMPs that increase the cancer stem cell population (13). More recently, stroma-derived MSCs from lymphomas have been shown to secrete monocyte/macrophage chemoattractants, which in turn promote tumor growth (14).

The identification and characterization of MSCs in pancreatic tumor growth is the focus of the current study. We use a genetically engineered mouse model of pancreatic cancer, the KC mouse (Ptf1a-Cre;LSL-Kras^{G12D}) (15) that expresses an oncogenic form of Kras, mirroring the most common genetic alteration in human PanINs and pancreatic cancer (16,17). KC mice develop PanINs in a step-wise manner that recapitulates human carcinogenesis (15). Our results show that MSC populations are present both in the normal murine pancreas (pancreatic MSCs, P-MSCs), and neoplastic mouse pancreas (carcinogenesis-associated MSCs, CA-MSCs). By performing functional comparisons of these two populations, we determined that CA-MSCs have an increased tumor-promoting potential, which is mediated, at least in part, by their unique ability to induce macrophage polarization to a pro-tumor, M2-like status.

Materials and Methods

Mice

Mice were housed in specific pathogen-free facilities of the University of Michigan Comprehensive Cancer Center. This study was approved by the University of Michigan

University Committee on Use and Care of Animals (UCUCA) guidelines. Ptf1a-Cre;LSL-$Kras^{G12D}$ (KC) animals were generated by crossing Ptf1a-Cre mice (18) with LSL-$Kras^{G12D}$ (15). Acute pancreatitis was induced as previously described (19) by two 8-hourly series of intraperitoneal injections with caerulein (Sigma) at a concentration of 75ug/kg over a 48-hour period.

Cell Culture

All cells were cultured in IMDM supplemented with 10% FBS and 1% penicillin/streptomycin (Gibco). Primary mouse pancreatic fibroblasts were derived from control or KC pancreata. Pancreata were minced with sterile scissors and subsequently digested in 1mg/mL collagenase. MSCs were sorted from cultures using Fluorescence Activated Cell Sorting as described below. For bone marrow MSC extraction, the tibia and femur was flushed with culture media. Collected marrow was plated after being extruded through a 20 G syringe to disassociate tissue. After 2 days, cultures were washed twice with PBS and adherent cells cultured for an additional week prior to FACS. Primary MSCs were verified using both flow cytometry for defined markers as well as functional testing of differentiation capacity into bone and fat. MSC differentiation was verified up to passage 10, and all experiments were performed on MSCs below this passage number. For MSC differentiation experiments, cells were plated following instructions on commercially available differentiation kits for osteogenesis, chondrogenesis, and adipogenesis (all Gibco). Bone-marrow derived macrophages were derived using an established protocol (20). Briefly, extruded bone marrow precursors were cultured in one week in growth media supplemented with 20% L929

conditioned media, 10% FBS, and 1% pen/strep. For RAW264.7 polarization experiments, neutralizing antibodies in PBS were used at indicated concentrations to block IL10 (R&D Systems #AF519) and IL6 (R&D Systems #MAB406).

Reverse Transcription Real-Time Quantitative PCR (RT-qPCR)

Cells for RNA extraction were collected in lysis buffer (Ambion). RNA was isolated using a PureLink RNA Mini Kit (Ambion) as per manufacturer instructions. Reverse transcription was conducted with a High-Capacity cDNA Reverse Transcription Kit (Applied Biosystems). RT-qPCR reactions were prepared with 1x SYBR Green PCR Master Mix (Applied Biosystems) and primers (**Table 4.1**) were optimized for amplification under the following reaction conditions: 95°C 10 minutes, followed by 40 cycles of 95°C 15 seconds and 60°C 1 minute. Melt curve analysis was included in the amplification protocol for all samples. Ppia (*Cyclophilin A)* and *Gapdh* were used as control housekeeping genes.

Western Blot

Protein was isolated from Raw264.7 cells in lysis buffer (50mM Tris pH 8.0, 1% Triton X-100, 130mM NaCL, 1mM Na3VO4*, 10mM Na4P2O7, 10mM NaF, 1mM EDTA). Equal amounts of protein were electrophoresed in SDS-PAGE gels and transferred to PVDF membranes (Bio-Rad). The following primary antibodies from Cell Signaling Technologies were used: AKT (1:1000, Cat# 9272), pAKT (Ser473) (1:1000, Cat# 9271), ERK (1:1000, Cat# 9102), pERK (Thr202/Tyr204) (1:1000, Cat# 9101), RalA (1:2500, Cat# 3526), STAT3 (1:1000, Cat# 9139), pSTAT3 (Tyr705) (1:1000, Cat#

9131). The following horseradish peroxidase-conjugated secondary antibodies from Bio-Rad were used (1:5000): Goat Anti-Mouse (Cat# 1721011) and Goat Anti-Rabbit (Cat# 1706515). Individual protein bands were visualized using Western Lightning Plus Enhanced Chemiluminescence (PerkinElmer, Cat# NEL103001EA) and film.

Flow Cytometry

Single cell suspensions were prepared from the pancreas as follows: tissues were minced with sterile scalpels prior to digestion in 1mg/mL collagenase (Sigma-Aldrich) at 37°C for 15min. Digested samples were then filtered through a 40μm strainer. Single cell suspensions were prepared in HBSS with 2% FBS for Fluorescence activated cell sorting (FACS). Antibodies used for MSCs were CD44-FITC (1:50, BD Pharm), CD73-PeCy7 (1:50, ebioscience), CD49a-PE (1:50, BD Pharm), and CD90-APC (1:50, BD Pharm). Antibodies used for immune cells were CD45-Pacific Orange (1:50, BD Pharm), CD11b-APCCy7 (1:50, BD Pharm), CD3-PE (1:50, BD Pharm), F4/80-PECy5 (1:50, ebioscience), CD64-PE (1:50, BD Pharm). FACS was performed on a MoFlo Astrios (Beckman Coulter) and data analyzed using Summit 6.1 Software.

Immunohistochemistry and Immunofluorescence

Primary antibodies used were CK19 (1:100, Iowa Developmental Hybridoma Bank), F4/80 (1:100, BMA Biomedicals), Ki67 (1:100, Vector Laboratories), Cleaved Capsase 3 (1:300, Cell Signaling). Images were taken with an Olympus BX-51 microscope, Olympus DP71 digital camera, and CellSens standard v1.6 software. For immunofluorescence, Alexa Fluor-conjugated (Invitrogen) secondary antibodies were

used. Cell nuclei were counterstained with Prolong Gold-DAPI (Invitrogen). The images were acquired using an Olympus IX-71 confocal microscope and FluoView FV500/IX software.

Statistical Analysis

Student's *t*-tests were used to compare experimental cohorts, and significance was established for p-values < 0.05. Significance values indicated by asterisks or pound signs are as follows: *p<0.05, **p < 0.01, ***p < 0.0005, ****p < 0.0001

Results

MSCs are Present in the Normal and in the Neoplastic Pancreas

MSCs are defined by their ability to differentiate into osteoblasts, chondrocytes, and adipocytes when exposed to appropriate differentiation media *in vitro.* To test whether we could identify a MSC population in the normal and neoplastic murine pancreas, we isolated pancreata from wildtype and littermate KC mice 3 weeks after the induction of acute pancreatitis. Wildtype pancreata have completed the tissue repair process by this time, whereas in KC pancreata, extensive PanINs surrounded by desmoplastic stroma are evident (**Figure 4.1A**) (15). Isolated bulk fibroblast populations from the pancreata were exposed to osteoblast, adipocyte and chondrocyte differentiation media. Tri-lineage differentiation was observed in the wildtype and in the KC-derived pancreata, indicating that a MSC population might exist in both settings (**Figure 4.1B**). MSCs have been isolated based on the expression of a panel of surface markers: $CD45^{-};CD44^{+};CD49a^{+}:CD73^{+};CD90^{+}$ (21). To determine whether these

markers were sufficient to isolate the MSC population in the pancreas, we isolated single-cell suspensions from wildtype and KC pancreata, 3 weeks after the induction of pancreatitis, and used fluorescent-activated cell sorting (FACS) to isolate and quantify cells expressing MSC markers. While $CD45^{-};CD44^{+};CD49a^{+}:CD73^{+};CD90^{+}$cells were present in both sample sets, their number was significantly higher in KC pancreata compared to the normal mouse pancreas (**Figure 4.2A**). To determine whether the surface markers did indeed identify the MSC population, we cultured $CD44^{+};CD49a^{+}:CD73^{+};CD90^{+}$ cells (putative MSCs, 4^{+}) as well as cells negative for all markers (4^{neg}) and performed *in vitro* differentiation assays with protocols promoting osteoblast and adipocyte lineages. In differentiation media, $CD45^{-};CD44^{+};CD49a^{+}:CD73^{+};CD90^{+}$ cells from both the normal and neoplastic pancreas could differentiate into osteoblasts -as determined by Alizarin Red staining of calcium deposits, and expression of the osteoblast marker Alkaline Phosphatase (**Figure 4.2B and 4.2C, top row)** - and adipocytes -as determined by Oil Red O staining of lipid droplets and expression of adipocyte marker Fatty acid binding protein 4 (Fabp4) (**Figure 4.2B and 4.2C, bottom row)**. In contrast, 4^{neg} cells did not differentiate into any of the lineages (**Figure 4.2B and 4.2C),** indicating that the combination of $CD44^{+}$, $CD49a^{+,}$ $CD73^{+}$ and $CD90^{+}$ surface markers identifies a subset of multipotent cells.

CA-MSCs have a Distinct Cytokine Expression Profile.

Since MSCs were present both in the normal and in the neoplastic pancreas, we set out to compare their functional characteristics. Hereby, normal pancreas-derived MSCs are referred to as P-MSCs, while MSCs derived from the neoplastic pancreas are

referred to as CA-MSCs (carcinoma-associated MSCs). In ovarian cancer, CA-MSCs are distinct from bone marrow and adipose-derived MSCs by the expression of *BMP2* and *BMP4*, and those factors confer a higher tumor-promoting ability to CA-MSCs (13). Thus, we measured the relative expression of *BMP2* and *BMP4* by qRT-PCR in isolated P-MSCs and CA-MSCs. We detected no difference in *BMP2* expression, while *BMP4* expression was decreased in CA-MSCs compared to P-MSCs (**Figure 4.2D).**

We have previously shown that pancreatic fibroblasts secrete a number of cytokines that regulate the infiltration of immune cells during pancreatic damage and repair and during carcinogenesis (22). Thus, we measured expression of those cytokines by qRT-PCR in freshly sorted P-MSCs and CA-MSCs. Interestingly, we observed a significant increase in several cytokines known to promote tumorigenesis, including *IL6*, *IL10*, and *TGFβ* (23-27) in CA-MSCs compared with P-MSCs (**Figure 4.3A)**. Then, we measured the expression of the same subset of cytokines in cultured CA-MScs and P-MSCs, respectively, and found a similar profile, with significantly elevated cytokines in CA-MSCs (**Figure 4.3B**). Similarly *M-CSF (Csf1)* and *GM-CSF (Csf2)*, cytokines known to regulate immune cell recruitment and function, were significantly elevated in CA-MSCs compared with P-MSCs. Finally, we compared paired bone marrow and pancreatic MSCs extracted from a control mouse (P-BM MSCs and P-MSCs) or a PanIN-bearing KC mouse (CA-BM MSCs and CA-MSCs). P-MSCs expressed higher levels of *IL6, Cox-2,* and *IL10* than their bone marrow counterparts. CA-MSCs expressed higher levels of *IL6*, *Cox-2*, *TGFβ,* and *IL10* than both P-MSCs and CA-BM MSCs (**Figure 4.4)**. These data indicate that MSCs extracted from the

neoplastic pancreas have unique characteristics, that are not shared by their counterpart extracted from the normal organ nor by MSCs extracted by different organs (in this case, the bone marrow) of a mouse bearing neoplastic changes in the pancreas.

MSCs Promote Pancreatic Tumor Growth

To determine the functional effect of MSCs on tumor growth, we performed subcutaneous co-injections of tumor cells and MSCs into immunocompetent mice using a syngeneic littermate approach. We used tumor cells isolated from the iKras*p53* mouse model (28) of pancreatic cancer (cell line: iKras*p53*#3 (29)). Tumor cells were injected at a 1:1 ratio with either P-MSCs or CA-MSCs (**see schematic in Figure 4.5A**). Co-injection of P-MSCs with iKras*p53*#3 cells promoted tumor growth, but co-injection with CA-MSCs promoted even larger tumor growth **(Figure 4.5B**). The histology of all three cohorts was similar with epithelial structures surrounded by abundant stroma (**Figure 4.5C**). Staining for CK19 to mark tumor cells revealed increased number of tumor cells in co-injections with CA-MSCs (**Figure 4.6A**). Consistently, we detected increased intratumor proliferation -as indicated by Ki67 staining- in co-injections with CA-MSCs. Immunofluorescence analysis revealed a notable increase in proliferating tumor CK19+ cells, indicating an increase in proliferating tumor cells (**Figures 4.6B and 4.6C)**.

Given our previous observation that CA-MSCs secreted a number of cytokines that are known to regulate macrophages, we sought to determine the effect of MSC co-injection on macrophage infiltration within the tumor. Thus, we stained tissues for F4/80,

a mature macrophage marker. We detected a significant increase in macrophages in the tumors derived from co-injection of tumor cells and CA-MSCs compared to tumor cells alone or co-injected with P-MSCs (**Figure 4.5C, inset**). To quantify macrophage numbers in the subcutaneous tumors, we performed flow cytometry for macrophages defined as $CD11b^{+};CD64^{+};F4/80^{+}$ cells. We found that tumors derived from the CA-MSC co-injection consistently had the highest population of macrophages compared to the other experimental cohorts, thus corroborating the histology (**Figures 4.5C, inset, and 4.6D**).

We repeated these experiments using tumor cells derived from the KPC mouse model (30) of pancreatic cancer (cell line: 13442) (**see schematic in Figure 4.7A**). Similar to co-injections with iKras*p53*#3 cells, CA-MSCs promoted the growth of larger tumors than P-MSCs (**Figure 4.7B**). Although overall histology was comparable between experimental cohorts (**Figure 4.7C**), increased intratumoral proliferation (**Figures 4.7D and 4.7E**) and macrophage infiltration (**Figures 4.7C, inset and 4.7F**) was again detected in tumors co-injected with CA-MSCs.

To determine whether MSCs were still able to promote tumor growth when injected at a lower ratio, we performed a parallel set of experiments by injecting tumor cells (13442) and MSCs at a 2:1 ratio. We found that at this lower ratio P-MSCs were unable to promote tumor growth, while in contrast CA-MSCs still promoted tumor growth, further validating the concept that CA-MSCs have increased tumor-promoting ability (**Figure 4.8A**).

Since our data indicated that CA-MSCs have different functional characteristics than P-MSC, we expanded our characterization to include bone-marrow derived MSCs (BM-MSCs). In the absence of rigorous lineage tracing studies, it is not known whether CA-MSCs derived from P-MSCs or, at least in part, from infiltrating BM-MSCs, as observed in other disease contexts (31,32). This is a question that warrants further studies that are beyond the scope of the current manuscript. BM-MSCs from a control mouse promoted tumor growth similarly to P-MSCs. However, CA-MSCs were able to promote significantly more tumor growth than their bone-marrow derived counterparts (**Figures 4.8B and 4.8C).** Thus, CA-MSCs have a unique tumor promoting ability; we then set out to understand the mechanistic basis for this finding.

Monocyte migration to the tumor stroma and subsequent differentiation into macrophages is a process orchestrated by an array of signaling molecules. To assess potential differences in these cytokine levels between tumor cohorts, we collected RNA from subcutaneous tumor tissue for RT-qPCR analysis. We found that expression of *Mcp-1*, a potent monocyte chemoattractant, did not differ between tumors co-injected with P-MSCs or with CA-MSCs but, at least for tumors derived from the 13442 line, was higher in the MSC-co-injected tumors than in the control group (**Figures 4.9A and 4.9C)**. Interestingly, we detected an increase in M-CSF in co-injections with CA-MSCs (**Figures 4.9B and 4.9D)**, a cytokine that supports the differentiation of monocytes into macrophages.

MSCs require Monocytes/Macrophages to Promote Tumor Growth

Macrophages have been shown to promote pancreatic growth (33). Thus, based on the observation that CA-MSCs promoted the highest infiltration of macrophages, we next tested whether this population's elevated tumor-promoting potential *required* macrophages. Thus, we co-injected tumor cells and MSCs into immunocompetent mice with concomitant depletion of monocytes and macrophages. Cd11b-DTR mice express the human diphtheria toxin receptor under the Cd11b promoter (**Figure 4.10A**). Administration of diphtheria toxin (DT) to Cd11b-DTR mice depletes all CD11b+ cells, including monocytes/macrophages (34). We performed a series of co-injection experiments with iKras*p53*#3 cells alone or in combination with P-MSCs or CA-MSCs. In a subset of each cohort, mice were injected with DT (**Figure 4.10B**). We found that tumor size was reduced by depleting CD11b+ cells in all experimental cohorts, underscoring the importance of myeloid cells in tumor growth. However, co-injections of iKras*p53*#3 cells with CA-MSCs were significantly more susceptible to myeloid cell ablation than any other experimental cohort, in terms of tumor mass changes (**Figure 4.10C).** We confirmed DT-mediated depletion by staining tumor tissues for F4/80; in all cohorts, DT administration significantly attenuated macrophage infiltration (**Figure 4.11, inset)**. While the tumor histology remained similar (**Figure 4.11**), immuno-staining for Ck19 revealed a reduction in the ratio of epithelial cells within the tumors (**Figure 4.12).** Moreover, while tumors derived from co-injections with CA-MSCs are more proliferative than the other cohorts, this increase in proliferation was abrogated upon myeloid cell depletion (**Figure 4.13**).

To determine whether the dependence on myeloid cells for tumor promotion was a unique property of CA-MSCs, or rather a common feature of fibroblasts derived from the neoplastic pancreas, we performed parallel co-injection experiments with non-MSCs ($CD45^-;CD44^-;CD49a^-:CD73^-;CD90^-$) cells sorted from the neoplastic stroma (CA-non MSCs) (**see schematic in Figure 4.14A)**. While these cells also promoted tumor growth, the extent of tumor mass reduction upon CD11b+ cell depletion was significantly less than in co-injections with MSCs (**Figure 4.14B**)**.** Thus, CA-MSCs have a unique dependence on myeloid cells, which led us to investigate the interaction between these cell types.

MSCs Promote Macrophage Differentiation and Polarization to a M2 Subtype

In order to interrogate whether MSCs directly regulate macrophage polarization we investigated their interactions *in vitro*. First, we investigated whether CA-MSCs promote the differentiation of monocytes into macrophages. For this purpose, we isolated and cultured mouse bone marrow precursors. After 1 week of culture in regular medium, about 25% of the cell population differentiates to macrophages, defined as $CD11b^+;CD64^+;F4/80^+$ cells by flow cytometry. As expected based on previous studies (20), exposure to M-CSF supplemented media led to differentiation of a uniform population of $CD11b^+;CD64^+;F4/80^+$ macrophages (**Figure 4.15**). We tested the effect of supplementing the culture medium with conditioned media from either P-MSCs or CA-MSCs, as well as P-nonMSCs and CA-nonMSCs (pancreatic fibroblasts or neoplastic fibroblasts). Both P-MSCs and CA-MSCs promoted macrophage differentiation in over 50% of the bone marrow precursors, with no significant difference

between the two populations. In contrast, only non-MSC fibroblasts from the neoplastic pancreas could also promote macrophage differentiation, although to a lesser extent than their MSC counterparts (**Figure 4.15**).

We next assessed whether P-MSCs or CA-MSCs regulated macrophage polarization. First, we performed RT-qPCR analysis for M1 and M2 markers on RNA collected from our subcutaneous co-injection experiments (**Figures 4.16A and 4.16B**). We found that tumors derived from co-injection with both P-MSCs and CA-MSCs had decreased expression of *iNos*, a M1 marker, compared with tumor cells injected alone. However, only co-injections with CA-MSCs tumor cells showed increased expression of *Arg1* and *CD206*, both M2 markers. Likewise, the expression of *IL10* – a cytokine known to regulate M2 differentiation- was significantly increased in co-injections with CA-MSCs (**Figures 4.16A and 4.16B)**. Importantly, these changes were observed both with iKras*p53* and KPC tumor cells.

To test whether MSCs directly regulated macrophage polarization to a M2 phenotype, we treated three independently derived cultures of bone marrow derived macrophages (BMDMs) with conditioned media from either P-MSCs or CA-MSCs for 12 hours (**see schematic in Figure 4.17A**). We found that both P-MSCs and CA-MSC-conditioned medium decreased *iNOS* expression in BMDMs compared with control medium, indicating suppression of the M1 subtype. However, only CA-MSC-conditioned medium promoted M2 polarization, as determined by *Arg1* expression (**Figure 4.17B)**. We then repeated this set of experiments using the mouse macrophage cell line RAW264.7 that can be polarized in culture. Conditioned media from P-MSCs had no

effect on the expression of *iNos* or *Arg1* in macrophages. In contrast, while conditioned media from CA-MSCs stimulated a four-fold increase in *iNos* expression, *Arg1* expression was increased over one hundred-fold. We also tested the effect of conditioned media from bone marrow MSCs, which have been reported to stimulate M2 macrophage polarization and *Arg1* expression in macrophages (35,36). We found that while CA BM-MSCs could promote *Arg1* expression, this effect was significantly less than CA-MSCs (**Figure 4.17C**)**.** Taken together, our data indicates that the ability to promote M2-like macrophage polarization is restricted to CA-MSCs.

As CA-MSCs expressed significantly higher *IL6* and *IL10* compared to P-MSCs, and these cytokines are known to regulate macrophage polarization, we tested whether production of these cytokines explained the unique ability of CA-MSCs to promote M2 polarization. Thus, we treated RAW264.7 macrophages with CA-MSC conditioned media with and without an IL6 neutralizing antibody or an IL10 neutralizing antibody and assessed *Arg1* expression. Consistent with IL6 stimulation, CA-MSC conditioned medium increased pSTAT3 levels in RAW264.7 macrophages compared to control medium, and this increase was abrogated by the anti-IL6 antibody but not by the anti-IL10 antibody (**Figure 4.18A**). Treatment with CA-MSC conditioned medium induced *Arg1* expression in RAW264.7 macrophages; this induction was partially abrogated by anti-IL6 and, to a lesser extent, by anti-IL10 treatment (**Figure 4.18B**). Concomitant treatment with anti-IL6 and anti-IL10 antibodies completely blocked the induction of *Arg1* expression, indicating that these two cytokines might act along parallel, non overlapping paths (**Figure 4.18B**). We then investigated the effect of CA-MSC

conditioned medium on the expression of M1 differentiation markers. We observed no change in *iNOS* expression, but a reduction of *IL12p35* upon treatment with conditioned medium (**Figures 4.19A and 4.19B**). This decrease was reversed with higher concentrations of either IL6 or IL10 inhibition (**Figures 4.19B**). Taken together, our results show that both P-MSCs and CA-MSCs can induce macrophage differentiation for a precursor population, but only CA-MSC specifically direct polarization to a tumor promoting M2-like subtype.

Discussion

Fibroblasts exist in every tissue and organ in the body and are a prevalent population within the pancreatic cancer stroma. Our understanding of their functional specificity, however, remains limited. Here, we have identified a sub-population of fibroblasts present both within the normal pancreas and in the neoplastic pancreas, with MSC characteristics, namely the ability to differentiate into chondrocytes, adipocytes and osteoblasts. We determined that MSCs from the neoplastic pancreas (CA-MSCs) have a unique ability to promote tumor growth, that depends on their ability to promote infiltration of monocytes/macrophages and their differentiation to a M2, tumor promoting, phenotype (**Figure 4.20**). Our study highlights the functional heterogeneity of stromal fibroblast populations, and the different functional properties of fibroblasts derived from the normal or neoplastic organ. Further, our study identifies novel interactions between the fibroblast population and the immune component of pancreatic cancer.

Acknowledgements

This project was supported by the NCI-1R01CA151588-01 to MPdM. EM was supported by a University of Michigan Program in Cellular and Molecular Biology training grant (NIH T32 GM007315) and a University of Michigan Gastrointestinal Training Grant (NIH T32 DK094775). ALB was supported by a University of Michigan Warner-Lambert Rackham Fellowship. The authors declare they have no conflict of interest. We would like to thank G Martinez-Santibañez and C Lumeng for protocols and reagents for macrophage experiments. We also thank L Cabrera for technical advice and reagents for MSC differentiation experiments.

Figures

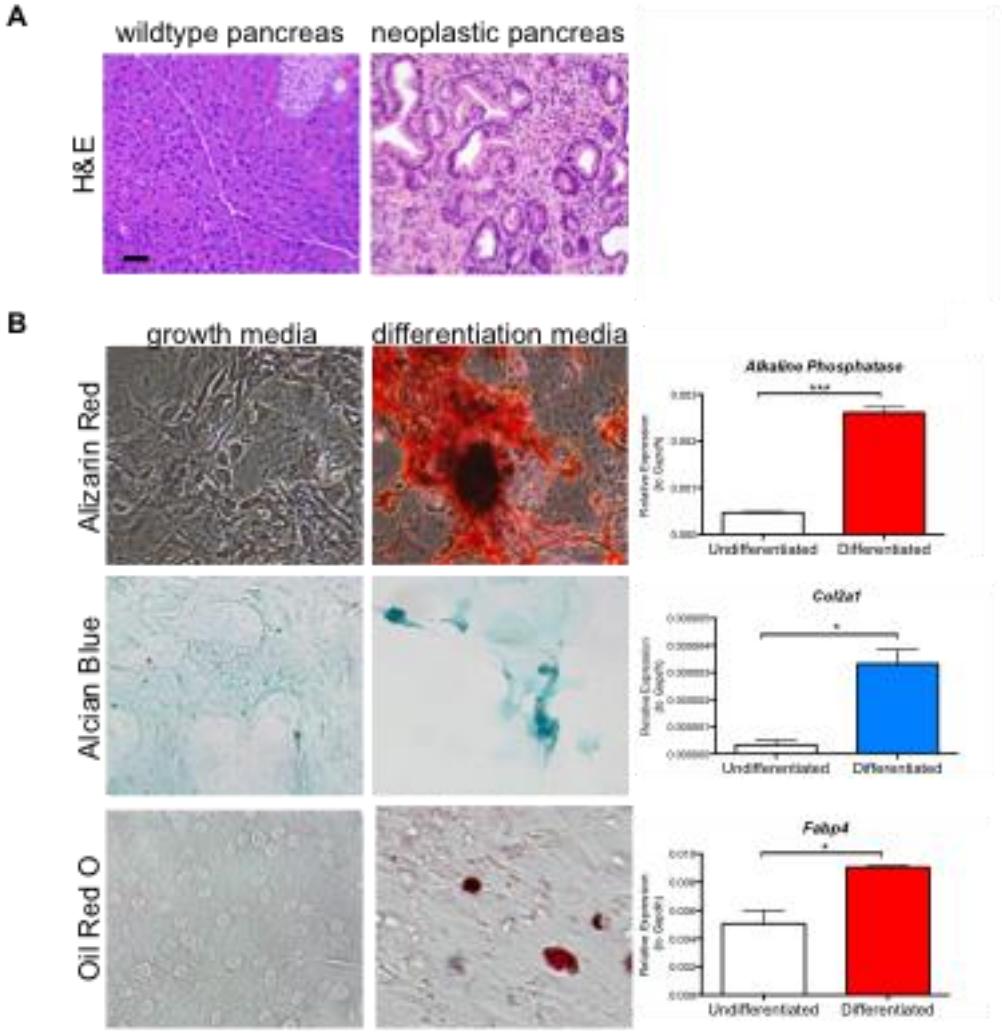

Figure 4.1: Mesenchymal Stem Cells (MSCs) are present in the pancreas

(A) H&E staining of wildtype (left) and KC (right) pancreas 3w post-caerulein-induced pancreatitis. Scale bar, 50μm. (B) Stromal cells isolated from the neoplastic pancreas can differentiate into osteoblasts (top row), chondrocytes (middle row), and adipocytes (bottom row).

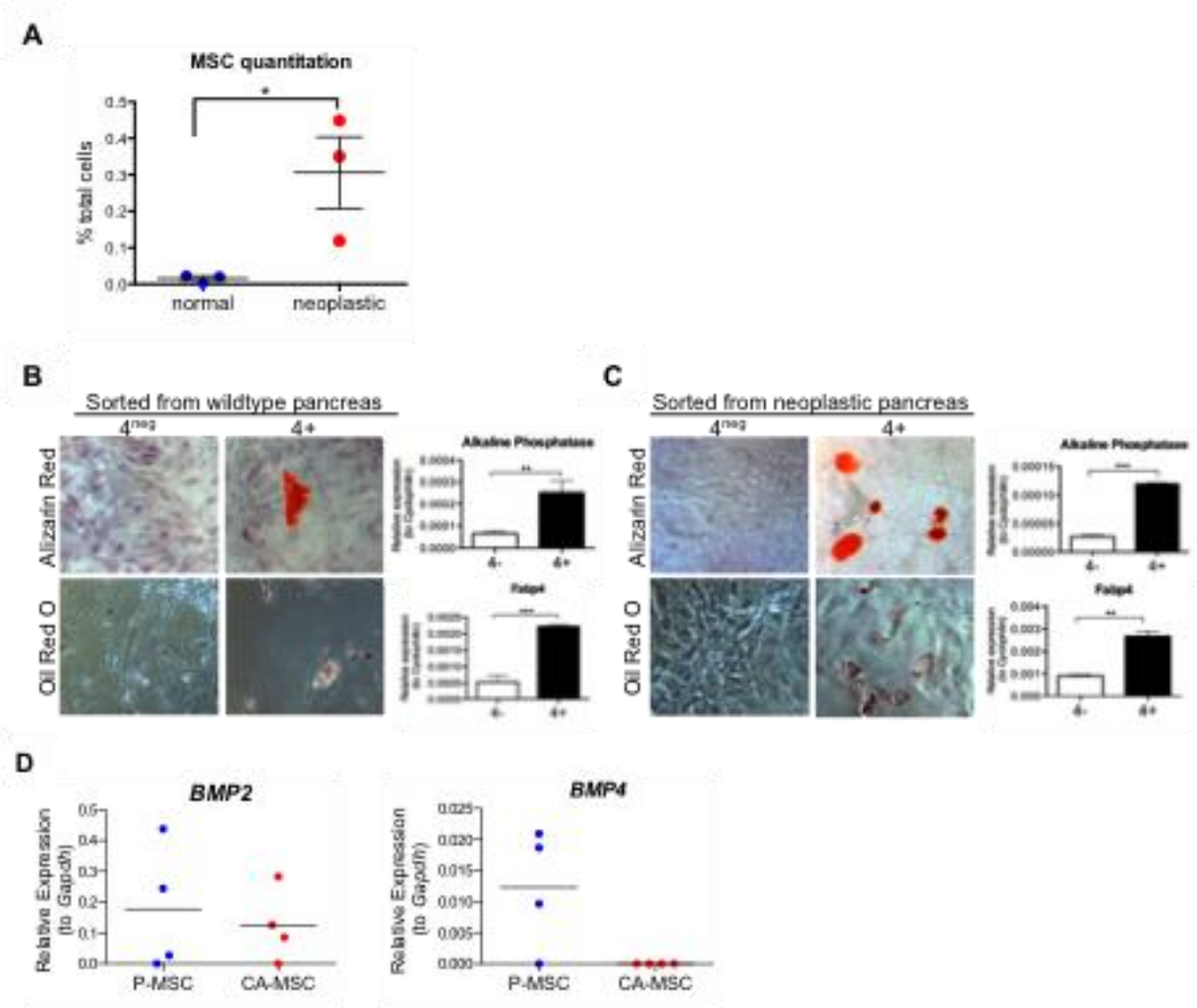

Figure 4.2: MSCs can be sorted from the normal and neoplastic pancreas

(A) Flow cytometry analysis of MSC populations in the wildtype and KC pancreas. (B) MSCs sorted from the normal pancreas (P-MSCs) can differentiate into bone (top row) and fat (bottom row) (C) MSCs sorted from the neoplastic pancreas (CA-MSCs) can differentiate into bone (top row) and fat (bottom row) (D) qRT-PCR for *BMP2* and *BMP4* on MSCs freshly sorted from the pancreas.

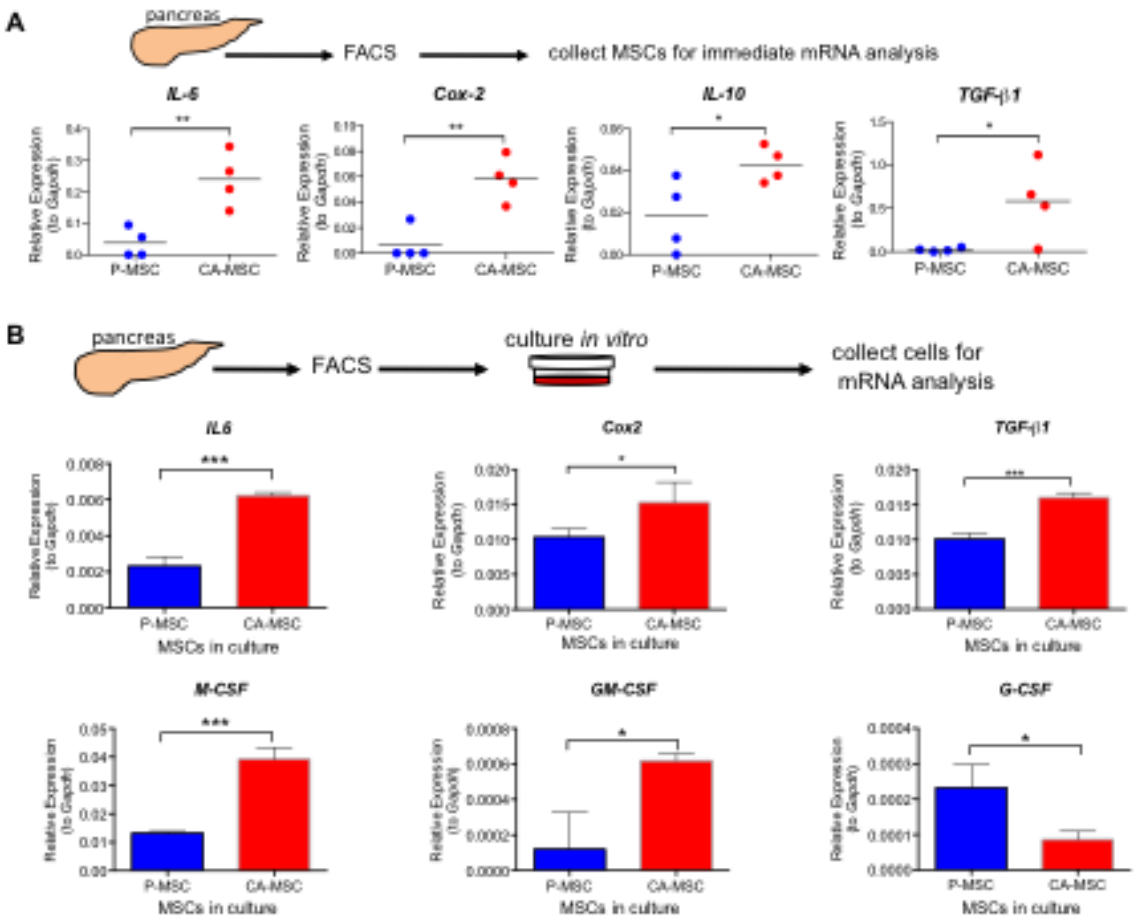

Figure 4.3: Differences in cytokine expression between MSCs from the normal and neoplastic pancreas

(A) qRT-PCR for *IL-6, Cox-2, IL-10* and *TGFβ-1* on MSCs freshly sorted from the pancreas. (B) Expression of *IL-6, Cox2, Tgfβ1, M-csf, Gm-csf,* and *G-csf* in MSCs cultured *in vitro*.

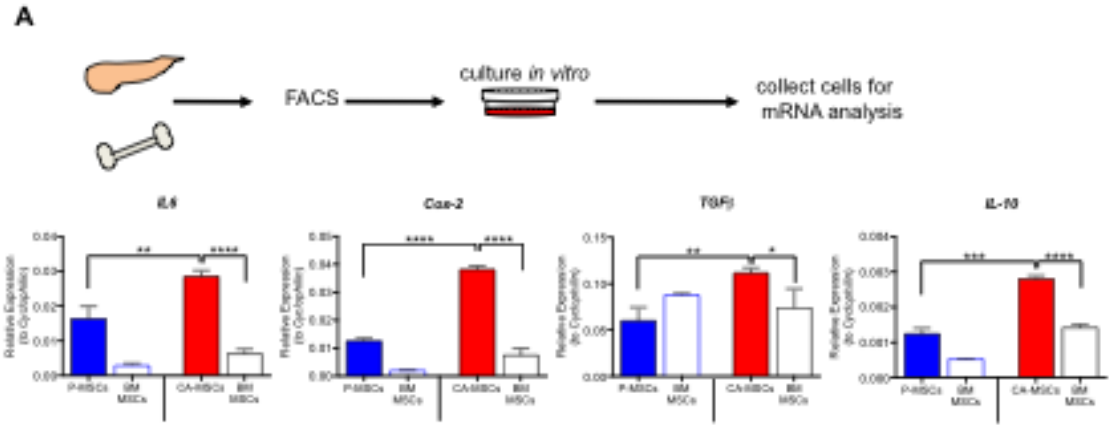

Figure 4.4: Differences in MSCs from the bone marrow and pancreas.

(A) Expression of *Il6, Cox2, Tgfβ1,* and *Il10* in bone marrow and pancreatic MSCs.

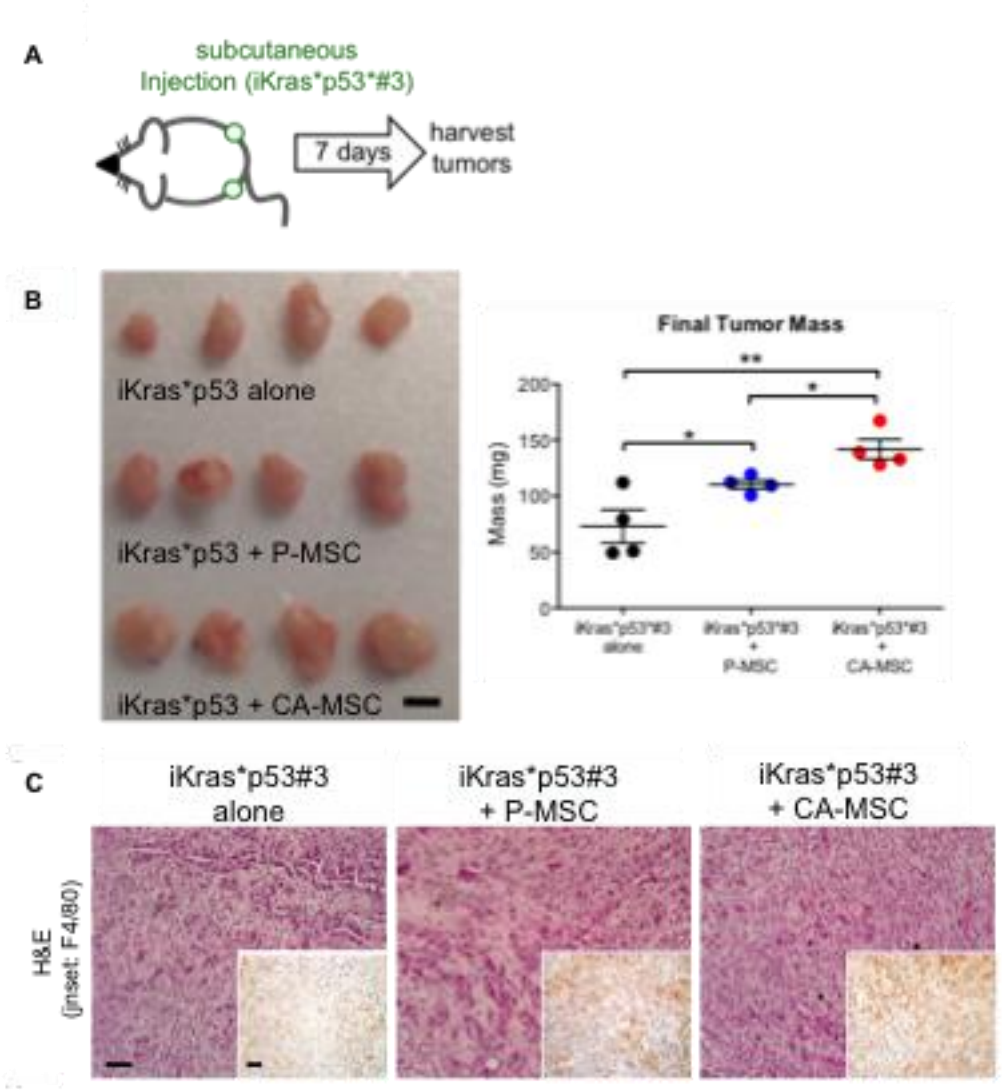

Figure 4.5: CA-MSCs promote tumor growth when co-injected with iKras tumor cells.

(A) Experimental design. (B) Gross tumor morphology and final tumor mass. Scale bar represents 0.5cm. (C) Histopathological analysis of tumors following co-injection. H&E staining, Scale bar represents 50μm. Inset F4/80 staining, scale bar represents 50μm.

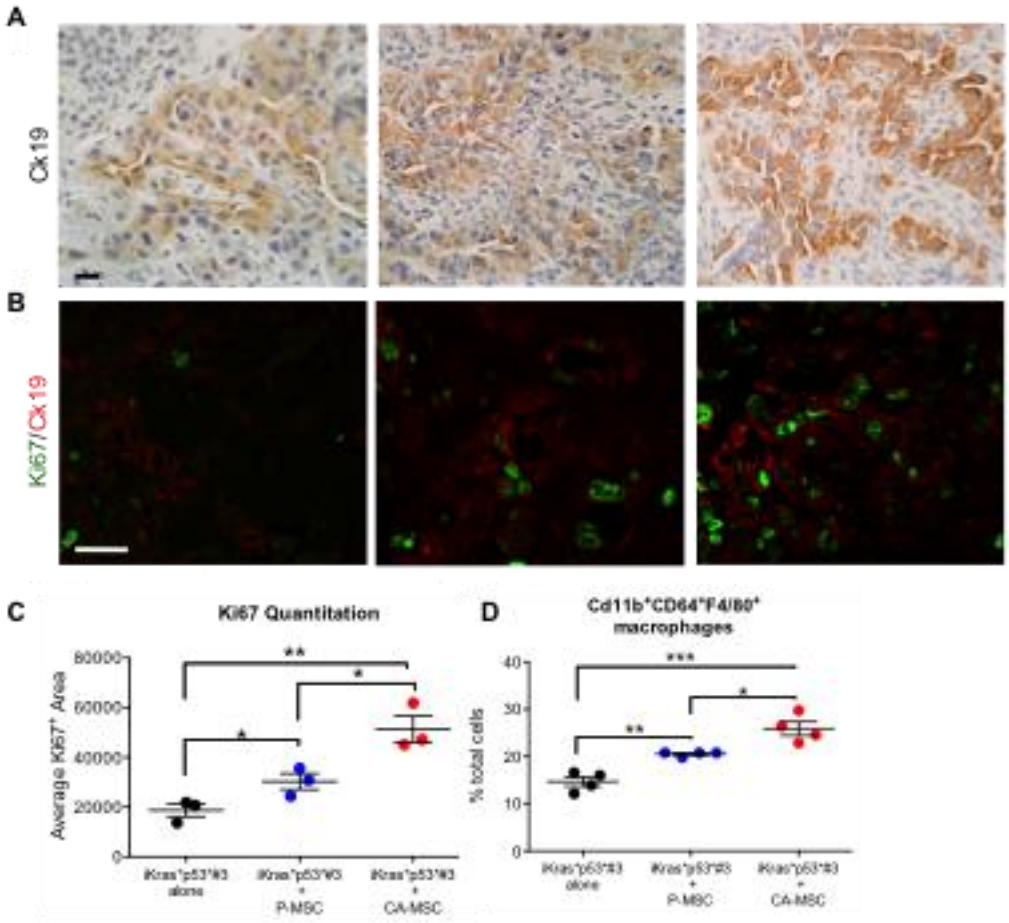

Figure 4.6: CA-MSCs promote tumor proliferation and macrophage infiltration.

(A) Immunohistochemistry for Ck19, scale bar represents 20μm. (B) Immunohistochemistry for Ki67 (green) and Ck19 (red), scale bar represents 20μm. (C)Quantitation of Ki67 staining. (D) Flow cytometry analysis of macrophages.

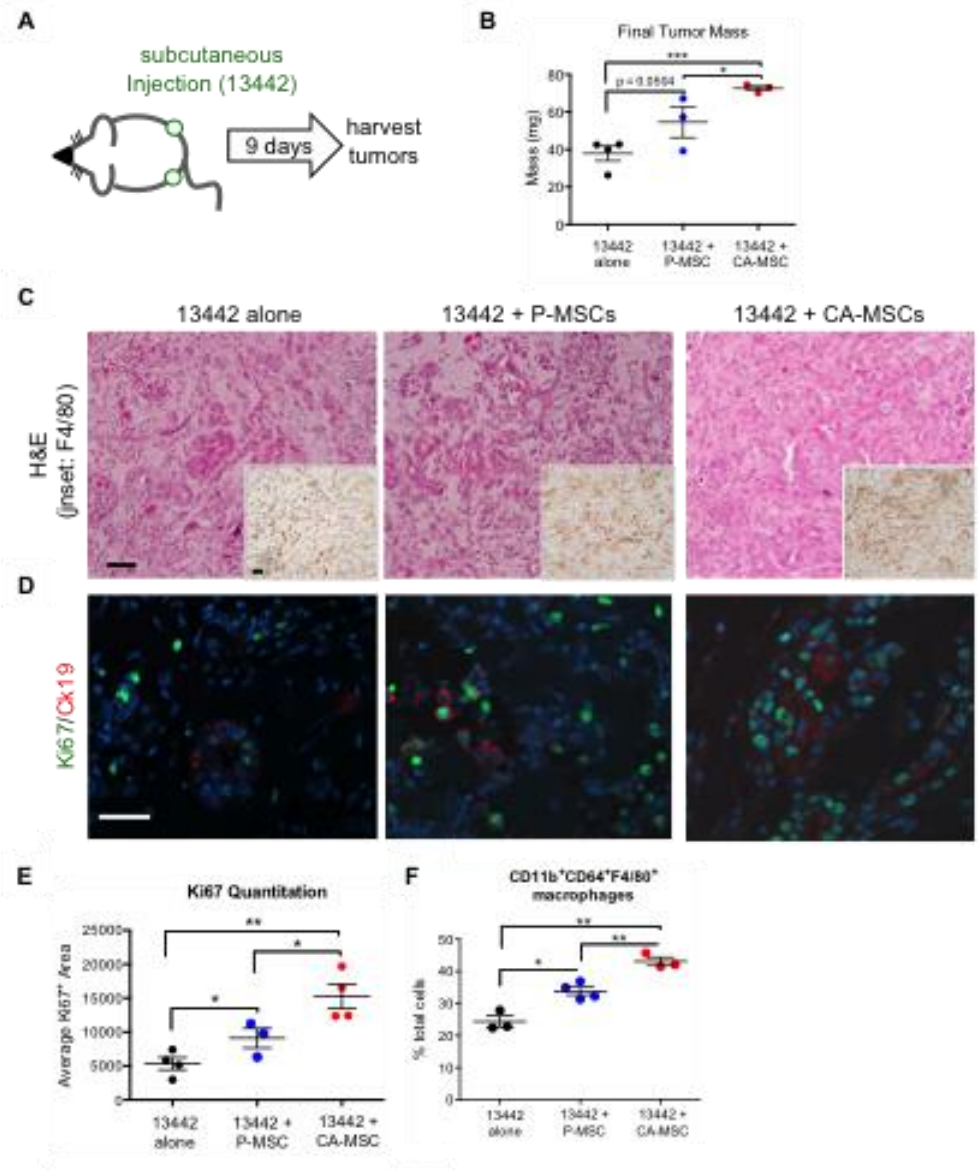

Figure 4.7: CA-MSCs promote tumor growth when co-injected with KPC tumor cells.

(A) Experimental design. (B) Final tumor mass. (C) Histopathological analysis of tumors from co-injection of 13442 KPC tumor cells with MSCs, scale bar: 50μm. Inset: antibody detection of F4/80. Scale bar: 20μm. (D) Antibody detection of Ki67, scale bar: 20μm. Inset: antibody detection of Ki67 (green) and CK19 (red). Nuclei marked by DAPI (blue), scale bar: 20μm. (E) Quantitiation of Ki67 staining. (F) Flow cytometry analysis of tumor CD11b+;CD64+;F4/80+ macrophages.

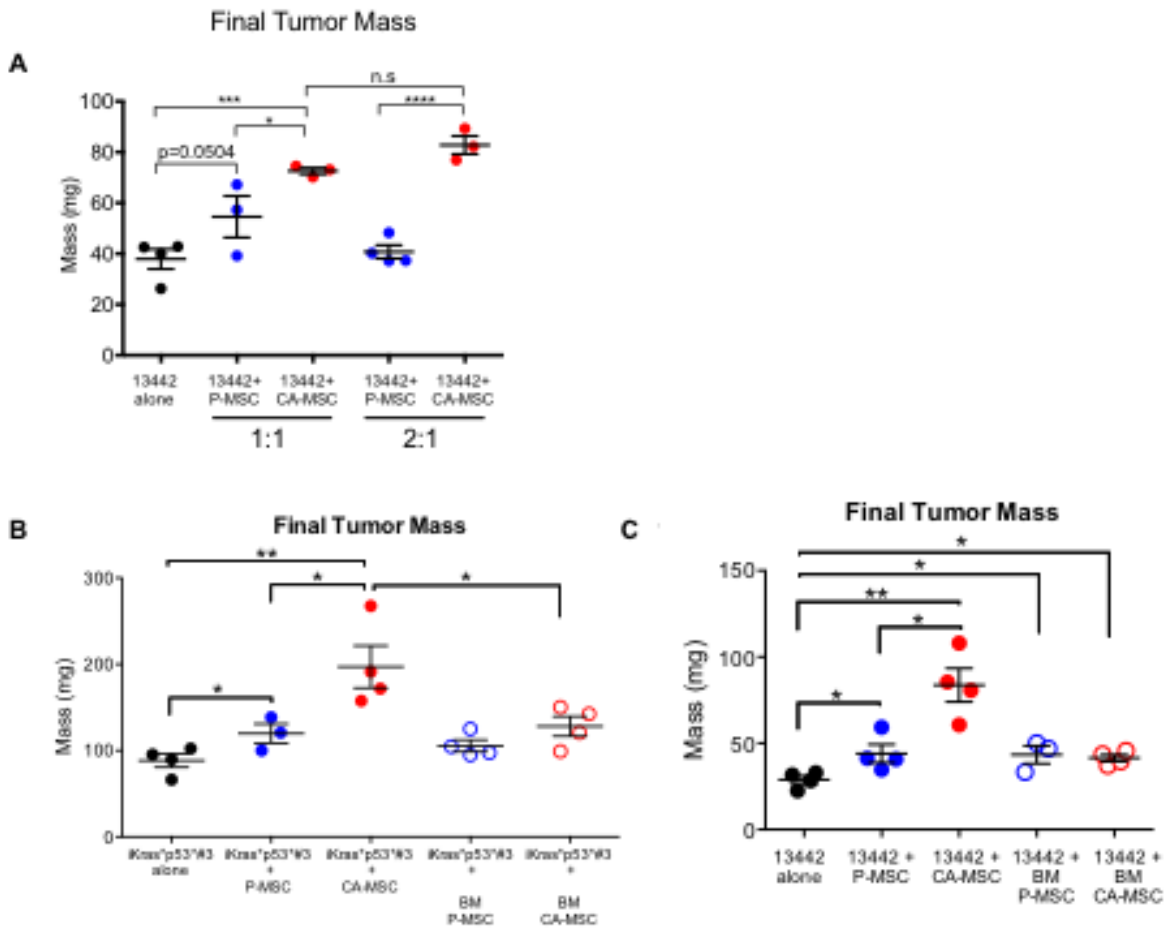

Figure 4.8: CA-MSCs promote tumor growth compared to their bone marrow counterparts.

(A) Final tumor mass for 13442 KPC tumor cells co-injected with MSCs at 2:1 and 1:1 ratios. (B) Final tumor mass of iKras*p53*#3 tumor cells co-injected with pancreatic and bone marrow MSCs. (C) Final tumor mass of 13442 KPC tumor cells co-injected with pancreatic and bone marrow MSCs.

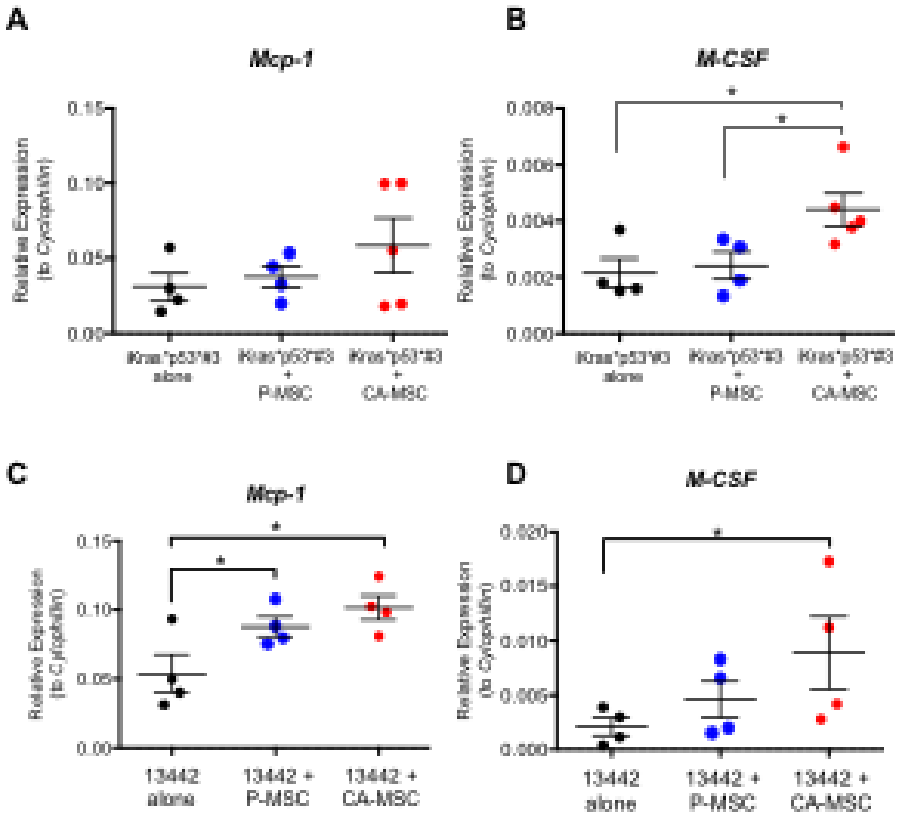

Figure 4.9: Tumors co-injected with CA-MSCs express the highest levels of *Mcp-1*.

qRT-PCR analysis for (A) *Mcp-1* and (B) *M-csf* in subcutaneous co-injection experiments with iKras*p53#3 cell line and MSCs. qRT-PCR analysis for (C) *Mcp-1* and (D) *M-csf* in subcutaneous co-injection experiments with 13442 cell line and MSCs.

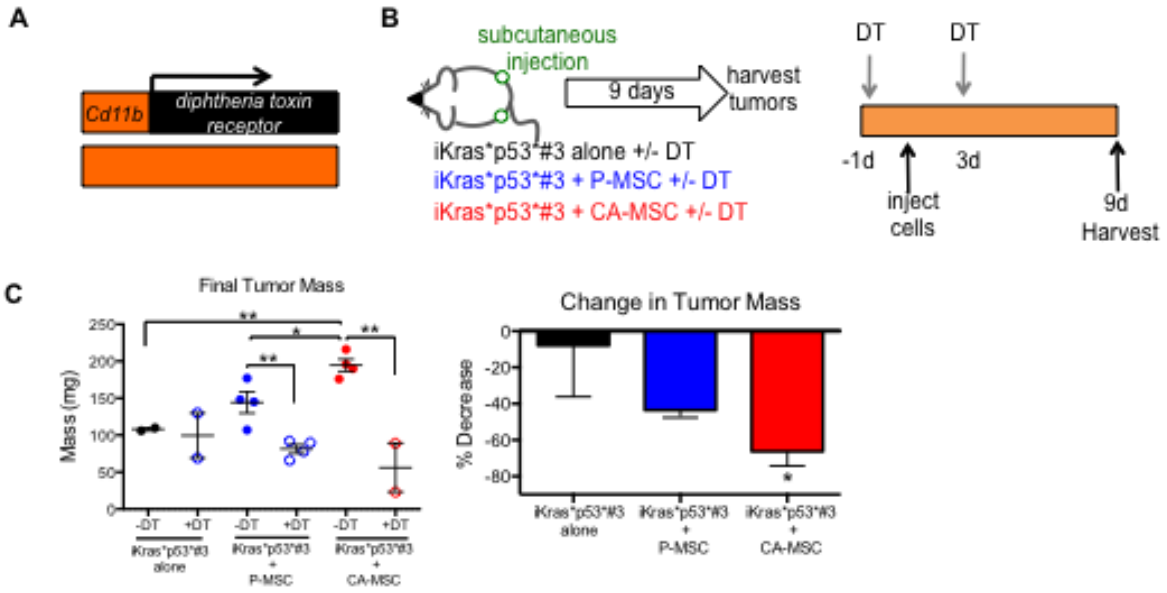

Figure 4.10: Myeloid cells are vital for CA-MSC-mediated tumor growth.

(A) Schematic for Cd11b-DTR mouse. (B) Experimental Design. (C) Left: Final tumor mass. Data is presented as mean ± SEM. Right: Percentage decrease in tumor mass.

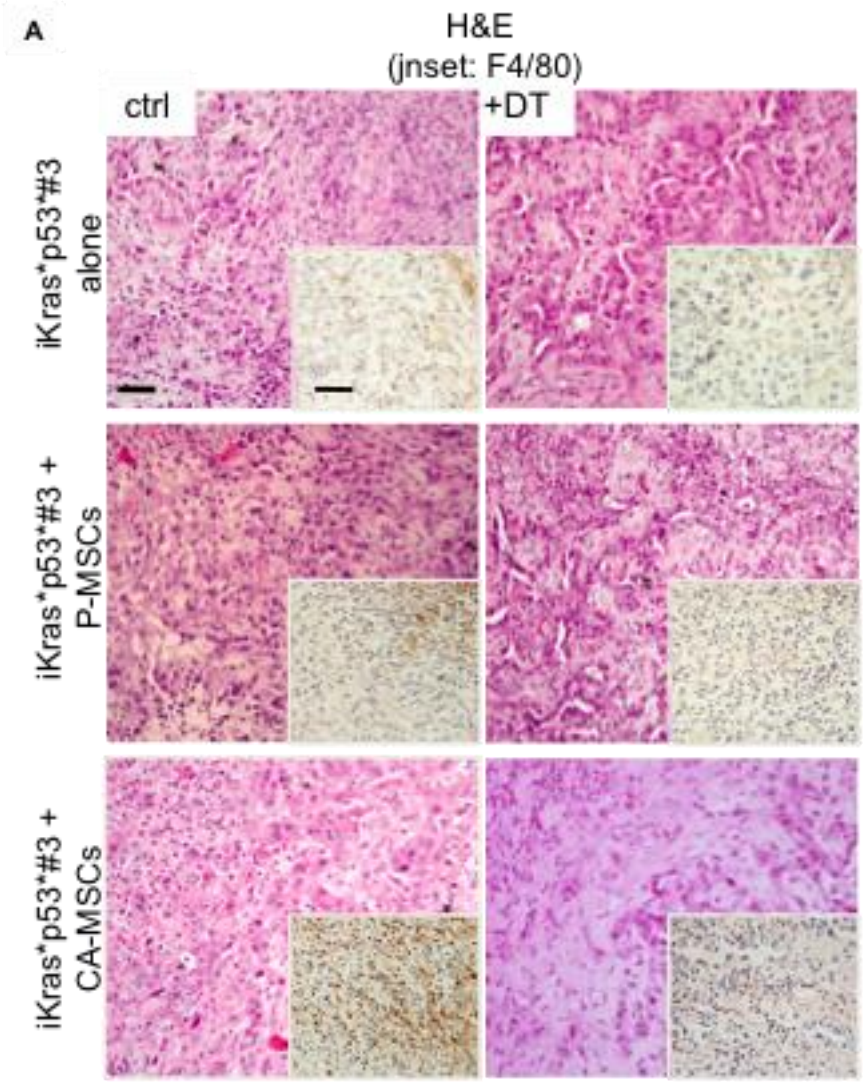

Figure 4.11: Myeloid cells can be depleted from tumors in CD11b-DTR mice.

(A) Histopathological analysis of tumors following co-injection. H&E staining, Scale bar represents 50μm. Inset F4/80 staining, scale bar represents 50μm.

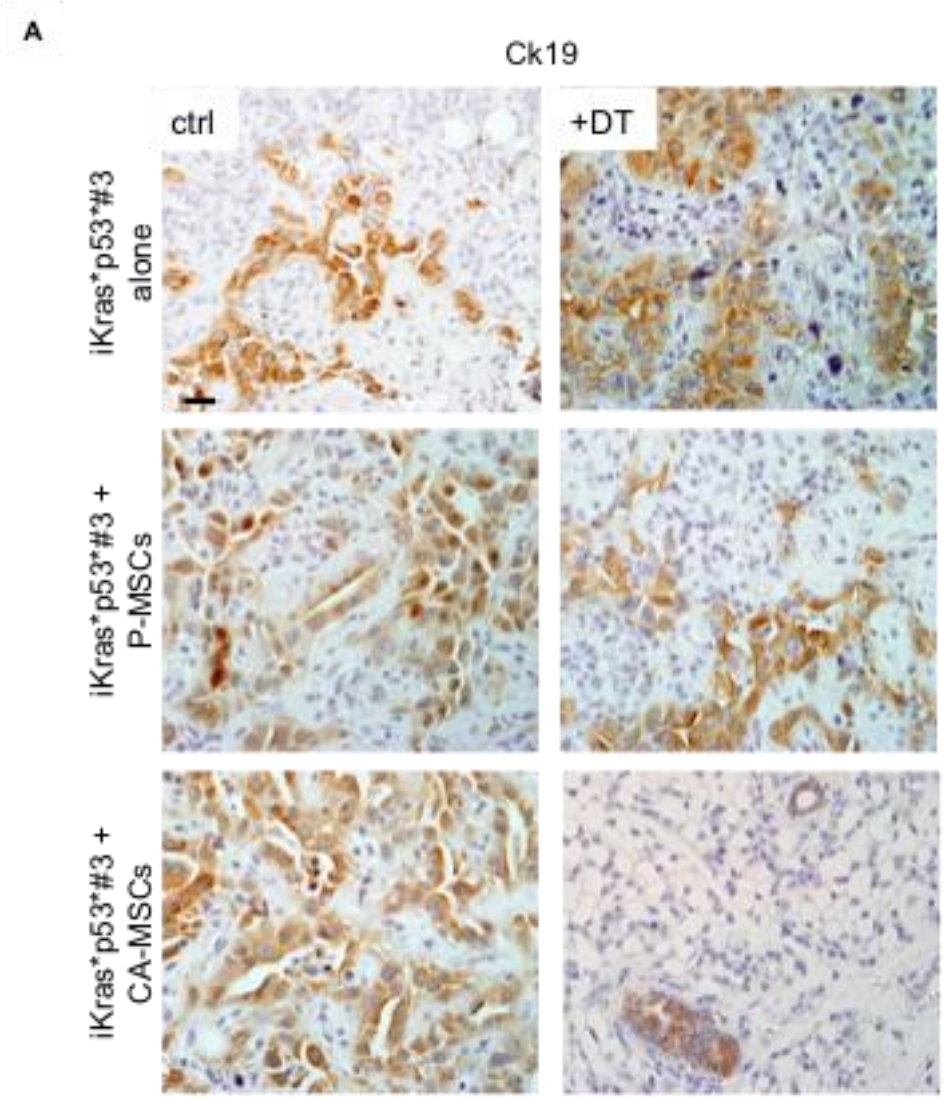

Figure 4.12: Tumor cell numbers are reduced upon myeloid cell depletion.

(A) Antibody detection of CK19, scale bar: 20µm.

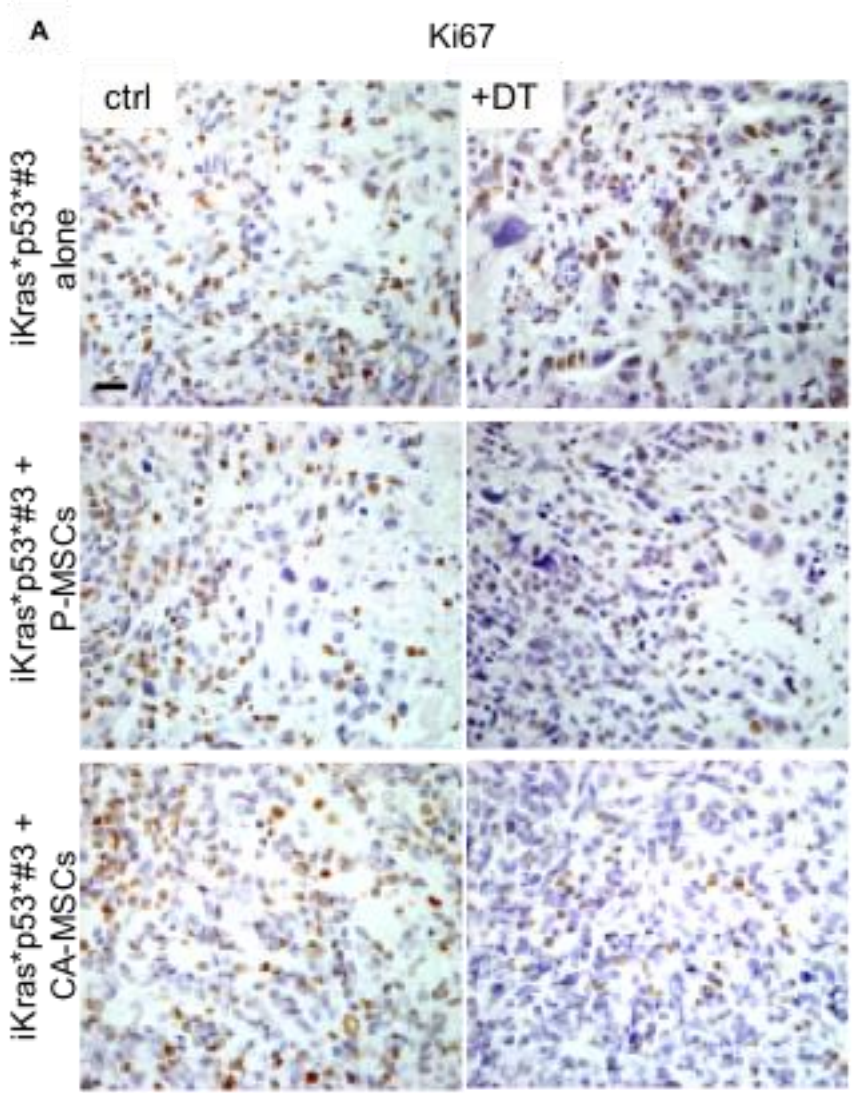

Figure 4.13: Myeloid cell depletion reduces the number of proliferating cells in tumors.

(A) Immunohistochemistry for Ki67, scale bar represents 20μm.

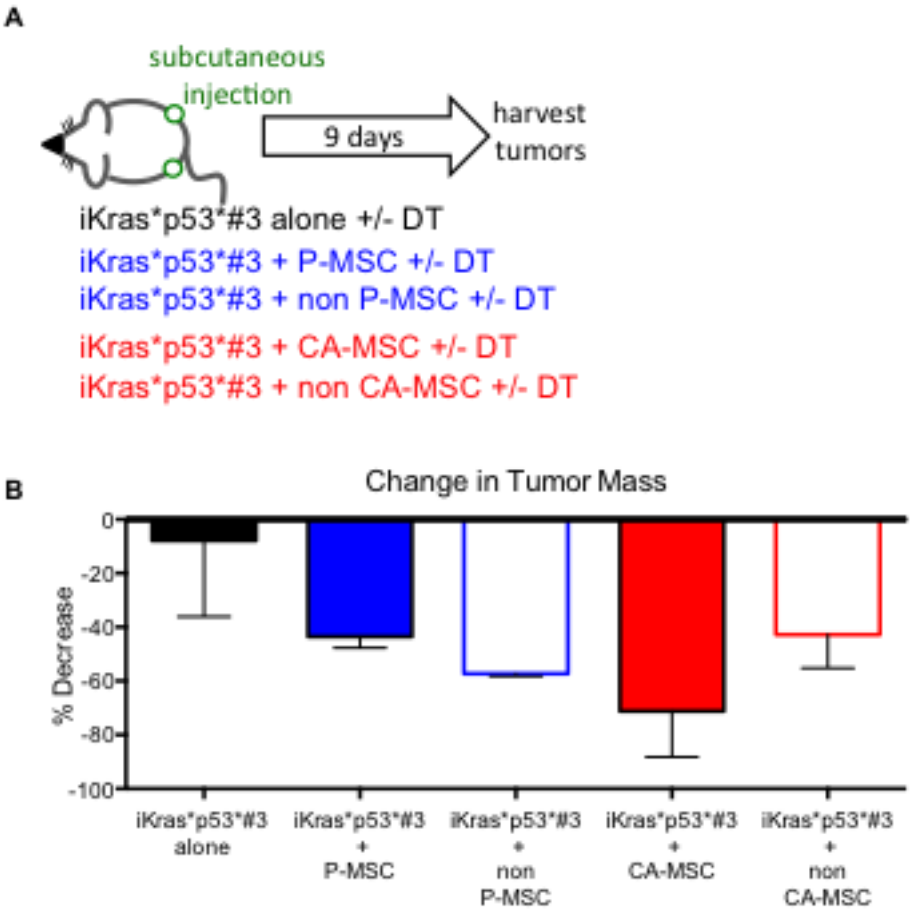

Figure 4.14: Myeloid cell depletion reduces tumor size.

(A) Experimental design. (B) Percent change in tumor mass after CD11b cell depletion.

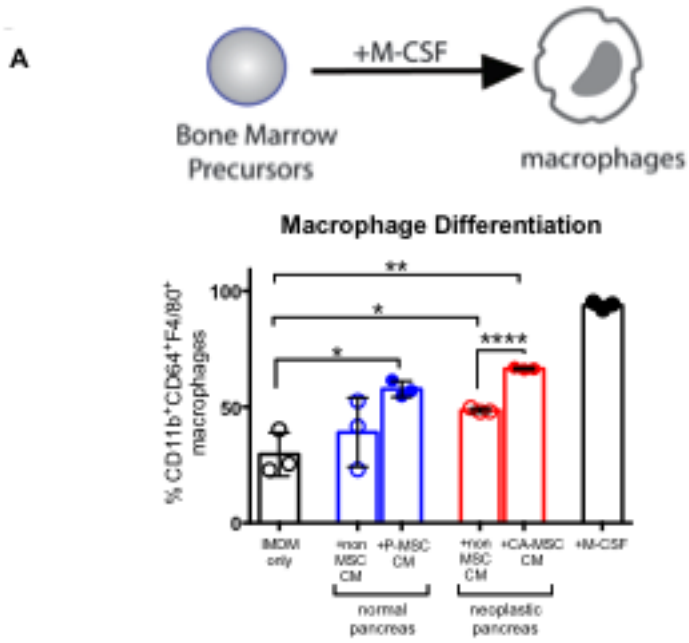

Figure 4.15: CA-MSC derived factors promote macrophage differentiation.

(A) Flow cytometry analysis of *in vitro* differentiated macrophages. Each data point represents bone marrow precursors from one mouse.

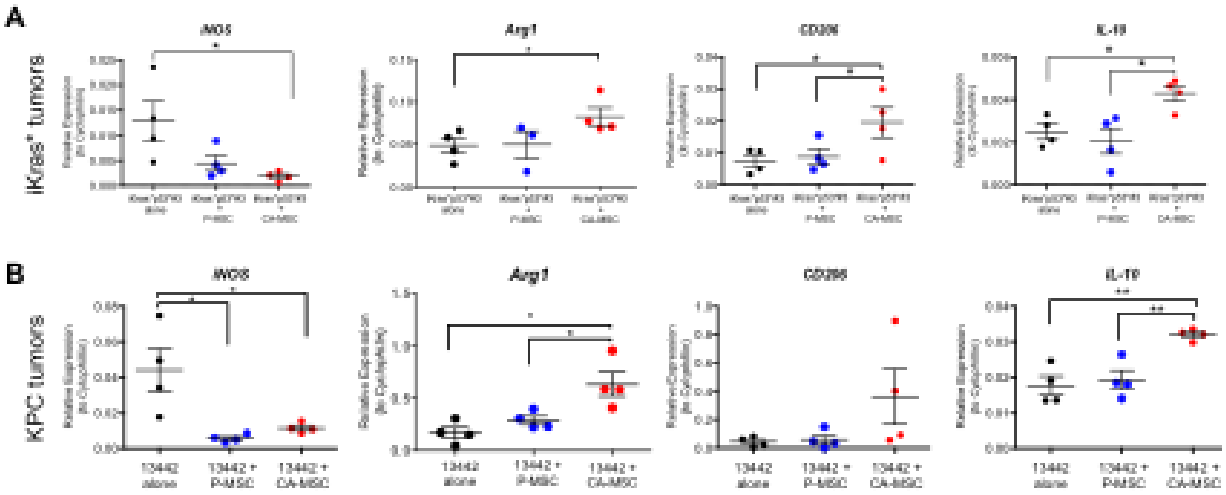

Figure 4.16: Tumor tissue from CA-MSCs co-injected with tumor cells express markers of M2-like macrophage polarization.

(A) RT-qPCR analysis of tumor tissue from co-injections of iKras*p53*#3 tumor cells with MSCs for *iNos, Arg1, Cd206, Il-10.* (B) RT-qPCR analysis of tumor tissue from co-injections of 13442 KPC tumor cells with MSCs for *iNos, Arg1, Cd206, Il-10.*

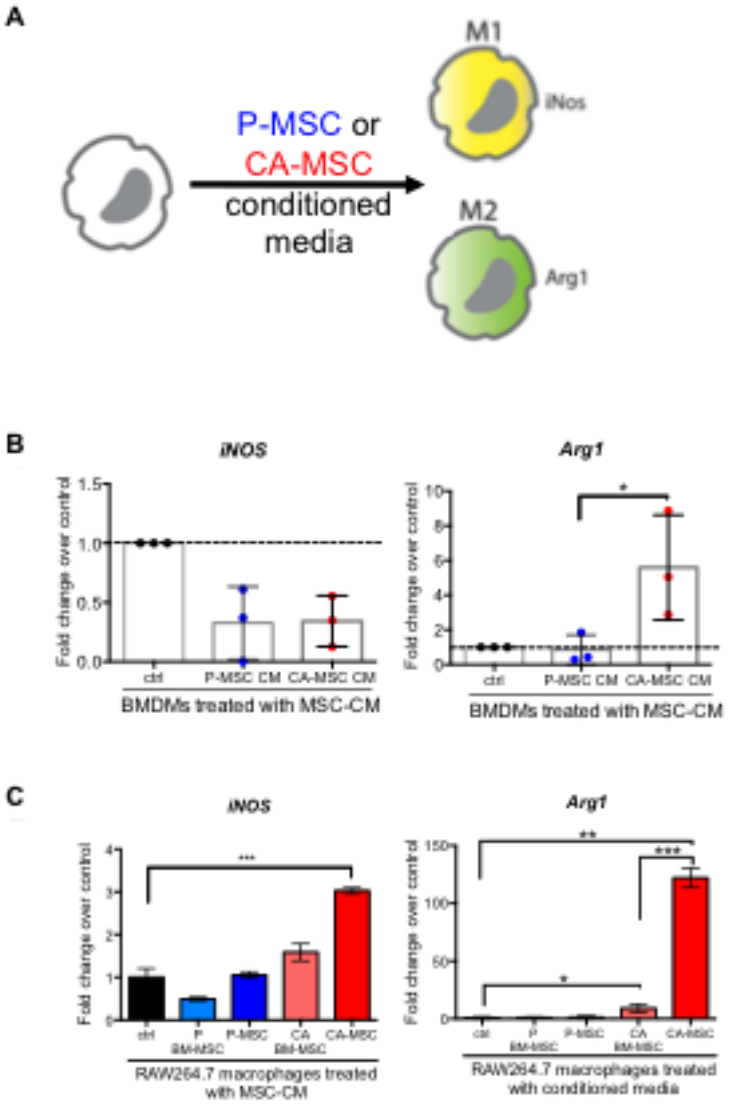

Figure 4.17: CA-MSC derived factors promote M2-like macrophage polarization *in vitro*.

(A) Experimental design. (B) qRT-PCR on BMDMs for *iNOS* (left) and *Arg1* (right). Each data point represents BMDMs from one mouse. (C) qRT-PCR on Raw264.7 macrophages for *iNOS* (left) and *Arg1* (right).

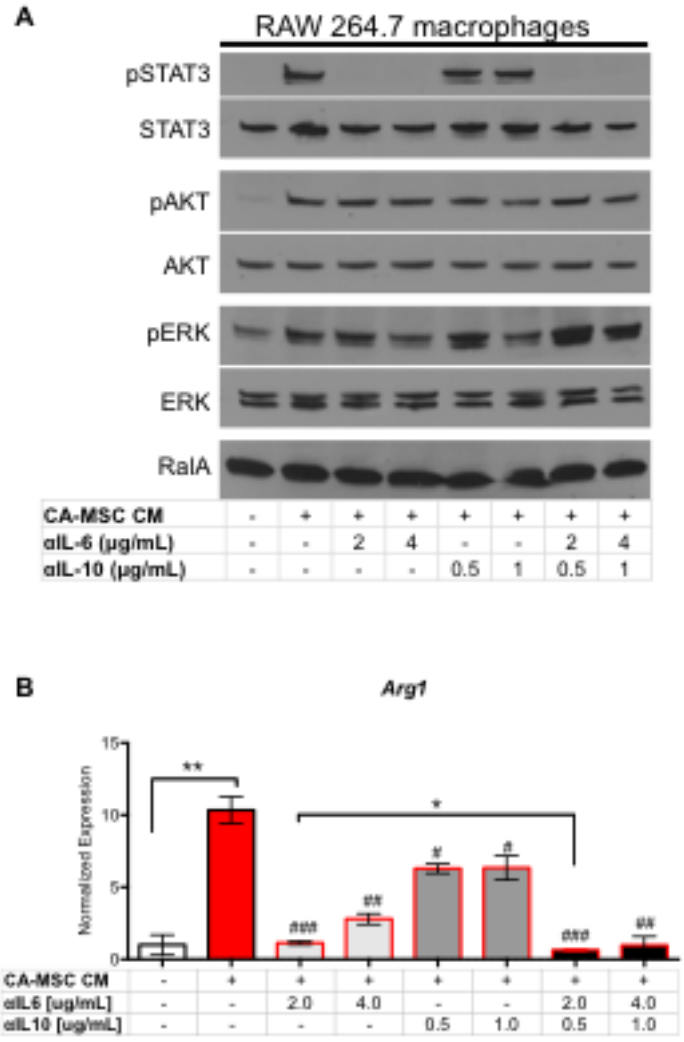

Figure 4.18: CA-MSC derived IL6 and IL10 promote M2-like macrophage polarization.

(A) Western Blot analysis of RAW264.7 macrophages treated with conditioned media and inhibitors. (B) qRT-PCR on RAW264.7 macrophages treated with conditioned media and inhibitors for *Arg1*. # indicate significant differences from CA-MSC stimulated cells.

Figure 4.17A Data/figure credit: Arthur L. Brannon and AnnaChiara Del Vecchio.

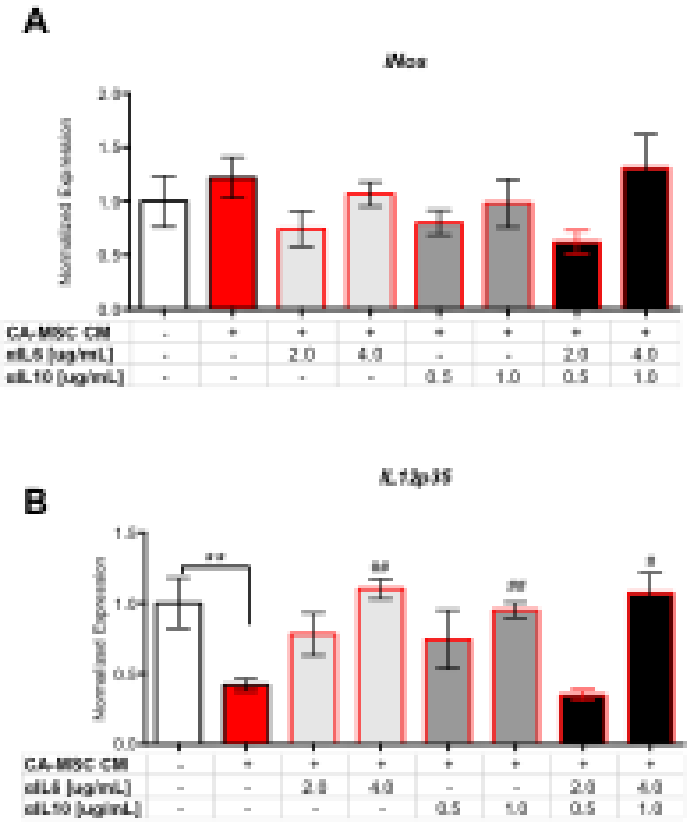

Figure 4.19: CA-MSC derived IL6 and IL10 suppress M1-like macrophage polarization.

(A) RT-qPCR analysis of RAW264.7 macrophages for *iNos*. (B) RT-qPCR analysis of RAW264.7 macrophages for *IL12p35*. # indicate significant differences from CA-MSC stimulated cells.

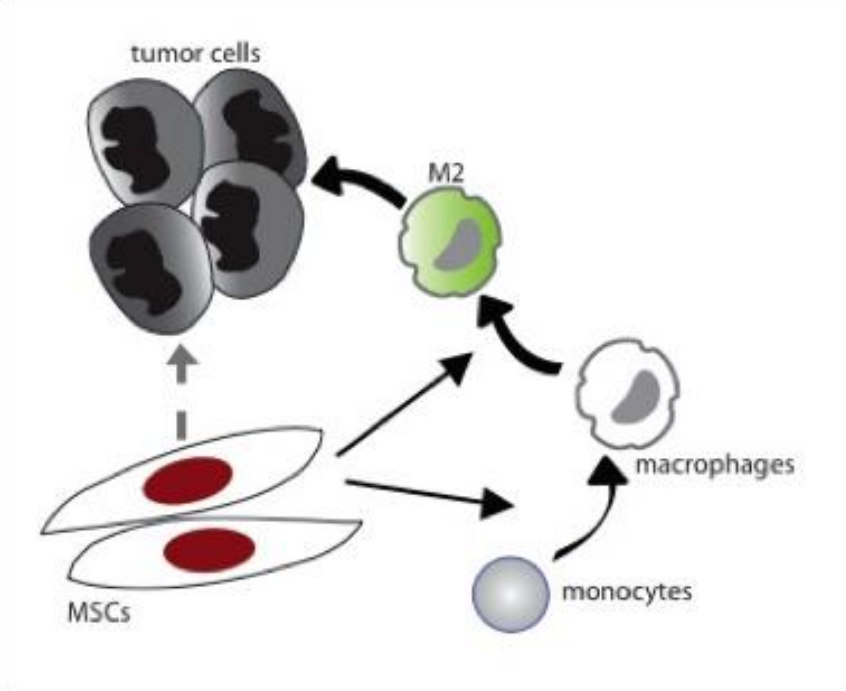

Figure 4.20: Working model wherein CA-MSC derived IL6 and IL10 promote M2-like macrophage polarization, which in turn promotes tumor growth.

Working model: CA-MSCs promote tumor growth, in part, by supporting the recruitment and polarization of M2-like macrophages.

Tables

Table 4.1: List of primers		
Primer	**Forward (5'-3')**	**Reverse (5'-3')**
Arg1	ctccaagccaaagtccttagag	aggagctgtcattagggacatc
BMP2	gggacccgctgtcttctagt	tcaactcaaattcgctgaggac
BMP4	ttcctggtaaccgaatgctga	cctgaatctcggcgacttttt
CD206	ggcaggatcttggcaacctagta	gtttggatcggcacacaaagtc
Cox-2	tgagcaactattccaaaccagc	gcacgtagtcttcgatcactatc
G-CSF	atggctcaactttctgcccag	ctgacagtgaccaggggaac
GM-CSF	atgcctgtcacgttgaatgaag	gcgggtctgcacacatgtta
IL6	ttccatccagttgccttcttgg	ttctcatttccacgatttcccag
IL10	gctcttactgactggcatgag	cgcagctctaggagcatgtg
IL12p35	cctcagtttggccagggtc	caggtttcgggactggctaag
iNOS	ccaagccctcacctacttcc	ctctgagggctgacacaagg
M-CSF	gacttcatgccagattgcc	ggtggctttagggtacagg
Mcp-1	ttaaaaacctggatcggaaccaa	gcattagcttcagatttacgggt
TGFβ1	tgacgtcactggagttgtacgg	ggttcatgtcatggatggtgc

References

1. Neesse, A., Michl, P., Frese, K. K., Feig, C., Cook, N., Jacobetz, M. A., Lolkema, M. P., Buchholz, M., Olive, K. P., Gress, T. M., and Tuveson, D. A. (2011) Stromal biology and therapy in pancreatic cancer. *Gut* **60**, 861-868
2. Hruban, R. H., Maitra, A., and Goggins, M. (2008) Update on pancreatic intraepithelial neoplasia. *Int J Clin Exp Pathol* **1**, 306-316
3. Clark, C. E., Hingorani, S. R., Mick, R., Combs, C., Tuveson, D. A., and Vonderheide, R. H. (2007) Dynamics of the immune reaction to pancreatic cancer from inception to invasion. *Cancer Res* **67**, 9518-9527
4. Apte, M. V., Park, S., Phillips, P. A., Santucci, N., Goldstein, D., Kumar, R. K., Ramm, G. A., Buchler, M., Friess, H., McCarroll, J. A., Keogh, G., Merrett, N., Pirola, R., and Wilson, J. S. (2004) Desmoplastic reaction in pancreatic cancer: role of pancreatic stellate cells. *Pancreas* **29**, 179-187
5. Hwang, R. F., Moore, T., Arumugam, T., Ramachandran, V., Amos, K. D., Rivera, A., Ji, B., Evans, D. B., and Logsdon, C. D. (2008) Cancer-associated stromal fibroblasts promote pancreatic tumor progression. *Cancer Res* **68**, 918-926
6. Ozdemir, B. C., Pentcheva-Hoang, T., Carstens, J. L., Zheng, X., Wu, C. C., Simpson, T. R., Laklai, H., Sugimoto, H., Kahlert, C., Novitskiy, S. V., De Jesus-Acosta, A., Sharma, P., Heidari, P., Mahmood, U., Chin, L., Moses, H. L., Weaver, V. M., Maitra, A., Allison, J. P., LeBleu, V. S., and Kalluri, R. (2014) Depletion of carcinoma-associated fibroblasts and fibrosis induces immunosuppression and accelerates pancreas cancer with reduced survival. *Cancer Cell* **25**, 719-734
7. Rhim, A. D., Oberstein, P. E., Thomas, D. H., Mirek, E. T., Palermo, C. F., Sastra, S. A., Dekleva, E. N., Saunders, T., Becerra, C. P., Tattersall, I. W., Westphalen, C. B., Kitajewski, J., Fernandez-Barrena, M. G., Fernandez-Zapico, M. E., Iacobuzio-Donahue, C., Olive, K. P., and Stanger, B. Z. (2014) Stromal elements act to restrain, rather than support, pancreatic ductal adenocarcinoma. *Cancer Cell* **25**, 735-747
8. Baertschiger, R. M., Bosco, D., Morel, P., Serre-Beinier, V., Berney, T., Buhler, L. H., and Gonelle-Gispert, C. (2008) Mesenchymal stem cells derived from human exocrine pancreas express transcription factors implicated in beta-cell development. *Pancreas* **37**, 75-84
9. Crisan, M., Yap, S., Casteilla, L., Chen, C. W., Corselli, M., Park, T. S., Andriolo, G., Sun, B., Zheng, B., Zhang, L., Norotte, C., Teng, P. N., Traas, J., Schugar, R., Deasy, B. M., Badylak, S., Buhring, H. J., Giacobino, J. P., Lazzari, L., Huard, J., and Peault, B. (2008) A perivascular origin for mesenchymal stem cells in multiple human organs. *Cell Stem Cell* **3**, 301-313
10. Gopurappilly, R., Bhat, V., and Bhonde, R. (2013) Pancreatic tissue resident mesenchymal stromal cell (MSC)-like cells as a source of in vitro islet neogenesis. *J Cell Biochem* **114**, 2240-2247

11. Joyce, J. A., and Pollard, J. W. (2009) Microenvironmental regulation of metastasis. *Nat Rev Cancer* **9**, 239-252
12. Karnoub, A. E., Dash, A. B., Vo, A. P., Sullivan, A., Brooks, M. W., Bell, G. W., Richardson, A. L., Polyak, K., Tubo, R., and Weinberg, R. A. (2007) Mesenchymal stem cells within tumour stroma promote breast cancer metastasis. *Nature* **449**, 557-563
13. McLean, K., Gong, Y., Choi, Y., Deng, N., Yang, K., Bai, S., Cabrera, L., Keller, E., McCauley, L., Cho, K. R., and Buckanovich, R. J. (2011) Human ovarian carcinoma-associated mesenchymal stem cells regulate cancer stem cells and tumorigenesis via altered BMP production. *J Clin Invest* **121**, 3206-3219
14. Ren, G., Zhao, X., Wang, Y., Zhang, X., Chen, X., Xu, C., Yuan, Z. R., Roberts, A. I., Zhang, L., Zheng, B., Wen, T., Han, Y., Rabson, A. B., Tischfield, J. A., Shao, C., and Shi, Y. (2012) CCR2-dependent recruitment of macrophages by tumor-educated mesenchymal stromal cells promotes tumor development and is mimicked by TNFalpha. *Cell Stem Cell* **11**, 812-824
15. Hingorani, S. R., Petricoin, E. F., Maitra, A., Rajapakse, V., King, C., Jacobetz, M. A., Ross, S., Conrads, T. P., Veenstra, T. D., Hitt, B. A., Kawaguchi, Y., Johann, D., Liotta, L. A., Crawford, H. C., Putt, M. E., Jacks, T., Wright, C. V., Hruban, R. H., Lowy, A. M., and Tuveson, D. A. (2003) Preinvasive and invasive ductal pancreatic cancer and its early detection in the mouse. *Cancer Cell* **4**, 437-450
16. Biankin, A. V., Waddell, N., Kassahn, K. S., Gingras, M. C., Muthuswamy, L. B., Johns, A. L., Miller, D. K., Wilson, P. J., Patch, A. M., Wu, J., Chang, D. K., Cowley, M. J., Gardiner, B. B., Song, S., Harliwong, I., Idrisoglu, S., Nourse, C., Nourbakhsh, E., Manning, S., Wani, S., Gongora, M., Pajic, M., Scarlett, C. J., Gill, A. J., Pinho, A. V., Rooman, I., Anderson, M., Holmes, O., Leonard, C., Taylor, D., Wood, S., Xu, Q., Nones, K., Fink, J. L., Christ, A., Bruxner, T., Cloonan, N., Kolle, G., Newell, F., Pinese, M., Mead, R. S., Humphris, J. L., Kaplan, W., Jones, M. D., Colvin, E. K., Nagrial, A. M., Humphrey, E. S., Chou, A., Chin, V. T., Chantrill, L. A., Mawson, A., Samra, J. S., Kench, J. G., Lovell, J. A., Daly, R. J., Merrett, N. D., Toon, C., Epari, K., Nguyen, N. Q., Barbour, A., Zeps, N., Kakkar, N., Zhao, F., Wu, Y. Q., Wang, M., Muzny, D. M., Fisher, W. E., Brunicardi, F. C., Hodges, S. E., Reid, J. G., Drummond, J., Chang, K., Han, Y., Lewis, L. R., Dinh, H., Buhay, C. J., Beck, T., Timms, L., Sam, M., Begley, K., Brown, A., Pai, D., Panchal, A., Buchner, N., De Borja, R., Denroche, R. E., Yung, C. K., Serra, S., Onetto, N., Mukhopadhyay, D., Tsao, M. S., Shaw, P. A., Petersen, G. M., Gallinger, S., Hruban, R. H., Maitra, A., Iacobuzio-Donahue, C. A., Schulick, R. D., Wolfgang, C. L., Morgan, R. A., Lawlor, R. T., Capelli, P., Corbo, V., Scardoni, M., Tortora, G., Tempero, M. A., Mann, K. M., Jenkins, N. A., Perez-Mancera, P. A., Adams, D. J., Largaespada, D. A., Wessels, L. F., Rust, A. G., Stein, L. D., Tuveson, D. A., Copeland, N. G., Musgrove, E. A., Scarpa, A., Eshleman, J. R., Hudson, T. J., Sutherland, R. L., Wheeler, D. A., Pearson, J. V., McPherson, J. D., Gibbs, R. A., and Grimmond, S. M. (2012)

Pancreatic cancer genomes reveal aberrations in axon guidance pathway genes. *Nature* **491**, 399-405
17. Jones, S., Zhang, X., Parsons, D. W., Lin, J. C., Leary, R. J., Angenendt, P., Mankoo, P., Carter, H., Kamiyama, H., Jimeno, A., Hong, S. M., Fu, B., Lin, M. T., Calhoun, E. S., Kamiyama, M., Walter, K., Nikolskaya, T., Nikolsky, Y., Hartigan, J., Smith, D. R., Hidalgo, M., Leach, S. D., Klein, A. P., Jaffee, E. M., Goggins, M., Maitra, A., Iacobuzio-Donahue, C., Eshleman, J. R., Kern, S. E., Hruban, R. H., Karchin, R., Papadopoulos, N., Parmigiani, G., Vogelstein, B., Velculescu, V. E., and Kinzler, K. W. (2008) Core signaling pathways in human pancreatic cancers revealed by global genomic analyses. *Science* **321**, 1801-1806
18. Kawaguchi, Y., Cooper, B., Gannon, M., Ray, M., MacDonald, R. J., and Wright, C. V. (2002) The role of the transcriptional regulator Ptf1a in converting intestinal to pancreatic progenitors. *Nat Genet* **32**, 128-134
19. Morris, J. P. t., Cano, D. A., Sekine, S., Wang, S. C., and Hebrok, M. (2010) Beta-catenin blocks Kras-dependent reprogramming of acini into pancreatic cancer precursor lesions in mice. *J Clin Invest* **120**, 508-520
20. Weischenfeldt, J., and Porse, B. (2008) Bone Marrow-Derived Macrophages (BMM): Isolation and Applications. *CSH Protoc* **2008**, pdb prot5080
21. Dominici, M., Le Blanc, K., Mueller, I., Slaper-Cortenbach, I., Marini, F., Krause, D., Deans, R., Keating, A., Prockop, D., and Horwitz, E. (2006) Minimal criteria for defining multipotent mesenchymal stromal cells. The International Society for Cellular Therapy position statement. *Cytotherapy* **8**, 315-317
22. Mathew, E., Collins, M. A., Fernandez-Barrena, M. G., Holtz, A. M., Yan, W., Hogan, J. O., Tata, Z., Allen, B. L., Fernandez-Zapico, M. E., and di Magliano, M. P. (2014) The transcription factor GLI1 modulates the inflammatory response during pancreatic tissue remodeling. *J Biol Chem* **289**, 27727-27743
23. Lesina, M., Kurkowski, M. U., Ludes, K., Rose-John, S., Treiber, M., Kloppel, G., Yoshimura, A., Reindl, W., Sipos, B., Akira, S., Schmid, R. M., and Algul, H. (2011) Stat3/Socs3 activation by IL-6 transsignaling promotes progression of pancreatic intraepithelial neoplasia and development of pancreatic cancer. *Cancer Cell* **19**, 456-469
24. Zhang, Y., Yan, W., Collins, M. A., Bednar, F., Rakshit, S., Zetter, B. R., Stanger, B. Z., Chung, I., Rhim, A. D., and di Magliano, M. P. (2013) Interleukin-6 is required for pancreatic cancer progression by promoting MAPK signaling activation and oxidative stress resistance. *Cancer Res* **73**, 6359-6374
25. Sharma, S., Stolina, M., Lin, Y., Gardner, B., Miller, P. W., Kronenberg, M., and Dubinett, S. M. (1999) T cell-derived IL-10 promotes lung cancer growth by suppressing both T cell and APC function. *J Immunol* **163**, 5020-5028
26. Amatangelo, M. D., Goodyear, S., Varma, D., and Stearns, M. E. (2012) c-Myc expression and MEK1-induced Erk2 nuclear localization are required for TGF-beta induced epithelial-mesenchymal transition and invasion in prostate cancer. *Carcinogenesis* **33**, 1965-1975

27. Yeh, T. S., Wu, C. W., Hsu, K. W., Liao, W. J., Yang, M. C., Li, A. F., Wang, A. M., Kuo, M. L., and Chi, C. W. (2009) The activated Notch1 signal pathway is associated with gastric cancer progression through cyclooxygenase-2. *Cancer Res* **69**, 5039-5048
28. Collins, M. A., Brisset, J. C., Zhang, Y., Bednar, F., Pierre, J., Heist, K. A., Galban, C. J., Galban, S., and di Magliano, M. P. (2012) Metastatic pancreatic cancer is dependent on oncogenic Kras in mice. *PLoS One* **7**, e49707
29. Jiang, W., Zhang, Y., Kane, K. T., Collins, M. A., Simeone, D. M., di Magliano, M. P., and Nguyen, K. T. (2015) CD44 regulates pancreatic cancer invasion through MT1-MMP. *Mol Cancer Res* **13**, 9-15
30. Hingorani, S. R., Wang, L., Multani, A. S., Combs, C., Deramaudt, T. B., Hruban, R. H., Rustgi, A. K., Chang, S., and Tuveson, D. A. (2005) Trp53R172H and KrasG12D cooperate to promote chromosomal instability and widely metastatic pancreatic ductal adenocarcinoma in mice. *Cancer Cell* **7**, 469-483
31. Quante, M., Tu, S. P., Tomita, H., Gonda, T., Wang, S. S., Takashi, S., Baik, G. H., Shibata, W., Diprete, B., Betz, K. S., Friedman, R., Varro, A., Tycko, B., and Wang, T. C. (2011) Bone marrow-derived myofibroblasts contribute to the mesenchymal stem cell niche and promote tumor growth. *Cancer Cell* **19**, 257-272
32. Kramann, R., Schneider, R. K., DiRocco, D. P., Machado, F., Fleig, S., Bondzie, P. A., Henderson, J. M., Ebert, B. L., and Humphreys, B. D. (2015) Perivascular Gli1+ progenitors are key contributors to injury-induced organ fibrosis. *Cell Stem Cell* **16**, 51-66
33. Zhu, Y., Knolhoff, B. L., Meyer, M. A., Nywening, T. M., West, B. L., Luo, J., Wang-Gillam, A., Goedegebuure, S. P., Linehan, D. C., and DeNardo, D. G. (2014) CSF1/CSF1R blockade reprograms tumor-infiltrating macrophages and improves response to T-cell checkpoint immunotherapy in pancreatic cancer models. *Cancer Res* **74**, 5057-5069
34. Duffield, J. S., Forbes, S. J., Constandinou, C. M., Clay, S., Partolina, M., Vuthoori, S., Wu, S., Lang, R., and Iredale, J. P. (2005) Selective depletion of macrophages reveals distinct, opposing roles during liver injury and repair. *J Clin Invest* **115**, 56-65
35. Cho, D. I., Kim, M. R., Jeong, H. Y., Jeong, H. C., Jeong, M. H., Yoon, S. H., Kim, Y. S., and Ahn, Y. (2014) Mesenchymal stem cells reciprocally regulate the M1/M2 balance in mouse bone marrow-derived macrophages. *Exp Mol Med* **46**, e70
36. Zhang, Q. Z., Su, W. R., Shi, S. H., Wilder-Smith, P., Xiang, A. P., Wong, A., Nguyen, A. L., Kwon, C. W., and Le, A. D. (2010) Human gingiva-derived mesenchymal stem cells elicit polarization of m2 macrophages and enhance cutaneous wound healing. *Stem Cells* **28**, 1856-1868

Chapter Five[1]

Future Directions

Pancreatic cancer has the highest accumulation of reactive stroma of all solid epithelial cancers; up to 90% of the bulk tumor can consist of stromal elements, and as little as 10% the tumor cells themselves (1). Adding further complexity to this disease, the various components of the reactive stroma, from fibroblasts to various immune cells, respond to signals from the tumor, and also signal to each other. The molecular crosstalk between the tumor and stroma as well as from cells of the stroma to each other profoundly impacts tumorigenesis. Understanding the nature of these various molecular conversations is an area of active investigation, with the hope of identifying pathways of therapeutic significance. My thesis work focused on the contribution of stromal components to pancreatic tumorigenesis and pancreatic repair, with a particular emphasis on the HH pathway.

The role of dosage-dependent HH signaling on pancreatic cancer

Tumor growth

[1] Portions of this chapter have been submitted as an invited review to *Cellular and Molecular Life Sciences*: Mathew, E, Allen BA, and Pasca di Magliano, M. Tentative title: Hedgehog Signaling in Pancreatic Cancer

The work in Chapter Two highlighted a dosage-dependent role of HH signaling on promoting tumor growth. By deleting two (*Gas1* and *Boc*) or three (*Gas1*, *Boc,* and

Cdon) HH co-receptors in fibroblasts, I was able to reduce their HH-responsiveness moderately or almost completely, respectively. Further, I used these fibroblasts to reveal a dosage dependant effect of HH-response on tumor promotion; fibroblasts with little or no HH-response did not promote tumor growth, but counterintuitively, fibroblasts with a moderate response to HH promoted the growth of large, vascular tumors (2). However, my data as presented did not exclude the possible role of CDON for mediating the tumor-promoting effect. While further experiments are needed on multiple, independent MEF lines, initial evidence indicates that both *Boc*$^{-/-}$*;Cdon*$^{-/-}$ and *Gas1*$^{-/-}$*;Cdon*$^{-/-}$ MEFs also show reduced HH response compared to their wildtype counterparts (**Figure 5.1A**). *Gas1*$^{-/-}$ MEFs also display reduced HH responsiveness compared to wildtype MEFs (**Figure 5.1B**). Although *Gas1*$^{-/-}$*;Cdon*$^{-/-}$ MEFs have not yet been tested in tumor growth assays, *Boc*$^{-/-}$*;Cdon*$^{-/-}$ and *Gas1*$^{-/-}$ MEFs are able to promote the growth of larger tumors, similarly to *Gas1*$^{-/-}$*;Boc*$^{-/-}$ MEFs (**Figure 5.1C**). Further analysis of the tumor tissue to assess vascularity is ongoing. While this data is preliminary, it supports our hypothesis that this effect is a result of HH-dosage and not a specific effect of CDON alone. However, additional experiments with distinct *Boc*$^{-/-}$*;Cdon*$^{-/-}$ and *Gas1*$^{-/-}$*;Cdon*$^{-/-}$ MEF lines, as well as single co-receptor knockouts are necessary to elucidate the relationship between HH-response and tumor promotion.

Gas1, Boc, and Cdon have functions aside from their role in the HH signaling pathway (3,4). However, evidence supporting the role of the HH-related function of these proteins on the development of accelerated, vascularized tumors was provided by Rhim et al., who found that KPC;*Shh*$^{f/f}$ mice develop larger, more vascular tumors than

KPC mice; interestingly, they detected increased *Ihh* expression in KPC;*Shh*$^{f/f}$ compared to KPC mice (5). The question then, is whether the generation of a KPC;*Shh*$^{f/f}$;*Ihh*$^{f/f}$ mouse, and thus a complete ablation of HH ligands in the neoplastic pancreas, would slow tumor progression. Further, tumor cells derived from tumor-bearing KPC, KPC;*Shh*$^{f/f}$, and KPC;*Shh*$^{f/f}$;*Ihh*$^{ff/}$ mice could be used in co-injection experiments with co-receptor knockout MEFs. As the subcutaneous co-injection experiments in Chapter Two were performed with tumor cells that expressed *Shh*, additional experiments with tumor cells expressing different amounts of *Shh* and *Ihh* would strengthen the hypothesis of a dosage-dependent role for paracrine HH signaling in pancreatic cancer.

Additional HH pathway components

The expression profile of Gas1 and Boc in the adult mouse pancreas mirrors that of Gli2 (**Figure 5.2A**). Likewise, by crossing reporter alleles of Gli2, Gas1, and Boc into KC mice, we see similar expression throughout the stroma during pancreatic tumorigenesis (**Figure 5.2B**). Hhip expression is also detected by qRT-PCR in the neoplastic pancreas of iKras* mice, and its expression decreases upon oncogenic Kras inactivation (**see Figure 3.11C**). However, this expression was determined by qRT-PCR of whole pancreatic tissue, and thus the identity of the cells expression Hhip remains unclear. Including *Gli2*$^{-/-}$, *Ptch1*$^{+/-}$ and *Ptch1*$^{+/-}$;*Hhip*$^{-/-}$ MEFs in our analysis would allow us to test the importance of additional HH pathway components in pancreatic tumor growth.

Tumor progression

The work in Chapter two focused on the effect of fibroblast response to HH on tumor growth, but did not deeply investigate any possible impact on tumor initiation and progression. Studies on KC;*Gas1*$^{-/-}$ and KC;*Boc*$^{+/-}$ mice revealed no overt differences in PanIN-formation and stroma accumulation compared to KC mice at 3 weeks following caerulein-induced pancreatitis. We also did not detect differences in tissue vascularity at this stage between KC, KC;*Gas1*$^{-/-}$ and KC;*Boc*$^{+/-}$ pancreata (**Figures 5.3A and 5.3B**). However, generating combination crosses, such as KC;*Gas1*$^{-/-}$;*Boc*$^{+/-}$ would allow us to test several aspects of co-receptor function on tumor initiation and progression. First, we could test whether expression of the co-receptors completely overlaps in fibroblasts, or whether distinct populations exist. Notably, Gas1 and Boc are co-expressed in the same fibroblasts in unperturbed pancreas from *Gas1*$^{+/-}$*;Boc*$^{+/-}$ adult mice **(Figure 5.4).** Likewise, we can determine whether Gli2 expression, which is comparable to Gas1 and Boc expression in the reactive stroma (**Figure 5.2A**), is truly co-expressed in the same set of cells, and whether distinct subsets exist. Preliminary analysis of KC;*Gli2*$^{+/-}$*;Boc*$^{+/-}$ mice three weeks following pancreatitis indicates a population of *Gli2*$^{+}$*;Boc*$^{+}$ fibroblasts in the reactive stroma.

Second, these crosses also allow us to test the importance of co-receptors on earlier stages of tumorigenesis. Mouse crosses to generate these genotypes are ongoing. Further, despite the difficulty in detecting the *Cdon-LacZ* reporter allele as a readout of co-receptor expression, crossing it into the KC model to generate additional combination knockouts would also allow us to interrogate the importance of all three co-

receptors on tumor initiation and progression in an autochthonous model of pancreatic cancer (**see Table 5.1**).

The identity of Gli1-expressing fibroblasts

In Chapter Three, we investigated the importance on Hedgehog signaling in pancreatic recovery, with a particular emphasis on Gli1. In the normal mouse pancreas, a small population of Gli1+ cells resides around blood vessels and ducts. During tumorigenesis, along with an increased fibroblast population in the reactive stroma, Gli1 expression is found in an increased subset of these cells (**Figure 5.6**). Notably, expression of Gli1 in the reactive stroma is not as prevalent as that of Gli2, Gas1, and Boc (**Figure 5.2**). Recently, perivascular Gli1-expressing cells were described in several organs including the kidney, lung, and heart (6). In culture, these cells displayed multipotency, a hallmark MSC property. Intriguingly, tissue-resident Gli1+ cells contributed significantly to organ fibrosis during induced tissue-damage; the contribution of bone-marrow derived cells was excluded through transplantation and parabiosis experiments. Specific ablation of Gli1+ cells decreased organ fibrosis, and as demonstrated in the heart, partially restored organ function that would normally be comprised by irreversible fibrosis (6). The source of organ fibrosis during chronic pancreatitis and pancreatic tumorigenesis is unknown. Given that organ fibrosis due to chronic pancreatitis is irreversible and increases the risk for pancreatic cancer, understanding the source and function of cells contribution to the fibrotic reaction is important for development of better clinical treatment.

Recently, our lab obtained the Gli1$^{eGFP/+}$ mouse, which allows FACS-sorting of Gli1 expressing fibroblasts (**see Fig. 5.7 for scheme**); this was not possible using the previous LacZ reporter allele. Further, crossing the Gli1$^{eGFP/+}$ mouse into the KC model of pancreatic cancer allowed us to characterize these cells in the context of pancreatic tumorigenesis. Preliminary experiments in the lab have found that Gli1+ fibroblasts in the pancreas display properties similar to MSCs. First, only Gli1+ fibroblasts FACS-sorted from the normal pancreas continue to grow in culture; although Gli1- cells are far more prevalent in both the tissue and from FACS-sorting, they do not persist *in vitro* (**Figure 5.8A**). Further, Gli1+ fibroblasts sorted from the both the Gli1$^{eGFP/+}$ and KC;Gli1$^{eGFP/+}$ mice can differentiate into bone and fat *in vitro*, thus demonstrating multipotency (**Figure 5.8B**). Further work is ongoing to functionally test the contribution of Gli1+ cells to pancreatic desmoplasia and tumor growth.

Heterogeneity of fibroblasts within the stroma and the response to HH

The collective body of evidence thus far has revealed that HH signaling in pancreatic cancer is more complex than previously thought. While canonical signaling is now established to occur in a paracrine manner from the tumor cells to the microenvironment, the identity of the HH responsive cells and the nature of their response is still not completely understood. The majority of HH-responsive cells are thought to be activated fibroblasts, which are commonly treated as a single homogenous group. In reality, however, activated fibroblasts are a heterogenous set of cells (7). Commonly used markers, including αSMA, Vimentin, and PDGFRα are not expressed by all CAFs in the microenvironment (7,8). It is possible then, that HH may

act upon these subsets in a different manner and elicit differential responses from these possible fibroblast subtypes. As the largest group of HH-responsive cells, activated fibroblasts have attracted significant research focus. However, while the tumor-to-fibroblast axis of paracrine hedgehog signaling has been relatively well-characterized, the nature of fibroblast response to HH stimulation has not. Thus, further understanding how fibroblast subsets respond to HH is critical to identify downstream pathways of possible therapeutic significance, as well as avoid unintended consequences of HH inhibition.

The Gli1$^{eGFP/+}$ mouse represents a possible system in which to test the differential response of fibroblasts to tumor-derived factors, such as HH ligand. After *in vitro* culture, FACS-sorted Gli1+ fibroblasts lose GFP expression, likely due to loss of tissue-derived signals to induce Gli1 expression. However, treating these fibroblasts with tumor-cell conditioned media or HH ligand induces Gli1 expression. Using GFP expression, Gli1+ and Gli1- cells can be FACS-sorted and further tested for differences between fibroblasts that upregulate Gli1 expression and those that do not.

In addition to signaling to the tumor cells, fibroblasts also communicate with immune cells and can modulate their behavior. Several Gli1 target genes, including *IL-6, Mcp-1,* and *mIL-8* are expressed by fibroblasts during pancreatic injury, and contribute to the recruitment of monocytes/macrophages as well as the polarization of macrophages (9). Extending these findings to fibroblast-immune cell communication during pancreatic tumorigenesis could identify possible therapeutic targets downstream of HH signaling.

Finally, the concept that activated fibroblasts promote tumor growth is also in question. Depletion of SMA+ activated fibroblasts led to accelerated pancreatic tumorigenesis. Further, although SMA-depleted tumors had reduced levels of vimentin and collagen I, these tumors were not sensitized to gemcitabine (10). While this study depleted only SMA+ stromal cells, and thus did not discern between other fibroblast subsets nor specific signaling pathways, it did challenge the idea that activated fibroblasts in the pancreatic tumor stroma act collectively to promote tumor growth.

Hedgehog signaling and the immune response to cancer

In addition to fibroblasts, myeloid cells are another highly prevalent cell population in the pancreatic cancer microenvironment (11). In other gastrointestinal tissues, HH signaling from the epithelium signals to fibroblasts as well as myeloid cells. For instance, in the stomach, *H.pylori* infection induced HH expression, which acted as a myeloid cell chemoattractant (12); mice lacking Gli1 were thus resistant to *H. pylori* induced recruitment to the infected stomach, reducing the overall cytokine response and ultimately preventing gastric metaplasia (13). In contrast to the stomach, where diminished HH response was protective, reduced response in intestinal myeloid cells was harmful. Following induced colitis, $Gli1^{LacZ/+}$ mice displayed a more dramatic cytokine response and consequently more severe intestinal tissue damage (14). Thus, HH-responsive myeloid cells in the gastrointestinal tissues respond to HH in a tissue-dependant manner.

During pancreatic tumorigenesis, a small population of macrophages also expressed Gli1 (9). Macrophages act on multiple aspects of tumorigenesis, from immunosuppression to chemoresistance (for review, see (15)), and are critical for pancreatic tumorigenesis (16). In contrast to fibroblasts, the functional heterogeneity of macrophage subpopulations in cancer is recognized and panels of surface markers allow for their further study (for review, see (17,18). However, any functional significance of Gli1 positive macrophages compared to their Gli1 negative counterparts in pancreatic cancer remains unknown.

In addition to macrophages, HH signaling can act upon other immune cells in the tumor stroma. For instance, various aspects of T cell behavior including anergy and differentiation into functional subsets, may also be affected by Hedgehog signaling (for review, see (19)). The effect of HH inhibition on the immune response is an open area of investigation.

Summary

Collectively, this dissertation work investigated the role of stromal components on pancreatic tumorigenesis. First, I assessed the role of HH co-receptors Boc, Cdon, and Gas1 on tumor growth. The role of these co-receptors on HH signaling has been studied in development, but remains poorly understood in cancer. Further, the results from Chapter Two highlight the importance of considering HH dosage when treating pancreatic cancer, as my data indicates that therapeutic benefit is only conferred upon almost complete blockade of the HH pathway. Secondly, I investigated the role of HH

signaling on pancreatic recovery from injury in Chapter Three. Currently, the most common form of pancreatic injury arises from pancreatitis, for which no specific treatment exists. While preclinical work indicated that complete HH inhibition in pancreatic cancer prolonged survival, I found that HH inhibition during pancreatitis precluded proper remodeling of the tissue, leading to residual tissue fibrosis. Finally, in Chapter Four, I investigated the presence and function of a specific subset of fibroblast-like cells – the MSC- on tumor growth. Further, I found that MSCs from the reactive stroma could promote the polarization of a tumor-promoting macrophage subtype. Taken together, this work sheds light on the complicated role of both the reactive stroma and HH signaling on pancreatic tumorigenesis.

Figures

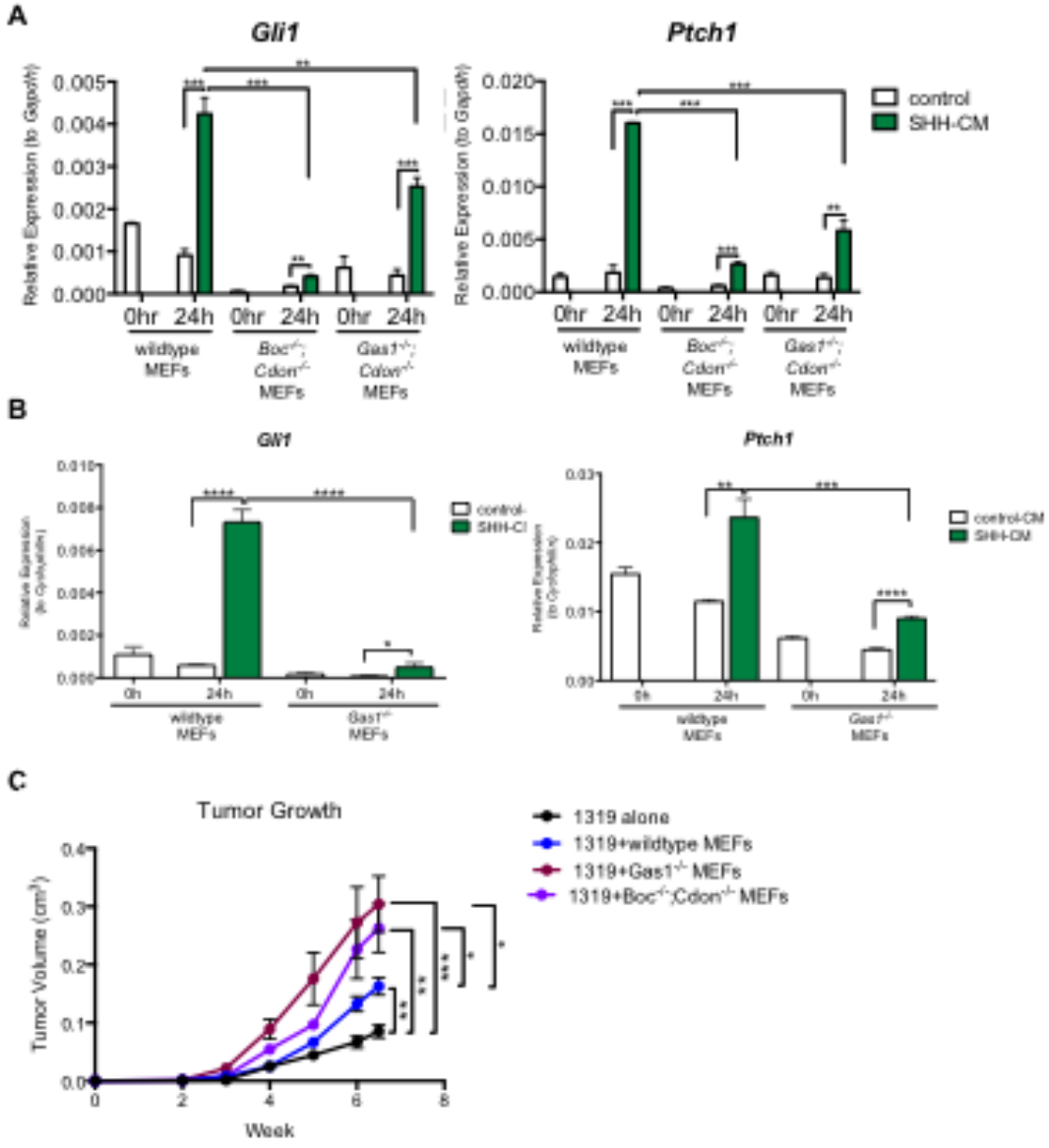

Figure 5.1: Dosage-dependent Hh response on tumor growth.
(A) RT-qPCR analysis of *Gli1* and *Ptch1* on SHH-stimulated wildtype, *Boc*$^{-/-}$*;Cdon*$^{-/-}$, and *Gas1*$^{-/-}$*;Cdon*$^{-/-}$ MEFs. (B) RT-qPCR analysis of *Gli1* and *Ptch1* on SHH-stimulated wildtype, and *Gas1*$^{-/-}$ MEFs. (C) Growth curve for subcutaneous tumors.

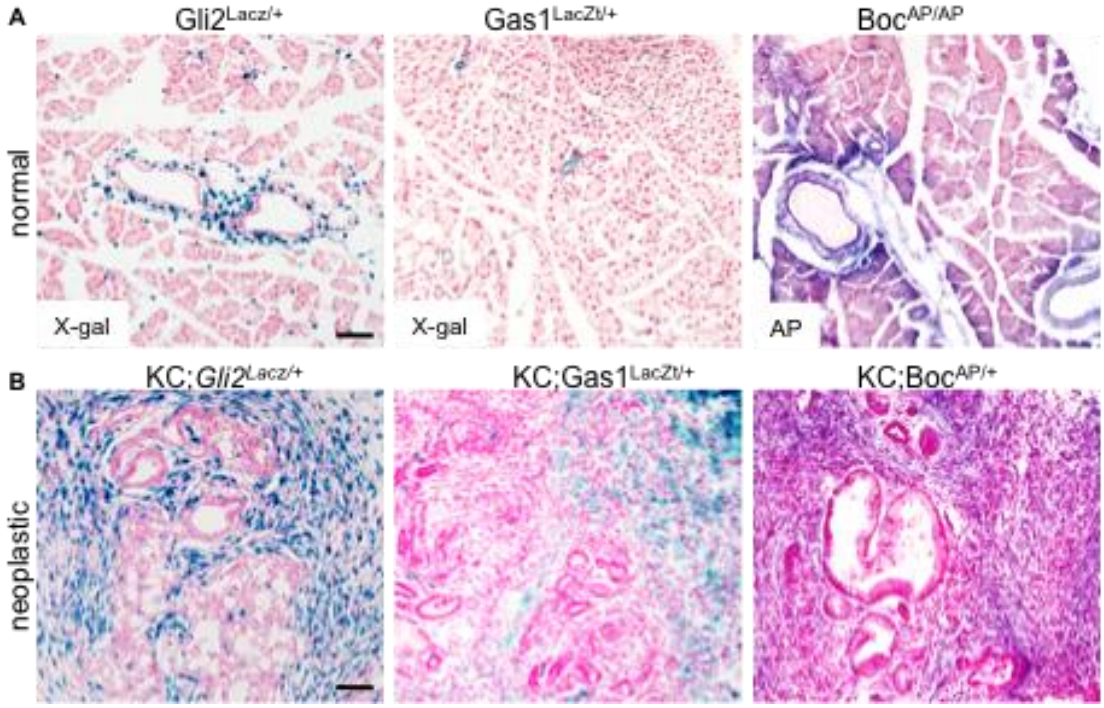

Figure 5.2: Gli2 expression is similar to that of Gas1 and Boc in the normal and neoplastic pancreas.

(A) Expression of *Gli2*^{LacZ} and *Gas1*^{LacZ} in the normal pancreas as detected by X-gal staining, and expression of *Boc*^{AP} in the normal pancreas as detected by Alkaline Phosphatase Staining (far right). Expression of *Gli2, Gas1,* and *Boc* is detected around blood vessels, ducts, and in scattered cells throughoutthe tissue. (B) Expression of *Gli2*^{LacZ}, *Gas1*^{LacZ}, and *Boc*^{AP} in the neoplastic pancreas indicates similar expansion of positive staining throughout the reactive stroma.). Scale bars, 50μm

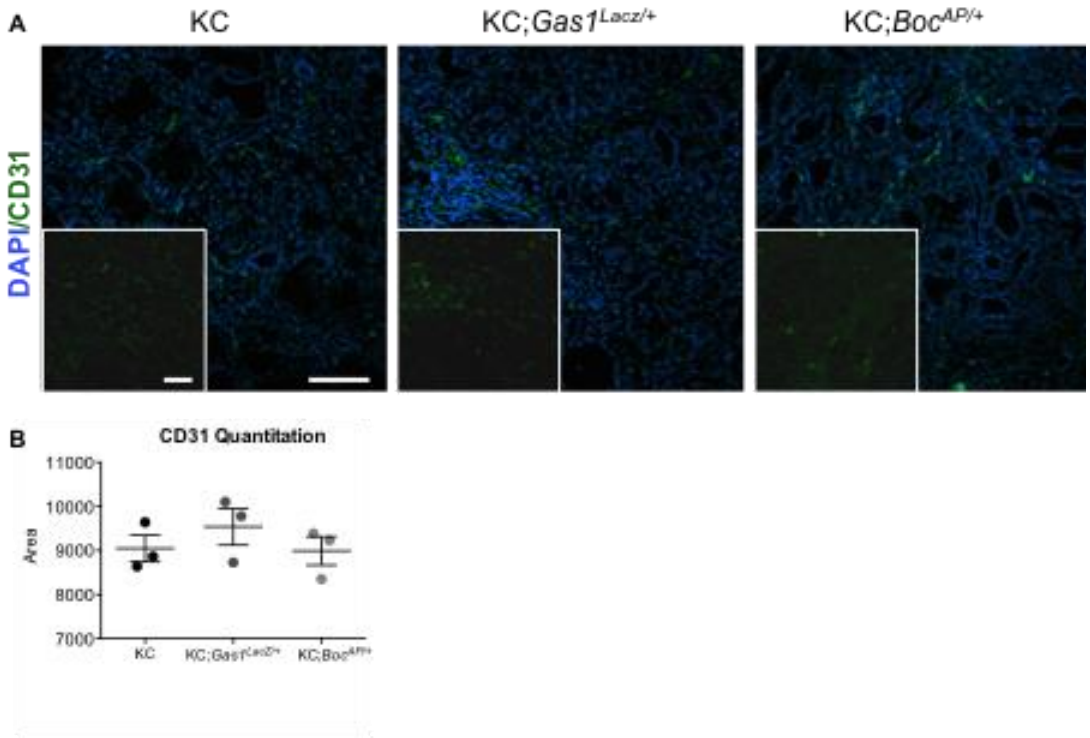

Figure 5.3: Tissue vascularity is comparable between KC, KC;*Gas1*$^{Lacz/+}$ and KC;*Boc*$^{AP/+}$ mice

(A) Antibody detection of CD31 in pancreata of KC, KC;*Gas1*$^{Lacz/+}$, and KC;*Boc*$^{AP/+}$ mice 3w following caerulein-induced pancreatitis. DAPI marks nuclei in blue. Scale bar for image and inset 20μm. (B) Quantitation of CD31+ stain. Total CD31+ area for each pancreas (n=3) obtained with ImagePro Plus Software on five randomized images from each pancreas.

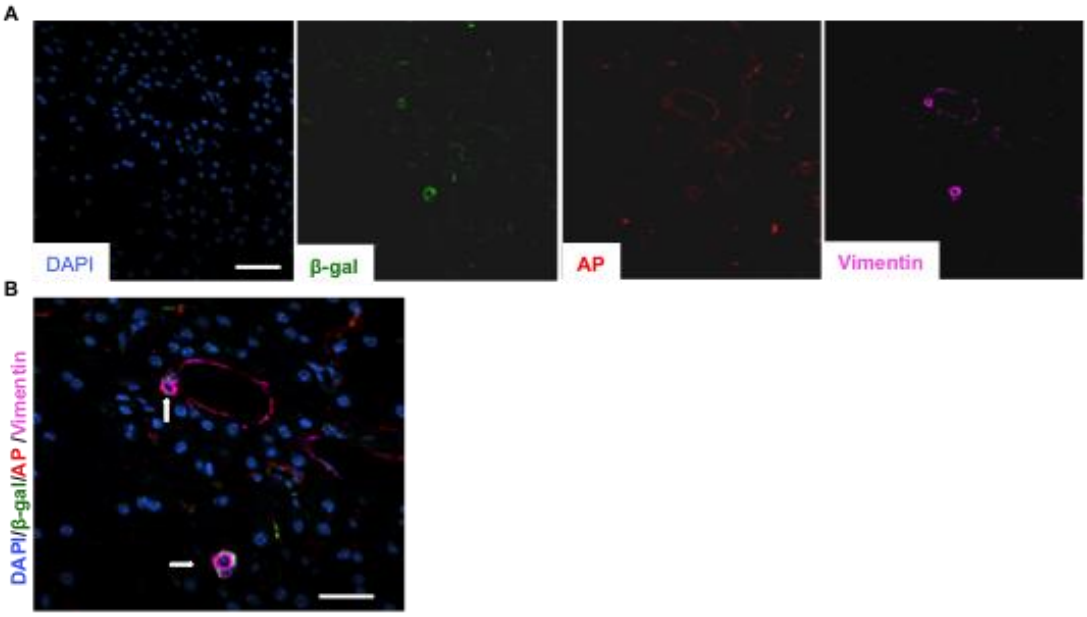

Figure 5.4: *Boc* and *Gas1* are expressed by fibroblasts and stellate cells in the adult pancreas.

(A) Single panel images of stains from *Gas1*$^{LacZ/+}$;*Boc*$^{AP/AP}$ for DAPI (blue), β-gal (green), AP (red), Vimentin (pink). (B) Merged image; white arrows indicate co-expression. Scale bar 20μm

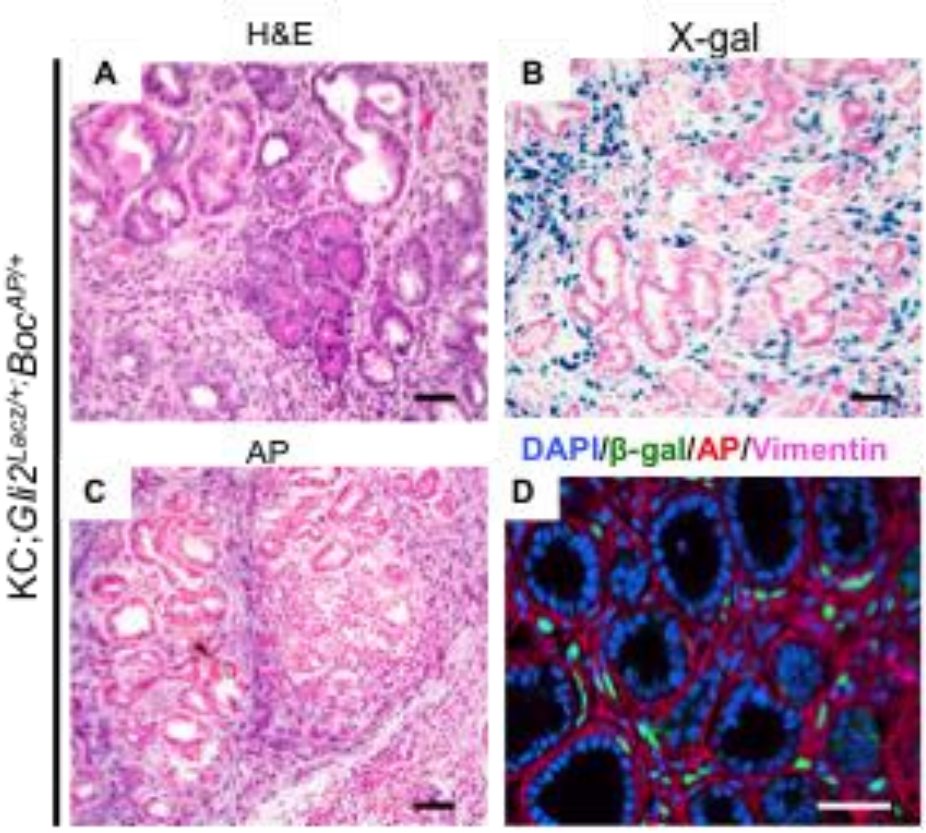

Figure 5.5: *Boc* and *Gli2* are expressed by fibroblasts in the stroma.
Analysis of KC;$Boc^{AP/+}$;$Gli2^{LacZ/+}$ pancreas three weeks following caerulein-induced pancreatitis. (A) H&E (B) staining for *Gli2* expression (C) AP staining for *Boc* expression. (D) Co-immunofluorescnece for *Gli2* (green), *Boc* (red), and Vimentin (pink). Scale bars, black: 50μm; white: 20μm.

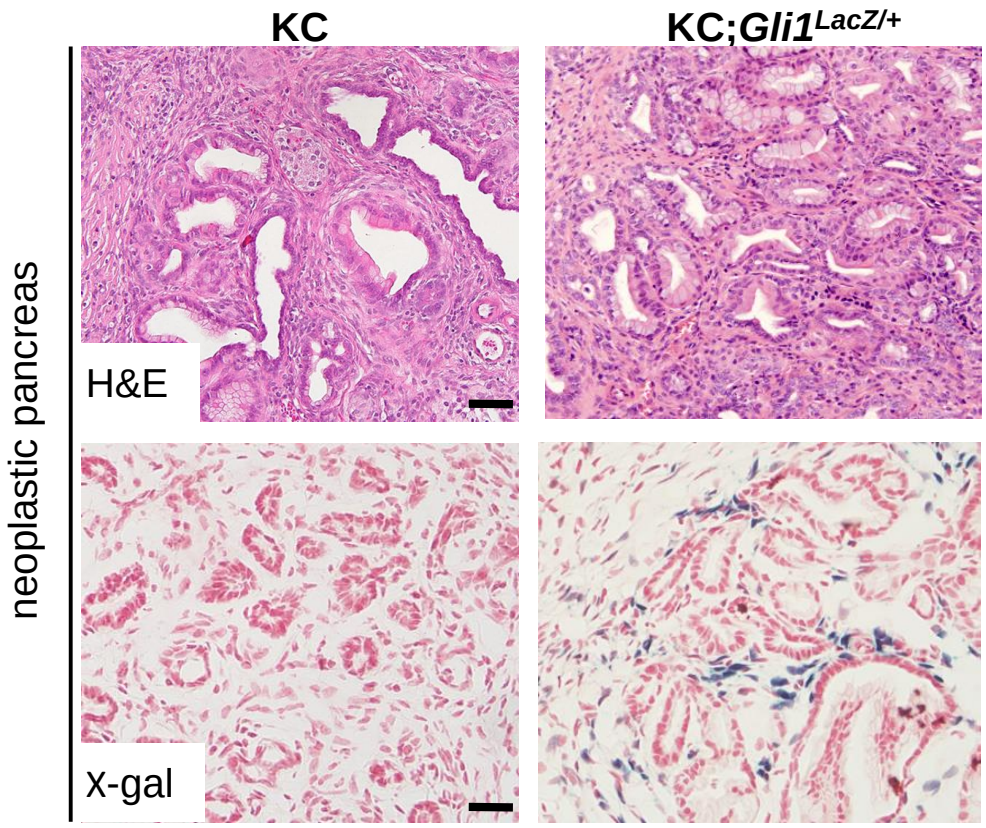

Figure 5.6: *Gli1* is expressed in the reactive stroma.
Analysis of KC (left) and KC;*Gli1*$^{LacZ/+}$ pancreas (right) three weeks following caerulein-induced pancreatitis. H&E staining (left) and X-gal staining (right) Scale bars, 50μm.

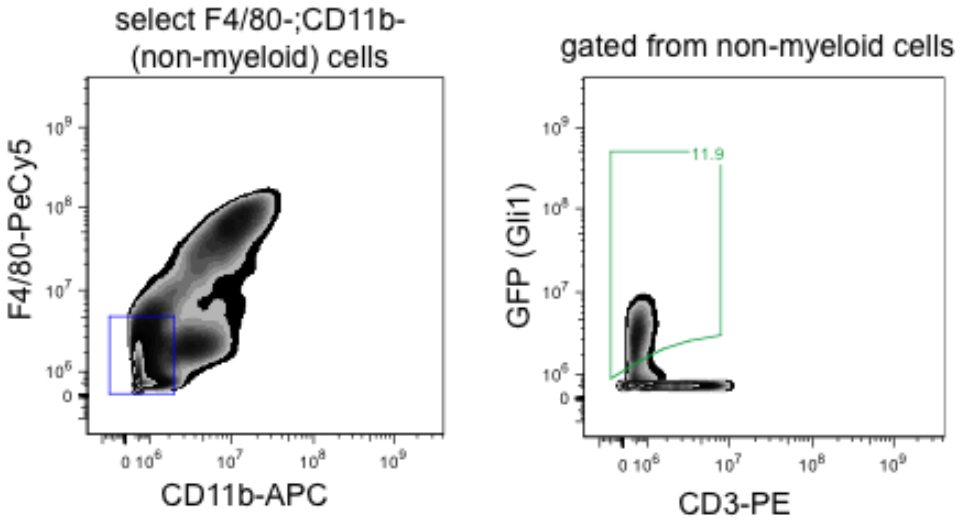

Figure 5.7: Gli1+ fibroblasts can be sorted from the pancreas.
Gli1+ fibroblasts can be sorted from the pancreas by negative selection for immune cell markers F4/80, CD11b, and CD3.

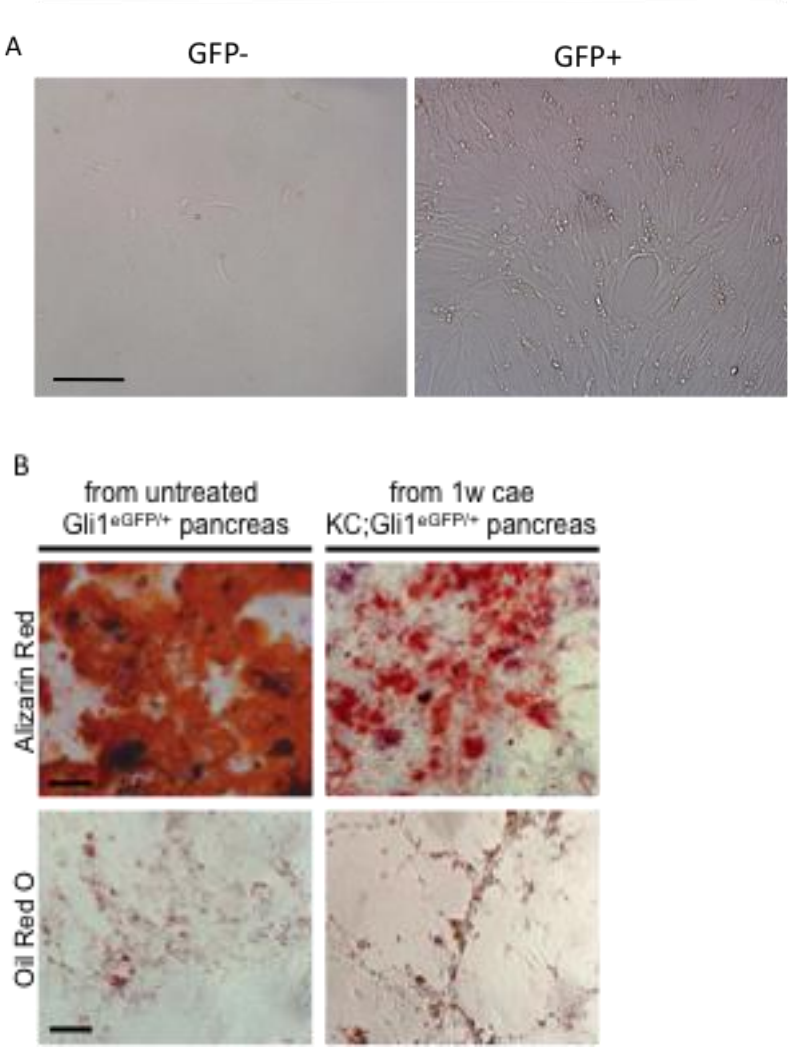

Figure 5.8: Gli1+ cells exhibit MSC-like properties *in vitro*.

(A) GFP+ fibroblasts persist *in vitro* while GFP- fibroblasts do not. Cells were sorted from a KC;Gli1$^{eGFP/+}$ mouse 1w after caerulein-induced pancreatitis. Scale bar, 250μm. (B) GFP+ cells from Gli1$^{eGFP/+}$ mice (left) and from KC;Gli1$^{eGFP/+}$ mice (right) are multipotent *in vitro*.

Tables

Table 5.1: Genotypes to test the effect of HH dosage on pancreatic tumor progression	
Genotype	**Co-receptor Status**
KC	All three co-receptors present
KC;*Gas1*$^{+/-}$	Missing one copy of *Gas1*
KC;*Boc*$^{+/-}$	Missing one copy of *Boc*
KC;*Boc*$^{+/-}$	Missing both copies of *Boc*
KC;*Cdon*$^{+/-}$	Missing one copy of *Cdon*
KC;*Gas1*$^{+/-}$;*Cdon*$^{+/-}$	Missing one copy of *Gas1* and one copy of *Cdon*
KC;*Boc*$^{+/-}$;*Cdon*$^{+/-}$	Missing one copy of *Boc* and one copy of *Cdon*
KC;*Boc*$^{-/-}$;*Cdon*$^{+/-}$	Missing both copies of *Boc* and one copy of *Cdon*
KC;*Gas1*$^{+/-}$;*Cdon*$^{+/-}$	Missing one copy of *Gas1* and one copy of *Cdon*
KC;*Gas1*$^{+/-}$;*Boc*$^{+/-}$	Missing one copy of *Gas1* and one copy of *Boc*
KC;*Gas1*$^{+/-}$;*Boc*$^{-/-}$	Missing one copy of *Gas1* and both copies of *Boc*
KC;*Gas1*$^{+/-}$;*Cdon*$^{+/-}$;*Boc*$^{+/-}$	Missing one copy of *Gas1, Cdon,* and *Boc*
KC;*Gas1*$^{+/-}$;*Cdon*$^{+/-}$;*Boc*$^{-/-}$	Missing one copy of *Gas1, Cdon,* and both copies of *Boc*

References

1. Lyssiotis, C. A., and Cantley, L. C. (2014) Targeting metabolic scavenging in pancreatic cancer. *Clin Cancer Res* **20**, 6-8
2. Mathew, E., Zhang, Y., Holtz, A. M., Kane, K. T., Song, J. Y., Allen, B. L., and Pasca di Magliano, M. (2014) Dosage-dependent regulation of pancreatic cancer growth and angiogenesis by hedgehog signaling. *Cell Rep* **9**, 484-494
3. Leem, Y. E., Han, J. W., Lee, H. J., Ha, H. L., Kwon, Y. L., Ho, S. M., Kim, B. G., Tran, P., Bae, G. U., and Kang, J. S. (2011) Gas1 cooperates with Cdo and promotes myogenic differentiation via activation of p38MAPK. *Cell Signal* **23**, 2021-2029
4. Kang, J. S., Mulieri, P. J., Hu, Y., Taliana, L., and Krauss, R. S. (2002) BOC, an Ig superfamily member, associates with CDO to positively regulate myogenic differentiation. *EMBO J* **21**, 114-124
5. Rhim, A. D., Oberstein, P. E., Thomas, D. H., Mirek, E. T., Palermo, C. F., Sastra, S. A., Dekleva, E. N., Saunders, T., Becerra, C. P., Tattersall, I. W., Westphalen, C. B., Kitajewski, J., Fernandez-Barrena, M. G., Fernandez-Zapico, M. E., Iacobuzio-Donahue, C., Olive, K. P., and Stanger, B. Z. (2014) Stromal elements act to restrain, rather than support, pancreatic ductal adenocarcinoma. *Cancer Cell* **25**, 735-747
6. Kramann, R., Schneider, R. K., DiRocco, D. P., Machado, F., Fleig, S., Bondzie, P. A., Henderson, J. M., Ebert, B. L., and Humphreys, B. D. (2015) Perivascular Gli1+ progenitors are key contributors to injury-induced organ fibrosis. *Cell Stem Cell* **16**, 51-66
7. Sugimoto, H., Mundel, T. M., Kieran, M. W., and Kalluri, R. (2006) Identification of fibroblast heterogeneity in the tumor microenvironment. *Cancer Biol Ther* **5**, 1640-1646
8. Erez, N., Truitt, M., Olson, P., Arron, S. T., and Hanahan, D. (2010) Cancer-Associated Fibroblasts Are Activated in Incipient Neoplasia to Orchestrate Tumor-Promoting Inflammation in an NF-kappaB-Dependent Manner. *Cancer Cell* **17**, 135-147
9. Mathew, E., Collins, M. A., Fernandez-Barrena, M. G., Holtz, A. M., Yan, W., Hogan, J. O., Tata, Z., Allen, B. L., Fernandez-Zapico, M. E., and di Magliano, M. P. (2014) The transcription factor GLI1 modulates the inflammatory response during pancreatic tissue remodeling. *J Biol Chem* **289**, 27727-27743
10. Ozdemir, B. C., Pentcheva-Hoang, T., Carstens, J. L., Zheng, X., Wu, C. C., Simpson, T. R., Laklai, H., Sugimoto, H., Kahlert, C., Novitskiy, S. V., De Jesus-Acosta, A., Sharma, P., Heidari, P., Mahmood, U., Chin, L., Moses, H. L., Weaver, V. M., Maitra, A., Allison, J. P., LeBleu, V. S., and Kalluri, R. (2014) Depletion of carcinoma-associated fibroblasts and fibrosis induces immunosuppression and accelerates pancreas cancer with reduced survival. *Cancer Cell* **25**, 719-734

11. Clark, C. E., Hingorani, S. R., Mick, R., Combs, C., Tuveson, D. A., and Vonderheide, R. H. (2007) Dynamics of the immune reaction to pancreatic cancer from inception to invasion. *Cancer Res* **67**, 9518-9527
12. Schumacher, M. A., Donnelly, J. M., Engevik, A. C., Xiao, C., Yang, L., Kenny, S., Varro, A., Hollande, F., Samuelson, L. C., and Zavros, Y. (2012) Gastric Sonic Hedgehog acts as a macrophage chemoattractant during the immune response to Helicobacter pylori. *Gastroenterology* **142**, 1150-1159 e1156
13. El-Zaatari, M., Kao, J. Y., Tessier, A., Bai, L., Hayes, M. M., Fontaine, C., Eaton, K. A., and Merchant, J. L. (2013) Gli1 deletion prevents Helicobacter-induced gastric metaplasia and expansion of myeloid cell subsets. *PLoS One* **8**, e58935
14. Lees, C. W., Zacharias, W. J., Tremelling, M., Noble, C. L., Nimmo, E. R., Tenesa, A., Cornelius, J., Torkvist, L., Kao, J., Farrington, S., Drummond, H. E., Ho, G. T., Arnott, I. D., Appelman, H. D., Diehl, L., Campbell, H., Dunlop, M. G., Parkes, M., Howie, S. E., Gumucio, D. L., and Satsangi, J. (2008) Analysis of germline GLI1 variation implicates hedgehog signalling in the regulation of intestinal inflammatory pathways. *PLoS Med* **5**, e239
15. Ruffell, B., and Coussens, L. M. (2015) Macrophages and therapeutic resistance in cancer. *Cancer Cell* **27**, 462-472
16. Mitchem, J. B., Brennan, D. J., Knolhoff, B. L., Belt, B. A., Zhu, Y., Sanford, D. E., Belaygorod, L., Carpenter, D., Collins, L., Piwnica-Worms, D., Hewitt, S., Udupi, G. M., Gallagher, W. M., Wegner, C., West, B. L., Wang-Gillam, A., Goedegebuure, P., Linehan, D. C., and DeNardo, D. G. (2013) Targeting tumor-infiltrating macrophages decreases tumor-initiating cells, relieves immunosuppression, and improves chemotherapeutic responses. *Cancer Res* **73**, 1128-1141
17. Murray, P. J., and Wynn, T. A. (2011) Protective and pathogenic functions of macrophage subsets. *Nat Rev Immunol* **11**, 723-737
18. Gordon, S., and Taylor, P. R. (2005) Monocyte and macrophage heterogeneity. *Nat Rev Immunol* **5**, 953-964
19. Crompton, T., Outram, S. V., and Hager-Theodorides, A. L. (2007) Sonic hedgehog signalling in T-cell development and activation. *Nat Rev Immunol* **7**, 726-735